Model Based Advisory Systems for Treatment of Type 1 Diabetes: On-Demand Treatment Recommendations as a Precursor to Fully Closed-Loop Drug Delivery

---

A Dissertation

Presented to

the faculty of the School of Engineering and Applied Science

University of Virginia

---

in partial fulfillment

of the requirements for the degree

Doctor of Philosophy

by

Paul Vereshchetin

May

2015

Abstract

Automated closed-loop drug delivery systems, in which continuous adjustments of treatment parameters are based on frequent sampling of physiological processes, have been studied for years and are largely envisioned for use in clinical settings where the system can be under constant supervision by a clinician. Recently, there have been efforts in using these systems as advanced treatment for chronic illnesses, which is timely since chronic illness rate is on the rise, but also raises the possibility that the system user may now be the patient (not a clinician). Indeed, miniaturization and smarter algorithms promise that one day these technologies can be taken out of the hospital and brought to patient's home. For example, recent clinical studies of artificial pancreas (AP) systems have demonstrated the feasibility of closed-loop treatment of Type 1 diabetes. While efforts to commercialize AP systems are underway, it is not yet clear that closed-loop treatment will appeal to a large segments of the patient population.

This work started with a desire to understand the factors that contribute to the success or failure of systems that (i) involve continuous measurement (as in the AP) but (ii) do not involve automated adjustment of all treatment parameters but rather present some treatment options to patients on demand where such options are model-based optimal recommendations. This approach accounts for human factors considerations and serves as a reasonable precursor to a fully closed-loop AP, but can be more readily adopted by the patients. The approach employs a model that addresses the risk asymmetry of the patient state space and takes advantage of a previously developed safety feature to create a semi-automated system.

One outcome of this work is a proposition of a controller design where individualization of the action of the system is achieved through the development of a mathematical model that is adapted to patient's individual physiology. Previous model-based advisory systems have generally relied upon a "population average" model and achieved individualization through careful construction of optimization objective

function. Such approach of defining state deviation penalties proved to be fragile because, for example, the patient's pump therapy parameters that the objective function becomes sensitive to are often misestimated. The *in silico* preclinical trials using the new controller design suggested dramatic improvement over conventional therapy by better keeping the blood glucose in range and reducing the risk of implications such as hypoglycemia, without requiring ad hoc tuning of objective function parameters.

In vivo validation of the bolus advisory system confirmed safe and effective operation at meal times, but, due to model uncertainty, demonstrated that a different approach should be employed to retain the efficacy in the timeframe immediately after meals. Consequently, the work continued with the advice request limited to meal times and correction boluses decoupled from meal boluses. In addition, the system's application was extended for multiple daily injection (MDI) therapy to serve a larger population. To address issues encountered earlier, the robustness of the system to uncertainty about the model's pharmacokinetic parameters was tested. In addition, the system's robustness to irregularities in the timing of long-acting insulin dose administration was tested, accounting for the reality of MDI therapy in practice. It was shown that the system can handle completely skipped long-acting insulin injections used in MDI therapy.

While the engineering design of automated systems for the management of chronic disease like Type 1 diabetes is a complex problem, it still does not encompass the larger challenge of designing human-machine systems of this sort. A formal framework is therefore proposed for holistic pre-design AP system analysis. In addition, a framework for risk identification is proposed that allows to locate and address the causes of suboptimal system performance.

APPROVAL SHEET

The dissertation

is submitted in partial fulfillment of the requirements

for the degree of

Doctor of Philosophy

AUTHOR

The dissertation has been read and approved by the examining committee:

Stephen D. Patek, Ph.D.

Advisor

William T. Scherer, Ph.D.

Marc D. Breton, Ph.D.

Stephanie Guerlain, Ph.D.

Sue Brown, M.D.

Accepted for the School of Engineering and Applied Science:

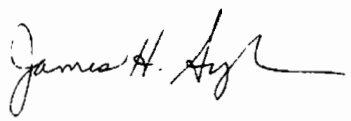

Dean, School of Engineering and Applied Science

May

2015

Acknowledgements

This work would not be possible without the guidance and support of my adviser, my colleagues, and the committee members.

I would like to express my deepest gratitude to my adviser Steve Patek who has been a patient mentor over all these years, Marc Breton who helped me understand the theory and harness the power of the simulator to be able to conduct my research, and Boris Kovatchev who has been a wise supporter of my research initiatives and a bright beacon helping to navigate the Artificial Pancreas waters.

I also extend my gratitude to Stephanie Guerlain who provided invaluable human factors input to my dissertation and always took so much time to supply the most detailed comments on how I can improve my manuscript, and to Sue Brown who was the clinical expert for me and always made sure my research was in line with real life patient needs.

I am particularly grateful to my committee chair Bill Scherer for supporting me not only in my research but also in my extracurricular activities that made my Ph.D. experience at U.Va. complete.

Finally, my friends and colleagues, and in particular Colleen Hughes, Andy Ortiz, Boyi Jiang, Benton Mize, and Antoine Robert deserve the most gratitude from me for always being willing to help, both at work and outside the office.

Contents

List of Figures

List of Tables

List of Abbreviations

AP – Artificial Pancreas

APS – Artificial Pancreas System

BG – Blood Glucose

CBGM – Capillary Blood Glucose Monitoring

CF – correction factor

CGM – Continuous Glucose Monitoring

CR – Carbohydrate ratio

DCCT – Diabetes Control and Complications Trial

EMMGK –Extended Meal Model for Glucose Kinetics

FDA – Food and Drug Administration

GUI – Graphical User Interface

HRM – Holistic Requirement Model

IOB – Insulin On Board

ID - Intradermal

IV - Intravenous

LQG – Linear Quadratic Gaussian

MDI – Multiple Daily Injections

MPC – Model Predictive Control

NPH – neutral protamine Hagedorn

PD - pharmacodynamics

PID – Proportional-Integral-Derivative

PK –pharmacokinetics

SC – subcutaneous

STA – Systemic Textual Analysis

SMBG – Self-Monitoring of Blood Glucose

T1DM – Type 1 Diabetes Mellitus

UKPDS – United Kingdom Prospective Diabetes Study

VBR – Virtual Basal Rate

Chapter 1

Introduction and Motivation

Closed loop control has been the staple of many control systems since its advantages were recognized in the early 20th century [1]. In the realm of governing mechanical processes, closed loop control was patented in the US as early as the 1860s, [2], [3]. And before that, self-governing devices like the centrifugal governor by Watts [4] and the pendulum clock by Huygens [5] trace the history of automatic control through centuries all the way back to antiquity when water clocks were first used in Greece.

While the complexity of such control systems has been growing at an ever increasing rate, the application of the engineering methods initially designed for mechanical inanimate systems also migrated into other fields, particularly biomedical applications of systems engineering. In fact, the field of control and systems has been applied to biological systems for many years: at least as early as the work of Walter Cannon on homeostasis in 1929 [6]. However, as Drs. Doyle III and Bequette note in the report The Impact of Control Technology [7], the impact of control and systems on devices and applications in the field of biology has only emerged in recent years.

This sort of application (biomedical applications of systems engineering) poses inherent risks due to several reasons:

- It is much less mature
- It has wide impact on human life as the actuation is directed at humans immediately
- It is more behavior dependent as the application is more individualized

There are specific challenges that have to be overcome in translating closed-loop techniques to practice. For instance, handling of both inter-patient and intra-patient variability. This problem is quite different

from engineering systems where uncertainty may be present, but it is typically of fixed (for example, stationary) structure [7]. In biology, the variability is profound, and the same subject can differ significantly from one day to the next, depending on such factors as stress, food quantity and quality, environment, and so on. In some specific situations, such as diabetes, the intra-subject variation in critical subject parameters (such as insulin sensitivity) far exceeds the inter-patient variability.

Besides technological and algorithmic challenges these biomedical applications of systems engineering also face the barriers of another kind – regulatory ones. To provide an example, for over 40 years there have been research and development progress in the area of what is called Artificial Pancreas – a type of therapy for type 1 diabetics where the insulin is infused automatically into the body of the patient by a system that makes the injection decisions based on the information available, such as glucose level continuously measured in subcutaneous (SC) tissues, insulin injection history, etc. (see [8] for a comprehensive review). However, there is no commercially available product on the market yet and such a product still remains a long-term prospect. One reason is that the Food and Drug Administration (FDA) in the US and similar agencies in other countries are very careful in considering applications for approval of systems with the features of closed loop. While these regulatory institutions have allowed prototype devices to be tested in clinical settings, the avenue to closed loops testing in a home environment remains unclear [9].

In this light, the primary hypothesis of this work is that it is possible to adapt model-predictive methods used in closed loop to create "advisory" systems that make the most out of available sensors, models, and actuators, but allow the patient and caregiver to maintain ultimate control authority. We deem these advisory systems – where the patient is ultimately in charge of the potent drug delivery –an alternative to automated drug-delivery systems and a natural stepping stone to marketable and viable closed loop solutions.

Chapter 2

Biomedical Background

It is impossible to consider biomedical engineering systems without delving at least to some degree in the contextual knowledge. This section provides all the background necessary to understand the rest of the research presented.

2.1 Type 1 Diabetes as a Control Problem

Type 1 diabetes mellitus (T1DM) is an autoimmune disease that is characterized by destruction of the insulin-producing beta-cells in the pancreas. This leaves the body without means of utilizing the glucose and leads to its increase in blood – hyperglycemia. As body cannot consume the glucose from the blood, it tries to obtain energy from breaking down fats. A byproduct of this process – ketones – cannot be completely gotten rid of by the body and so the ketones concentration builds up leading to ketoacidosis (diabetic coma). Chronic hyperglycemia injures the heart and incurs poor blood circulation. This might lead, among other things, to foot ulcers that, when untreated, lead to the amputation of the toes, foot, or even part of the leg. Besides foot damage, hyperglycemia leads to neuropathy (nerve damage), nephropathy (kidney damage), and retinopathy (eye damage). According to the American Diabetes Association (ADA), blood glucose levels above 130 mg/dl before a meal and above 180 mg/dl 2 hours after a meal should be considered hyperglycemic [10].

To prevent hyperglycemia in type 1 patients, exogenous insulin is used. The insulin facilitates the uptake of glucose by tissues and thus decreases its concentration in blood. The overall insulin-glucose interaction system is depicted in Figure 1 (the graphic is adopted from [8]). However, the amount of insulin necessary in any given case is hard to calculate precisely. Overdosing insulin leads to another clinical complication – hypoglycemia, or low blood glucose. If the hypoglycemia is not treated, it leads to a

seizure, unconsciousness, and eventually to death. According to the American Diabetes Association, blood glucose levels below 70 mg/dl should be considered hypoglycemia [11].

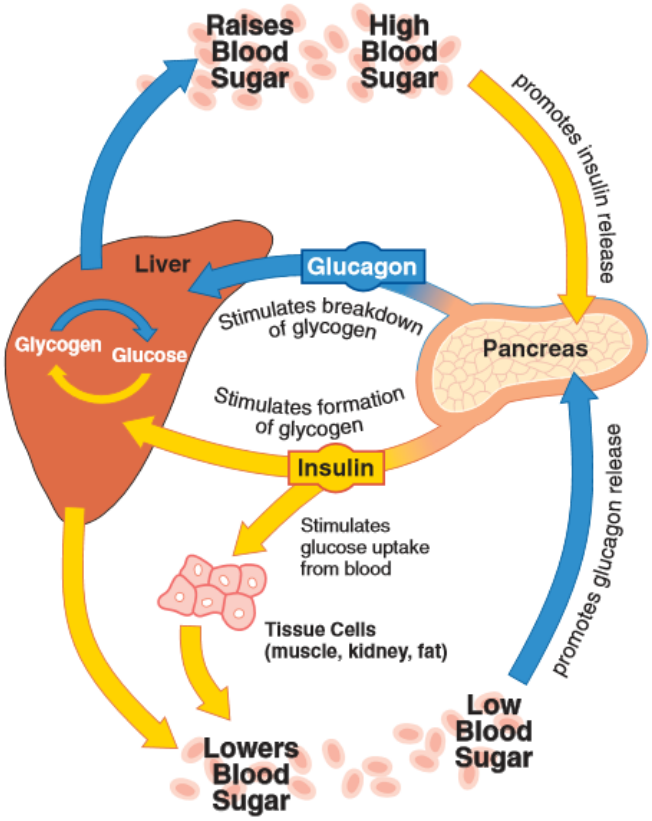

Figure 1. Insulin-glucose metabolic interaction.

2.2 Types of Insulin

There are different types of insulin, different methods of its administration, and different therapies available to treat hyperglycemia. The most used types of insulin are presented in Table 1 along with their main characteristics.

Table 1. Common types of insulin and their characteristics.

Type of Insulin	Onset Time	Peak Time	Action Time
Rapid-acting insulin (e.g. lispro)	5 min	1 h	2 – 4 h
Short-acting insulin (e.g. regular insulin)	30 min	2 – 3 h	3 – 6 h
Intermediate-acting insulin (e.g. NPH)	1 - 2 h	4 – 12 h	12 – 18 h
Long-acting insulin (e.g. glargine)	1 – 2 h	-	20 – 24 h
Ultralong-acting insulin (e.g. degludec)	1 – 2 h	-	Up to 40 h

2.3 Insulin Delivery Methods

There are three main ways of delivering insulin into the body:

- Subcutaneous (SC) injection
- Intradermal (ID) injection
- Intravenous (IV) injection

There are also other ways of administration that are being investigated:

- Transbuccal (through the cheek) administration [12], [13].
- Oral administration to digestive tract [14].

- Inhalation [15]. While after the failure of the Pfizer's product, giants like Novo Nordisk and Eli Lilly scrapped their inhalable insulin research, there is a newer product Afrezza by MannKind that was recently approved by FDA.
- Intranasal administration [16].
- Transdermal administration [17], [18].
- Transconjunctival (through eyes) delivery [19].

2.4 Current off-the-Shelf Devices for Diabetes Management

- Self Monitoring of Blood Glucose (SMBG) device, or capillary BG monitoring (CBGM) device. Comes with strips on which the patient squeezes a blood drop after pricking their finger with a lancet (fingerstick). The strip is then plugged into the device and the BG level is shown on the screen.
- Continuous Glucose Monitoring (CGM) device. Consists of the sensor with a needle that is inserted under the skin and the receiver that wirelessly receives glucose data from the sensor every 5 minutes. Receiver shows the trend and current level on the screen. One drawback of this system, as compared to SMBG, is that the glucose level is measured in subcutaneous tissue, not in the blood, and therefore there is a delay and lower accuracy. FDA does not recommend making decisions solely based on CGM readings – SMBG test should be in place to assess BG more precisely before any insulin is injected.
- Insulin pen (replacing relatively more archaic syringes). Provides a way to carry out an intradermal injection of insulin. Uses either replaceable cartridges or comes as a disposable device with prefilled insulin of certain type and brand. The injections are either basal insulin (long-acting insulin) or boluses (rapid-acting insulin).
- Insulin pump. Most of the pumps consist of a tube that goes from the pump (carried on the belt in a cradle) to the insertion site on the body where a needle permanently stays in the body, subcutaneously. The insulin is injected every 5 minutes in small amounts to emulate the body's

natural production (basal insulin) and big amounts are injected at certain times by the command of the user, e.g. at meal times (boluses). There are also pumps in which the insulin cartridge is part of the insertion site (the so called pod), and the interface is located on a wireless devices that is not connected to the site with a tube.

Chapter 3

Literature Review

The sections provides overview of the models and control systems in the realm of Artificial Pancreas systems and of the insulin administration peculiarities in the corresponding context.

3.1 State of the Art

Model Predictive Control (MPC) was developed mainly for the chemical industry in the US and France in the 1960s and 1970s [20]. Since then, it has been used extensively in the applications of controlling various dynamical systems, and attempts have been made in the field of type 1 diabetes control as well. The pursuit of the elusive goal of closed-loop control for Type 1 Diabetes Mellitus (T1DM) continued with renewed vigor after the seminal 1993 Diabetes Control and Complications Trial (DCCT), [21] (for similarly impactful United Kingdom Prospective Diabetes Study (UKPDS) for type 2 diabetes see [22]), that showed that intensive glycemic control reduces the complications of the disease, such as retinopathy and stroke. Another boost was given by the JDRF initiating the artificial pancreas project and providing corresponding funding to numerous research centers in 2006 [23].

Reactive algorithms like Proportional-Integral-Derivative (PID) control (e.g. [24]) underperformed in the Artificial Pancreas settings in the past due to the lags of the input and actuation signals which results from the subcutaneous nature of the glucose sensors and insulin pumps. The subcutaneous medium of the glucose measure and insulin injection is not the medium where the interaction of the manipulated variable (glucose) and actuation tool (insulin) occurs, and a reactive controller may result in unstable system behavior and system oscillation [25]. Indeed, this kind of systems worked well in AP applications where the IV route was used, and therefore the delays were eliminated [26], [27]. But IV route is too invasive and cumbersome to be a part of a commercial AP system.

That is why lately researchers have been concentrating on other, model-based solutions. Among well-known earlier model-based approaches is the Model-Based Algorithm by Parker and Doyle III, [28], and their follow-on work studying an Advanced Model Predictive Control, [29]. Later Magni et al. published the design of Model Predictive Control, [30] and followed up with its Run-to-Run tuning, [31]. Another advanced MPC strategy was investigated by Hovorka et al. in [32]. Other encouraging MPC systems results are described in [33], [34], and [35]. In addition, a modular structure for AP systems has been developed by Patek et al., [36]. This approach enabled design flexibility, and should allow for incremental testing, regulatory approval, and deployment of AP control systems

Boston researches have been investigating bihormonal control, where the action of insulin, if needed, can be counter-regulated by the hormone glucagon which raises the concentration of glucose in the blood, [37]. This system, called by the authors Bionic Pancreas (glucagon, along with insulin, is naturally produced in the pancreas by alpha-cells, while insulin is produced by beta-cells), requires not one, but two insulin pumps one of which is used for insulin delivery and another one for glucagon delivery. While the study results were encouraging, a bihormonal system allows for more aggressive control (since any action can be always counter-regulated) and therefore might be potentially more dangerous.

Finally, the state-of-the-art simulation system was developed at U.Va. with the help of collaborators from California and Italy, [38]. The Simulator – Simulink-implemented simulation environment – contains a cohort of 300 *in silico* patients, is approved by the FDA as a substitution for animal trials, and allows researchers to develop. test, tune, and validate AP algorithms, [39].

3.2 Call for Advisory Systems

With all the development on the side of fully automatic control described above, there is hardly any research published about advice-on-demand types of systems. There might be an additional source of confusion in the fact that there is a method called Advisory Mode Control used for testing and validation of closed-loop control algorithms. Under this name, the test is common in the petrochemical industry for prototyping and has been used with type 1 diabetes control algorithms as well, for instance in [40] and [41]. It consists of testing an MPC controller on historical clinical data and presents value *per se*, but does not have any relation to the advisory mode being proposed in this work. In contrast to the proposed advisory system, the Advisory Mode Control still administers insulin on a frequent basis (e.g. every 5 minutes) and is an instantiation of an MPC control.

There have been early attempts to introduce so called decision support systems, such as Computer Assisted Insulin Dosage Adjustment by Schiffrin et al. in 1985 [42], Computer-Assisted Diabetic Management by Deutsch et al. in 1990 [43], or DIAS – the Diabetes Advisory System by Hejlesen et al. in 1997 – see [44] and the system's further evaluation in [45] (not to be confused with DiAs – Diabetes Assistant software platform developed at U.Va. and described in [46]). However, these systems were developed at the times of lower computational power, bulkier devices, their algorithms were based on limited previous experience, and they would usually run on desktop computers of physicians to assists them in assigning therapy to type 1 diabetics.

There is another work that used the word 'advisory' in it, [47] by Zarkogianni et al. The discussed system is called Insulin Infusion Advisory System for Type 1 Diabetes Patients. However, the word 'advisory' (or any other mention of any 'advice') is used in the paper only twice – in the title and in the abstract where the title is repeated. Other than that, the system presented is a pump-based MPC system, where, natural to MPC, a calculation based on an optimization function is performed at each step until the end of prediction horizon and only the first element of the suggested control sequence is applied to the system.

Interestingly, in most of the works that describe closed-loop insulin infusion systems, the subjects' opinion of the system operation is not studied, or at least not reported, and in the case of computer simulation studies, is not considered at all. There seems to be a gap therefore since the systems under consideration should be designed to ultimately serve the patients and their input would be invaluable for every stage of the design. While an argument can be made that all diabetes patients would support the arrival of AP, as with many a design in real life, users (patients) might have a mental model of the system that is different from the mental model of the designers (engineers and physicians). Discrepancy between these mental models is studied in the field of human factors and is proved to sometimes be dangerous to the user of the system [48].

3.3 Models

Since model-based control is considered, it is important to have a full picture of the models that are used in the control systems for type 1 diabetes. A great summary on the models developed to measure, control and simulate type 1 diabetes centered systems is given in the review [49] by Cobelli et al. Arguably the two most cited models are the meal model by Dalla Man, [50], and the Minimal Model by Bergman, [51], the latter also having useful extensions accounting for subcutaneous oral glucose sensing and insulin transport as described in [52]. Another useful transformation of the Bergman's model uses the logarithmic space to reflect the difference of the risk weight attached to the deviations of the same magnitude from the target that are directed towards hypo- or hyperglycemia – see [53] for a detailed description and compare to the symmetrization by Kovatchev et al. in [54].

3.4 Independent Insulin Profiles Evaluations

In addition to considering the literature of model-based control in type 1 diabetes, another relevant topic is the types of insulin, with its characteristics like onset time, peak time, and action time, and other peculiarities of the drug's pharmacokinetics and pharmacodynamics. Besides drug descriptions published

by manufacturers, there have been numerous studies published that independently examine the characteristics of the drug, e.g. [55] by Gillies et al. for insulin glargine or [56] by Birkeland et al. investigating new ultralong-acting insulin degludec. There are also insightful studies comparing different insulins, e.g. [57] by Porcellati et al. comparing long-acting insulins glargine and detemir, or [58] by Heinemann et al. comparing long-acting insulin glargine to intermediate-acting insulin neutral protamine Hagedorrn (NPH). Finally, there are review papers, like [59] by Porcellati, Bolli, and Fanelli covering just basal insulins, or [60] by Hirsch covering all insulin analogues. Many such independent study results were used in this work when deriving models.

3.5 Literature Review Conclusion

This literature review shows that there is a gap in the research of control in type 1 diabetes. Namely, little has been done to consider a model-based advisory system (where the advice is supplied on-demand) as a substitute for a closed-loop fully-automated system. On the other hand, as we explained in the Introduction, advisory system may be the necessary ramp for the technology-based solutions that would lead to the acceptance of type 1 diabetes closed-loop controls – accepted by both regulators and patients. In addition, there is no formal framework proposed to facilitate the design of such systems.

Chapter 4

Semi-Autonomous Advisory System in Risk Space

For the reasons described in Chapter 1, it has been a struggle to find models for control that could completely trusted and thus we ask ourselves whether the models we *do* have can be used at all. While from the engineering point of view Artificial Pancreas systems might be attainable in the very near future, practically it might be a long time before they are widely available and accepted. Medical establishment, patients, and regulatory institutions are wary of fully automatic systems that inject potentially lethal drug and thus are reluctant to easily accept AP systems.

However, we believe that there is still a way to benefit from these models without engaging with a fully automatic AP, but instead building a system where control action would be initiated not at every step like in an MPC, but *on demand* – that is when the patients decides it is time to administer a bolus. This approach addresses the issues that any fully-automatic system has – that automatic control removes the intellect of the user, which can be an additional safeguard when the data and device function are subject to error.

We call this on-demand concept an advisory mode or advisory system – the system in which the correction insulin is not immediately injected upon the calculation, but instead presented to the user for their approval, cancellation, or modification – that is, advised. In other words, we do not make the patient fully give up control, but we do take the computational burden off the patient.

In this work, a two-module hierarchical system is considered; (i) there is a lower level automation of the basal rate modification that continuously provides minor changes that have little (in terms of BG change

and not in terms of clinical importance) influence on the system; (ii) there is another level of correction or meal bolus that provides a much bigger impact on the metabolical balance.

4.1 Methods

Our hypothesis is that it is possible to adapt model-predictive methods to create an advisory system that supplies the patient with numerically optimized value upon which the patient makes a decision. The resulting advisory system should perform better than conventional therapy.

In this chapter, we employ the logarithmic risk function developed by Kovatchev et al [57] to transform the metabolical model developed by Bergman et al [51]. This transformation allows us to: (i) adequately weigh hypo- and hyperglycemia risks in the objective function; and (ii) linearize [61] the metabolical model in log space.

We then discretize [62] the model, identify its parameters and convert it to state-space representation. Kalman Filter estimation is used to provide the best estimate of the current metabolic state. Using the model, a model-based prediction is built and an objective function about it is formulated. This results in a linear-quadratic optimization in which a closed-form solution can be derived.

We then conduct computer simulations using *in silico* population to validate the optimal controller that we designed. Various scenarios are constructed including conditions of erroneous therapy parameter values and misestimations by virtual patients. The results are evaluated using time in range, time under 70mg/dl, time over 180 mg/dl**,** risk parameters like Low Blood Glucose Index and High Blood Glucose Index [54], and variability parameter of Average Daily Risk Range [63].

4.2 Human-Automation Integration

As automation becomes more and more ubiquitous, the problems associated with human-machine interaction attract more attention from scholars. As far as back as in 2004, Lee and See highlighted that automation is often problematic because people fail to rely upon it appropriately [64]. In fact, this problem consists of two reciprocal issues:

- People trust automation when it's not appropriate – they over-rely on it.
- People are not always willing to put sufficient trust in automation – they under-rely on it.

Lee and See call these two ways of not appropriate use of automation *misuse* and *disuse*, respectively [64].

As any closed-loop system, AP closed-loop systems require relinquishing some or all control to an automated system, which takes patients time to adapt to [65]. The adaptation period can in fact be stressful and instead of taking the burden of managing the disease away, the system can create an additional mental burden of coping with it. There are anecdotal evidence that fully automated systems that take diabetes management out of the patient's hands can be anxiety-inducing for some patients [65]

Supporting such evidence is this comment from the recent ATTD 2015 conference by a patient: "Even if we can get to a fully automated system, it may not work for everyone. There should be different levels of automation. Perhaps these systems should be designed for specific age groups. What works for an adult may not work for a teenager… I would like to see the gradual introduction of these types of systems. If you gave me a fully self-driving car today, I wouldn't use it. It would take me many months before I could build the confidence. We can't just give patients the artificial pancreas and tell them to go out and start using it right away." [65]

In a 2012 study by Shepard and Gonder-Frederick, one of the notable findings was the difficulty the patients had with trusting the technology and relinquishing personal control of daily diabetes management to an automated system, [66]. Nearly all participants (n = 56), emphasized the importance of being able to

override the system's advice, if desired. This feedback from the patients strengthens our thesis of the necessity of the advisory mode in every closed-loop system and warrants the development of an advisory system as a precursor to full automation. In fact, a discussion we conducted in a limited focus group [67] showed that while patients would welcome a fully automatic system, they would still prefer to retain the chance to take over by disabling the automation, e.g. on the days when they feel particularly sensitive about their control.

Therefore, there is a very fine line between the patient's desire to get rid of the burden of constant dose contemplation and desire to fully relinquish control of the key everyday decisions that are critical for their health and life. Thus keeping the human in the loop to some degree is important not only in an objective way – because the final check by the user increases safety (and, in another context, lifts alleviates the responsibility of the designers to facilitate the regulatory approval) – but also subjectively, in the sense that it provides the comfort and sense of security experienced by the patient.

To avoid both misuse and disuse of automation, the user (the patient) should be allowed to choose whether to rely on it or not. In the very specific case of Artificial Pancreas systems, such freedom of choice lies in advisory systems like the one we propose.

4.3 Two –Module System

While, as explained above, the optimal advisory correction mode should be an optional feature of an AP system, preliminary simulations showed that to achieve optimal efficiency of the advisory mode, one part of the system should remain fully automatic.

Particularly, overly aggressive advice (stemming from high penalty on the deviation of blood glucose from the target) can lead to hypoglycemia incidents. However, reducing the advice's hyperglycemia mitigation capacity decreases the time in range and other control quality statistics and therefore makes the benefits of the system less pronounced.

A hybrid control is therefore designed: consisting of (i) open-loop decision support – the advisory part; and (ii) closed-loop monitoring – the safety part. Specifically, to alleviate the aggressiveness of the advice and at the same time keep the injection amounts within optimal values relative to hyperglycemia treatment, a safety system developed by Hughes et al. [52] was put in place.

Originally, this safety system employs two algorithms for attenuating insulin pump injections, which are referred to as Brakes and Power Brakes: the former is a pump attenuation function computed using CGM information only, and the latter is an attenuation function in which a metabolic state observer with insulin and meal inputs is used in addition to CGM information to inform the level of pump attenuation [36].

We use the latter one and this way the safety system compensates through basal attenuation the advices that otherwise would be overly aggressive. Simulations showed that the safety system's action is enough to eliminate all significant lows of this nature. Thus the advisory system consists of two main modules: the bolus advisor and meal-informed power brakes (Figure 2), both of which continuously process insulin history, CGM data, and meal information. The bolus advisor is invoked episodically by the patient and provides correction bolus advice using a model-predictive approach (using the risk space control model, described below). At the same time, meal-informed power brakes function by continuously constraining basal insulin delivery based on the predicted risk of hypoglycemia.

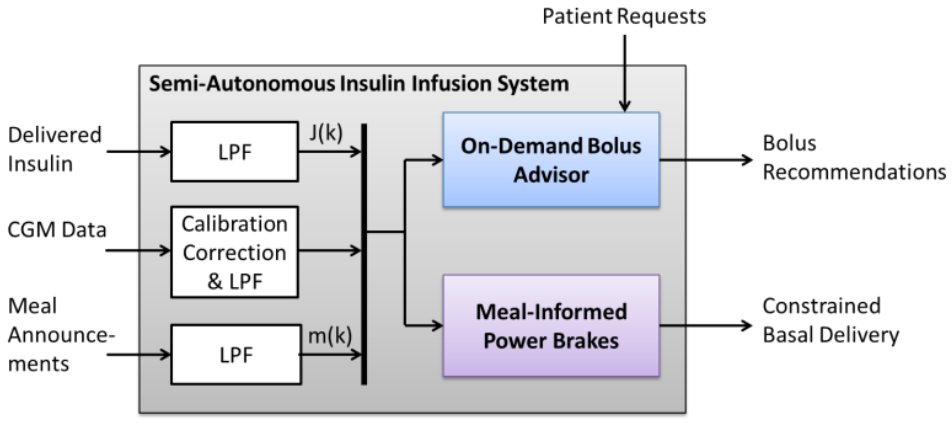

Figure 2. System algorithm schematic design.

4.4 Advantage of Risk Space and the Log Model

One of the challenges that are peculiar to designing control algorithms for blood glucose in Type 1 diabetics is the asymmetry of the risk associated with deviations from the euglycemia target or euglycemic target range. For instance, being 50 mg/dl above the target of 115 mg/dl (that is at 165 mg/dl) is not of concern for the most of type 1 patients and lies well within the range recommended by the American Diabetes Association [68]. On the other hand, being 50 mg/dl below that target – that is at 65 mg/dl – is hypoglycemic and constitutes significant health risk.

To correct for this discrepancy, various control methods have been proposed that reflected the asymmetrical nature of BG risk and acted accordingly ([69], [70], and [71]). However, these systems have the significant drawback of requiring on-line numerical solvers for computing insulin doses at each stage, even when the underlying model is linear, [53]. Kovatchev et al. in [54] designed a symmetrization function that reflects the asymmetry of risk by equating the risks of severe hypoglycemia (20 mg/dl) and severe hyperglycemia (600 mg/dl) and equating the risks associated with endpoints of the clinically recommended [70, 180] mg/dl target range. Efficiency measures from [72] reported later in this work (LBGI and HBGI – Low and High Blood Glucose Indices) are also based on this BG symmetrization function. However, the prospective use of the existing risk symmetrization function as a criterion for model-based control presents a challenge since online numerical methods are generally required to compute optimal actions, [30].

Here we use another "risk space" based approach that uses a model that describes the relationship between the logarithm of plasma glucose and the logarithm of remote compartment insulin. This representation of the model has two major benefits: it expresses the multiplicative dependence on remote-compartment insulin in glucose clearance in a linear fashion; and it enables a close approximation of the risk symmetrization as a quadratic function of the state vector in the new coordinate system (Figure 3).

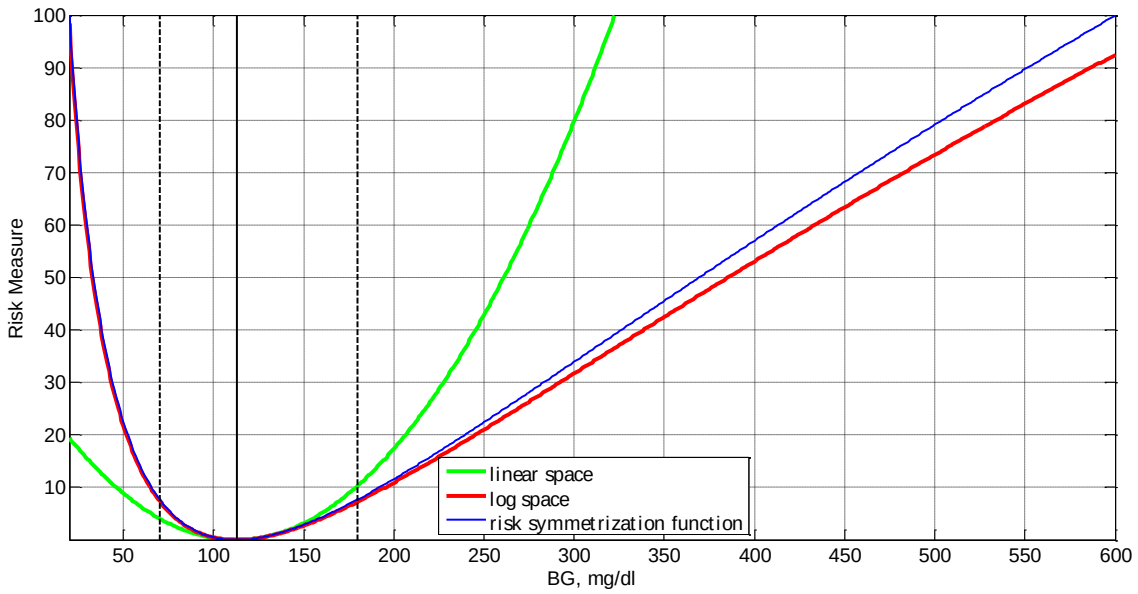

Figure 3. Comparison of Logarithmic "Risk Space" to Risk Symmetrization Function.

As a foundation, the meal model by Bergman et al [51] is used:

$$\dot{G(t)} = -\big(S_G + X(t)\big)G(t) + S_G G_b + \frac{Q_2(t)k_{abs}f}{V_G BW} \quad \textbf{(1)}$$

$$\dot{X(t)} = -p_2 X(t) + p_2 S_I \left(\frac{I_P(t)}{V_I BW} - I_b\right) \quad \textbf{(2)}$$

It is extended with a compartmental insulin transport model to account for insulin kinetics:

$$\dot{I}_{SC1}(t) = J(t) - k_d I_{SC1}(t) \quad \textbf{(3)}$$

$$\dot{I}_{SC2}(t) = k_d I_{SC1}(t) - k_d I_{SC2}(t) \quad \textbf{(4)}$$

$$\dot{I}_P(t) = k_d I_{SC2}(t) - k_{cl} I_P(t) \quad \textbf{(5)}$$

where $J(t)$ is the subcutaneous insulin injection actuated by the pump. The compartmental structure of the model is depicted in Figure 4.

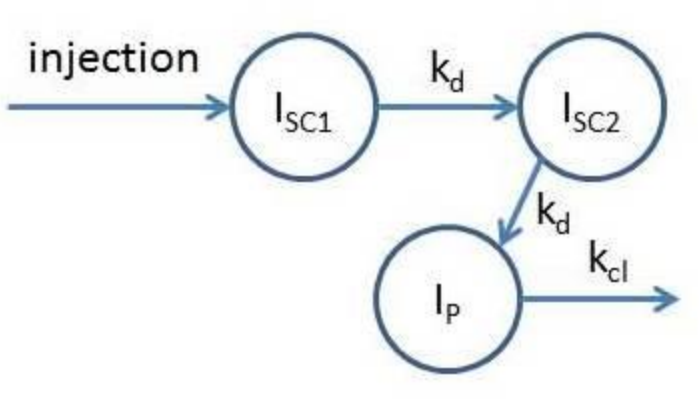

Figure 4. Insulin Transport Compartmental Model.

The model is further extended with a compartmental gut model:

$$\dot{Q}_1(t) = -(a_d + a_1)Q_1(t) + m(t) \quad \textbf{(6)}$$

$$\dot{Q}_2(t) = -a_2 Q_2(t) + a_d Q_1(t) \quad \textbf{(7)}$$

$$\dot{d}(t) = a_1 Q_1(t) + a_2 Q_2(t) \quad \textbf{(8)}$$

where $m(t)$ is ingested carbohydrates and $d(t)$ is the rate of appearance of glucose in blood. The compartmental structure of the model is depicted in Figure 5.

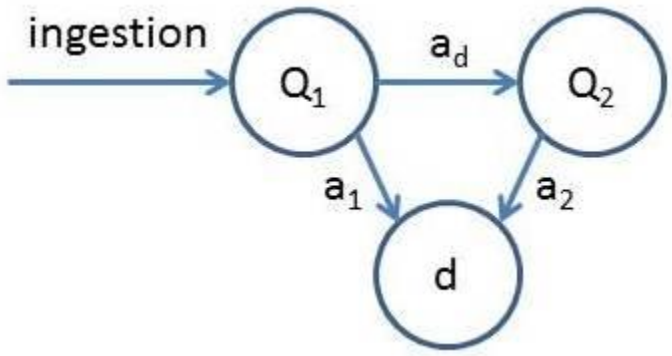

Figure 5. Carbohydrate Absorption Compartmental Model.

In logarithmic coordinates, we employ the model based on Eq. (1) - (2) and developed by Jiang et. al [73]:

$$\dot{ln}\left(\frac{G(t)}{G_b}\right) = -p_1 ln\left(\frac{G(t)}{G_b}\right) - p_2 ln\left(\frac{X(t)}{X_b}\right) + p_6 d(t) \quad \textbf{(9)}$$

$$\dot{ln}\left(\frac{X(t)}{X_b}\right) = -p_4 \ln\left(\frac{X(t)}{X_b}\right) + p_4\left(\frac{I_P(t)}{V_I BW} - I_b\right) \quad \textbf{(10)}$$

The parameters p_1, p_2, p_6, p_4, and BW (body weight), are patient-specific, have interpretations similar to those in the standard Bergman's minimal model of glucose kinetics [51]. The p parameters' values are obtained through a regression equation given available physiological information. The process is described in detail in [73]. The gut and insulin transport parameters V_I, k_d, k_{cl}, a_d, a_1, and a_2 are population average and are obtained as described in [52]. Basal glucose concentration G_b is set to 112.5 mg/dl as a fixed reference. I_b is calculated as equal to $\frac{I_P(t)}{V_I BW}$ at steady state. To calculate the value of the latter, $J(t)$ from (3) is fixed at the patient's average basal rate and then the equations (3) - (5) are used to obtain the value of $I_P(t)$. The value of X_b is never used on its own and only the value of $\ln\left(\frac{X(t)}{X_b}\right)$ is ever used, so X_b is not estimated.

State-space form of equations (3) - (5) can be written as

$$\begin{bmatrix} \dot{I}_{SC1}(t) \\ \dot{I}_{SC2}(t) \\ \dot{I}_P(t) \end{bmatrix} = \begin{bmatrix} -\kappa_d & 0 & 0 \\ \kappa_d & -\kappa_d & 0 \\ 0 & \kappa_d & -\kappa_{cl} \end{bmatrix} \begin{bmatrix} I_{SC1}(t) \\ I_{SC2}(t) \\ I_P(t) \end{bmatrix} + \begin{bmatrix} 1 \\ 0 \\ 0 \end{bmatrix} J(k) \quad \textbf{(11)}$$

State-space form of equations (6) - (7) can be written as

$$\begin{bmatrix} \dot{Q}_1(t) \\ \dot{Q}_2(t) \end{bmatrix} = \begin{bmatrix} -(a_d + a_1) & 0 \\ a_d & -a_2 \end{bmatrix} \begin{bmatrix} Q_1(t) \\ Q_2(t) \end{bmatrix} + \begin{bmatrix} 1 \\ 0 \end{bmatrix} m(t) \quad \textbf{(12)}$$

Finally, state-space form of equations (9) - (10) can be written as

$$\begin{bmatrix} \dot{ln}\left(\frac{G(t)}{G_b}\right) \\ \dot{ln}\left(\frac{X(t)}{X_b}\right) \\ \dot{\Delta}(t) \end{bmatrix} = \begin{bmatrix} -p_1 & -p_2 & 0 \\ 0 & -p_4 & 0 \\ 0 & 0 & -\frac{1}{720} \end{bmatrix} \begin{bmatrix} ln\left(\frac{G(t)}{G_b}\right) \\ ln\left(\frac{X(t)}{X_b}\right) \\ \Delta(t) \end{bmatrix} + \begin{bmatrix} p_6 \\ 0 \\ 0 \end{bmatrix} d(t) + \begin{bmatrix} 0 \\ \frac{p_4}{V_I BW} \\ 0 \end{bmatrix} I_P(t) + \begin{bmatrix} 0 \\ -p_4 I_b \\ 0 \end{bmatrix} \quad \textbf{(13)}$$

The new Δ term included in the state vector is introduced to account for model discrepancy and is calculated as

$$\Delta(\mathrm{t}) = \widehat{ln}\left(\frac{X(t)}{X_b}\right) - ln\left(\frac{X(t)}{X_b}\right) \tag{14}$$

More details about the Δ term can be found in [73].

It will be helpful later to be able to feed the whole insulin state $[I_{SC1}(t),\ \ I_{SC2}(t),\ \ I_P(t)]$ into the equation (13) and not just $I_P(t)$. For that purpose, the equation (13) can be rewritten as

$$\begin{bmatrix} \dot{ln}\left(\frac{G(t)}{G_b}\right) \\ \dot{ln}\left(\frac{X(t)}{X_b}\right) \\ \dot{\Delta}(t) \end{bmatrix} = \begin{bmatrix} -p_1 & -p_2 & 0 \\ 0 & -p_4 & 0 \\ 0 & 0 & -\frac{1}{720} \end{bmatrix} \begin{bmatrix} ln\left(\frac{G(t)}{G_b}\right) \\ ln\left(\frac{X(t)}{X_b}\right) \\ \Delta(\mathrm{t}) \end{bmatrix} + \begin{bmatrix} p_6 \\ 0 \\ 0 \end{bmatrix} d(t) + \begin{bmatrix} 0 & 0 & 0 \\ 0 & 0 & \frac{p_4}{V_I BW} \\ 0 & 0 & 0 \end{bmatrix} \begin{bmatrix} I_{SC1}(t) \\ I_{SC2}(t) \\ I_P(t) \end{bmatrix} + \begin{bmatrix} 0 \\ -p_4 I_b \\ 0 \end{bmatrix} \tag{15}$$

(11), (12), and (14) and then discretized to the following (details in Appendix A):

$$i(k+1) = A_I i(k) + B_I J_{basal}(k) + B_I u_{bolus} \tag{16}$$

$$q(k+1) = A_Q i(k) + B_Q m(k) \tag{17}$$

$$x(k+1) = A_C x(k) + B_C d(k) + B_{CI1} i(k) + B_{CI2} \tag{18}$$

where $J_{basal}(k)$, u_{bolus}, $m(k)$, and $d(k)$ are scalars.

Notice that in (16), the input $J(t)$ from (3) is broken down into its basal and bolus components - $J_{basal}(k)$ and u_{bolus} respectively. The reason that the latter does not have a step index, is that we assume the advised bolus is the only bolus within the considered time horizon and happens at step (k), while the basal is constant and administered at every step throughout whole time horizon.

4.5 State Estimation

State estimation within the adviser is accomplished through a combination of feedforward estimation and Kalman filtering (Figure 6). Another example of this technique can be found in [74].

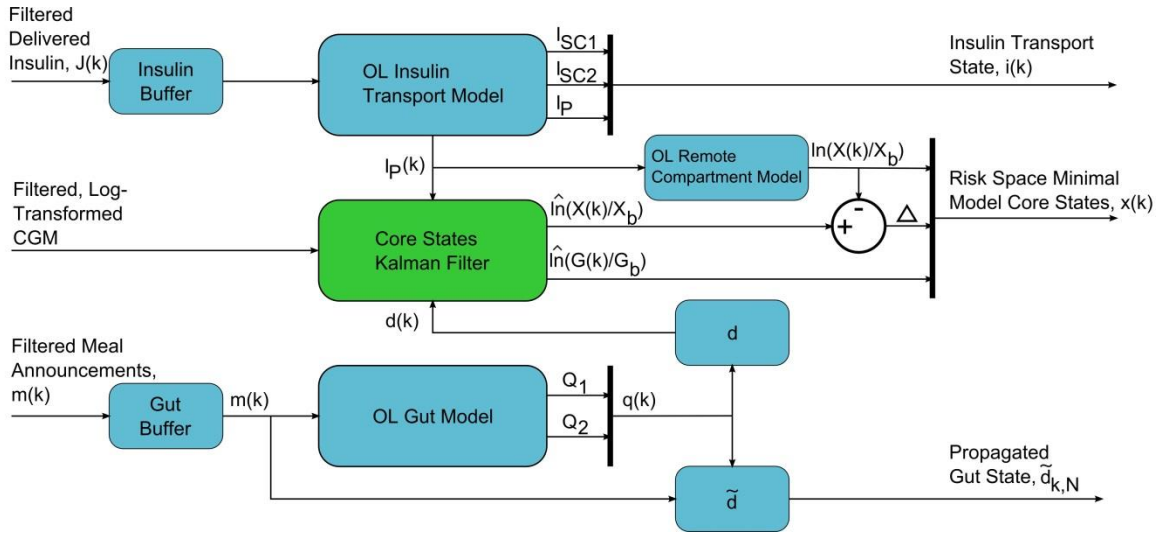

Figure 6. State Estimation and Feed-Forward Models.

In Figure 6, the module 'OL Insulin Transport Model' uses equation (16) to "estimate" (in an open loop fashion) insulin transport states, and the module 'OL Gut Model' uses equation (17) to "estimate" gastrointestinal transport states. The results are then fed into the Kalman filter, which uses CGM data to estimate the "core" states of the risk space control model, expressed by equation (18).

The buffer modules in Figure 6 "protect" the state estimation from taking into account the meal and insulin that is taken at the advice calculation step. Insulin buffer also serves the purpose of delay the insulin absorption. More about these two modules can be learned in [73].

The module 'OL Remote Compartment Model' uses the discretized version of equation (2) to "estimate" the insulin action core state which is then used for Δ calculation. The module d calculates the rate of appearance of glucose. Finally, the module $\tilde{d}$ propagates the state of the rate of appearance through the whole time horizon according to the equation presented later in the chapter.

4.6 Optimization Model

Matrix composition and manipulation can be found in Appendix B.

The evolution equation of the insulin transport state all the way to the end of the horizon can be written as:

$$\tilde{\imath}_{k,N} = \mathcal{A}_I i(k) + \Gamma_{I1}\mathcal{B}_I J_{basal} + \Gamma_{I1} u_{bolus}(k) \quad \textbf{(19)}$$

Thus equation (19) provides the evolution of the insulin transport system from the start of the horizon k to its end at $k + N - 1$ given only insulin state at step k, bolus amount at step k, and the basal value that is constant for all steps.

The same can be done with the evolution equation of the carbohydrate transport as was done with the insulin transport equation – the state evolution all the way to the end of the horizon can be written out as:

$$\tilde{d}_{k,N} = \mathcal{C}_Q\big(\mathcal{A}_Q q(k) + \mathcal{B}_Q m(k)\big) \quad \textbf{(20)}$$

Thus equation (20) provides the evolution of the gut transport system from the start of the horizon k to its end at $k + N - 1$ given only gut state at step k and meal input at step k.

Finally, the same can be done for the core model – the state evolution all the way to the end of the horizon can be written out as:

$$\tilde{x}_{k,N} = \mathcal{A}_C x(k) + \Gamma_{C1}\tilde{d}_{k,N} + \Gamma_{C2}\mathcal{A}_I i(k) + \Gamma_{C2}\Gamma_{I1}\mathcal{B}_I J_{basal} + \Gamma_{C2}\Gamma_{I2} u_{bolus}(k) + \Gamma_{C3}\mathcal{B}_{CI2} \quad \textbf{(21)}$$

The matrices $\mathcal{A}_I$, Γ_{I1}, $\mathcal{B}_I$, $\mathcal{A}_Q$, $\mathcal{B}_Q$, $\mathcal{C}_Q$, $\mathcal{A}_C$, Γ_{C1}, Γ_{C2}, Γ_{I2}, Γ_{C3}, and $\mathcal{B}_{CI2}$ are defined in Appendix B.

Since the core states are logarithms of fractions that at perfect control should be equal to 1 – in particular, $G(k)$ should be equal G_b and $X(k)$ should be equal X_b at every step k (and Δ should be equal zero) – a cost function can readily use $x(k)$ value for calculating the penalty for deviation.

$$F(u) = \sum_{i=k+1}^{k+N} x(i)' q(i) x(i) \quad \textbf{(22)}$$

where *N* is a planning time horizon, and *q(i)* is a penalty coefficient.

Using the matrix manipulation work done above, equation (22) can be written in a form that does not use the summation:

$$F(u) = \tilde{x}_{k,N}{}' \mathcal{Q} \tilde{x}_{k,N} \tag{23}$$

where $\mathcal{Q}$ is a 3Nx3N matrix with 3x3 $q(i)$ matrices on its diagonal. In other words, the following minimization problem must be solved by choosing the right bolus value at time step k:

$$\min_{u_{bolus}} \tilde{x}_{k,N}{}' \mathcal{Q} \tilde{x}_{k,N} \tag{24}$$

To put this in perspective, equation (24) is "located" inside the orange 'Minimization Problem Solution' module in Figure 7.

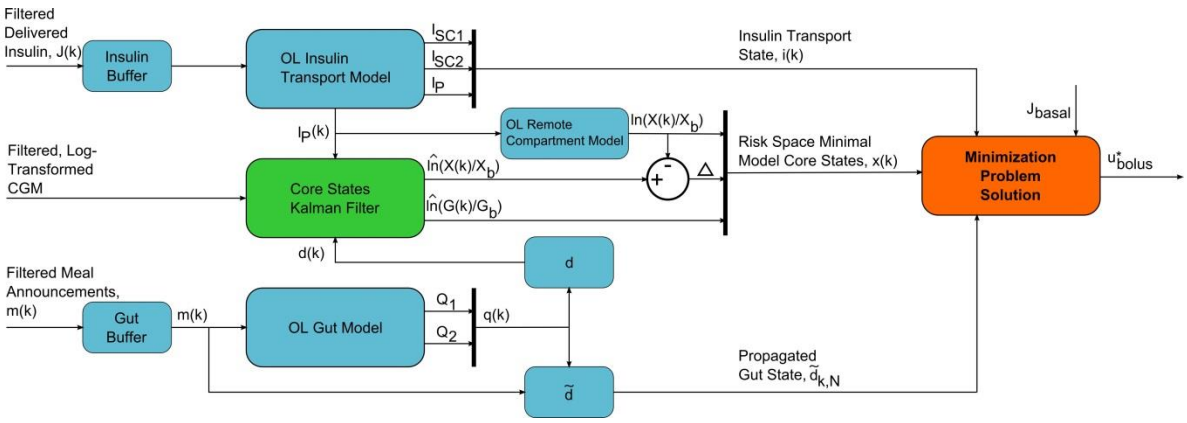

Figure 7. Optimization Step In the System's Context.

This optimization problem is to be solved every time the patient requests an advice – between the meals – and also at meal time when the algorithm is run automatically. A possible scenario for one day is presented in Figure 8.

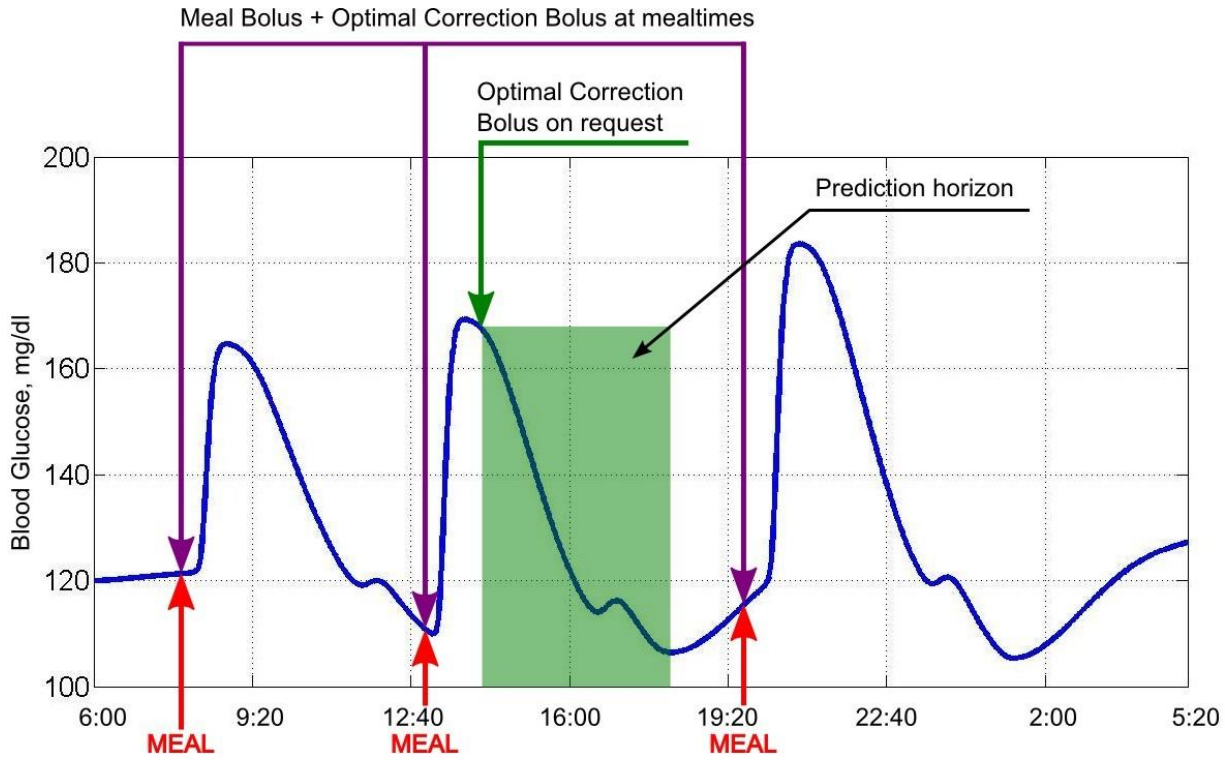

Figure 8. A One-Day Scenario.

The Q penalty matrix from (23) and (24) is constructed in such a way that only the glucose state, $ln\left(\frac{G(k)}{G_b}\right)$, deviation is penalized. Particularly, going along the main diagonal of Q, every second and third element is equal to zero in order not to penalize the two other states in the core triple.

In addition, the main diagonal elements that penalize the glucose state take values from 0 to 1 in proportion to how much time elapsed since the last meal (taken at time step k). The implementation is such because the glucose data should be "trusted" less in post-prandial proximity as the model might struggle with producing an accurate prediction at that time, while far in the future after the meal the model performs better.

The details of the penalty matrix construction are presented in Appendix C.

The value of the optimal bolus to administer at time step k is obtained by equating the derivative of (23) to zero and solving for u_{bolus}.

$$u^*_{bolus} = -\Phi^{-1}\left(\Theta^1\hat{x}(k) + \Theta^2\tilde{d}(\kappa) + \Theta^3 i(k) + \Theta^4 J_{basal} + \Theta^5\right) \quad \textbf{(25)}$$

where

$$\Phi = \Gamma_{I2}{}'\Gamma_{C2}{}'\mathcal{Q}\Gamma_{C2}\Gamma_{I2} \quad \textbf{(26)}$$

$$\Theta^1 = \Gamma_{I2}{}'\Gamma_{C2}{}'\mathcal{Q}\mathcal{A}_C \quad \textbf{(27)}$$

$$\Theta^1 = \Gamma_{I2}{}'\Gamma_{C2}{}'\mathcal{Q}\Gamma_{C1} \quad \textbf{(28)}$$

$$\Theta^1 = \Gamma_{I2}{}'\Gamma_{C2}{}'\mathcal{Q}\Gamma_{C2}\mathcal{A}_I \quad \textbf{(29)}$$

$$\Theta^1 = \Gamma_{I2}{}'\Gamma_{C2}{}'\mathcal{Q}\Gamma_{C2}\Gamma_{I1}\mathcal{B}_I \quad \textbf{(30)}$$

$$\Theta^1 = \Gamma_{I2}^{\prime\Gamma_{C2}\prime}\mathcal{Q}\Gamma_{C3}\mathcal{B}_{CI2} \quad \textbf{(31)}$$

where all the matrices are defined earlier and the values for $\mathcal{Q}$ are determined as described above.

4.7 Pre-Clinical *In Silico* Validation

The results of pre-clinical *In Silico* validation can be found in [53]. To evaluate the developed semi-automated insulin advisor relative to conventional CSII therapy, (mealtime boluses only without low-glucose insulin attenuation), *In Silico* pre-clinical trials were conducted using the 100 adult subjects that accompany the U.Va./ U. Padova FDA-accepted type 1 Simulator. For each experimental setting, results are presented in terms of (i) percentage time in the range of [70 mg/dl 180 mg/dl], and (ii) percentage time under 70 mg/dl (hypoglycemia).

In the first experiment, the case where the patient's simulated carbohydrate ratio is miscalibrated (within a range of values) was studied. In this scenario, the meal is underinsulinized to varying degrees, and the bolus advisor is triggered one hour after the meal to compensate for the inadequate bolus. Each of the *in silico* subjects is challenged with three meals in a 24 hour period, with a breakfast of 0.7 g/kg at 08:00, lunch of 1 g/kg at 13:00, and a dinner of 1 g/kg at 20:00. Mealtime corrections are also computed by the bolus advisor, but this is done without knowledge of the meal amount. The meal-informed power brakes are enabled for the duration of the experiment. As can be seen in Figure 9, the risk-space correction advice serves to reduce the time in the hyperglycemia, especially in the case of heavily underinsulinized

meals. The incidence of hypoglycemia in either case is negligible: 0.01 percent time on average below 70 for the entire *in silico* population, with and without the optimal correction.

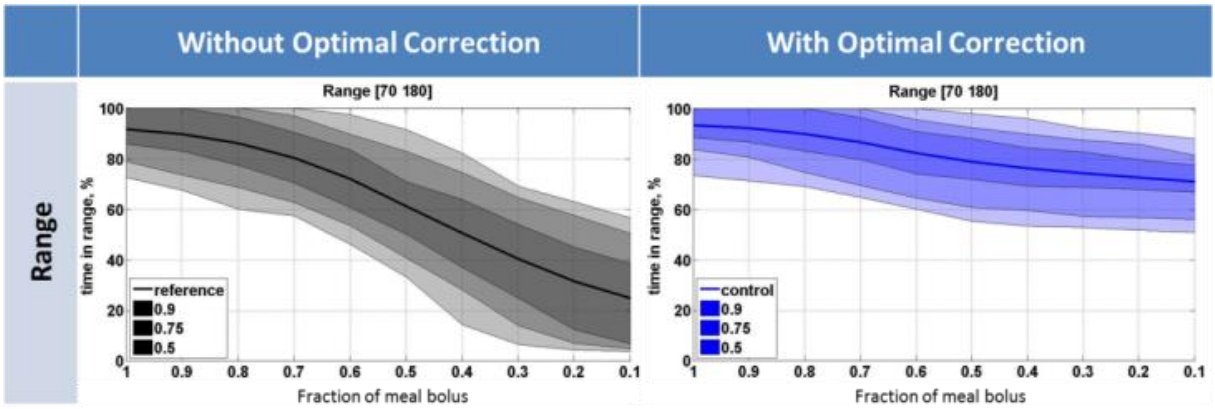

Figure 9. CR miscalibration. Average percentage time in range is shown with thick solid lines, accompanied by 50, 75, and 90% envelopes.

In the second experiment, a more challenging scenario was studied – the actual carbohydrate content of a meal ranged from -50% to +50% of the true value. (With the incorrect estimate of the size of the meal, the estimate of the patient's state will be thrown off for the timeframe after the meal.) Each *in silico* subject experienced a 0.8 g/kg meal, and the meal-related insulin dose was computed using the patient's carbohydrate ratio. The adviser is called one hour after each meal. Mealtime corrections are also computed by the bolus advisor, but this is done without knowledge of the meal amount. The meal-informed power brakes are enabled for the duration of the experiment. As can be seen in Figure 10, the bolus advisor manages to improve upon conventional therapy with up to 50% under- and over-estimation of carbohydrates in meals. It is worth noting that the improvement in the case of 50% underestimation is relatively small, due probably to the fact that the Kalman Filter has to "catch up" to the truth that a large meal was taken. The improvement in the case of overestimation is due mostly to hypo-mitigating effect of the meal-informed power brakes, which indeed manage to prevent hypoglycemia.

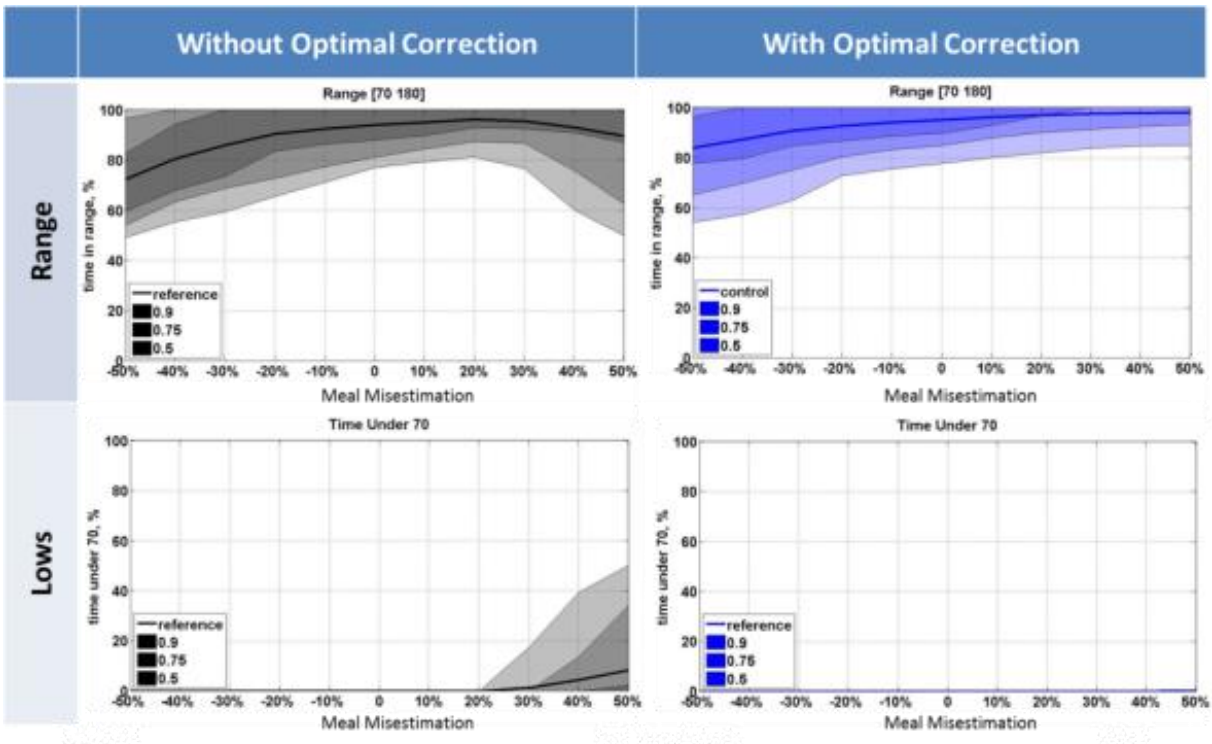

Figure 10. Carb content is misestimated from -50% to +50%.

In the third experiment, the ability of the system to provide correction bolus advice at different times after meals was explored. Returning to a 24-hour simulation scenario, each subject experiences three meals: breakfast of 0.7 g/kg at 8:00, lunch of 1 g/kg at 13:00, and dinner of 1 g/kg at 20:00. In each case the patient receives 50% of his/her meal bolus due to miscalibrated carbohydrate ratio. In separate runs we provide advice at different times after the underbolused meal, ranging from 15 to 240 minutes. Again, the advisor is also invoked at meal times, and the meal-informed power brakes are continuously enabled. From Figure 11 it can be seen that the advisory system manages to represent an improvement over the no-advice condition, even when the advisor is invoked 15 minutes after the underbolused meal. Again, the incidence of hypoglycemia in either case is negligible: 0.04 percent time on average below 70 for the entire *In Silico* population, with and without the optimal correction.

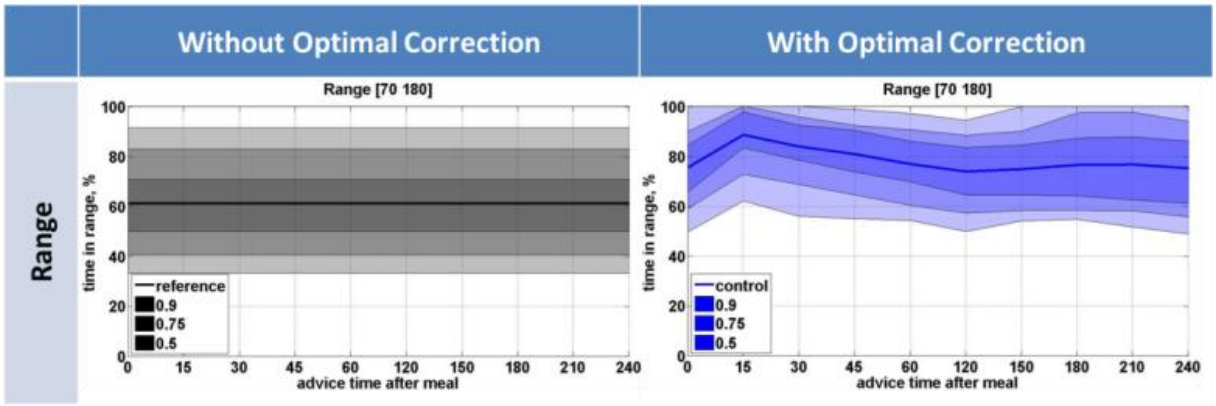

Figure 11. Advice request at different times relative to the meal.

4.8 Clinical Experience

In-silico performance reported in 4.7 *Pre-Clinical In* Silico Validation suggested testing the systems in a human clinical trial. "Early feasibility study of adaptive advisory/automated (AAA) control of type 1 diabetes" was conducted at the Center for Diabetes outpatient guesthouse as part of the University of Virginia Health System.

In experimental session (Figure 12), subjects were admitted to guesthouse at 18:00 (6:00pm) and were discharged 40 hours later at 09:00 (09:00am) on day 3 of the admission. Breakfast, lunch and dinner were served around 07:00, 12:00 and 19:00 respectively. A 45-min physical exercise session was conducted starting at 14:00. After the initialization of AAA control, Safety Supervision Module (SSM) and Basal Rate Modifier (BRM) [75] were active throughout the whole admission period while Advisory Module was only active during day time (07:00 – 23:00). Blood glucose readings, CGM data (DexCom® Gen4), carbohydrate amount of meals served, and insulin administration data were collected during the study.

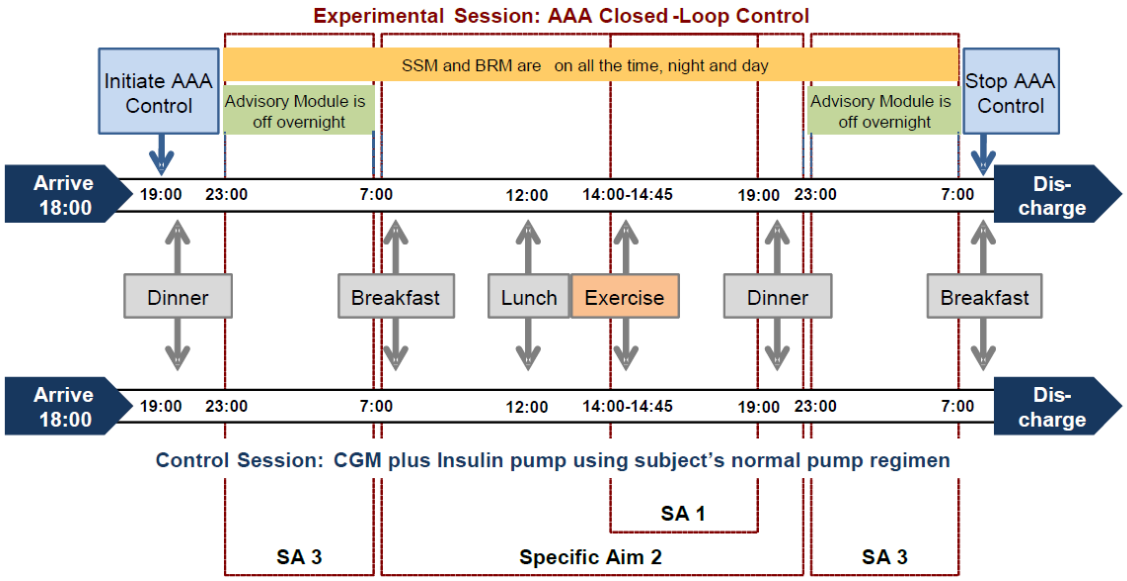

Figure 12. Study Design.

For the pilot experimental session, two subjects were recruited. Correction bolus were advised to the subjects as part of the meal time boluses and as standalone correction boluses. At some times the advice would be accepted; at other times the advice would be modified (in effect, not accepted).

When in clinical trial setting, the performance of the system did not match that of *in silico* validation. Due to inadequate amounts of insulin advice in some cases, the advisory module had to be suspended after the pilot and was not used in the study. However, even though the advisory system was not used with the subject following the experimental session, the advice was still calculated at each meal and correction bolus administration. This enables the analysis of the data from the third subject in the context of the advisory system as well

When in the trial, before the system can be engaged, CGMS must be "warmed up" for two hours. Because of that, and as the trial started right before at dinner time, the time values in the following plots and table (where in minutes) start shortly after 120 minutes – the two hours that the CGMS was working before the system was engaged.

4.8.1 Subject 1

Table 2 presents the sizes of the meals that the subject consumed as estimated by the subject along with the true amount. The true amount comes from the dietary data on the food packaging. The estimated amount is chosen from 3 present values corresponding to a small, medium, or large meal as perceived by the subject.

Table 2. Subject 1 Meals Parameters.

Meal	Carbs amount as estimated by the subject	Actual Carbs Amount
Dinner	55	40
Breakfast	30	90
Lunch	30	62
Snack	30	Unknown

As can be seen in the Table 2, subject 1 often heavily underestimated the amount of food eaten – sometimes acknowledging only a third of the meal. The snack was of such kind that the actual carbs amount for it could not be known.

Note that we use the terms ‘estimation’ or ‘misestimation’ in this context as if the patient always applies a conscious process trying to determine the carbohydrate content of meals to calculate the meal bolus based on their Carbohydrate Ratio. There are few comments to be made about this:

1. Small degree of misestimation is inevitably universal in meal bolus calculations. Also. often the meal amount is actually grossly misestimated (see again Table 2). Therefore, in systems context, it might be more appropriate to treat this input as a stochastic process in the first place.
2. Many patients (especially type 2 patients) never actually estimate the size of the meal that way and are not aware of their Carbohydrate Ratio. Instead, they just guess the amount of insulin for the meal based on their subjective perception of how much insulin this kind of meal would require.

3. Other patients (also particularly type 2 patients) actually engage in a therapy of fixed dose meal bolus when, for example, lunch bolus is the same across all days, and the patient tries to consume the type of meal that would be appropriate for this amount of insulin. In other words, the meal is adjusted to insulin, not the other way round.

In Table 3, the most relevant data for subject 1 is presented:

- Date and time correspond to the moment when the insulin was recorded by the advisory system. This times differs only slightly from the time when the insulin was actually delivered or from the time when the meal was acknowledged by the subject, but it is the most relevant as it identifies the time when the advice was calculated.
- Meal Insulin was calculated based on the subjects carbohydrate ratio, which was
    - 8 g/U from midnight to 8:00am
    - 7 g/U from 8:00 am to noon
    - 8 g/U from noon to midnight
- Advised Correction is the system's advice that could be negative and then is subtracted from meal insulin.
- Taken Correction is the insulin that was actually injected as the correction part of the bolus (whether the advised value or the advised value modified).
- Injected Insulin is the sum of the Meal Insulin and Taken Correction.
- Blood glucose was measure only at meal times (and was recorded as '-1' by the system at times of standalone correction bolus).

Table 3. Subject 1 Trial Data.

Ins Del Date	Ins Del Time	Meal, g	Meal Insulin, U	Advised Corr, U	Taken Corr, U	Injected Insulin, U	SMBG, mg/dl
12-Dec	7:19:50 PM	55	6.875	-1.516501502	-1.516501502	5.4	79
12-Dec	10:51:34 PM	0	0	0.652767971	0.652767971	0.7	-1
13-Dec	7:43:57 AM	30	3.75	0.206295608	0.206295608	4	89
13-Dec	10:07:12 AM	0	0	-0.397666921	3	3	-1
13-Dec	12:06:58 PM	30	3.75	-2.825166911	-2.825166911	0.9	142
13-Dec	2:05:29 PM	0	0	0.202807103	0.202807103	0.2	-1
13-Dec	3:09:06 PM	30	0	0		0	110
13-Dec	4:02:05 PM	0	0	0		0.5	-1

Blue entries in Table 3 identify the case when the subject did not follow the advice and manually adjusted the final value. Red entries in Table 3 identify a snack that was not recorded through the meal screen and was not bolused for. The last row identifies a manual bolus overriding the system that was later administered by the subject when BG went high due to the snack taken an hour earlier.

The two plots in Figure 13 shows CGM traces along with other information, notably the tags for insulin administered. Note that the times in the x axis are 1 hour ahead of real time due to a bug in the online monitoring system.

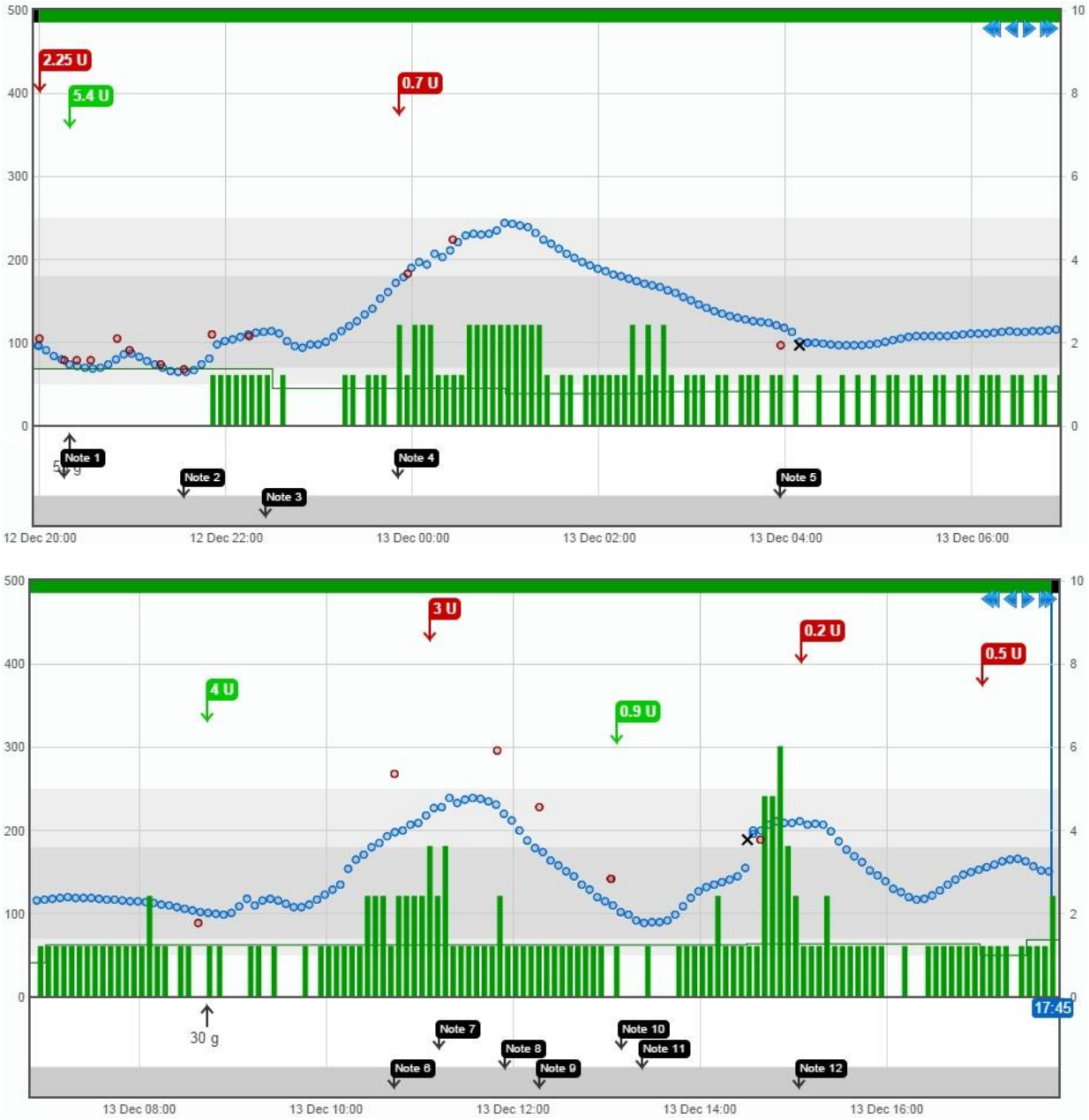

Figure 13. Record of Remote Monitoring for Subject 1.

Green insulin tags correspond to meal total boluses, red tags correspond to standalone corrections. The first red tag of 2.25 U corresponds to the insulin injected within 4 hours before the trial and acknowledged as IOB at the start of the trial. The snack is missing completely from the second plot between the two last

red tags as it was not acknowledged. Notice also, that while the lunch insulin tag is present (0.9 U shortly after 13:00), there is no gram amount indicated under the trace as in previous meals. This was another glitch in the remote monitoring system that did not affect the operation of the advisory system in any way.

4.8.2 Subject 2

Table 4 presents the sizes of the meals that the subject consumed as estimated by the subject along with the true amount. The true amount comes from the dietary data on the food packaging.

Table 4. Subject 2 Meals Parameters.

Meal	Carbs amount as estimated by the subject	Actual Carbs Amount
Dinner	69	86 (out of 130)
Breakfast	44	47
Lunch	44	35
Snack	20	Unknown

The snack was of such kind that the actual carbs amount for it could not be known.

In Table 5, the most relevant data for subject 2 is presented.

Table 5. Subject 2 Trial Data.

Ins Del Date	Ins Del Time	Meal, g	Meal Insulin, U	Advised Corr, U	Taken Corr, U	Injected Insulin, U	SMBG, mg/dl
12-Dec	7:45:53 PM	69	4.6	-1.523850433	-1.523850433	3.1	76
12-Dec	9:28:19 PM	0	0	0	1.8	1.8	-1
13-Dec	7:51:08 AM	44	2.933333	0.786566958	0.9	3.8	143
13-Dec	10:13:39 AM	0	0	1.897781336	1.897781336	1.9	-1
13-Dec	12:08:27 PM	44	2.933333	-3.580077935	-3.580077935	0	121
13-Dec	3:54:15 PM	20	1.333333	-0.094281241	-0.094281241	1.2	178

As in Table 3, in Table 5, blue entries identify the cases when the subject did not follow the advice and manually adjusted the final value. However, this subject adjusted the values only marginally, within 15% change.

The two plots in Figure 14 shows CGM traces along with other information, notably the tags for insulin administered.

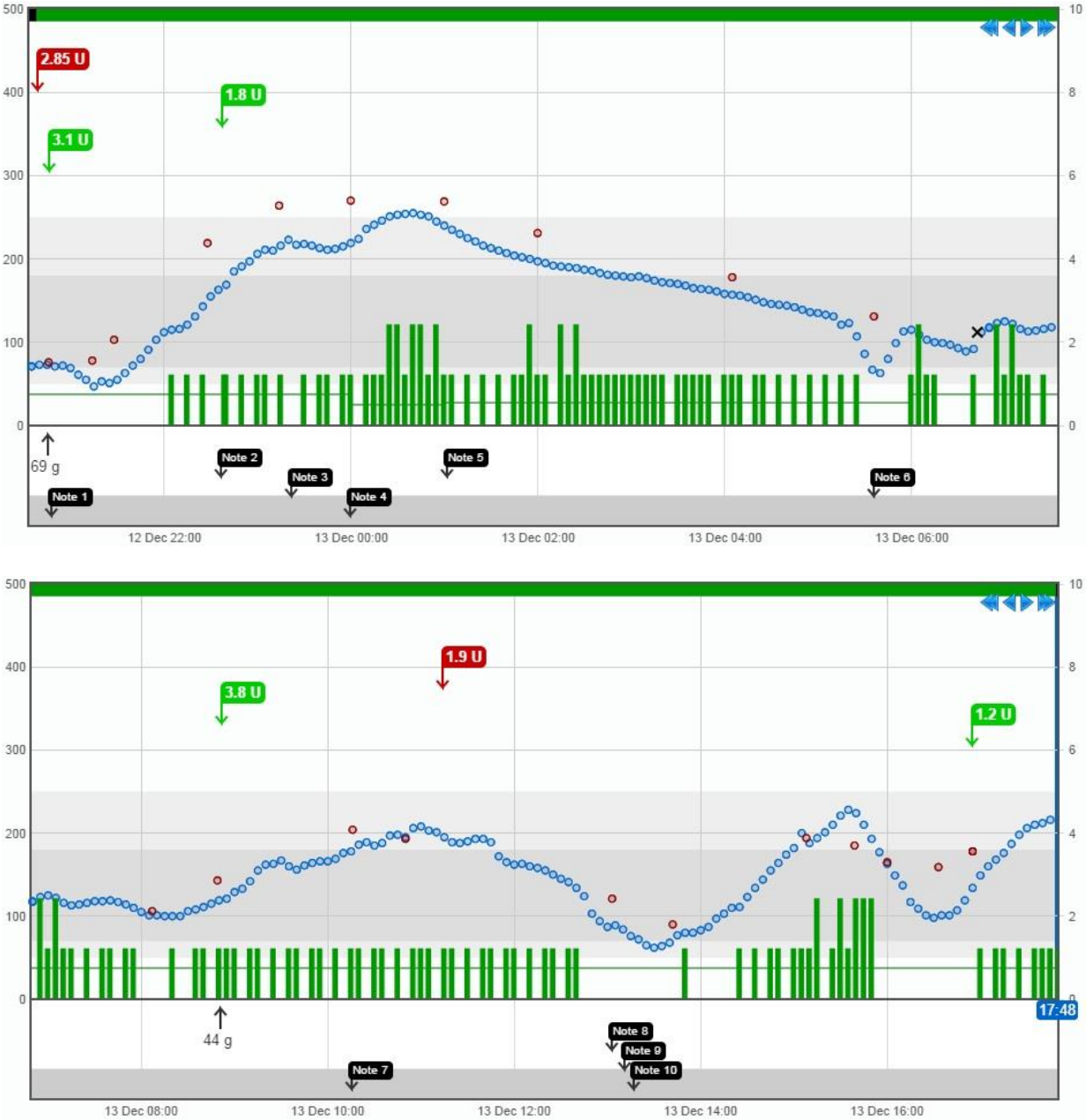

Figure 14. Record of Remote Monitoring for Subject 2.

Note that 1.8U tag in the beginning of the trial is green-coded while it was not a meal. This is just another glitch of the remote monitoring system. Also, the lunch at 12:05pm is missing from the visualization due to another glitch.

4.8.3 Subject 3

As was explained before, while subject 3 did not use the advisory system functionality, the system still produced and saved advice values based on system inputs and thus enables some analysis of the algorithm performance.

Table 6 presents the sizes of the meals that the subject consumed as estimated by the subject along with the true amount. The true amount comes from the dietary data on the food packaging. As this was not the pilot part anymore, but the actual study, the timeline was a little longer and more meals were consumed.

Table 6. Subject 3 Meals Parameters.

Meal	Carbs amount as estimated by the subject	Actual Carbs Amount
Dinner	39	41
Snack	19	Unknown
Breakfast	59	69
Lunch	59	44
Snack	19	Unknown
Dinner	39	37

The snacks were of such kind that the actual carbs amount for it could not be known.

In Table 7, the most relevant data for subject 2 is presented.

Table 7. Subject 3 Trial Data.

Ins Del Date	Ins Del Time	Meal, g	Meal Insulin, U	Advised Corr, U	Taken Corr, U	Injected Insulin, U	SMBG, mg/dl
6-Jan	7:43:56 PM	39	3	0.66450351	0	3	171
6-Jan	10:01:48 PM	19	1.5	0.352606671	0	1.5	164
7-Jan	7:52:20 AM	59	2.4	-0.552580421	0	2.4	88
7-Jan	10:48:41 AM	0	0	2.042974697	1.4	1.4	-1
7-Jan	11:32:42 AM	0	0	0	0.5	0.5	-1
7-Jan	1:01:01 PM	59	2.5	-1.03387802	0	2.5	148
7-Jan	6:48:12 PM	0	0	0	1.5	1.5	-1
7-Jan	8:17:05 PM	39	2.1	-1.561021423	0	2.1	158
7-Jan	10:24:10 PM	0	0	1.991751405	0.8	0.8	-1

Since no advice was followed by design, nothing is highlighted blue in Table 7. Also, for some correction boluses, particularly at 11:30am and 6:48pm, the adviser did not produce any internal advice as the bolus was implemented manually through the insulin pump leaving the advisor unaware.

Three plots in Figure 15 shows CGM traces along with other information, notably the tags for insulin administered. Again, due to a remote monitoring system software bug, all the times in the plots are 1 hour ahead: for example, the 1.5U snack at first night that appears to be at 11:00pm, actually occurred at 10:00pm.

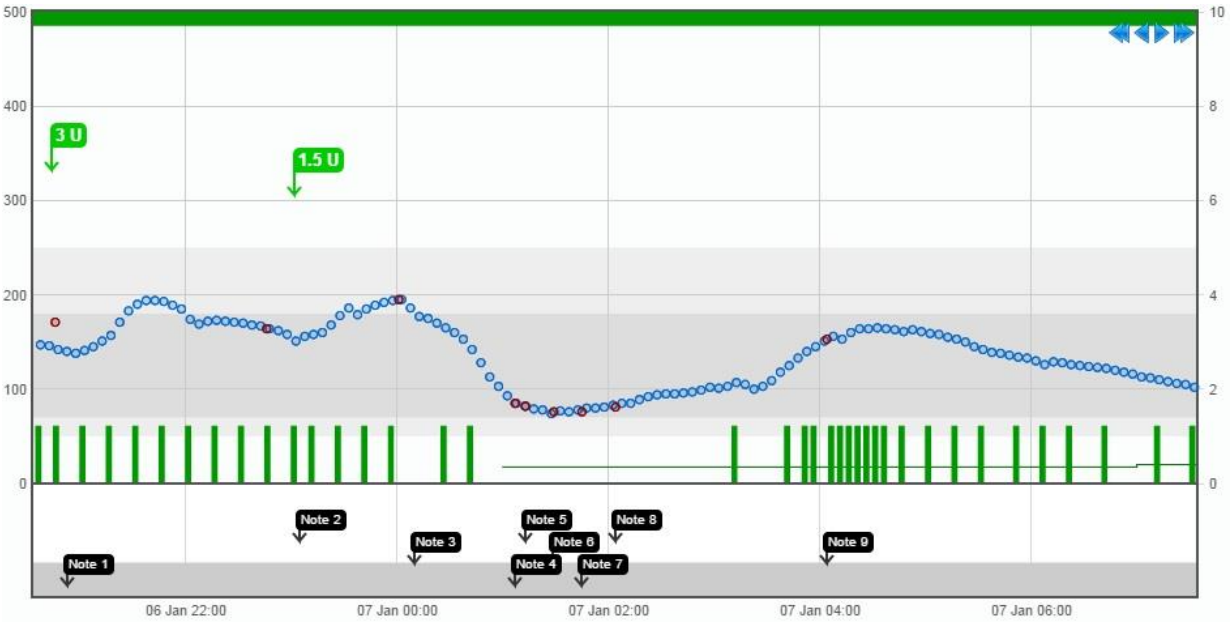
500
400
300
200
100
0
10
8
6
4
2
0
3 U
1.5 U
Note 1
Note 2
Note 3
Note 4
Note 5
Note 6
Note 7
Note 8
Note 9
06 Jan 22:00
07 Jan 00:00
07 Jan 02:00
07 Jan 04:00
07 Jan 06:00

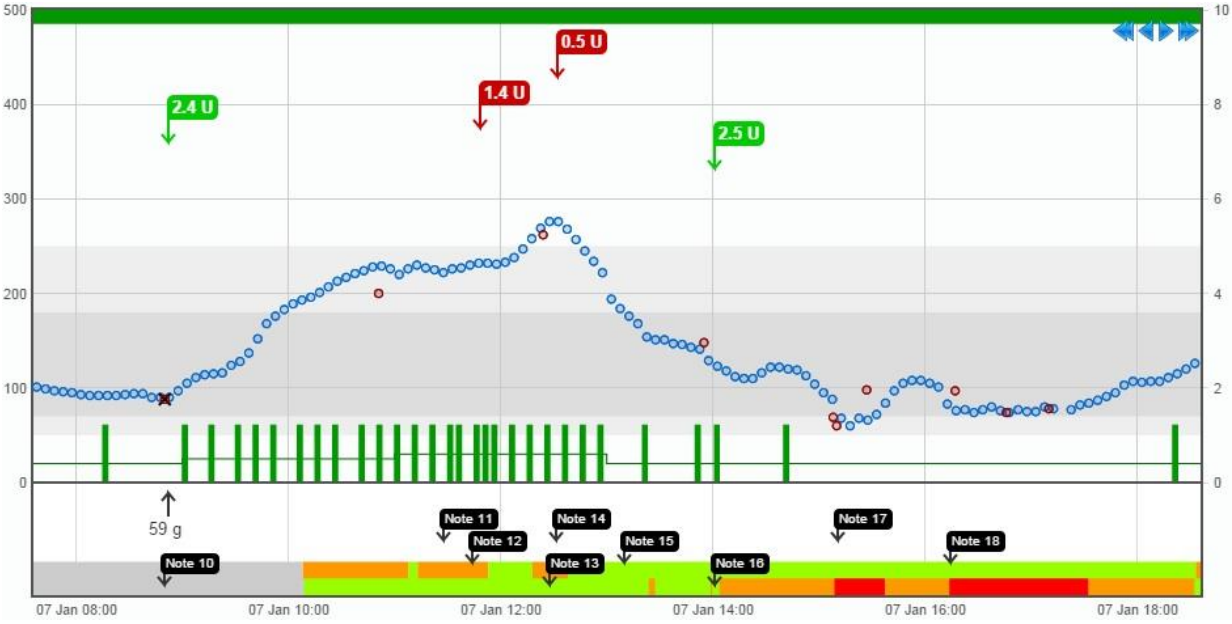
500
400
300
200
100
0
10
8
6
4
2
0
2.4 U
1.4 U
0.5 U
2.5 U
59 g
Note 10
Note 11
Note 12
Note 13
Note 14
Note 15
Note 16
Note 17
Note 18
07 Jan 08:00
07 Jan 10:00
07 Jan 12:00
07 Jan 14:00
07 Jan 16:00
07 Jan 18:00

Figure 15. Record of Remote Monitoring for Subject 3.

4.9 Post-Trial Analysis.

Now as the data from the trial is introduced and described, several cases of bolus miscalculation will be closely analyzed.

Generally speaking, the advice can be miscalculated in two ways:

- Too little insulin – underbolusing
- Too much insulin – overbolusing

In the following, several examples from the trial are presented along with the analyses of the reasons leading to miscalculations.

4.9.1 Trial Reconstruction in the Simulator

To analyze the reasons behind inadequate advices during the pilot trial, the three subjects described above were "reconstructed" in the Simulator [39]. To accomplish this, for each subject, the following was implemented:

- CGM data exported from the trial's remote monitoring system was converted into Simulator-loadable vector.
    - 2 hours of the sensor "warm-up" were retrospectively added as equal to the first known CGM value in the trial
- The same was done with the insulin data from the trial.
- Patient therapy parameters values were used
    - Body weight was taken as is
    - Carbohydrate Ratio was calculated for the simulation purposes as an average of the subject's CR profile weighted according to the time of day.
    - Correction Factor was incorporated similar to CR.
    - Basal rate was incorporated similar to CR.
- A scenario was constructed with
    - The same simulation time as the length of the trial
    - Meals of the same size as the ones administered and at the same time as in the trial

In the examples below, the prediction curves demonstrated are results on the simulations run based on the above.

4.9.2 Underbolusing Case 1

An example of underbolusing in subject 1 is presented in Figure 16. While the system advised 0.7U of insulin at 10:50pm (remember that online monitoring system has the time shifted one hour), BRM [75] had to increase the basal rate starting approximately at the same time and for the next two hours.

As presented in Table 2, a 40-gram of carbohydrates meal was served at 7:20pm (entered in the system as 55 grams). However, there was no blood glucose increase until almost three hours later, approximate at 10:00pm (Figure 16).

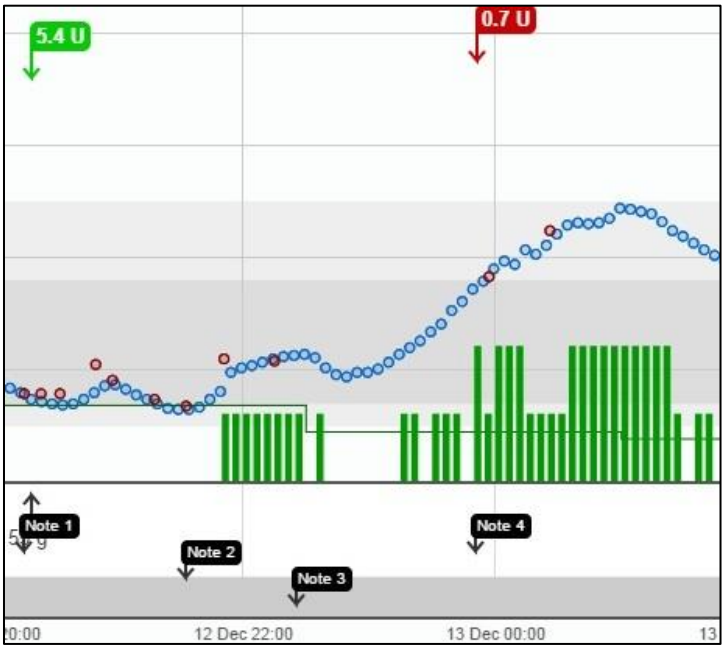

Figure 16. Underbolusing.

Using the Simulator-based trial reconstruction, the predictions for this time of the trial were observed (Figure 17). X axis units are 5-minute steps and each red curve corresponds to a 4-hour prediction calculated at a given time. As can be seen, during the BG climb present, the predicted glucose is rapidly decreasing. The advice calculated based on such prediction is therefore very conservative not to lead to hypoglycemia.

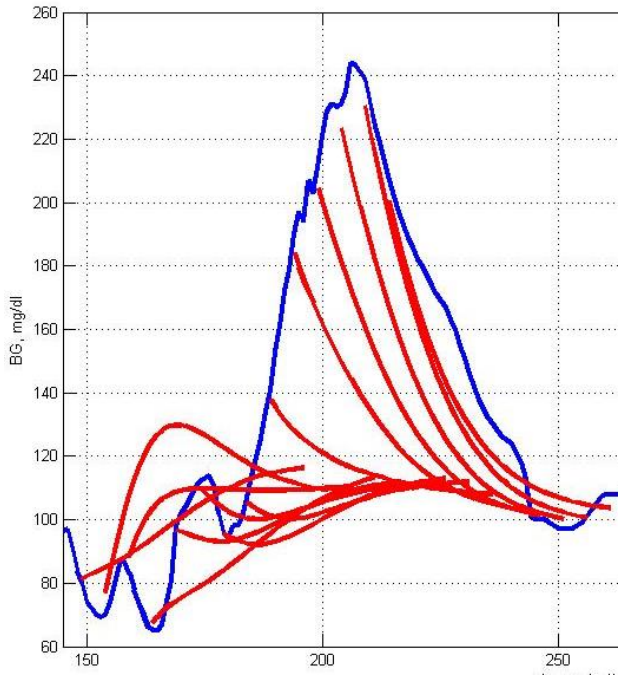

Figure 17. Real-Data Simulated Predictions.

A possible reason for the inaccuracy of BG prediction is the inability of the model to characterize delayed meal absorption. Mixed meals that contain fat have a substantial impact on the post-prandial glucose response and the meal content in this case could have contributed to this delayed absorption since in the cases of the other two meals for this subject BG started climbing within an hour (Figure 13). The tuning of the model [73] could not account for this effect and therefore the prediction was inaccurate leading to underbolusing by the adviser.

4.9.3 Underbolusing Case 2. Reconstruction Using Net Effect.

In addition to reconstructing the trial in the way described above, we have an opportunity of also learning what would have happened in the cases when the patient "disagreed" with the adviser if the patient actually followed the advice. For example, the second bolus from Table 5 can be analyzed. This is done using the Net Effect simulator by Patek et al [76]

Net Effect, in one sense, is a method of using continuous glucose monitoring and insulin pump data to extract a BG variability signature represented by oral carbohydrate net effect, which can be "fed" back into the mathematical model to (i) reproduce the original BG time series from the original record of insulin delivery and (ii) be used to approximate the effect of a modified schedule of insulin delivery [76]. Thus Net Effect, in its other meaning, is the signal that the Net Effect simulator produces and which is further used alongside modified insulin delivery to obtain a modified "what-if" glucose trace.

To obtain the Net Effect signal for subject 2, we used the insulin and CGM data from the clinical trial and parameter of the subject collected at admission. The result of recovered CGM produced by the Net Effect simulator is presented in Figure 18 (blue curve).

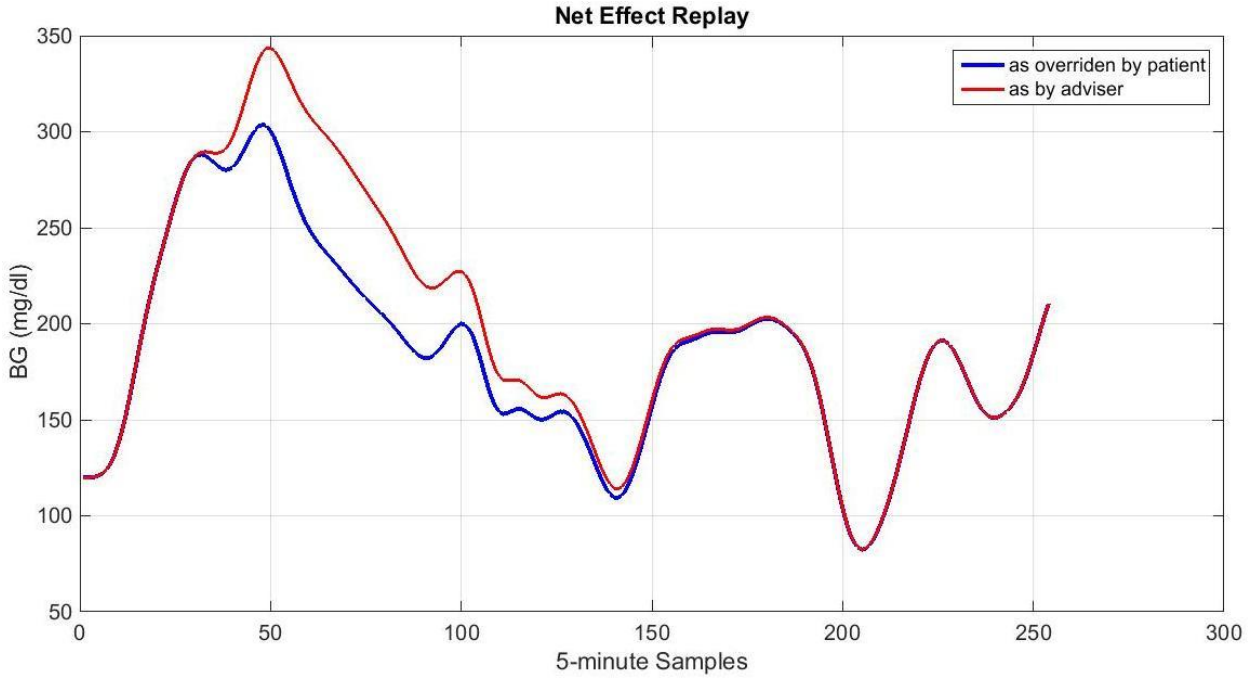

Figure 18. Net Effect replay with the advised zero bolus that would have led to hyperglycemia.

The 9:28 pm bolus request is considered which corresponds to the step 25 in Figure 18. During the trial, the adviser advised the patient to take the bolus of 0 Units or, in other word, not to take the bolus. However, the patient overrode the suggested value and instead administered 1.8 Units of rapid-acting

insulin. This led to a timely descent of the patient's BG (blue curve). The red curve in Figure 18 shows what would have happened if the patient had accepted the advised value of 0 Units. In that case, the BG would have continued to rise into a significant hyperglycemia that would peak out at about 11:30pm (step 50 in Figure 18).

4.9.4 Overbolusing Case 1. Reconstruction Using Net Effect

An example of overbolusing in subject 2 is presented in Figure 19. At 10:13am (11:13 am in the plot) the subject requested an advice and 1.9U was suggested by the system. In about 2 hours an alarm went off alerting the team that the BG was below 90 mg/dl. The advice was therefore inadequate as it led to a hypo alarm. It is worth noting that for the meal administered at 12:08pm (missing from the plot due to the remote monitoring system glitches), the advisory system suggested a negative correction bolus that resulted in a zero total bolus.

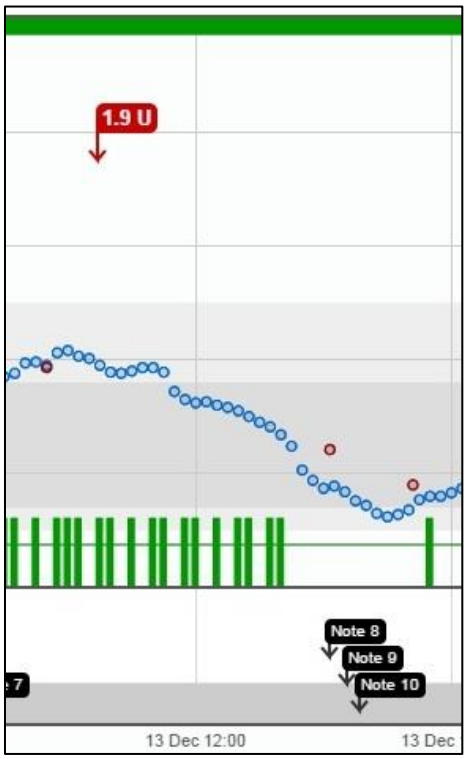

Figure 19. Overbolusing 1.

After reconstruction in the Simulator, the cause of the problem was identified as another poor prediction but in this case one that had predicted glucose level higher than it turned out to be (Figure 20). Given the prediction that the system used, one can see that the system indeed made an optimal decision as with the 1.9U advised the predicted glucose was converging to the target 112.5 mg/dl as shown in the figure.

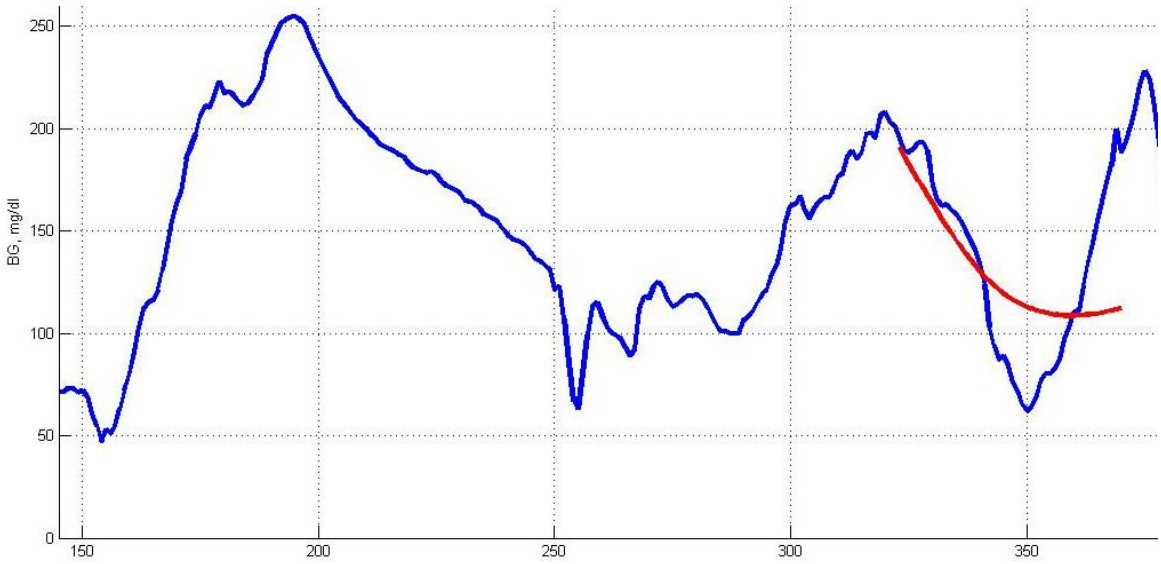

Figure 20. Real-Data Simulated Prediction.

We further explore this case of overbolusing by again employing the Net Effect simulator. To obtain the Net Effect signal for subject 2, we used the insulin and CGM data from the clinical trial and parameter of the subject collected at admission. The result of recovered CGM produced by the Net Effect simulator is presented in Figure 21 (red curve).

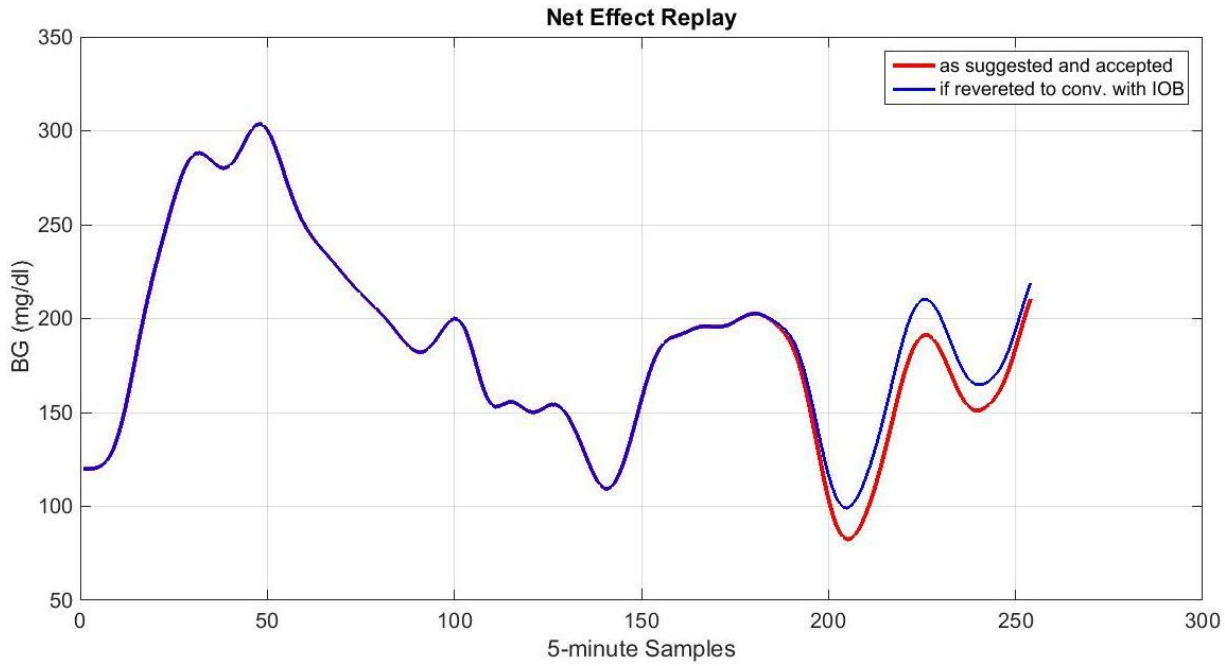

Figure 21. Net Effect replay with bolus smaller than one that led to hypoglycemia.

In Figure 21, red curve (most of the time hidden by the blue curve) repeats exactly what happened in subject 2 during the trial. CGM recovered by Net Effect is smoother than the original CGM (Figure 20), but it preserves all the main feature of the BG pattern in the trial. The 1.9U bolus of 10:13am is "administered" at step 177 in Figure 21. The original 1.9U bolus led to hypoglycemia observed in the plot around step 205.

Net Effect simulator allows us to see what would have happened in subject 2 had an alternative therapy been used. For example if the conventional CF calculation was used and IOB was taken into account: at 201 mg/dl, the target of 112.5 mg/dl, CF of 50 and IOB of 0.525579 (IOB is constantly kept track of by the system) the bolus would been 1.24 U. The blue curve in Figure 21 reflects the case when only 1.24 U of rapid-acting insulin is administered at 10:13am instead of 1.9 U. In this case, the hypo is avoided and the patient stays above 100 mg/dl.

4.9.5 Overbolusing Case 2

For another overbolusing case subject 3 can be considered. Although the system was suspended during the admission of subject 3, the would-be scenario of the system operation can still be reconstructed in the Simulator having all the data from the subject 3 session.

As a would-be overbolusing, the real bolus of 0.8U at 10:24pm (11:24 pm in the plot) can be used – Figure 22. To learn what the advisory system would suggest as a bolus in this case, we run the simulation for all the subject 3 parameter and real data until 10:24pm and then " request" the advice.

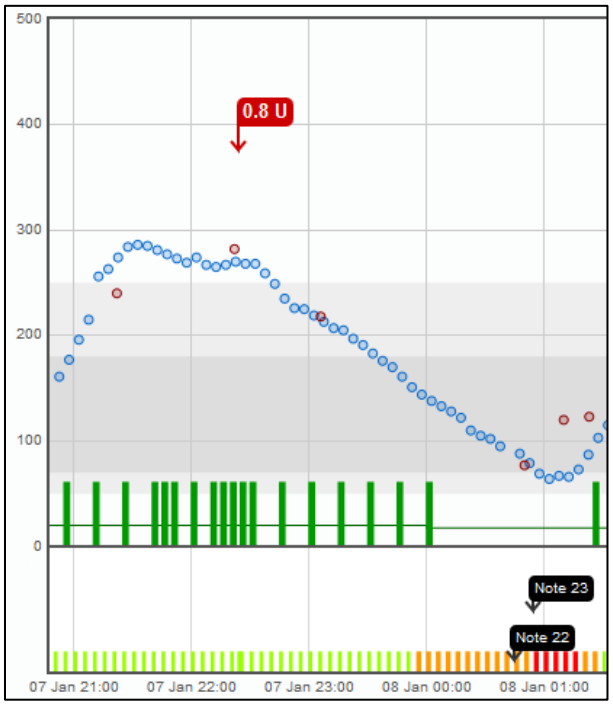

Figure 22. Overbolusing 2.

This results in the adviser suggesting 2 Units of insulin. Importantly, we do not know that an actual correct value of this bolus would be, but given that 0.8U resulted in hypoglycemia, it is clear that 2U would have resulted in even more sever hypoglycemia.

Let us look at the prediction that the advisory system would have used – Figure 23. In addition to the trace of real CGM data from the trial, the figure contains the trace of the Δ state.

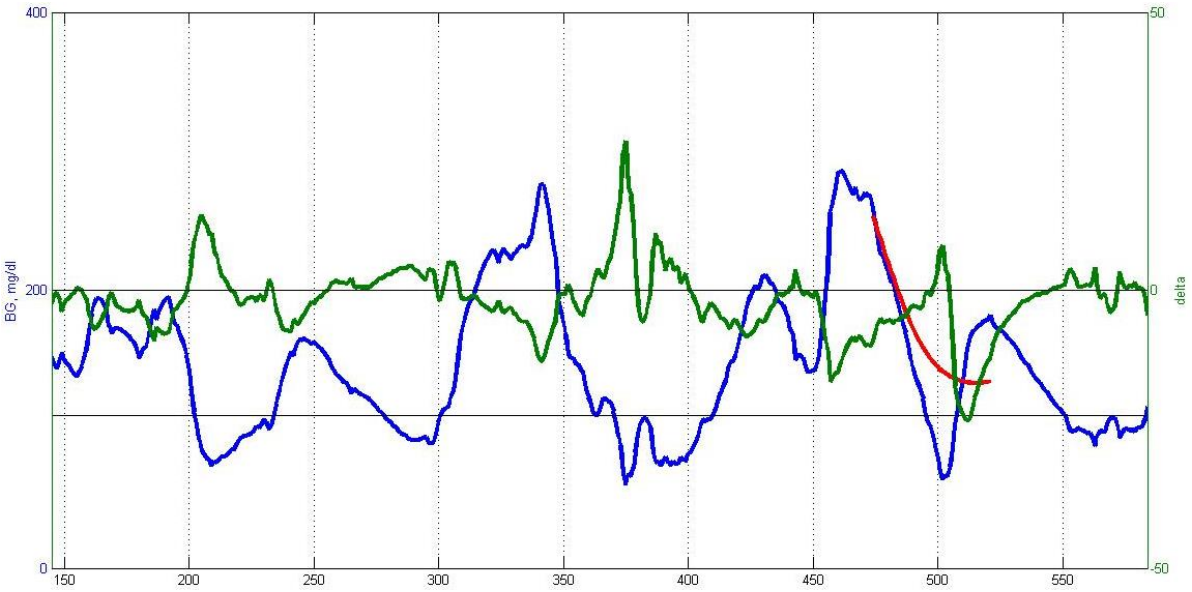

Figure 23. CGM and Delta; Prediction at 0.8U.

Remember, that Δ is calculated as the difference (see equation (14)) between the estimated insulin action and the insulin action fed-forwarded by the model described in equation (2). When Δ is negative, the system "thinks" that Kalman Filter underestimates the insulin action in the system. This would generally result in larger advice to compensate for that underestimation.

Figure 24 shows the same scenario with the prediction by the system had the injected insulin been the advised 2.0 Units. While the prediction is still inaccurate, the end of glucose trace "lands" precisely on the target 112.5 mg/dl (remember that the end of the trace is what counts for the optimization model - Figure 74). In reality, 2.0 U would have resulted in severe hypo.

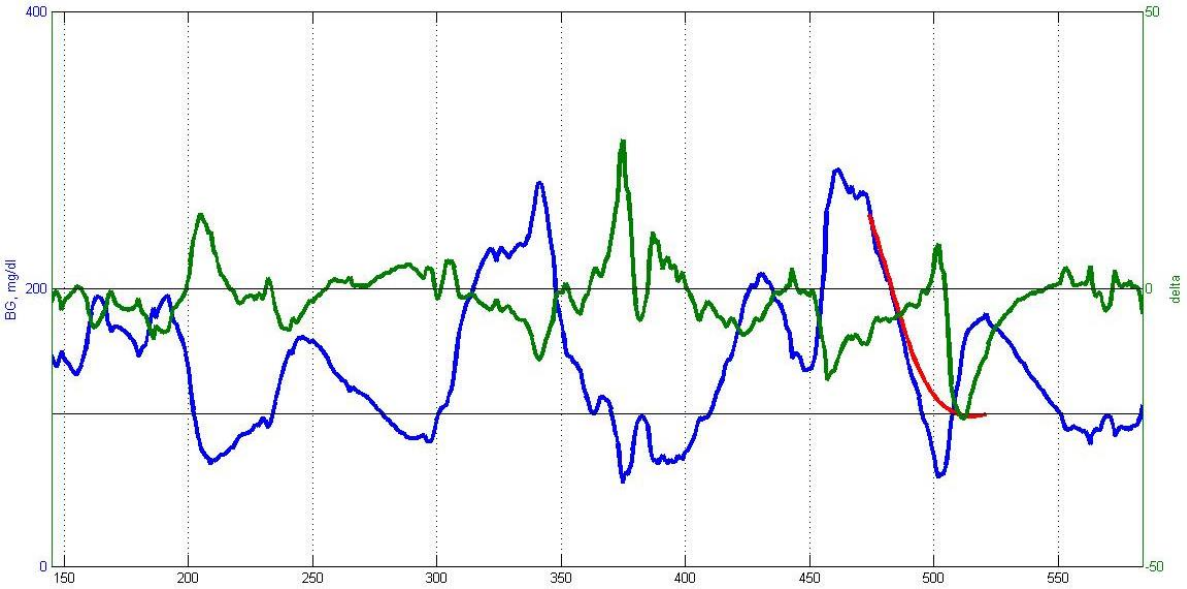

Figure 24. CGM and Delta; Prediction at "optimal" 2.0U.

Note that in Figure 24, the 2.0 Units are advised at the time when Δ is negative and well below 0. To further demonstrate the interconnection between the Δ state and the advice value, Figure 25 demonstrates the would-be advice value for any moment of advice request. Compare to Figure 24 to see the close relation between the values of Δ and advice. Not always, but most of the time the advice value is negative when Δ is positive and positive while Δ negative. The absolute magnitude of the advice also corresponds to the value of Δ.

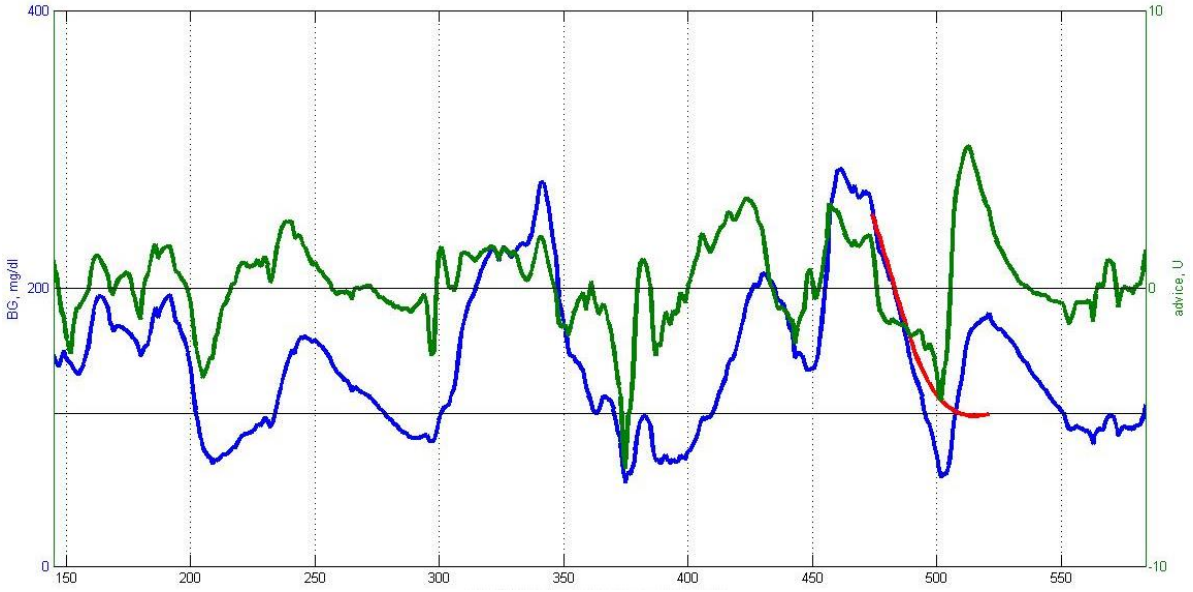

Figure 25. CGM and Advice; Prediction at "optimal" 2.0U.

Therefore, the advice value does not only depend on the prediction incorporated into the objective function, but also on the performance of the Kalman Filter underlying model, feed-forward insulin action log model and resulting Δ.

4.9.6 Prediction Quality

To see prediction quality for the whole trial admission, the following plots were created: Figure 26 – Figure 29. In the plots, red strokes show 3-step prediction segments for certain time in the future. For example, the plot titled “steps 7 to 9” shows, for each step, three steps of prediction calculated at the given step that are 7, 8, and 9 steps in the future. Magenta vertical lines designate meals. Note that the advisory system would withhold advice for certain time after meals (30 to 90 minutes depending on the meal’s fat content), therefore there are no predictions plotted right after meals, and the more so with farer prediction.

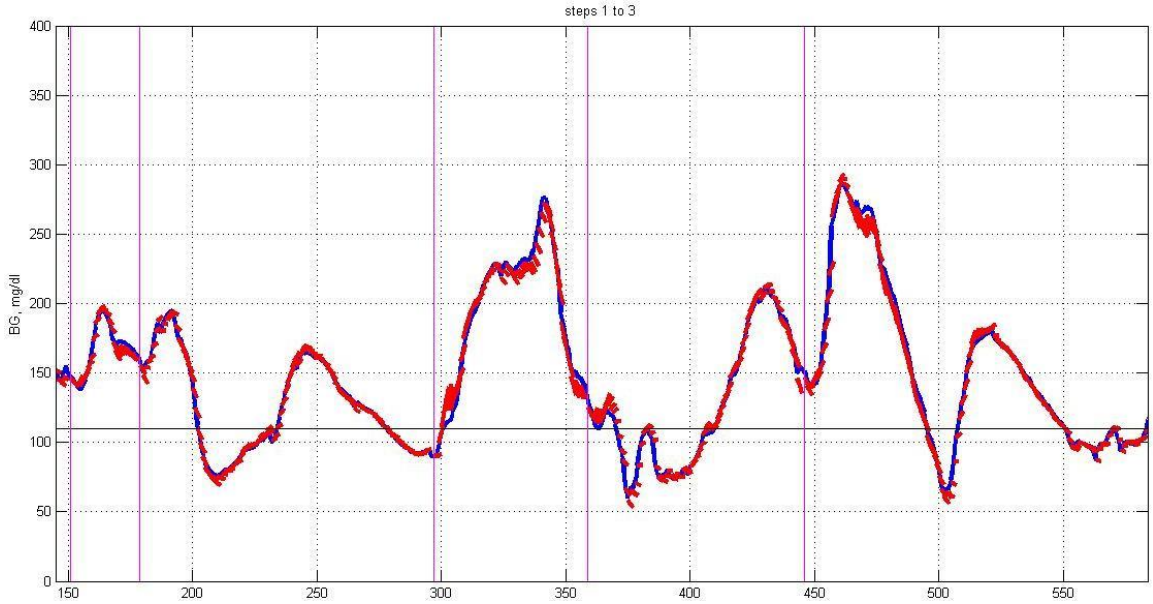

Figure 26. Steps 1 to 3 Three-Step Prediction Segments.

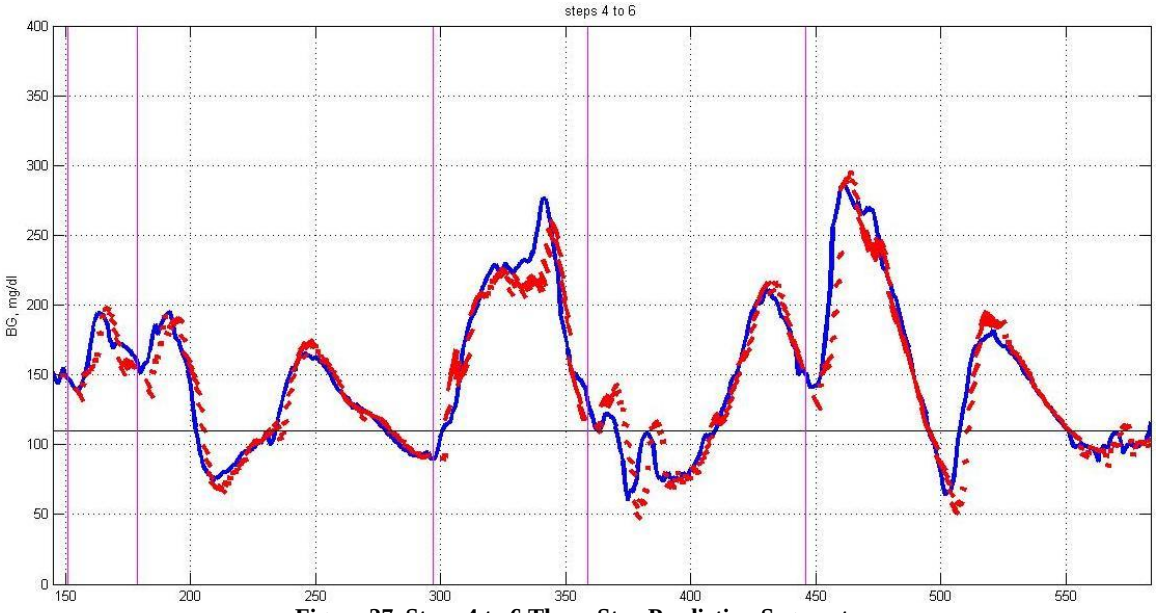

Figure 27. Steps 4 to 6 Three-Step Prediction Segments.

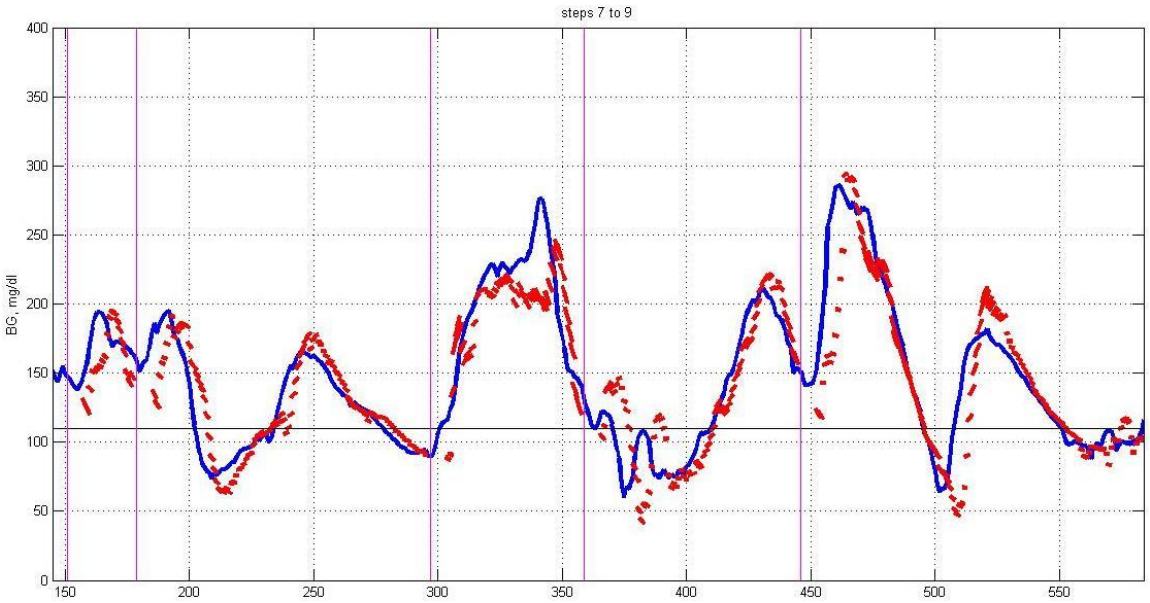

Figure 28. Steps 6 to 9 Three-Step Prediction Segments.

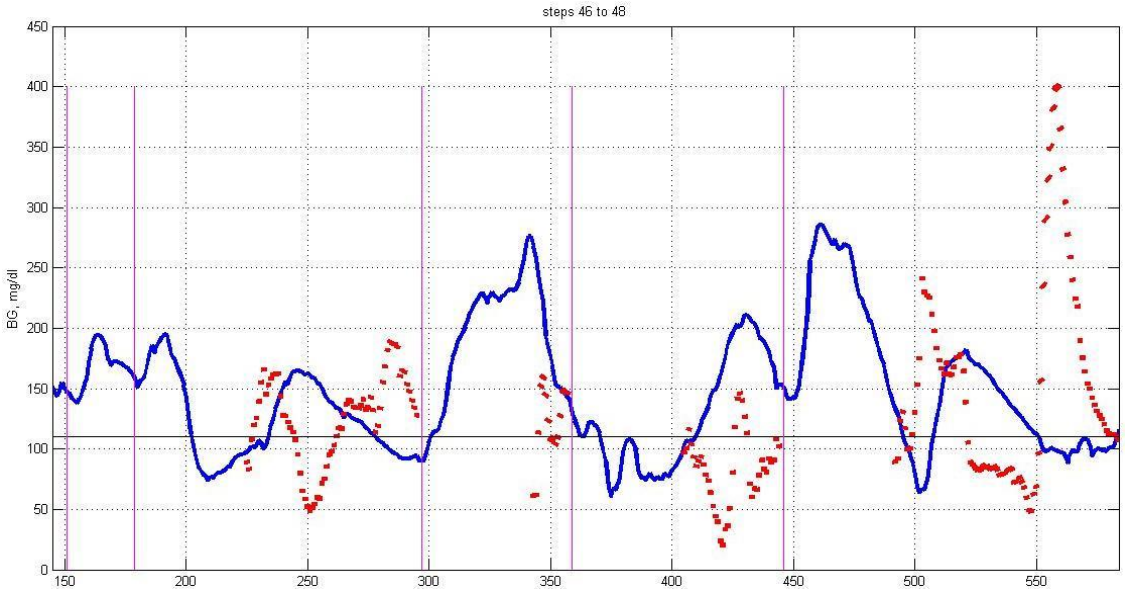

Figure 29. Steps 46 to 48 Three-Step Prediction Segments.

The plots demonstrate that while it is possible to have accurate prediction within short time horizon (up to 6-9 steps or 30-45 minutes), long-term predictions like 4-hour predictions, almost always result in inaccuracy.

However, in many prediction cases in these plots, the inaccuracy should be attributed to the fact that prediction "does not know" about the upcoming meals – for example, in Figure 29, steps 46 to 48 of the

prediction calculated at step 170 do not have a chance to be correct as the system is not aware of the meal coming at the step 179.

In some cases though, the prediction is correct despite the meal in the future because the meal absorption was delayed – Figure 30.

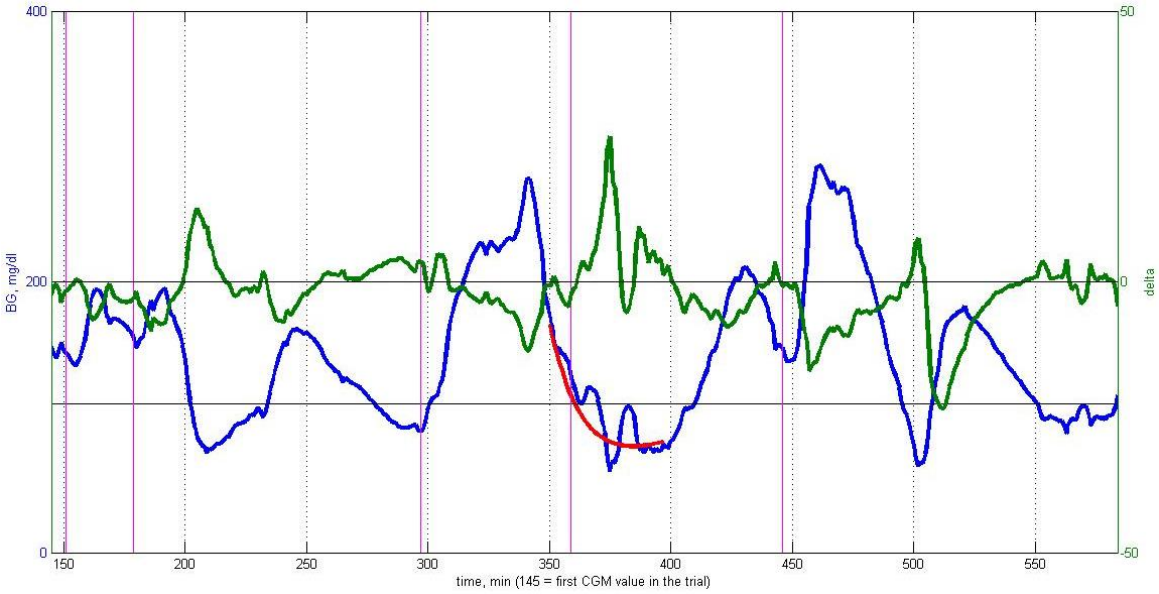

Figure 30. Example of Accurate Prediction.

After the pilot trial and the post-trial analysis presented above. there are several directions in which such advisory systems can be improved. As will be explained in Chapter 6, risks of one nature can be mitigated by actions in a different category of risks causes.

In particular:

- To partially counter overbolusing, a safety measure should be included to ensure that overly large amounts of insulin are not injected.
    - For example, a constraint based on Insulin On Board can be applied to the final recommendation of the advisory system.
- Provide proper training to patient before the system is used to mitigate things like carbs misestimation.

- Better models should be built or current models should be tuned differently to be able to better account for real-life patient metabolical dynamics.

Chapter 5

MDI Therapy Based On the Advisory System

As the previous work shows, advisory system based on a long-term prediction has the weakness of being inadequate when the prediction is not right. In its turn, the prediction, might be working well in simulations but, as clinical trial demonstrated, it might underperform in human subjects due to a very high inter- and intra-patient variability. Particularly, there is a big discrepancy between meal absorption rates even within the same subject. This post-prandial PD uncertainty suggests limiting advice to meal times only.

At the same time only 20% of Type I diabetics in the US use insulin pumps in the first place which is a prerequisite to the usage of an AP of any kind or an advisory system as in Chapter 4 (this number is even lower in other countries) [77]. The rest of the patients are still on Multiple Daily Injections (MDI) therapy. In MDI, there is no insulin pump that would deliver basal insulin every 5 minutes, but insulin syringes or pens are used instead for delivering long-acting insulin.

A particular feature of MDI therapy is that it involves types of insulins different in their pharmacokinetics (PK) and pharmacodynamics (PD) when in the body. Therefore an auxiliary aim of this chapter is to augment the simulation platform existing in Artificial Pancreas and used in our advisory system work to reconcile metabolism of different insulins and create a framework for design and testing of control systems to be incorporated into MDI therapy.

To that end, we devise a system that accommodates MDI therapy patients and has features that allow it to circumvent the drawbacks that the system of Chapter 4 has at its current stage:

1. Decoupling meal bolusing from correction bolusing. The meal bolus is thus taken care of through conventional CR-based therapy or other rule of thumb.

2. Restricting the correction bolusing through the advice to meal times only.

Additional rationale for the second point comes from the clinicians stating that MDI patients tend not to inject any correction insulin between meals, in order to decrease the total number of injections per day. Therefore confining the times of corrections to only meal times does not significantly limit the application of the system.

Conceptually, the system is designed for operation in the framework presented in Figure 31.

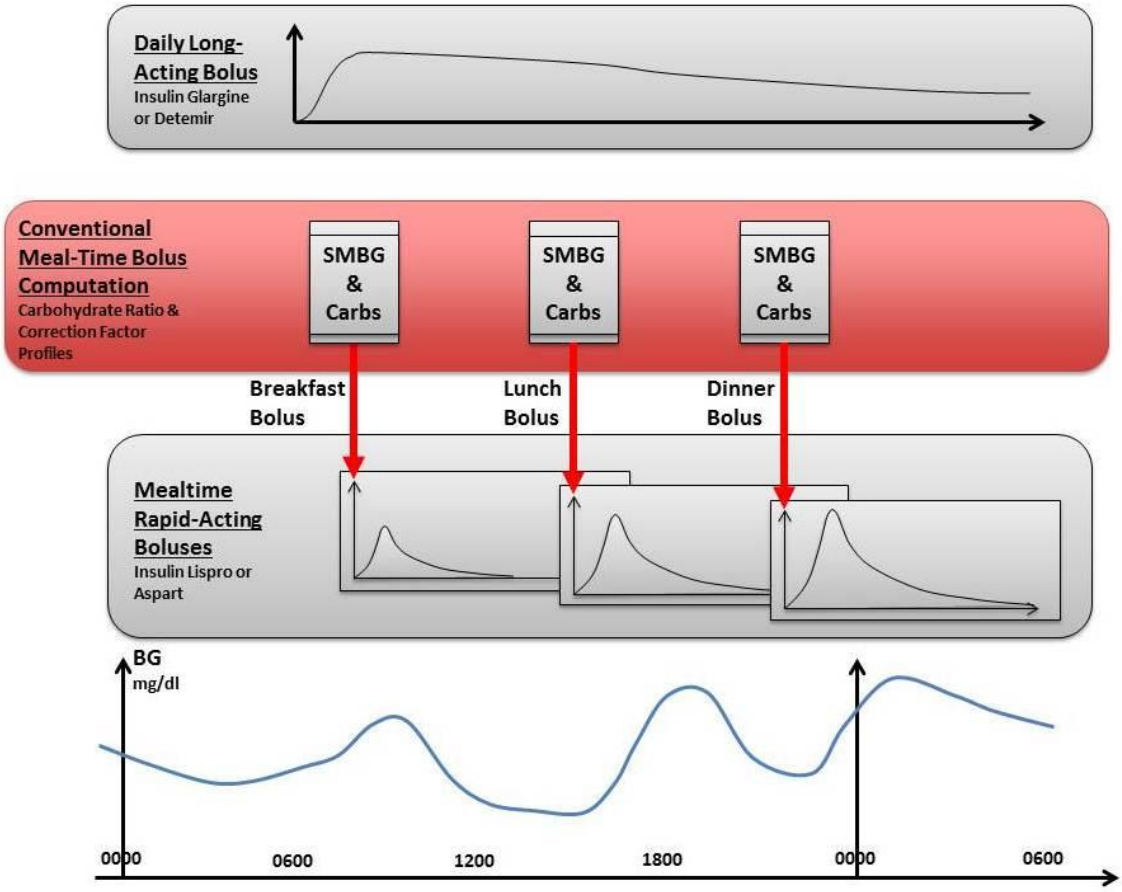

Figure 31. MDI Daily Scenario.

Applying the system to this scenario modifies the therapy leading to another scenario, presented in Figure 32.

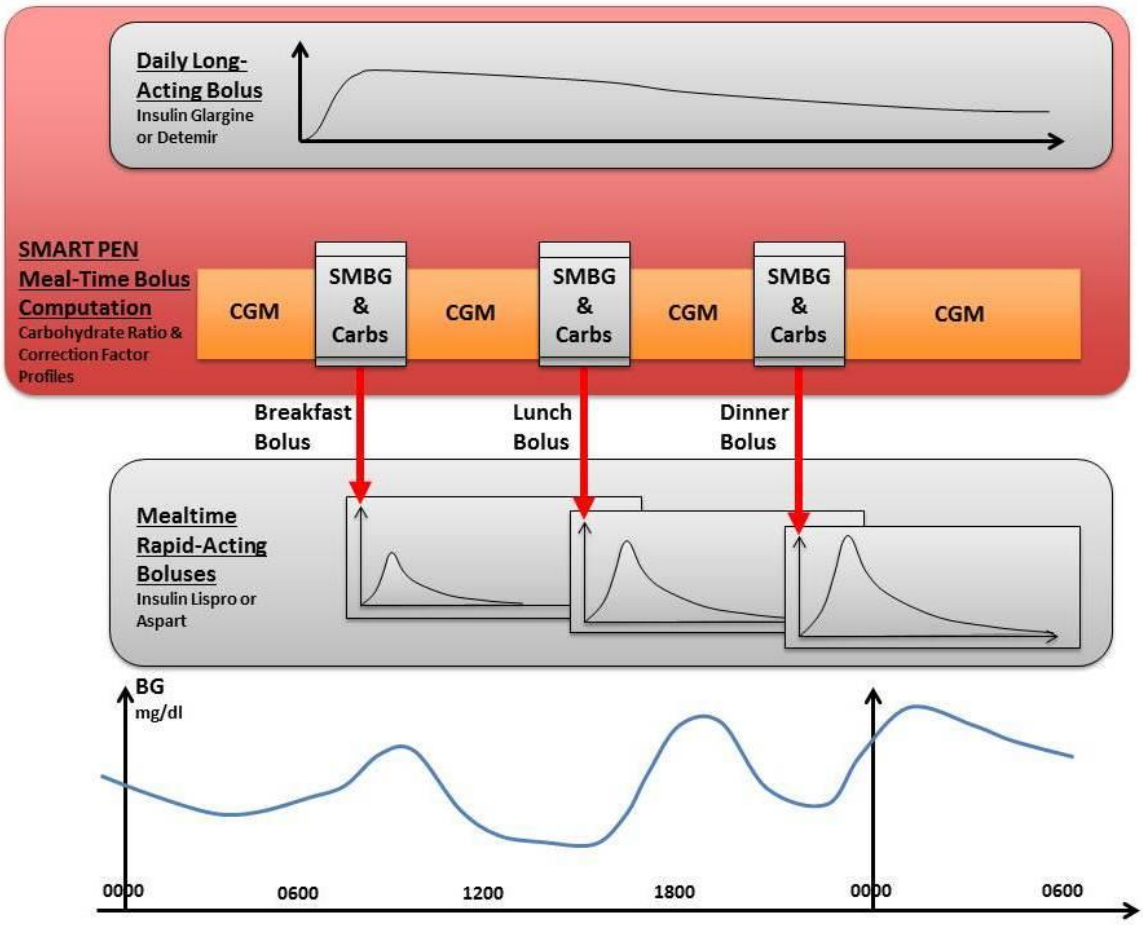

Figure 32. Smart Advisor Applied to MDI Scenario.

5.1 Methods

We use pharmacokinetic and pharmacodynamics data analysis to design a model structure that would allow for modeling of long-acting insulin. We further identify the model using the data set provided.

The resulted model is then discretized and converted to state space representation. Kalman Filter estimation is used to provide the best estimate of the current metabolic state. Using the model, a model-based prediction is built and an objective function is formulated about it. Linear regression is performed to derive the dependency between the patient's parameter and the aggressiveness factor. This results in a linear-quadratic optimization in which a closed-form solution can be derived.

We then conduct computer simulations using *in silico* population to validate the optimization controller that we designed. Various scenarios are constructed including conditions of erroneous therapy parameter values and misestimations by virtual patients. The results are evaluated using time in range, Time under 70mg/dl, Time over 180 mg/dl**,** risk parameters like Low Blood Glucose Index and High Blood Glucose Index [54], and the variability parameter of Average Daily Risk Range [63].

Further, we conduct robustness analysis by varying pharmacokinetic parameters and complacency degree of the patient.

5.2 New Insulin Transport Model

To adapt the framework to MDI therapy, we needed to develop a new model, or augment the existing one, since in the AP framework only rapid-acting insulin is used, while in MDI therapy, rapid-acting insulin is used for boluses and long-acting insulin is used for basal injections. There are other, less common, types of MDI therapy where, for example, intermediate-acting insulin is used, or insulins are mixed together, but we are going to consider the most common MDI therapy type of rapid-long combination. The long-acting insulin was providing the basal rate while the rapid-acting insulin was providing meal and correction boluses.

To enable the development of the advisory system, one particular long-acting insulin was chosen – insulin glargin. Insulin glargine pharmacodynamics is often conceptualized as having rapid time (two or three hours) to peak concentration and staying perfectly flat over the remaining hours of the day. However, a more detailed analysis shows that there is:

- significant variation in insulin concentration throughout the day (unlike in idealized curves found in [78])
- significant inter-patient variability in PK characteristics.

Based on PK/PD clamp data from 19 Type 2 subjects of [79], we have observed that, depending on the patient, glargine concentration can taper off in less than 24 hours, or sometimes remains in the system longer. All 19 subjects' PKs are illustrated in Figure 33 where x axis represents minutes and y axis represents plasms insulin concentration in pmol/l.

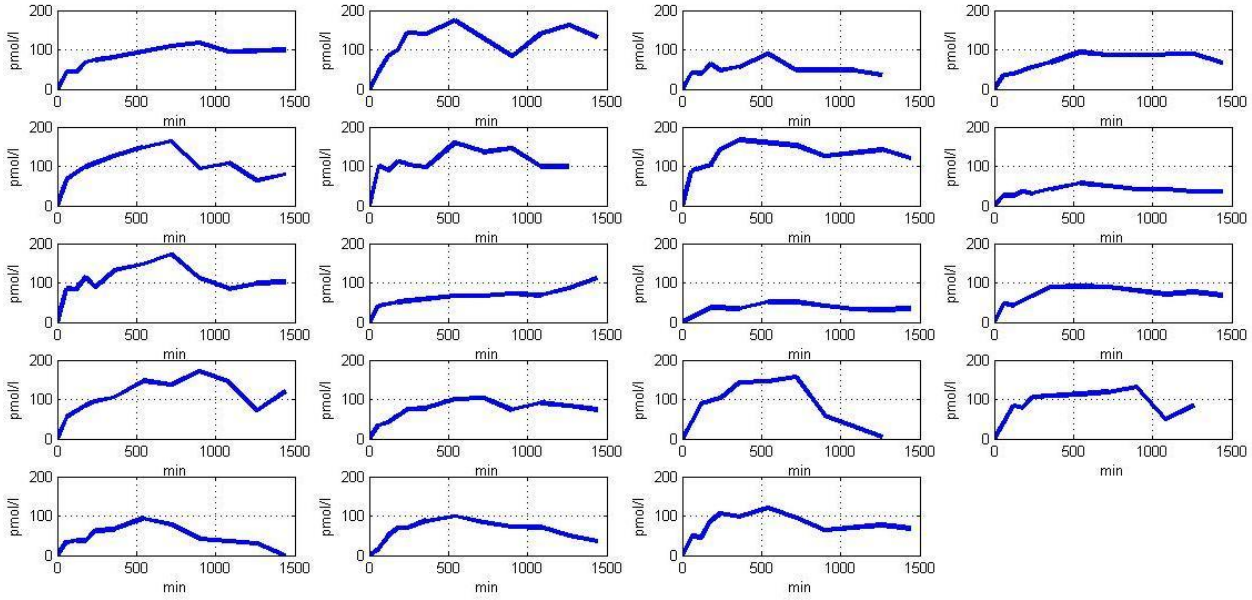

Figure 33. Inter-Subject PK Variability.

Assumption was made that it would be possible to develop a simple model for subcutaneous insulin glargine PK by modifying an existing compartmental model for subcutaneous rapid-acting insulin through the addition of an extra compartment accounting for the breakdown of insulin hexamers. The insulin transport part of the existing meal model [50] used in the Simulator was augmented with an additional compartment that allowed to simulate the slow absorption of long-acting insulin (Figure 34).

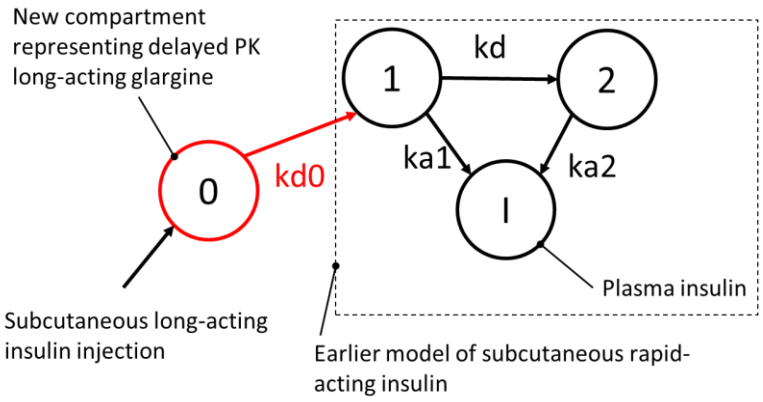

Figure 34. New 3-Compartment Insulin Transport Model.

To determine the population average value of the parameter k_{d0}, we fit the model to the data from the Hompesch's study [79]. Even after cleaning the data and deleting obvious outliers, great variability can be seen (Figure 35).

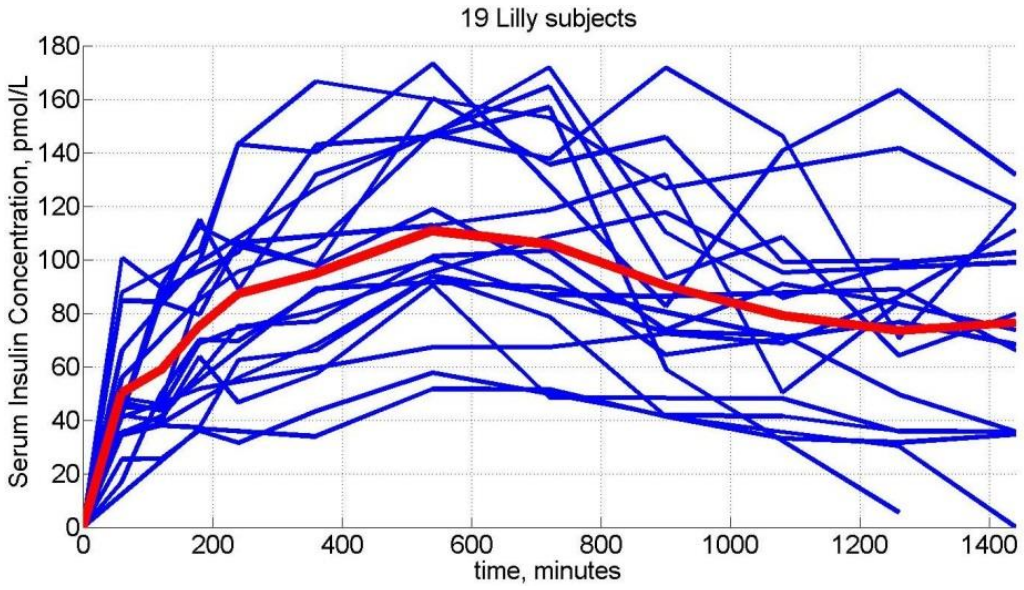

Figure 35. Average Insulin PK of the Data.

Other insulin transport parameters are the *in silico* patient-specific parameters derived similar to those described in Chapter 4.

After adding the new compartment, the subcutaneous injection is "pushed back" one compartment, as compared to the model from [50], and the insulin transport injections of the meal model are modified as from

$$\dot{I}_{SC1}(t) = J(t) - (k_{a1} + k_d)I_{SC1}(t) \quad \textbf{(32)}$$

$$\dot{I}_{SC2}(t) = k_d I_{SC1}(t) - k_{a2} I_{SC2}(t) \quad \textbf{(33)}$$

to

$$\dot{I}_{SC0}(t) = J_1(t) - k_{d0} I_{SC0}(t) \quad \textbf{(34)}$$

$$\dot{I}_{SC1}(t) = k_{d0} I_{SC0}(t) + J_2(t) - (k_{a1} + k_d)I_{SC1}(t) \quad \textbf{(35)}$$

$$\dot{I}_{SC2}(t) = k_d I_{SC1}(t) - k_{a2} I_{SC2}(t) \quad \textbf{(36)}$$

where $J(t)$ is rapid-acting insulin injection in the pump-equipped system of Chapter 4, $J_1(t)$ is long-acting insulin injection of the new system, and $J_2(t)$ is rapid-acting insulin injection of the new system.

The averages of the data and the plasma concentration curves produced by the fitted model with population average long-acting insulin transport parameter is in Figure 36.

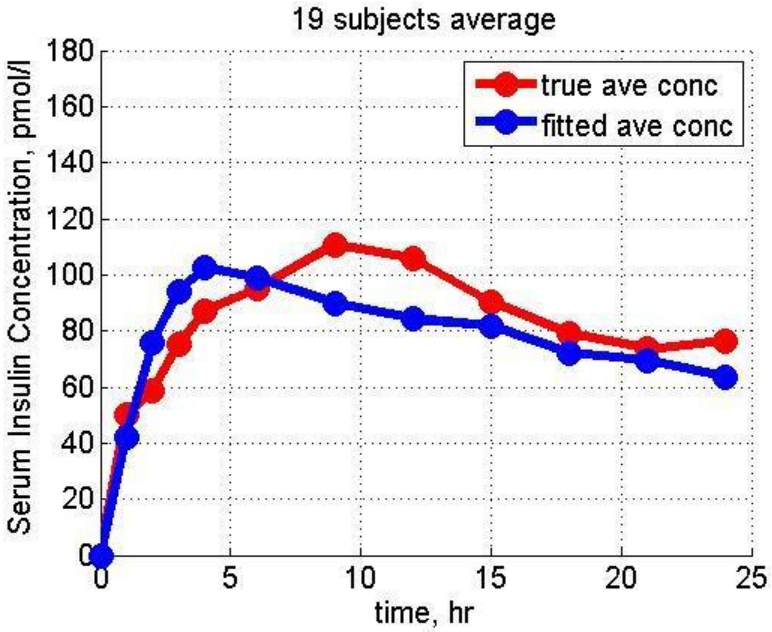

Figure 36. Fitted average concentration and real data.

Judging from the fits (see Appendix H), it is possible that a more complex model, perhaps another compartmental model with more compartments and corresponding parameters k_{d0}, k_{d1}, k_{d2} and so on, could do a better fit.

However, under this kind of inter-patient variability, it is important to avoid overfitting so that the model is useful within simulations based on population average parameters of *in silico* subjects. That is this simple one-compartment model is kept and oriented around the average PK curves available in the literature [78], [80], [58].

5.3 Meal Model Modularization and Modification of the Industry Standard Simulator

After the new insulin transport model is designed, a simulation environment is needed to conduct pre-clinical *In Silico* validation. The simulator used in Chapter 4 is not equipped for this purposed due to two reasons:

- It is equipped with pump simulation, but not pen/syringe simulation that is required for MDI scenarios.
- The metabolical model used in it is not modular and thus does not allow easy modification of its subsystems (meal transport, insulin transport, etc.).

To solve the first problem, the pump module was removed from the Simulator and two separate pen modules were built: one pen for long-acting insulin for MDI basal injections and one pen for rapid-acting insulin for boluses.

To solve the second problem, the one-block central model configuration in the Simulator was dismantled and reassembled with the insulin transport modules operating "outside" of the rest of the model. More details to both these solutions are presented in Appendix I.

The latter transformation is useful outside of solving this particular problem of adapting the Simulator [39] to MDI systems. Generally, such modularization of the system into the subsystems of independent dynamics of various states provides the ability to:

- easily modify a particular subsystem and quickly verify the effects of the modification to the system overall
- separate concerns specific to a particular subsystem
- minimize the dependency between the various subsystems to allow efficient maintenance of the program

Now a simulation platform is established. Such simulation framework is essential not only for validation of an already designed system, but for the design process itself, especially when of complex systems. The new Simulator allows for two types of insulin delivery:

- daily insulin glargine injections
- injections of rapid acting insulin at meal times (or between meals) according to a prescribed "meal/correction" scenario

Thus, the simulator is uniquely equipped to support evaluation of both (i) conventional insulin pen therapy and (ii) enhanced "Smart Pen" insulin therapy.

5.4 Virtual Basal Rate and u^{LA}

Long-acting insulin injection results in a relatively quick increase of the insulin concentration with gradual decay until the next injection is administered (or until the insulin clears off completely from the system).

When starting an MDI therapy with long-acting insulin as the source of basal concentration, the initial few days are considered a "burn-in" period during which, given proper titration, the insulin is "stacked" until the desired fasting BG is attained [81]. After the stacking period is over, a hypothetical plasma insulin concentration oscillates about some average value. *In Silico*, any number of fasting days can be simulated to observed such effects – Figure 37.

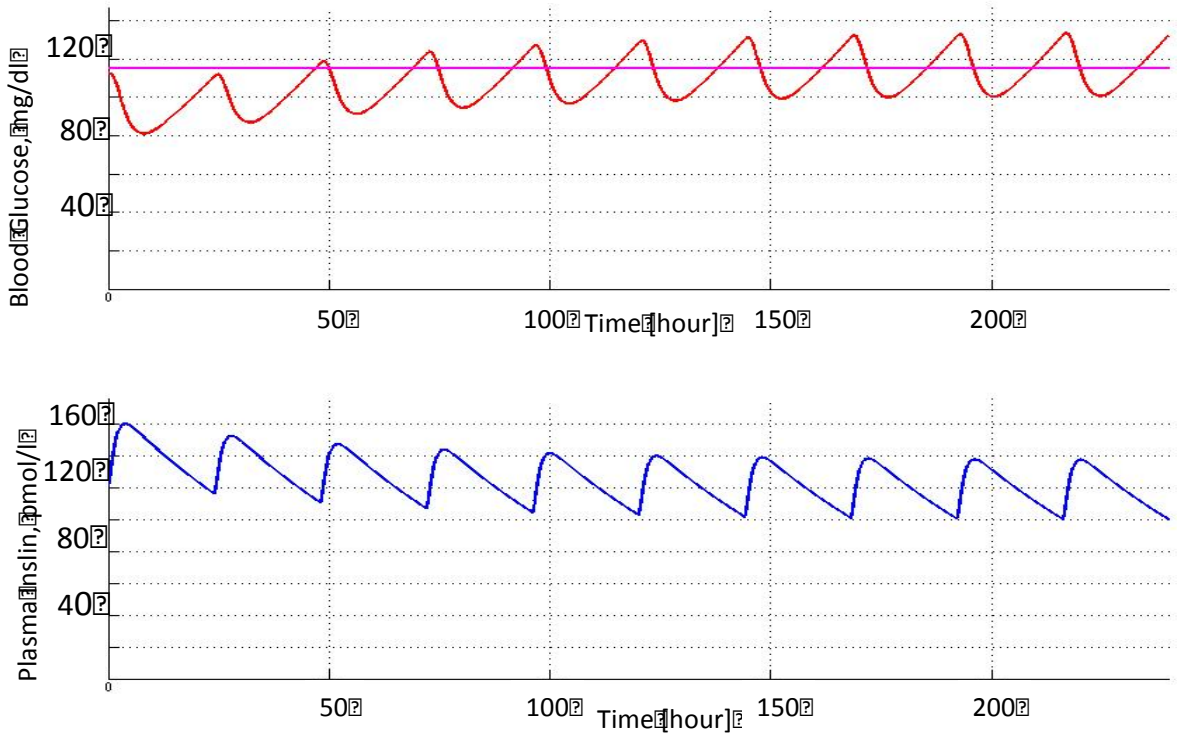

Figure 37. Simulator output for population average patient using the average PK model.

The figure shows the output of the Simulator for the population average *In Silico* patient in a scenario in which the patient only takes the daily insulin glargine injection and experiences no other metabolic disturbances. Specifically, the *In Silico* patient does not eat and consequently does not require supplementary rapid-acting insulin at meal times. For the patient in Figure 37, the daily glargine dose (35.23 U) was manually titrated to achieve an average BG of 115 mg/dl. The fluctuations in both BG and plasma insulin concentration are due to the non-ideal PK characteristics of insulin glargine. Note that, like in real patients it takes several days of simulated time for the patient to settle into a regular 24-hour pattern of BG and plasma insulin fluctuations. This period is not showed in Figure 37.

In contrast to plasma insulin concentrations observed in Figure 37, insulin pumps that are used in the traditional Artificial Pancreas framework provide flat basal insulin concentration profile. Since an AP-like system has already been developed in Chapter 4, it would be beneficial to represent the mathematics of

the MDI therapy system in such a way so that the algorithmic machinery from the pump-equipped system could be utilized.

This is achieved by introducing the concept of the Virtual Basal Rate (VBR). VBR is the equivalent basal rate that would be set on an insulin pump (a value per each time step) to achieve exactly the same BG profile as achieved with a long-acting insulin injection. Technically, VBR is the output of the "0" compartment of the new insulin-transport model of Figure 34 which in the Simulator is implemented in the units of pmol/kg/min, but for the ease of understanding can be converted into U/hr (the units in which the basal rate is usually set on insulin pumps). For example, the *In Silico* population average adult who achieves, on average, the BG of 115 mg/dl using long-acting insulin injections, would have their VBR as in Figure 38 (note the stacking period shown for the first several days)

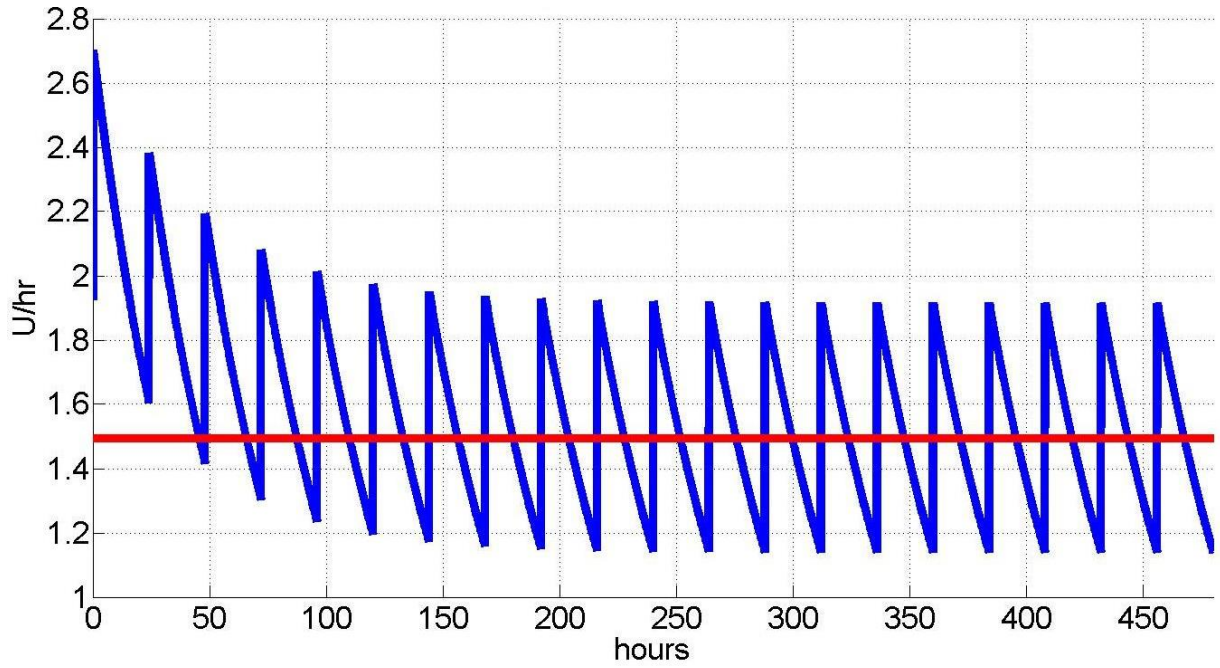

Figure 38. Virtual Basal Rate of a population average In Silico adult across 20 days.

The average of this curve (red horizontal line in Figure 38) is what the ideal basal rate would have been for a subject had they used an insulin pump instead of being on MDI therapy. The discrepancy between the actual "0" compartment of a subject and this ideal rate is what conventional MDI therapy does not have knowledge about but the proposed system does and what is taken advantage of. Within the framework of this work, this discrepancy is called u^{LA} – Figure 39.

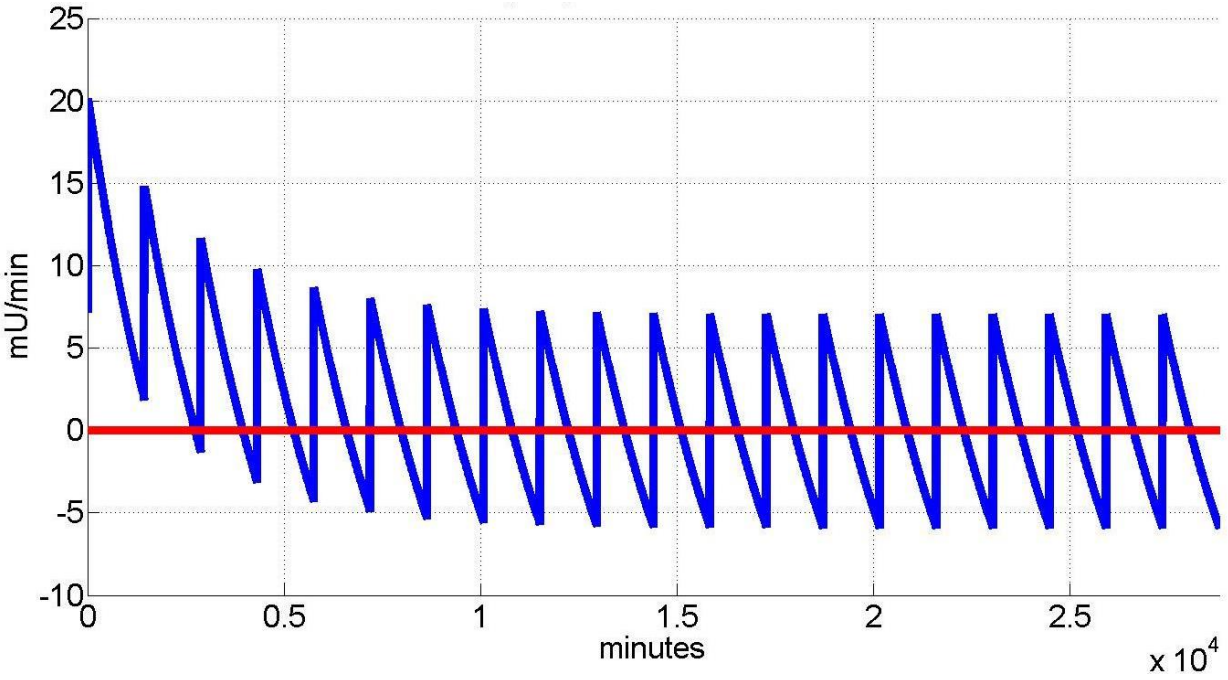

Figure 39. u^{LA}, deviation from the perfect basal rate.

The concept of VBR enables to embed the slower PK and PD rates, resulting from the injection of the long-acting insulin, along with the faster-PK-PD part of the Simulator, under one analytical roof. This allows to accommodate the previously developed simulation framework for the optimization of the MDI therapy.

5.5 State Estimation

In summary, the structure of the subcutaneous glargine PK model makes it possible to interpret the 24-hour pattern of plasma insulin fluctuations as resulting from an equivalent insulin pump (continuously varying) basal rate profile. For example, the 24-hour pattern in plasma insulin concentration for the population average *In Silico* patient in Figure 37 can be implemented via the equivalent insulin pump basal rate profile of Figure 38: $1.493 + u^{LA}(t)$, with $u^{LA}(t)$ being an appropriate, patient-specific basal rate deviation signal, as shown in Figure 39. In fact, a simulation can be run in the original Simulator to validate this. The average population subject is run under the basal pump rate modified continuously as described above. This results in the insulin concentration and corresponding BG levels presented in Figure 40.

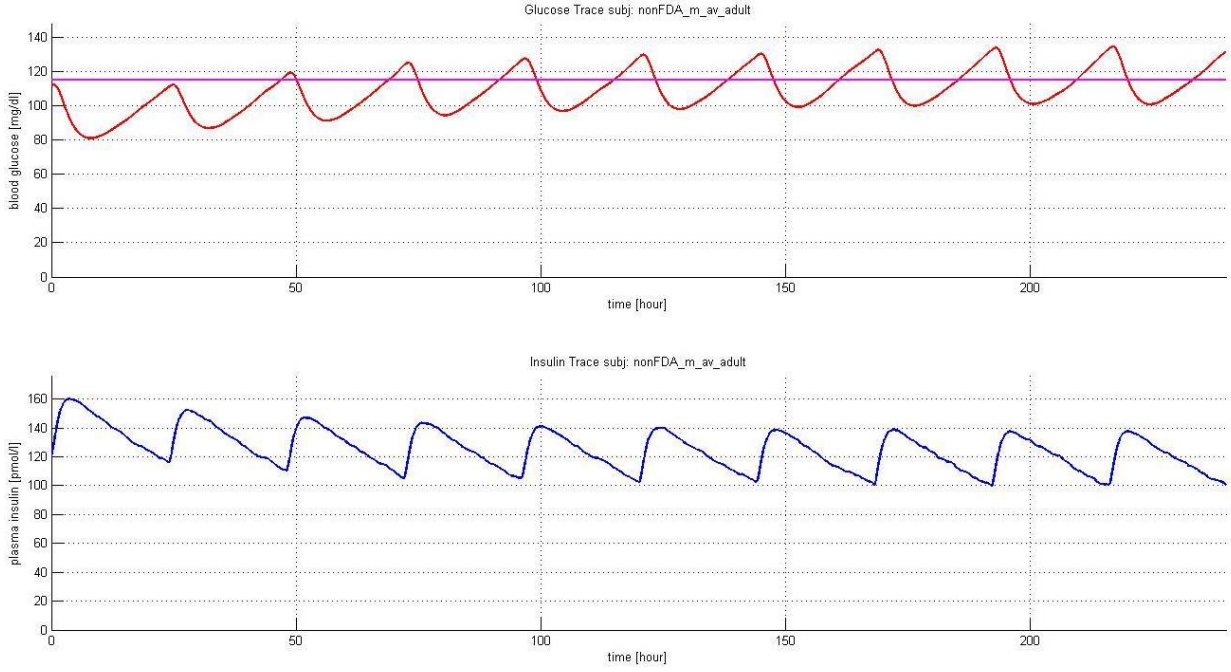

Figure 40. VBR applied to pump-equipped Simulator.

Observe that the traces in Figure 40 are equivalent to the traces in Figure 37 bar the jagged shape of the plasma insulin concentration. The latter is the result of the pump hardware limitations (inability to dose with more precision than 0.05 U/hr) that is encoded in the Simulator.

The notion of a "virtual basal rate profile" makes it possible to account for the time-variability of glargine PK within the LQG framework. Specifically, the u^{LA} signal becomes an input into the Kalman filter state observer in exactly the same way that continuously adjustable basal insulin enters in a closed-loop artificial pancreas application. Ultimately, the u^{LA} signal allows for the implicit assessment of a glargine IOB, creating the opportunity for improved correction bolus computations throughout the day.

A schematic diagram of u^{LA} feeding the KF is shown in Figure 41. To interpret the figure, suppose that the patient is interested in advice about an optimal correction bolus at discrete time k. (Note: We use a discrete-time implementation of LQG, where, corresponding to the frequency of CGM samples (mg/dl), each discrete stage corresponds to a five-minute sampling interval.) The patient may be requesting this advice as a supplement to a meal-time bolus or as a standalone correction bolus; if the former, then the patient will take responsibility for computing the meal-component of the bolus based on his/her estimate of meal carbohydrates.

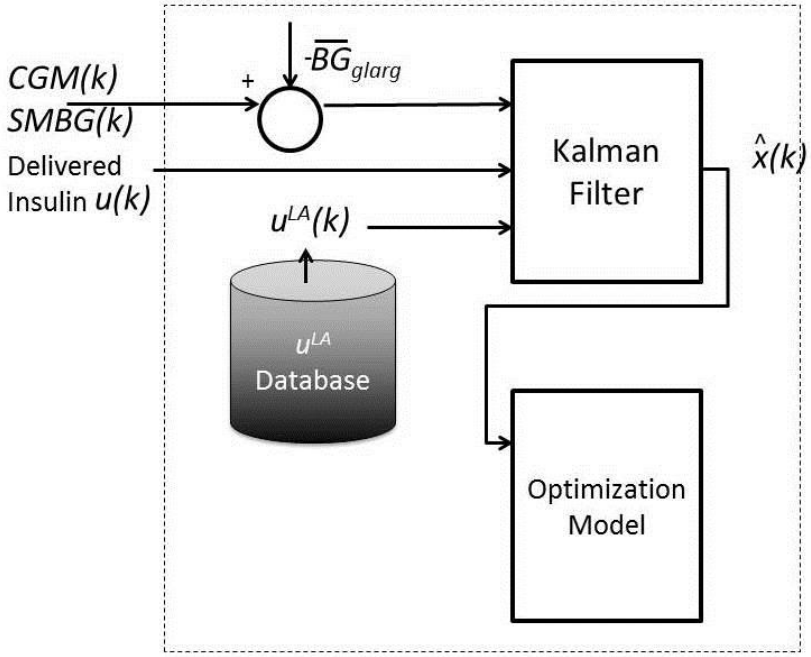

Figure 41. Schematic diagram of u^{LA} informing KF.

5.6 Optimization Model

To make further use of u^{LA}, we adopt a linear discrete-time model derived from the "minimal model" [51] extended to account for subcutaneous sensing, subcutaneous injection of rapid acting insulin, and oral consumption of carbohydrates:

$$x(k+1) = Ax(k) + Bu(k) + Bu^{LA}(k) \quad \textbf{(37)}$$

where *k* is a discrete time index, *x* is a vector of metabolic state variables, and *u* is a rapid-acting insulin injection. *A* and *B* are discrete state-space system representation matrices of the EMMGK model [51]. As you can notice we do not include the meal component into (37) since the meals are taken care of separately. Then we design a quadratic objective function:

$$F(u) = u'Ru + \sum_{k=\kappa}^{\kappa+N} (Cx(k) - \Delta)'Q(Cx(k) - \Delta) \quad \textbf{(38)}$$

where *N* is a planning time horizon, *Q* and *R* are positive semidefinite and definite weighting matrices, respectively, *C* is such that $y(k) = Cx(k)$ is the patient's plasma BG at stage *k* relative to the operating point, Δ is a desired BG offset of how much a patient would like to change their long-term average blood glucose level, and $x(\kappa)$ is Kalman filter estimate of the patient's metabolic state at the time of the meal bolus.

After some matrix algebraic manipulations with (37) we obtain a vector $\tilde{x}(\kappa)$ of predicted states all the way until the end of the prediction horizon:

$$\tilde{x}(\kappa) = \boldsymbol{A}\hat{x}(\kappa) + \boldsymbol{B}\tilde{u}^{LA}(\kappa) + \boldsymbol{B}_0 u \quad \textbf{(39)}$$

where $\boldsymbol{A}$, $\boldsymbol{B}$, and $\boldsymbol{B_0}$ are block matrices built of the matrices from (37) and $\tilde{u}^{LA}$ is the vector of predicted u^{LA} values up to the time horizon.

Now, through the use of (39), we can convert (38) into

$$F(u) = \left(\boldsymbol{C}\tilde{x}(\kappa) - \tilde{\Delta}\right)'\boldsymbol{Q}\left(\boldsymbol{C}\tilde{x}(\kappa) - \tilde{\Delta}\right) + u'Ru \quad \textbf{(40)}$$

where $\boldsymbol{C}$ is a block matrix constructed of C's from (38), $\boldsymbol{Q}$ is a block matrix constructed of Q's, and $\tilde{\Delta}$ is a block matrix constructed of Δ's.

Now we can find u^* that minimizes (40) as:

$$u^* = K^1\hat{x}(k) + K^2\Delta + K^3\tilde{u}^{LA}(k) \quad \textbf{(41)}$$

where $\hat{x}(k)$ is the states estimates vector from the Kalman filter, and

$$K^1 = \Phi^{-1}\Theta^1 \quad \textbf{(42)}$$

$$K^2 = \Phi^{-1}\Theta^2 \quad \textbf{(43)}$$

$$K^3 = \Phi^{-1}\Theta^3 \quad \textbf{(44)}$$

and, in turn,

$$\Phi = \boldsymbol{B'}_0\,\boldsymbol{C'QCB}_0 + R \quad \textbf{(45)}$$

$$\Theta^1 = -\boldsymbol{B'}_0\,\boldsymbol{C'QCA} \quad \textbf{(46)}$$

$$\Theta^2 = \boldsymbol{B'}_0\,\boldsymbol{C'Q} \quad \textbf{(47)}$$

$$\Theta^3 = -\boldsymbol{B'}_0\,\boldsymbol{C'QCB} \quad \textbf{(48)}$$

5.7 Pre-Clinical *In Silico* Validation

To test the effectiveness of the system. an *in silico* validation in the Simulator [39] is required. The Simulator consists of three sub-populations of *in silico* patients – 100 children, 100 adolescents, and 100adults – totaling at 300 subjects. The evaluations are conducted using the 100 adults. However, the current population is unsuited to serve as a proper reference population for two reasons:

1. The glargine dose and timing is absent in the original Simulator that is equipped with pump only. While the Simulator was modified in provide for pen use and glargine PK and PD, the *In Silico* population that the Simulator is based on lacks these parameters in their parameter sets.

2. The therapy parameters of carbohydrate ratio and correction factor are tuned for *In Silico* subjects perfectly – that is, under these parameters and the controlled environment of the Simulator, the handling of disturbances like meals is handled in a perfect fashion that does not require any additional control actions. However, that does not correspond to real life where patients are prone to misestimate and misuse these therapy parameters.

5.7.1 LA Insulin Parameters for *In Silico* Cohort

To address the first point, each *In Silico* subject's glargine dosage must be titrated to first achieve the perfect BG that would be attainable only in the controlled conditions of the Simulator. Then this perfect therapy can be modified to achieve the realistic titration for every subject.

As glargine is basal insulin, the titration can be done without the meals and other disturbances. Using the 100 adults subjects, the following conditions for the titrations are formulated:

1. The minimum long-term BG must be above 90 mg/dl.
2. The average long-term BG must be above 112.5 mg/dl.

6-day simulations are used. Essentially, the subject is titrated by pushing the average BG down to 112.5 mg/dl but not allowing the minimum BG fall below 90 mg/dl (algorithmically, the titration is done in log space). The results of the titration are presented in Figure 42.

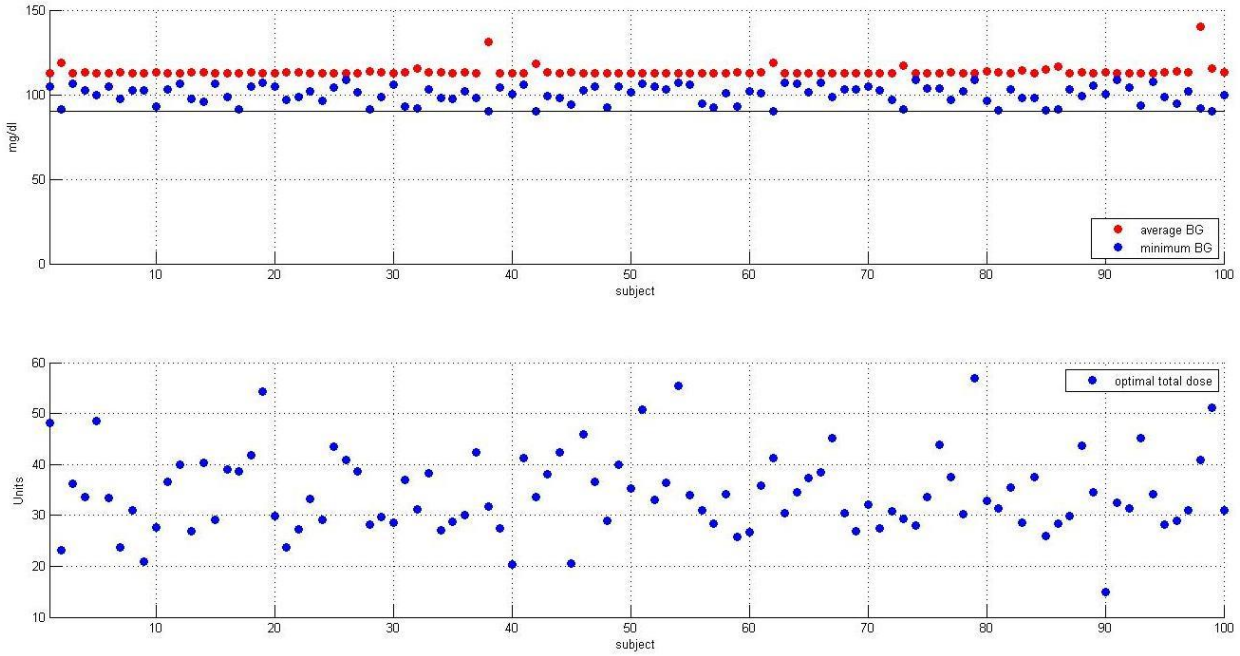

Figure 42. Titration results.

The top graph presents the average BG achieved for every subject (in red) and the minimum BG for every subject. Minimum BGs do not go below 90 mg/dl while the average is close from above to 112.5 mg/dl bar few exceptions. The bottom graph presents the corresponding perfectly titrated doses of glargine corresponding for every subject.

The titration described above resolves the second obstacle discussed earlier – that of not having the glargine parameters in the Simulator for each *In Silico* subject. Now the perfect dose is known, and the timing used during the titration (one injection a day) can be used as the perfect timing parameter. Since the titration was done under the idealistic conditions with no meal disturbance, the reference time can be chosen as any time of the day, for example 8:00am.

5.7.2 Behavioral *In Silico* Populations

To resolve the second obstacle – that of not having realistic parameter values for the reference therapy – we introduce the concept of reference populations. The concept is graphically described in Figure 43.

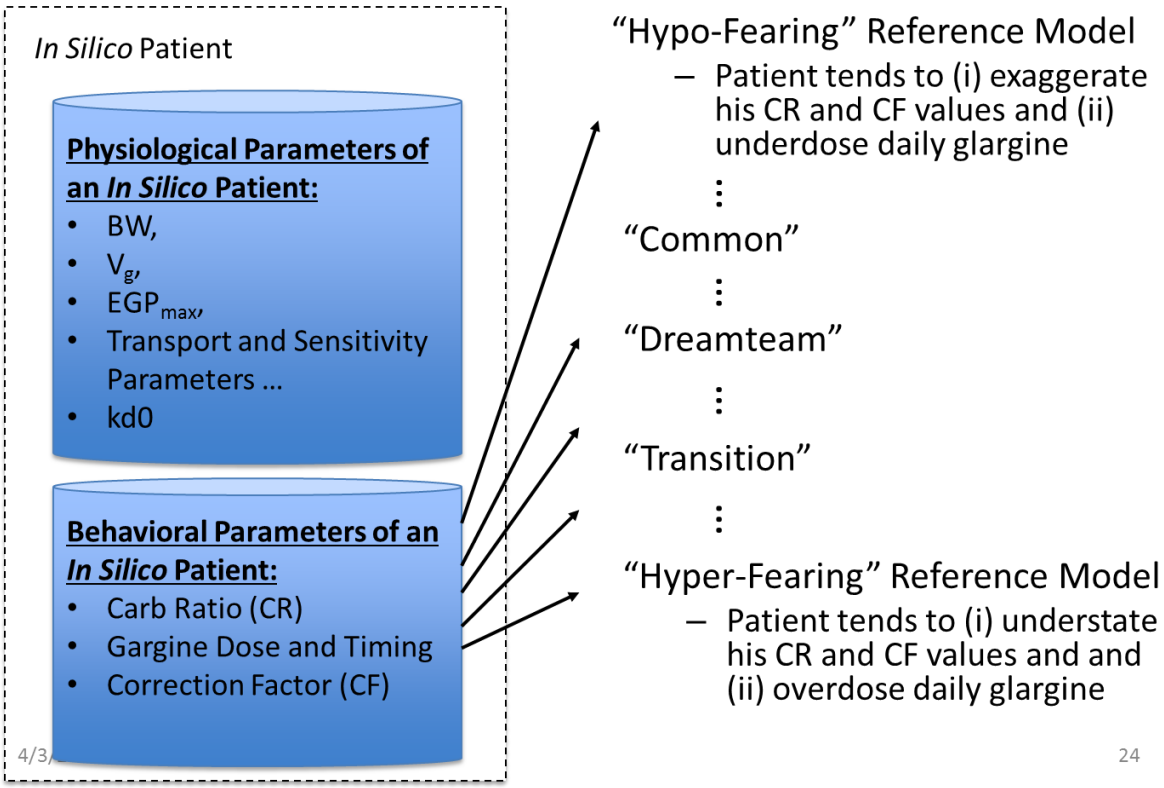

Figure 43. Reference populations concept.

As shown in Figure 43, by slightly varying the values of CR, CF, and glargine dose and timing, various *In Silico* populations can be created that differ in their "behavior".

As a preliminary evaluation, we have created a reference MDI therapy population model in which daily long-acting insulin doses and rapid-acting mealtime correction factors and carb ratios have been titrated to achieve an average A1c of 7.98% (standard deviation = 0.52), an average percentage time above 180 mg/dl of 46.6%, and an average percentage time below 70 mg/dl of 0% (Appendix J). This primary reference treatment model could be taken to represent a hypoglycemia-fearing group patients that tend to gravitate to higher levels of BG. In this case, the objective of the algorithm is to reduce A1c without significantly increasing the risk of hypoglycemia.

It is important to keep in mind that HbA1c that is measured in clinical setting – glycated hemoglobin – has a different meaning when used in our *in silico* validation. It would be incorrect to equate HbA1c that

is a form of hemoglobin that is measured to identify the average plasma glucose concentration over prolonged periods of time to the A1c ('Hb' omitted intentionally) that results from a reversed formula of [82] based on the average BG over just two days of simulation. That is why the primary focus of the results should be the average BG values. Still, we report A1c to provide an approximate relation to what the therapy could result in if used in real patients long term.

Another important disclaimer (addressed later in this chapter) is that in real population glargine injection time varies. Usual times are before breakfast and at bedtime. In addition, some people split their daily dose in two parts and administer them separately at these two times. For our purposes here we have chosen a scenario with just one glargine injection a day, which occurs in the morning at 6:00 AM with 100% compliance.

In the validation simulations, parameters are programmed the same way they were programmed in the simulations conducted to create this population (Appendix J). In particular:

- The carbohydrate ratio for each *in silico* patient is based upon the subject's ideal carbohydrate ratio. A random number between 1.0 and 1.1 was generated and then applied as a factor to that CR to emulate an overstatement.
- The correction factor for each *in silico* patient was modified similarly.
- The long-acting insulin part of the insulin transport in the simulation environment is characterized by the coefficient kd0 (as described in 5.2 New Insulin Transport Model). Its nominal value is 0.00028.
- The daily LA insulin dose is titrated for each subject to achieve, on average, the A1c of around 8 % across two days.
- All subjects/profiles are run under 2-day scenarios with the meal plan of:
    - first day:
        - 0.5 g CHO/kg for breakfast at 8:00 AM

        - 0.9 g CHO/kg for lunch at 2:00 PM
        - 0.7 g CHO/kg for dinner at 8:00 PM
    - and second day:
        - 0.5 g CHO/kg for breakfast 8:00 AM
        - 0.9 g CHO/kg for the dinner 8:00 PM

For all of the *in silico* results presented below a universal formula for choosing an appropriate q-parameter for each patient is used:

$$q = 10^{\beta_{ho0}+\beta_{ho1}BW+\beta_{ho2}TDI} \quad \textbf{(49)}$$

where BW refers to the patient's body weight in kilograms and TDI is the patient's total daily insulin requirement in Units. In practice this formula would be taken as an initial starting point for patients encountering the algorithm for the first time. The other design parameter $\Delta\overline{BG}_{desired}$ was individually numerically tuned for each *in silico* patient.

Another behavioral population that is highlighted in Figure 43 is "hyper-fearing" population. This *in silico* cohort consists of patients who tend to have lower BG values, perhaps reflective of "hyper-fearing" individuals, who are prone to understating their carbohydrate ratios and correction factors. These virtual patients are created by again randomly tweaking adults from the original *in silico* cohort but this time the other direction. Particularly,

- The carbohydrate ratio for each *in silico* patient is based upon the subject's ideal carbohydrate ratio. A random number between 0.9 and 1.0 was generated and then applied as a factor to that CR to emulate an understatement.
- The correction factor for each *in silico* patient was modified similarly.
- The daily LA insulin dose is titrated for each subject to achieve, on average, the A1c of around 5.2 % across two days.

- The meal scenario and kd0 parameter for the *in silico* patients are the same as for "hypo-fearing" population.

In running the *in silico* trial, a universal formula was used to calculate the patient-specific control parameter *q*, similarly to (49):

$$q = 10^{\beta_{hr0}+\beta_{hr1}BW+\beta_{hr2}TDI} \quad \textbf{(50)}$$

(50) differs from (49) only in its β coefficients.

5.7.3 Results

Some representative *in silico* trial results are illustrated in Figure 44. Each plot shows a comparison between the reference MDI therapy model (black "std" trace) and the advisory system (red "opt" trace). Note that hour 0 corresponds to 6:00 AM (assumed to be the time of the daily injection of insulin-glargine). Five meals are administed over the course of two days, as described above, and are easily identifiable on the plots by the corresponding BG spikes that follow them. From the plots one can see the difference in the pairs of traces leading to lower average glycemia under the advisory system. The LQG algorithm, informed by continuous monitoring (and with its patient-adapted q and $\Delta\overline{BG}_{desired}$ values), makes different decisions about the amount of insulin to be injected as the correction part of the pre-meal bolus compared to the "decision" made by the reference therapy.

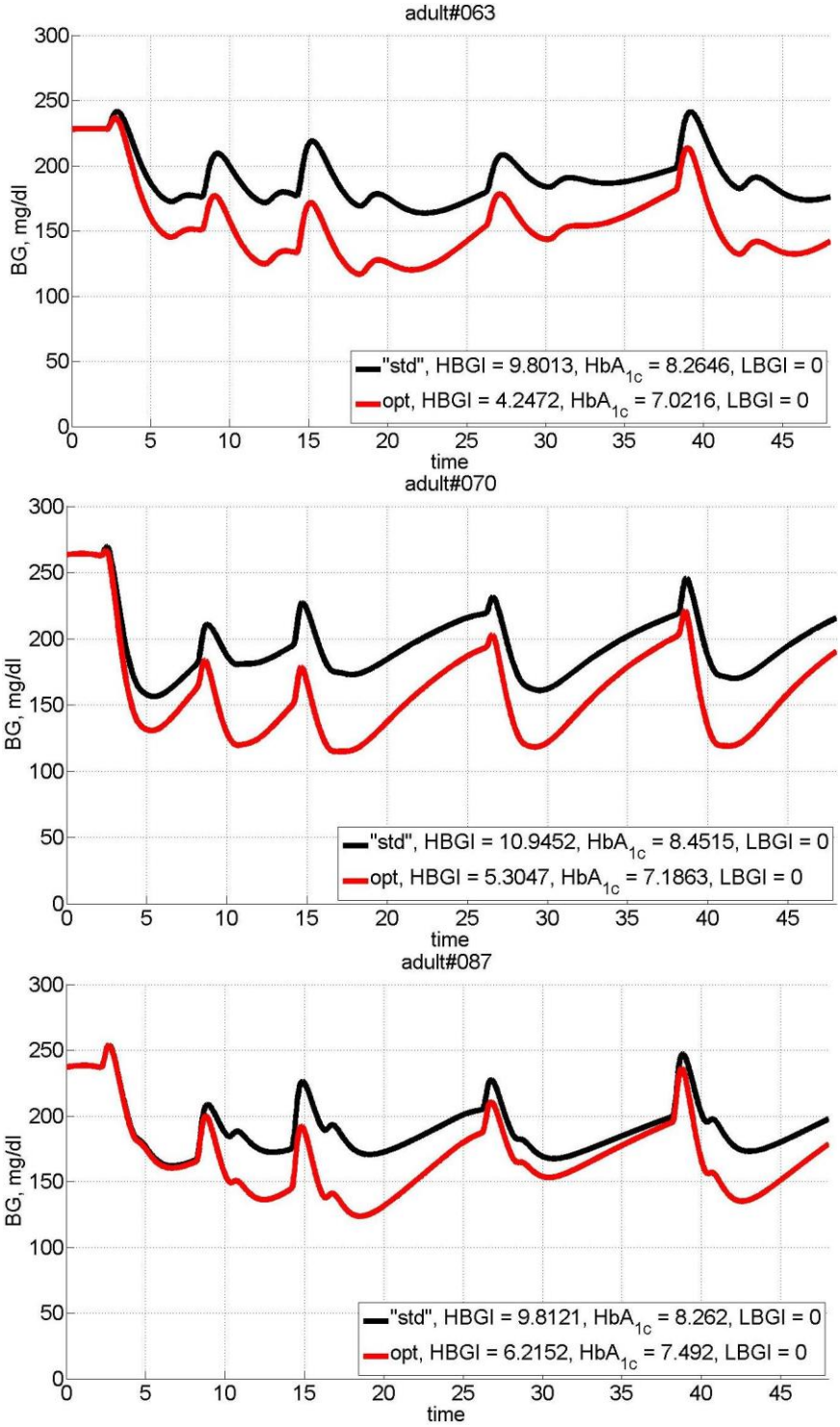

Figure 44. Examples of reducing A1c by the MDI advisory system in "hypo-fearing" subjects.

A summary of the key statistics of the nominal *in silico* evaluation appears in Table 8 below. As can be seen, the Smart Pen LQG Algorithm is capable of reducing HbA1c by over one percentage point (from 7.98% to 6.79%) without significantly increasing the risk of hypoglycemia. Note that "LBGI" refers to the low blood glucose index, a measure of the patient's risk of hypoglycemia, where in this setting any LBGI (introduced in [54]) below 1.5 can be regarded as essentially "no risk". Similarly, "HGBI" is a measure of the risk of hyperglycemia [54].

Table 8. *In silico* evaluation.

	LBGI	**HBGI**	**A1c**	**Time above 180 mg/dl, %**	**Average BG**	**Time below 70 mg/dl, %**
Reference Therapy	0.001 (0.008)	8.64 (2.72)	7.98 (0.52)	46.6 (18.78)	182 (14.6)	0 (0)
Smart Pen LQG (nominal case)	0.594 (0.724)	5.44 (1.67)	6.79 (0.5)	19.9 (9.58)	148 (14.3)	0.047 (0.27)

Few preliminary runs were also done for the "hyper-fearing" population. Figure 10 below shows sample *in silico* trial results for three subjects from this cohort. Note that in each case the Smart Pen LQG Algorithm has the effect of significantly decreasing the risk of hypoglycemia, while maintaining very low blood glucose concentrations. One caveat here is that the Type 1 simulator used in this study does *not* include a model of counter-regulation and is prone to underestimating low BG values as a result. More generally, it is impossible to draw general conclusions from three *in silico* trial results. Still, the results do illustrate that the Smart Pen LQG Algorithm has the potential to accommodate the needs of different kinds of patients.

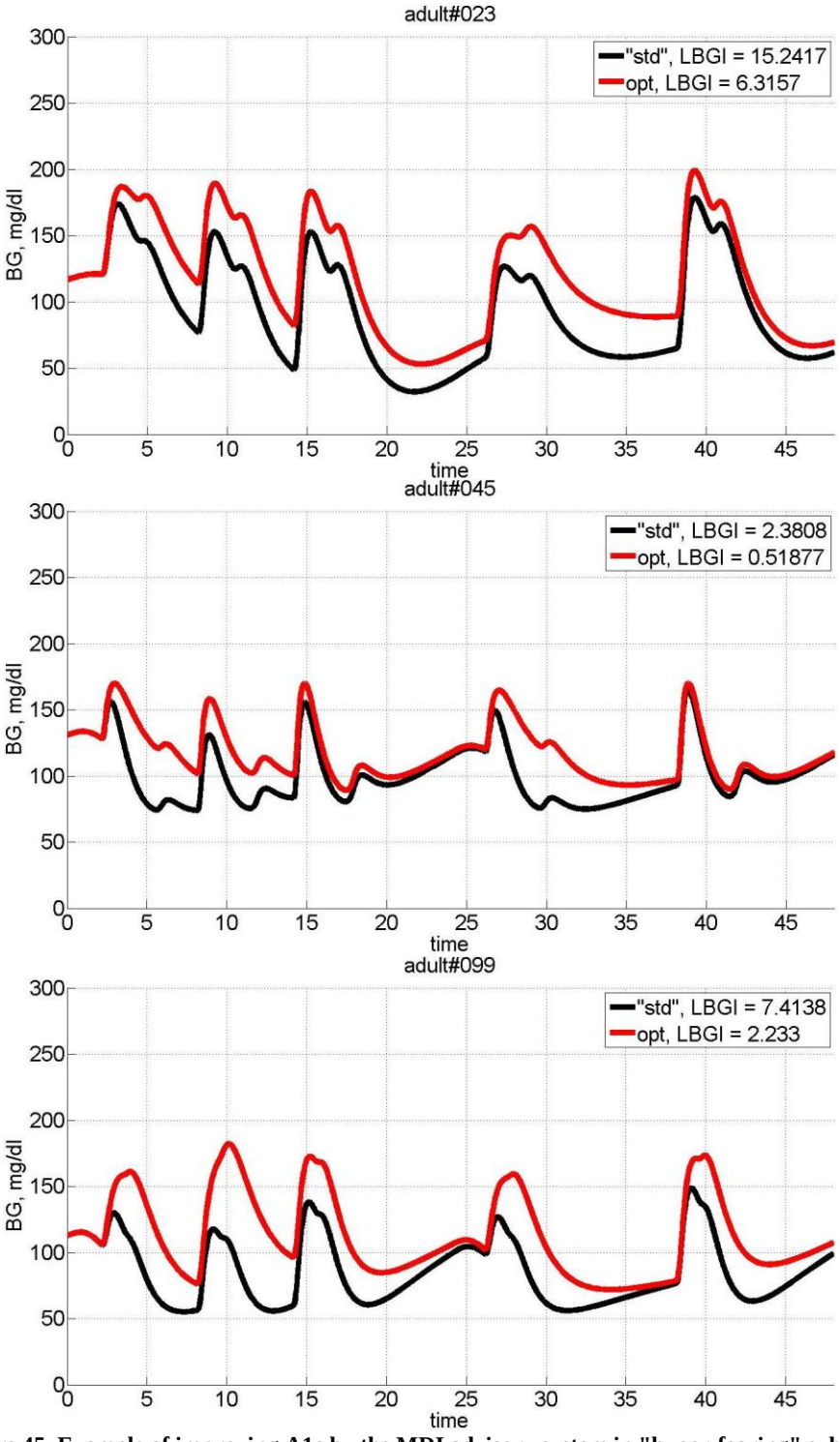

Figure 45. Example of improving A1c by the MDI advisory system in "hyper-fearing" subjects.

5.8 Robustness and Real Life Application

5.8.1 Pharmacokinetics Parameter Uncertainty

To test the robustness of the algorithm against uncertainty about the patient's glargine PK characteristic, we ran a sensitivity analysis in which each patient's true kd0 was adjusted by +/-25% and +/-10%, respectively, relative to the population average value. The results are shown in Table 9 below.

Table 9. Testing under four robustness scenarios.

	LBGI	HBGI	A1c, %	Time above 180 mg/dl, %	Average BG	Time below 70 mg/dl, %
Reference Therapy	0.001 (0.008)	8.64 (2.72)	7.98 (0.52)	46.6 (18.78)	182 (14.6)	0 (0)
Smart Pen LQG, 0.75*kd0	0.444 (0.623)	6.83 (2.36)	7.21 (0.56)	29.52 (12.3)	160 (15.9)	0.02 (0.2)
Smart Pen LQG, 0.9*kd0	0.497 (0.65)	5.86 (1.81)	6.94 (0.49)	23.01 (10.19)	152 (14.06)	0.011 (0.08)
Smart Pen LQG, 1.0*kd0 (nominal case)	0.594 (0.724)	5.44 (1.67)	6.79 (0.5)	19.9 (9.58)	148 (14.3)	0.047 (0.27)
Smart Pen LQG, 1.1*kd0	0.738 (0.87)	5.21 (1.6)	6.65 (0.53)	17.52 (9.1)	144 (15.23)	0.27 (0.95)
Smart Pen LQG, 1.25*kd0	1.069 (1.33)	5.07 (1.79)	6.47 (0.59)	15.2 (8.74)	139 (17.02)	1.25 (3.43)

Note that even when the Smart Pen LQG algorithm is tuned with the "wrong" kd0 value, it is still capable of significantly reducing A1c relative to the Reference Therapy model.

Figure 46 below illustrates a tradeoff that has emerged in the sensitivity analysis. Namely, under the advisory system, A1c and LBGI are traded off as the "true" value of kd0 varies from 75% nominal to 125% nominal (smaller kd0 corresponds to a slower absorption of glargine.) For all cases, the Smart Pen LQG

Algorithm results in lower A1c values than the reference MDI model (shown as a red dot), yet this comes at the expense of slightly greater risk of hypoglycemia.

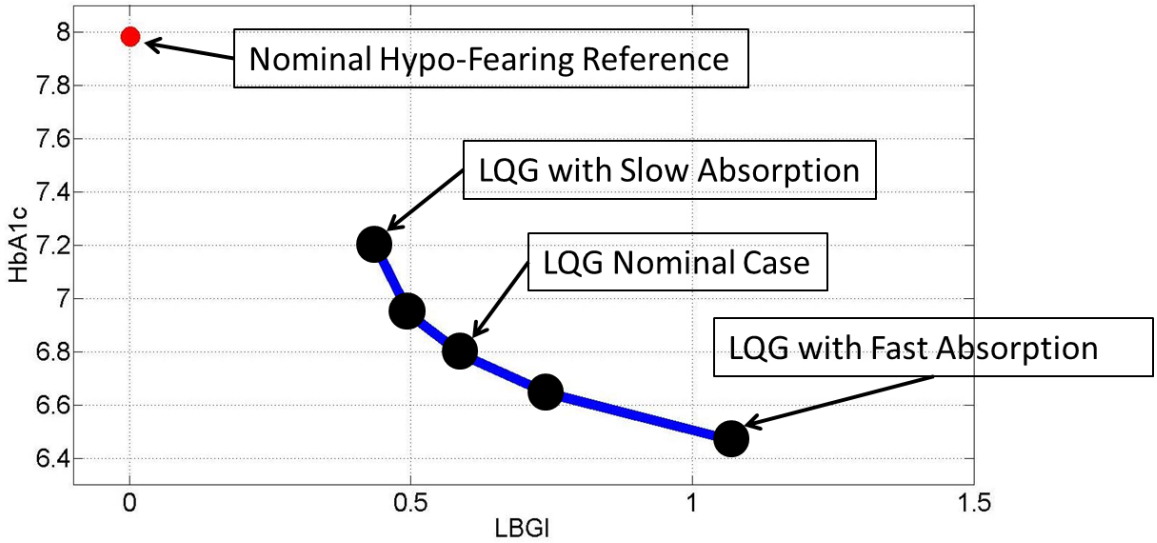

Figure 46. A1c plotted against the risk measure LBGI.

5.8.2 Behavior-Based Therapy Uncertainty

In real patients, the time of long-acting insulin injections is not uniform across the days. For example, the patient injects their long-acting insulin at 7am one day, at 7:15am on the next day, at 6:55am on the day after that and so on. To address this, we design another set of simulations that put a "jitter" around the injection times.

We Run a 30-day simulation for each *in silico* subject, with 3 meals a day, where the long-acting insulin injection times written in the scenario files are pregenerated and are uniformly distributed around the default time of the injection, Figure 47.

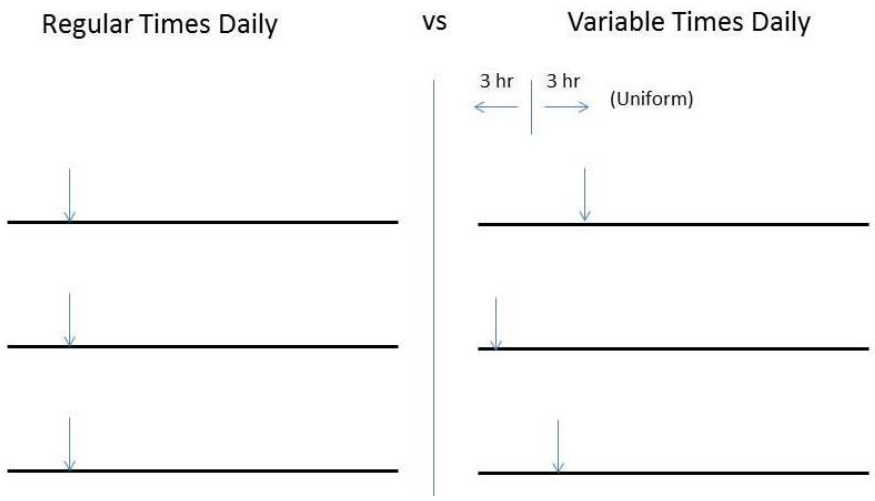

Figure 47. Varying long-acting insulin administration.

The meal regimen is the same as in simulation described above. The results of such simulation without the advisor are in Table 10.

Table 10. Varying glargine administration in hypo-fearing population without advisor.

Without Advisor	Mean BG mg/dl	A1c %	%<70	%>180	% 70-180	LBGI	HBGI	ADRR
Without Jitter	173.5	7.94	0.03	37.6	62.4	0.03	7.27	7.3
With Jitter	176.9	7.95	0	40	59.95	0	7.7	7.7

Predictably, the introduction of variability in long-insulin time administration decreases time in range and increases the hyperglycemia risk and variability indices. Then we run the simulation under the operation of the adviser. The results are in Table 11.

Table 11. Varying glargine administration in hypo-fearing population with advisor.

With Advisor	Mean BG mg/dl	A1c %	%<70	%>180	% 70-180	LBGI	HBGI	ADRR
Without Jitter	131.6	6.35	0.68	10.4	88.9	0.46	2.31	2.77
With Jitter	132.6	6.35	0.52	10.3	89.2	0.4	2.34	2.74

While the introduction of the varying glargine administration did marginally reduce the efficacy of the advisor, it did not have impact as significant as in the case of the simulations without the adviser. Thus in the case of the varying glargine administration, the advisory system not only retained, but improved the advantage over the conventional therapy, reducing A1c for over 1.5%.

Finally, we test the scenario of a glargine injection being completely skipped. We run 10-day simulation skipping the 3rd injection, both with and without the adviser. Results are in Table 12

Table 12. Skipped glargine injection on the 3rd day out of 10.

	Mean BG mg/dl	A1c %	%<70	%>180	% 70-180	LBGI	HBGI	ADRR
Without Advisor	165	7.95	0.1	34.2	65.7	0.08	6.75	6.83
With Advisor	128.7	6.36	0.92	8.87	90.2	0.53	2.1	2.6

The advisory system again maintains significant advantage over the conventional therapy in all measures, even when a long-acting insulin injection was skipped.

5.8.3 Real-Life Tracking of the Virtual Basal Rate

In silico, u^{LA} for every subject was obtained by running a simulation for 20 days with no meal disturbances, then saving the data and using a 2-day part of it for the validation runs. Clearly, this approach is not possible in real life. Importantly, not only it is impossible to "run" a patient for 20 days with no meals, but the 100% compliance with 6:00 am injections is not realistic either. Whatever time for the daily injection the patient chooses, it might varying every day depending on their daily situation or an injection might be skipped altogether. Moreover, the patient can have not one but two long-acting insulin injections a day.

To address these issues, we designed a "u^{LA} generator" that can generate Virtual Basal Rate and consequently u^{LA} by using only accessible parameters of the patient's therapy.

The generator makes use of the discretized equation of the long-acting insulin SC compartment (34). Converted into state-space form, this SC compartment state is propagated until the next daily (or half-daily) injection in 5-minute steps. This process is repeated until the steady state is achieved. This steady state is understood as the time when the contents of the compartment at the time of each consecutive injection are equal for the first time. It is regarded as the end of long-acting insulin stacking after which the VBR is oscillating around the average in a consistent fashion.

From the steady state, the concentration of the long-acting insulin SC compartment is calculated as follows:

$$I_{SC0} = \frac{a^{n-1} b J_{LA}}{1 - a^n} \quad \textbf{(51)}$$

where a and b are known population average parameters resulted from the discretization of (34), n is the number of steps between long-acting insulin injections, and J_{LA} is the patient's prescribed long-acting insulin injection amount. Note that n depends on the number of long-acting insulin injections a day and thus accommodates both once and twice daily injections (or more which is uncommon)

This provides the foundation for the generator which then uses the (34) to produces the u^{LA} "on the fly" as required by the rest of the system. This approach, unlike the pregenerated Virtual Basal Rate curves allows to track the deviation from the average VBR whenever the long-acting insulin is injected or even skipped, as long as the system is timely informed about each new injection.

5.8.4 MDI Advisory System Prototyping Experience

As described above, to take the advantage of the Virtual Basal Rate including the time when it is especially useful like when a long-acting insulin injection is skipped, it is imperative to inform the system when the long-acting insulin injections take place and how much insulin is injected.

In the course of this work, a working prototype of the MDI advisory system was created using Android smartphone development platform on which another diabetes technology system is built – DiAs [46]. A prominent part of the prototype was the user interface which provided for the interaction between the patient and the system. To accommodate the u^{LA} generator as described above, the following screen was included in the user interface (Figure 48).

Figure 48. Long-acting insulin information entry via user interface.

Every time the patient injects long-acting insulin, they are required to access this Graphical User Interface (GUI) screen and enter the amount of insulin they just injected or are about to inject. The time of the injection is saved automatically when the user approves the entry.

During the prototyping and especially during the user interface design, numerous iterations were done on what the interface should actually be, what kind of information it should present or require, what kind of visuals should be used for that and so on. Interestingly, these conversations usually took place between the researchers, a pharmaceutical/medical device company and physicians, but never involved actual patients. The designed process proved to be prolonged and "painful" which was a motivation for the top-down approach described in Chapter 6 of this dissertation. Every consensus that was reached would be later overturned, but what we present here was the version approved at the time of writing.

For example, it was determined that an additional screen must be following the screen in Figure 48 to double check whether the amount was entered correctly and require a final confirmation (Figure 49).

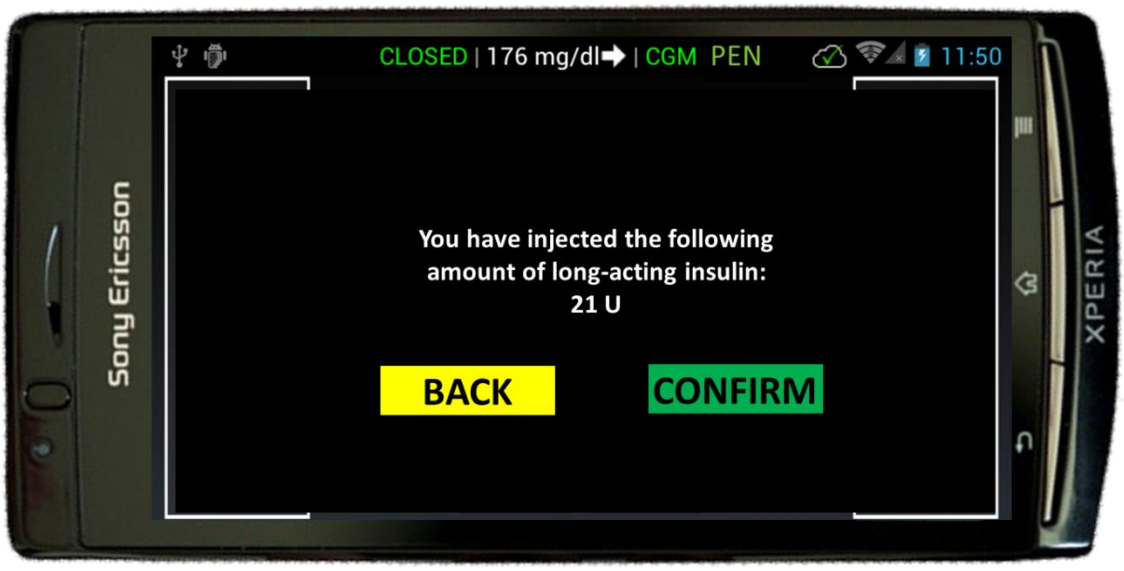

Figure 49. Long-acting insulin entry confirmation screen.

Much thought was given to the behavioral aspect of using the system. For example, a patient might enter the long-acting insulin injection information before the injection and then after the injection intend to mistakenly do it again. This duplicate information in the database would result in a lot of "IOB" insulin which would negatively affect the system's performance. To address such scenario, an additional screen was implemented that would remind the user about past injections if the long-acting insulin entry screen is entered too often (thus implying that the previous visit and entry were forgotten) – Figure 50.

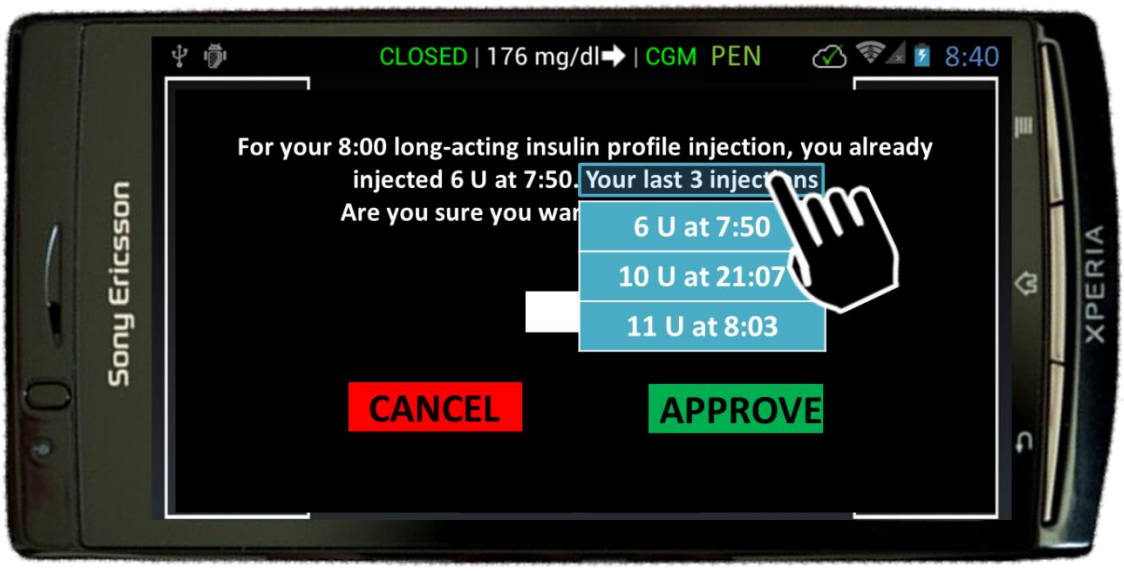

Figure 50. Long-acting insulin injection screen if entered again shortly.

This interface would provide information about the past three injections. Still, the patient is able to enter the long-acting insulin value, approve it, and proceed to the confirmation screen. This override capacity is implemented for the case when the first injection (supposedly few minutes ago) was too small by mistake and the patient intends to add the missing long-acting insulin. Note that all of these challenging cases will be successfully tacked by the u^{LA} generator and no insulin will be missing in the system.

While all the interface screen can be found in Appendix K, we present here one more detail that pertains to what was discovered in Chapter 4 – that we cannot always rely on models and there must be a substitute therapy to revert to when the conditions are especially challenging.

For example, the screen that presents the optimally calculated correction advice at the time of meals (Figure 51) also indicates how big or small this correction is relative to what the conventional therapy for this patient would produce (green font in the upper part of the screen).

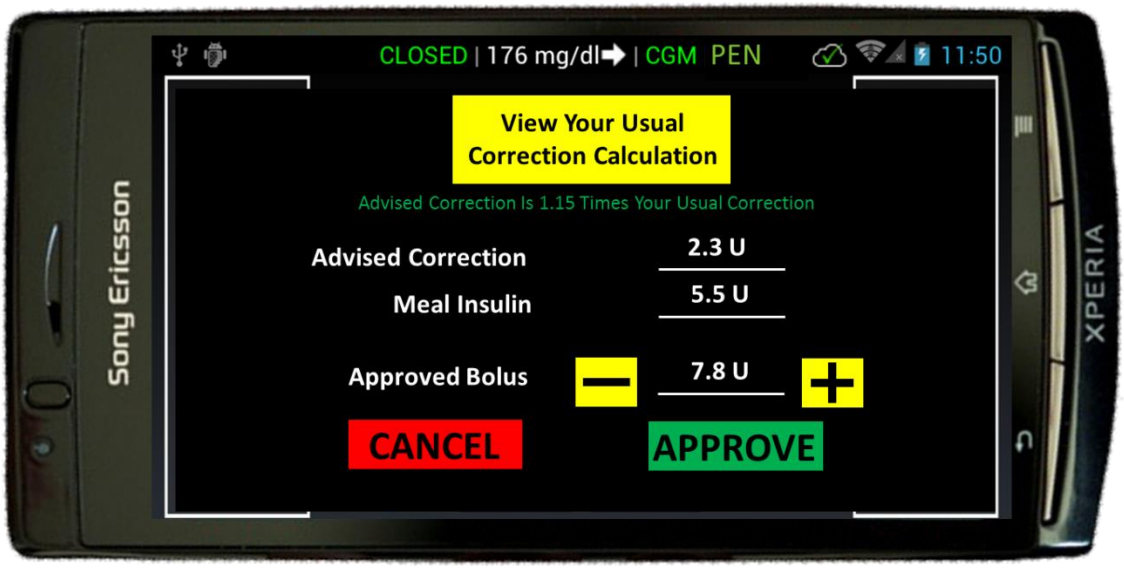

Figure 51. Advice Screen.

The button 'View Your Usual Correction Calculation' allows the user to see what their conventionally calculated correction is exactly to make a more informed decision about whether to accept the advice – Figure 52.

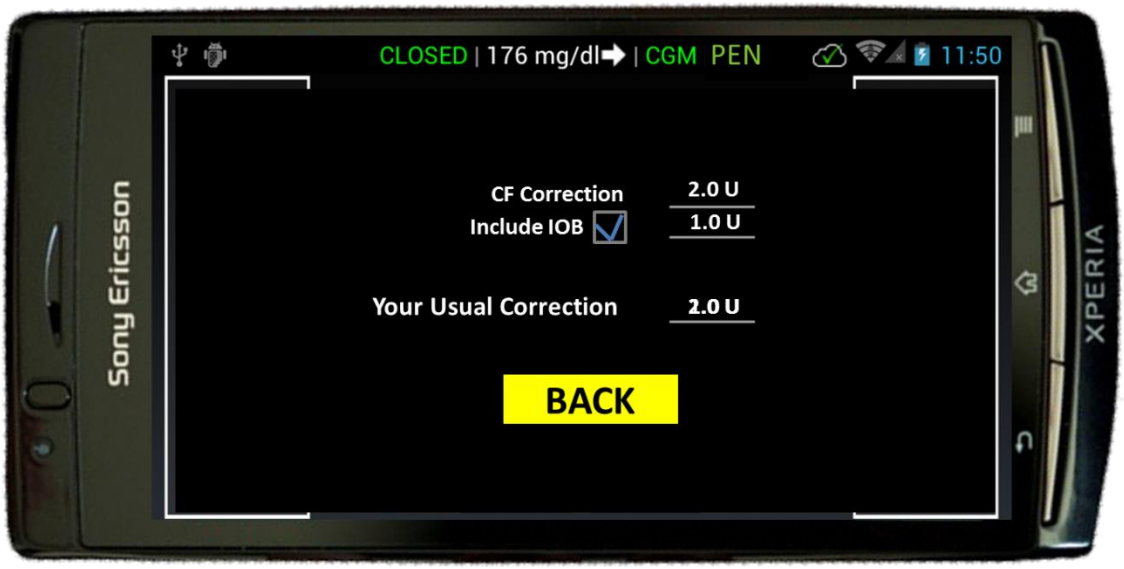

Figure 52. Conventional correction calculation screen.

The screen contains a check-box that allows the patient to calculate the conventional correction in two different ways depending what their individual conventional therapy actually is: with or without IOB included. The IOB corresponds to the Insulin On Board calculated as in [83].

Finally, note that the indicator message of the corrections ration from Figure 51 can take a different color – red – if a certain ratio threshold is exceeded. For example, if we believe that the advised correction should not exceed the conventionally calculated value by more than 25% and this threshold is passed, the red color of the message would indicate to the patient that it would be safer to revert to the conventionally calculated values (Figure 53).

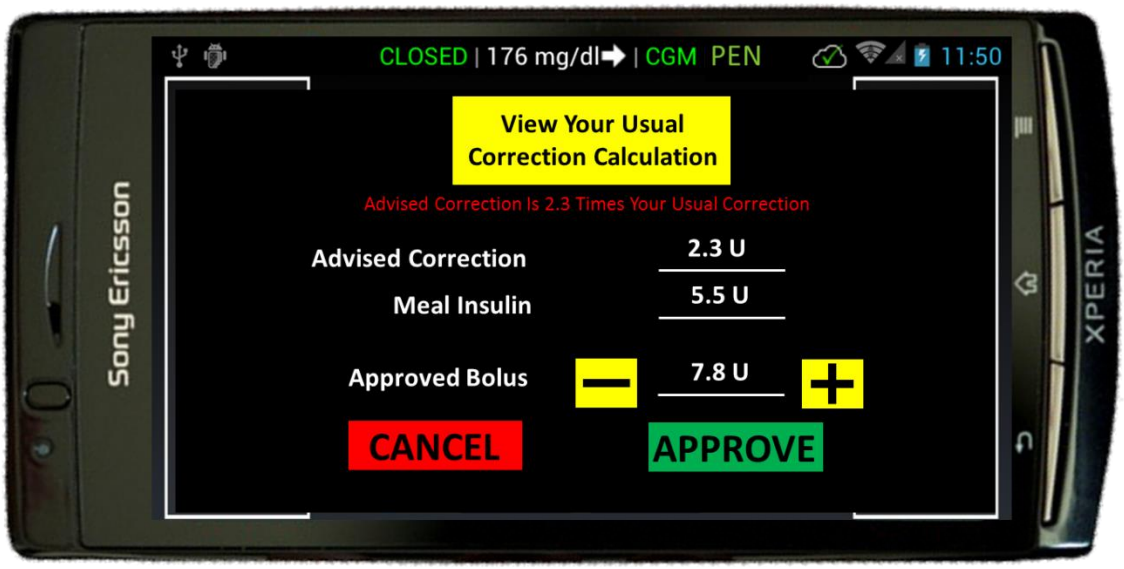

Figure 53. Advice screen with an alert.

This section described how the experience of the work from Chapter 4 and Chapter 5 led us to closer consider the behavioral aspects of diabetes technology. The next chapter generalizes our experience with a comprehensive top-down approach that should facilitate design process of similar systems.

Chapter 6

Diabetes Technology Systems Design Methodology

6.1 What is success?

The work presented so far was centered on developing algorithms that would successfully control blood glucose in type 1 diabetics. However, very little attention was devoted to type 1 diabetics themselves. While there was some discussion about human-automation relationship and human-machine interfacing, the fact that the system did not perform as well in real life as *in silico* indicates that not all real life factors were taking into account.

It is only natural for an engineer to concentrate on the engineering system. However, when it comes to systems engineering, there is much more contextual investigation to be done to ensure that the system is deployable and that there will be no additional constraints on its operation once it's deployed. In biomedical engineering systems like AP, a lot of context is found in patients. The result of engineering design in such a system is not just the algorithm or technology, but *a therapy.*

Biomedical engineering support systems, which AP is, pose an interesting case of engineering systems in that the operator of the system is also the object of the system's action. An important part of such system's architecture is the information flow from the user to the system. The volume and quality, or in this context, the user's compliance and commitment, defines how efficient if effective at all the system can be. In other words the patient benefits the more from the system the more they are willing to commit to its usage. Less obviously, more efficient system can anticipate more involvement from the patient

encouraged by the results. These psychological factors cannot be left out of consideration when designing such a system.

- Will system accommodate any type of patient?
- If not, which one or several audiences should the system be designed for?
- What amount of commitment can the system anticipate?
- Will the system be able to take the illness management burden away without incurring additional mental burden of using the system?

These and other questions cannot be answered without obtaining the opinion of the very user of the system. [84]

The methods below allow to "fill in" the pieces that are not obvious while working on the engineering part per se. However, these pieces are essential to the system if it is ever to become a product people would actually use. This larger scale framework requires methods that structure the problem of integrating the system into real life and that point out what requirements from any and every potential stakeholder have been missed so far. It is then necessary to work on satisfying these requirements. In fact, it is preferable to run this kind of qualitative analysis of the potential system first, not to fall victim of the Pareto principle.

Since many approaches described in this section are used in consumer product industry, applying them to biomedical systems poses additional difficulties *and* additional value because of the very close tie between the user and the device/system. In the case of artificial pancreas systems, the user and the system are connected in literal sense and not only the user's action drives the system, but also the system's action drives the user in the most impactful way. Hence the importance of considering all the ramifications of such system's deployment and operation.

6.2 Methods

We use stakeholder mapping method – a simpler version of stakeholder influence mapping – to map out all the stakeholders of the Artificial Pancreas community. Particularly, we brainstorm all the potentially influenced and influential parties and then lump them into a tractable number of stakeholder groups.

Consequently, we conduct a holistic requirement analysis (or holistic requirements model – HRM) informed by these stakeholders. In particular, we design a survey which questions directly correspond to the requirements groups of HRM. We ask respondents submit answers to these questions and use thematic analysis to convert their replies into actionable and relevant requirements.

In addition, we adopt the use of Ishikawa diagram – a cause-effect tool that allows to identify groups of risks to structure and simplify risk mitigation. We design our own 7D Ishikawa diagram that pertains specifically to Artificial Pancreas systems.

6.3 Stakeholder Influence Map

A simplified version of a tool widely used in systems analysis – Stakeholder Influence Map [85] was used. Omitted are the influences between the stakeholders since the goal of the study is to poll them individually and not infer their relationships.

We start by brainstorming all the stakeholders of the AP system universe, and then identify the groups that, according to the Stakeholder Influence Map tool [85], we *must* get requirements from (in parenthesis, is the corresponding number of respondents for each group that we ultimately polled):

- Patients
    - Tech savvy patient (64)
    - Naive patient (3)
    - Patient with special needs (1)
- Parents of patient (45)

Also, the groups that we *should* get requirements from:

- Spouses/partners of patients (2)
- Physicians (2)
- Certified Diabetes Educators (12)
- Diabetes technology researcher s (2)
- Medical device companies (2)
- Regulators (1)

And finally, the groups that we will *ignore* for the time of this study:

- Hospitals employees (other than physicians)
- Insurance companies
- Advocacy Groups
- Governmental funding sources
- Policy makers (legislative branch)
- Private sponsors
- General public

We ignore some stakeholders for now as their impact on the AP systems *design process* is not as significant as that of the others', but at the same time it is challenging to elicit responses from them.

Also, from a product development point of view, this is not a comprehensive list as more of the commercialization stakeholders would be taken into account (e.g. marketing, sales, etc). However, commercialization is out of the scope of this work and therefore corresponding stakeholders are left out for the purpose of this analysis.

6.4 Holistic Requirements Model

Holistic Requirements Model (HRM) is a systems approach tool [86] that provides an analysis framework to help define the system's requirements. It consists of five distinct groups of requirements and represented graphically in the Figure 54.

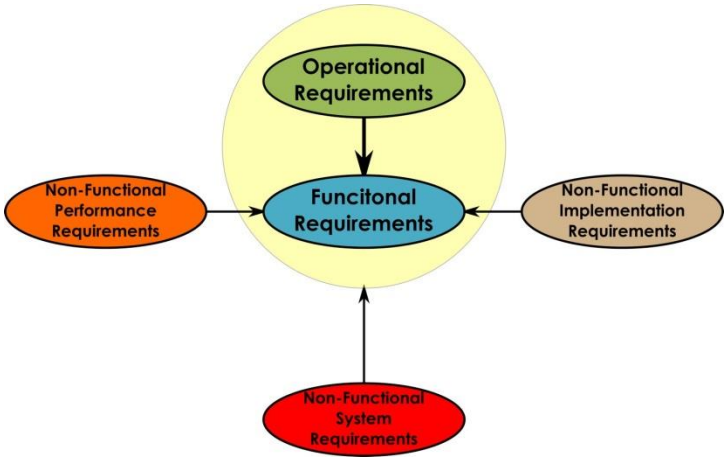

Figure 54. Holistic Requirements Model

Every system has two types of requirements:

- Operational requirements
- Functional requirements

Operational requirements define what the purpose of the system is overall. Operational requirements are often omitted since they are deemed obvious to the user/developer of the system. However, operational requirements help ensure that the mental models of the engineers and end users match and that the development process is conducted accordingly. Also, specifying the operational requirements helps to make the set of functional requirements more comprehensive.

Functional requirements define what the system needs to do in order to fulfill the operational requirements. The functional requirements, however, do not provide information about how something

must be done or how well – only what needs to be done. In addition, functional requirements should be implementation-independent.

In addition, there are non-functional requirements to the system. These are usually constraints and (unlike the functional requirements) define how something should be done and how well it should be done. There are three categories of non-functional requirements:

- Performance requirements – how well a function is to be performed.
- System requirements – define large scale constraints like size of weight of the system, safety, cost, etc.
- Implementation requirements – using what technology the system should be built and possibly in what legislative framework.

6.4.1 Survey

When designing the survey, we aimed to map each type of requirements into a question. One exception was the non-functional system requirements category which we generalized into a quantitative performance question related to the whole system. We did this as we anticipated many functional requirements that would be very hard to quantify the performance for. Thus, the five types of requirements produced five questions:

- What would the purpose of the system be overall?
- In particular, what functions would the system need to perform to fulfill its purpose?
- Keeping in mind that no system can be perfect, what is the lowest percentage of the time that the system would need to work perfectly to be safe? [80%, 85%, 90%, 95%, 100%]
- What would the very basic feature of the system be, *without* which it would be unusable? Alternatively, what characteristic would make it unusable?
- How do you envision your system working? What parts of existing technology should it use or be built upon?

6.4.2 Thematic Analysis and Scores

The total sample size summed up to 134 respondents. This qualitative study resulted in 536 free form text-based responses which required thematic analysis [87] to be performed to process the results into a meaningful HRM. In processing the results, we generally followed the six phases of thematic analysis that Braun and Clarke proposed [88].

It was deemed useful to include certain weights or scores for each requirement to indicate its importance. Such weights could be inferred from the number of times this requirement was mentioned in the responses. However, calculating such scores was not straightforward and it is important to note that in thematic analysis, more instances do not necessarily mean the theme itself is more crucial [88]. Some generic mechanics of how responses would map into categories are presented in Appendix L.

The answers varied significantly in their length and nature and did not always map directly in the category the corresponding question intended for. For example, one answer to question 1 was 16 characters long, while another answer to the same question was 1,373 characters long. Such long answers usually "fed" more than one category (and several requirements in each).

When processing the answers, we assisted the thematic analysis by the algorithm proposed by Burge [86] (Figure 55).

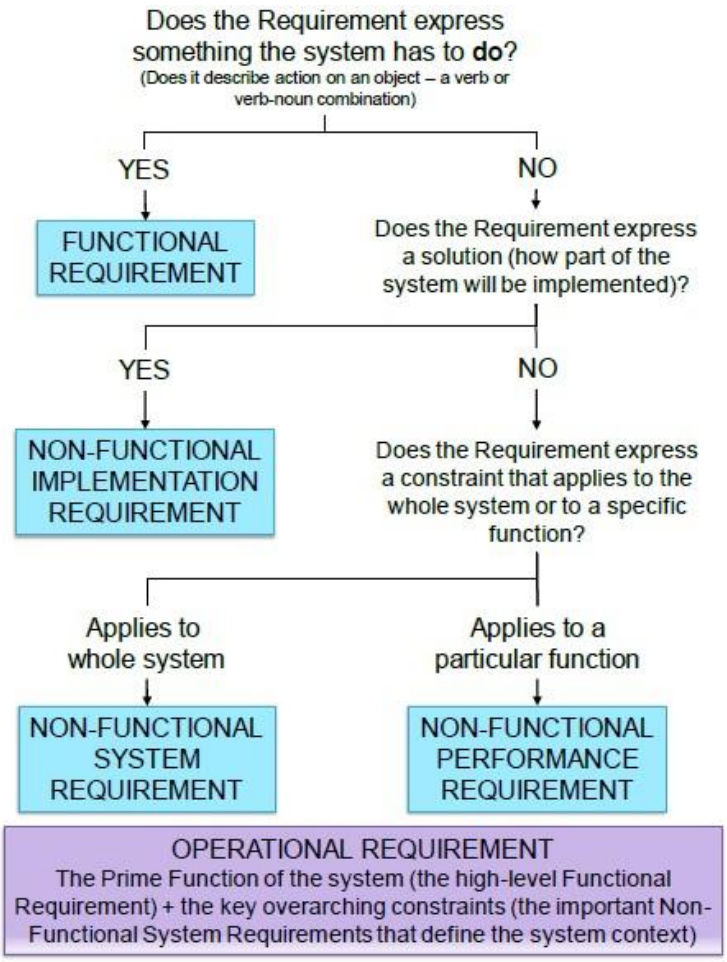

Figure 55. HRM Requirement Processing Algorithm.

Therefore, the scores should not be considered proxies for the number of people mentioning a requirement. Nor should they be considered weights of importance because the answers varied widely in the language they used – sometimes being very strong statements and sometimes assuming optionality. Often, the requirement would not be mentioned because it is obvious (see A1C score in Table 13). The scores only provide a "soft" reference of how much a certain requirement is on the mind of the stakeholders.

6.4.3 Responses and Resulting HRM

The resulting HRM had 4 groups of requirements:

- Operational requirements
- Functional requirements
- Non-functional implementation requirements
- Non-functional system requirements

Plus the system-level performance requirement expressed in the desired percent of the time the system would need to be working perfectly.

The operational requirements are presented in Table 13. This one and all the following tables also present the relatives score values.

Table 13. Operational Requirements.

	Score
Increase time in range	52
Control diabetes with little to no input from the patient	40
Closed Loop	28
Take the burden away	23
Mimic healthy pancreas	17
Prevent hypos to keep the patients safe	14
Help analyze patterns and trends in BG and habits	9
Reduce BG variability	7
Lead to good A1c	2

Functional requirements were divided into several subcategories for easier interpretation.

Table 14. Functional Requirements Related to Information Usage.

	Score
Monitor glucose	68
Check *blood* glucose	11
Account for food carbohydrate content	19
Account for food protein content	2
Account for food fiber content	2
Account for physical activity	16
Account for stress/adrenaline	8
Account for illness	7
Account for bolus	2
Account for basal	2
Account for menstrual cycle/hormonal change	4
Account for age-related differences	1
Monitor ketones/unexplained highs	2
Track all other relevant data	3
Use historical data, not just current data	5
Account for IOB	2
Monitor system components	1

Table 15. Functional Requirements Related to Injections.

	Score
Inject insulin	78
Inject glucagon	55
Provide insulin dosing recommendations	2
Suspend insulin if needed	10
Suspend glucagon if needed	1
Provide temporary basal	1
Automatically adjust basal	28
Automatically administer boluses (insulin and/or glucagon)	18
Prevent lethal dose injection	1
Provide quick preset carb bolus (e.g. for 15 grams)	1
Provide BG thresholds for automatic insulin/glucose delivery	1

Table 16. Functional Requirements Related to Advanced/Other Functions.

	Score
Provide remote monitoring/control	33
Correct for miscalculated carbs	1
Predict changes in blood sugar	17
Allow customizable parameters (be patient-specific)	14
Provide data for export and analysis	10
Provide food database/dairy	5
Account for intra-patient variability	1
Do not require calibrations / *blood* glucose testing	7

Illustrate glucose patterns specific to time of day	4
Distinguish different highs	1
Do not require carb counting	5
Allow override/turnoff	6
Detect exercise, fat in meals, fast/slow carbs without input	2
Do safety self-checks	1

Table 17. Functional Requirements Related to Alerts/Interface.

	Score
Alerts for taking meal insulin	1
Alerts for other insulin if needed	1
Alerts for missed meals	1
Out of range BG alerts	3
Reservoir refill alert	2
Various alerts, predictive alerts, components issues alerts	21
Alerts for long-term events like eye exam, dental cleaning, etc.	1
Show BG trend as arrow	1
Show snapshot of current BG	1
Alerts with GPS data in case of emergency	1

Note that there were almost no explicit interface requirements. However, many information functions implied interface functions. For example ‘Account for food carbohydrate content’ can imply ‘Allow for the input of carbohydrates’. This is done via Systemic Textual Analysis [89] and some results are present later in this work.

Implementation requirements are presented in Table 18.

Table 18. Implementation Requirements.

	Score
Insulin pump	69
Glucagon pump	21
CGM	73
One site / smaller sites / fewer sites	15
Tubeless	13
Remote monitoring system	8
Dual chamber pump	8
Touch screen	3
Heart rate monitor	2
Mac compatibility/iOS	1
Signal interference protection	1
Refillable insulin cartridge	1
Large insulin reservoir	1
One device	33
Rugged	6
Waterproof/water-resistant	7
Shockproof	1
Childproof	1
Rechargeable	2
Rechargeable wirelessly	1
Smartphone	26

Multiplatform	14
Wireless between devices (Bluetooth, WiFi, NFC)	16
Open source	1
BTLE pump	1
BTLE CGM	1

There were responses where certain available device or technology was mentioned. They are listed in Table 19. When a particular feature of the device/technology was explicitly mentioned, it was reflected in this table as well and it incremented the score for the corresponding functional, implementation, or system requirement.

Table 19. Particular Devices/Technology Mentioned.

	Score
Dexcom (Dexcom, Inc., San Diego, California) - high accuracy CGMS	21
Dexcom Share	1
Abbott Libre (Abbott Laboratories, North Chicago, Illinois)	1
Omnipod – tubeless; integrated BG meter	7
Tandem t:slim (Tandem Diabetes Care, Inc., San Diego, California) – touch screen	4
Animas Vibe - integrated Dexcom G4 CGMS	1
Medtronic Minimed – insulin suspension	2
Asante Snap (Asante Solutions, Sunnyvale, California)	1
Calibra Finesse (Johnson & Johnson, New Brunswick, New Jersey)	1
One-Touch BG meter (Johnson & Johnson, New Brunswick, New Jersey) – insurance coverage	1
Bayer Contour (Bayer AG, Leverkusen, Germany)	1

Abbot Freestyle Lite (Abbott Laboratories, North Chicago, Illinois)	1
Nightscout (open source, DIY project)– remote glucose monitoring	8
MyFitnessPal (myfitnesspal.com) – food diary	2
Fitbit (Fitbit, Inc., San Francisco, California) – food diary	1
Bionic Pancreas	2
iPhone (Apple, Inc., Cupertino, California)	6
iCloud (Apple, Inc., Cupertino, California)	1
Contact lenses BG measuring	1
Temporary tattoo BG measuring	1

System requirements define the constraints that affect the whole or a significant proportion of the system [86] and are reported in Table 20.

Some responses implied performance metrics, but were not quantitative. For example, "fast insulin" describes performance but does not define how fast exactly (e.g. via onset time in minutes) the insulin must be. Such requirement cannot be meaningfully used as a performance requirement which must be quantitative, but cannot be omitted either since it was important for the respondent. Such requirements were therefore also reported in Table 20.

Table 20. System Requirements.

	Score
Small/portable	35
Accurate glucose readings	27
Easy to set-up, use, troubleshoot by children, teens, adults, seniors, caregivers, medical team, people with special needs	23
Minimal invasiveness (number of fingersticks a day and insertions)	19

Minimal number of devices	2
Inexpensive and/or covered by primary and secondary insurances and Medicare	10
Configurable automation	10
Safe	8
Adaptive to patient (by adjusting basal, CR, CF, etc.)	4
Stable glucagon	4
Insulin faster than currently existing	3
Not hackable	1
Cool look [sic]	1
Discreet	1
Long battery life	1
Long-lasting infusion set	1
Long-lasting sensor	1
Sensor robust for all activities	1
Less delay between BG and SCG	1
No computer necessary to use	1

The requirements category that was not included into the HRM presented the question: "Keeping in mind that no system can be perfect, what is the lowest percentage of the time that the system would need to work perfectly to be safe?". The summary of responses is in Figure 56.

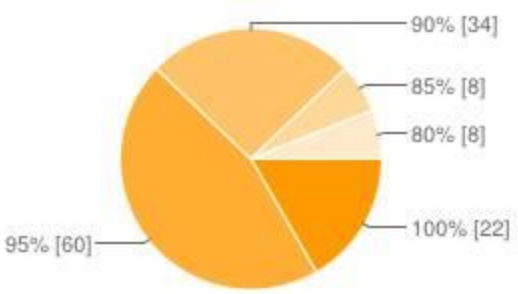

100%	22	17%
95%	60	45%
90%	34	26%
85%	8	6%
80%	8	6%

Figure 56. System Level Performance Requirement.

6.4.4 Two Schools of Thought

A significant feature of the survey results was that there were conflicting responses. The obtained mutually exclusive requirements suggested several possible technological solutions and therefore several HRMs – one for each solution.

Overall, the study produced four distinct implied solutions, although their HRMs would overlap in many requirements. Here, the solutions are listed in the order of decreased attention, with the first two being approximately equally prevalent in the responses:

1. External: one-device Artificial Pancreas
2. External: mobile-device-based multiplatform Artificial Pancreas
3. Internal: Implantable Artificial Pancreas
4. Other: Smart Insulin

For the purposes of this work HRMs will not be composed for the solutions 3 and 4 since attention to them among the respondents was very limited and, conceptually, they are out of the scope of the technological solutions implied in this study. The aggregate score of all the requirements unique to the implantable solution was 28. More about implantable artificial pancreas can be learned in [90].. The aggregate score for smart insulin was 1. More about smart insulin can be learned in [91].

Considering the solutions 1 and 2, one can infer two "schools of thought" of AP systems. One school of thought can be roughly represented by the industry and proposes the one-device solution. The other school of thought can be roughly represented by researchers in academia and proposes the multi-platform solution.

Figure 57 depicts a schematic representation of a composite HRM for solutions 1 and 2 and reflects the structure of a generic HRM from Figure 54. The graphics of Figure 57**Error! Reference source not found.** are conceptual idealized images of the two schools of thought. The composite HRM includes operational, functional, implementation, and system requirements that were common for both types of solutions; it also includes implementation requirements that were unique for each solution. In Table 18, the unique implementation requirements for solutions 1 and 2 were reported in the middle and the bottom of the table, respectively.

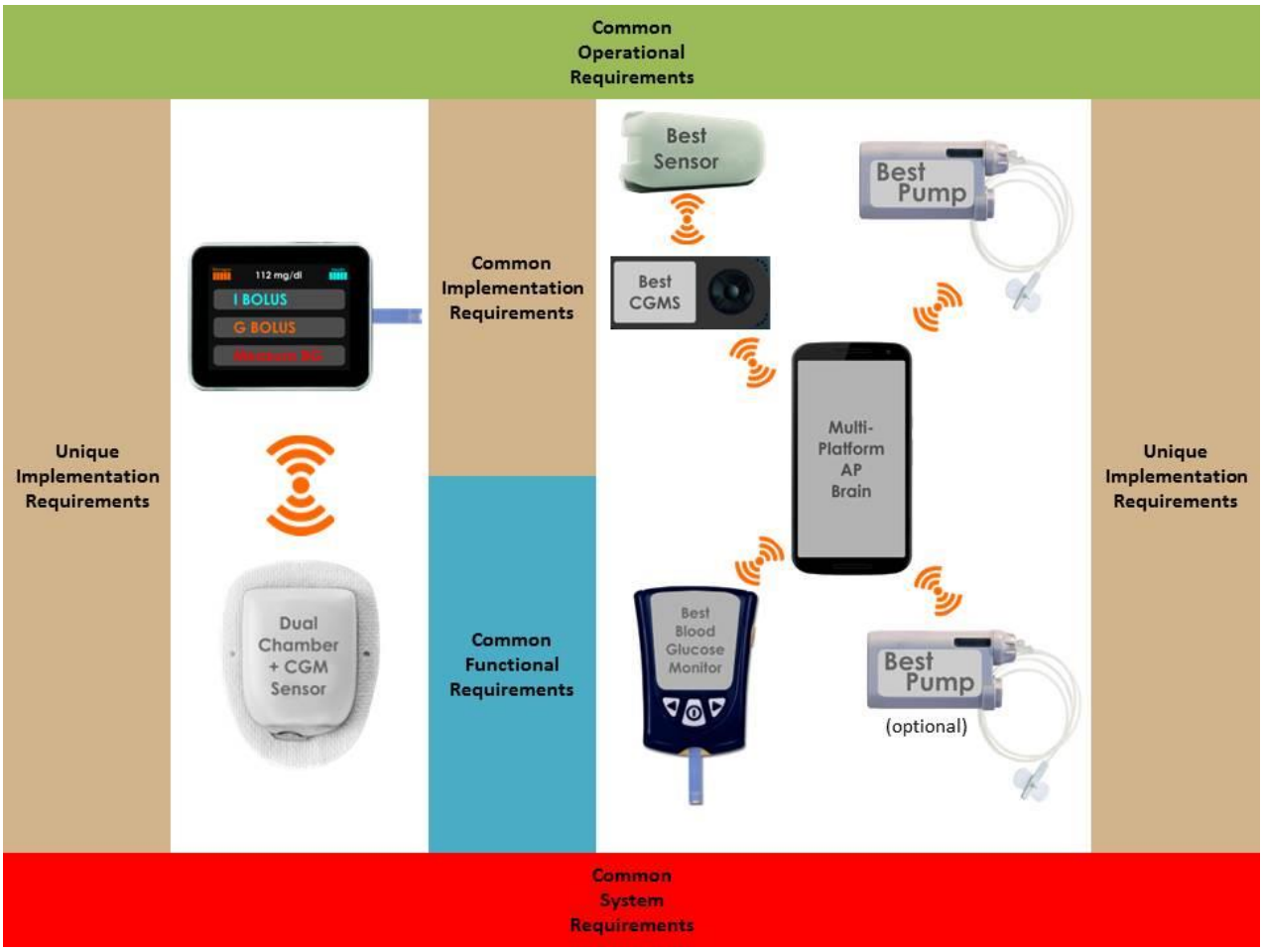

Figure 57. AP Systems Two Schools of Thought.

Solution 1 implies an external, fully integrated one-device Artificial Pancreas system where an insulin pump, [an optional] glucagon pump, a CGMS, a blood glucose meter, and the AP "brain" itself are all housed in one device. Examples of the developments that are leading to this solution are found in the industry. Some of them are:

- Medtronic MiniMed 530G (Medtronic plc, Northridge, California)
- Animas Vibe (Johnson & Johnson, New Brunswick, New Jersey)
- Omnipod (Insulet Corporation, Billerica, Massachusetts)

The advantage of solution 1 is its compact design and ability to integrate several devices in one. The assumption of this solution is that industry players have necessary resources to design and manufacture any device form factor. That is also the reason that requirements like 'waterproof' are only included into solution 1 specific implementation requirements. Thus, the extreme idealistic case for this solution would be a one device and one site with no tubes as depicted in Figure 57.

However, there are currently several industry players in the field and the best relevant technologies are divided but not shared among them. Therefore it is hard to imagine one company that would possess, for example, the best pump *and* the best sensor *and* the rest of the technologies/features to integrate them into the perfect one-device solution that all patients would prefer.

Solution 2 implies that the AP "brain" could be installed on any portable device (e.g. smartphone, tablet, or smartwatch), ideally being able to communicate with any kind of pump (insulin and glucagon), CGMS, and other devices, and controls them according to its decisions. Examples of the developments that are leading to this solution are found in the academic research community. Some of them are:

- DiAs - Diabetes Assistant (Center for Diabetes Technology at the University of Virginia, Charlottesville, Virginia)
- Bionic Pancreas (Boston University and Massachusetts General Hospital, Boston, Massachusetts)
- Artificial Pancreas by Doyle III et al. (University of California, Santa Barbara, California)

Since it is, in a sense, an open source platform, researchers and developers are free to use the peripheral devices – pumps, CGMS, etc. – that perform the best. However, they do not possess manufacturing capabilities and the least number of devices possible in the solution 2 is two – the smartphone and a one-device solution from the industry if existing.

There were many responses that carried more value than just the score.

Responses show that patients might have a wide range of BG values in mind that they consider “good”. For example, one person expressed desire to be in “tight control” of between 65 and 200 mg/dl, while another person wanted it “normal” between 70 and 140 mg/dl, and yet another between 80 and 120 mg/dl. This demonstrates the need for customizable parameters of the system.

Only few times respondents referred to monitoring *blood* glucose more or less specifically. The most explicit comment called for monitoring ”blood glucose (not interstitial glucose)”.

Large number of responders indicated that glucagon needs to be available in the system along with insulin, with some of them emphasizing that glucagon is as important as insulin. One provided reason was that it “is critical, because hypoglycemia can cause unawareness and inability to care for oneself.”

Some answers implied the necessity of configurable automation. For example, “Give up control to the user if not sure – if user does not respond, go default basal (pump mode in DiAs), and send sms/email to doctor/support”. Another example: “Manual for meals, rest automated”.

6.5 Systemic Textual Analysis

Systemic Textual Analysis (STA) is concerned with the analysis of expressed user requirements with the purpose of interpreting, expanding, and clarifying requirements and identifying missing one [89].

The survey produced 107 requirements for the corresponding HRM. It makes sense that each function's performance could be quantified and that each function is implemented in a certain way. This is fundamental logic behind STA. STA fills the missing components of a HRM – functions, performance, or implementation – based on the components that are present in the HRM. Graphically, the concept is depicted in Figure 58.

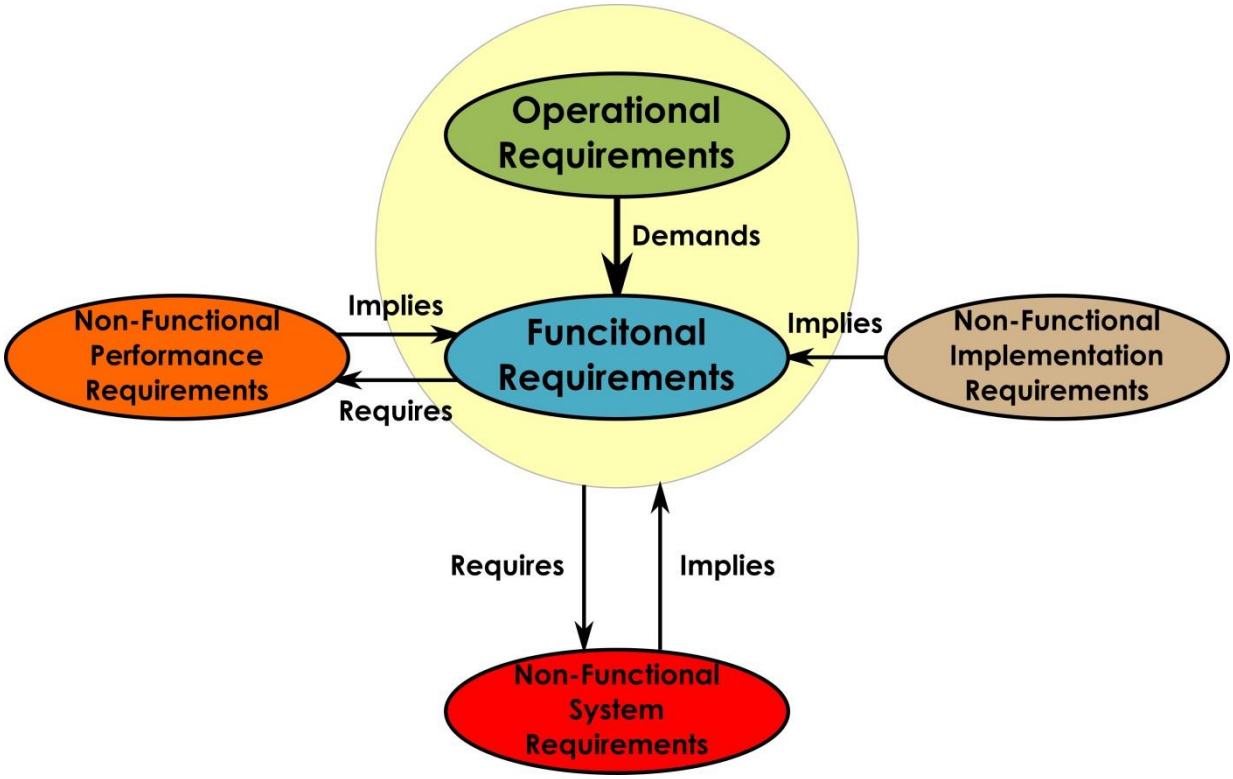

Figure 58. Systemic Textual Analysis Graphical Representation.

To put it in words:

1. An implementation requirement (e.g. insulin pump) is a solution to a functional requirement (inject insulin). Therefore, given the former it is possible to deduce the latter.
2. A performance requirement (e.g. blood glucose must be measure with MARD of 9% accuracy) defines how well a particular system function has to perform. Therefore, given the latter it is possible to deduce the latter (measure blood glucose).
3. To provide completeness, each functional requirement needs the associated performance requirement.
4. System-functional requirements relationship is akin to (2) and (3) from above.

Since we omitted performance requirements question from the original survey (for the reasons described in 6.4.1 Survey), Table 21 presents an example of filling in requirements between functional and non-functional implementation requirements of an AP system.

Table 21. STA Example for AP System.

Functional Requirement	Non-Functional Implementation Requirement
Show snapshot of current BG	Interface (allowing for BG output)
Account for age-related differences	Interface (allowing for age input)
Out of range BG alerts	Speaker, vibration, light

Notice, that implementation requirements in the right column of the Table 21 were not in the original implementation requirements in Table 18. However, it is clear that these implementation requirements are necessary to fulfil what stakeholders put forward as their functional requirement. While in the stakeholders' responses such requirements might be omitted because they are obvious, for the engineers designing the AP system it is essential that the requirements table is exhaustive and everything is taken into account. That is exactly what STA is for.

Another example of functional (or operational) requirements implying other groups of requirements is the inference of performance requirements. Below are few example of such inferred performance requirements with the corresponding functional or operational requirements that imply them.

Table 22. Another example of STA.

Operational/Functional Requirement	Non-Functional Performance Requirement
Increase time in range	The range maintained must be from *x* to *y* mg/dl
Lead to good A1C	The A1c of *x* must be maintained
Monitor glucose	Provide glucose reading every *x* minutes
Inject insulin	Inject insulin with the hardware increment of *x*
Provide temporary basal	Provide temporary basal of *x* % of current basal
Check *blood* glucose	Require *x* number of fingersticks a day

6.5.1 Performance requirements

To learn what the values of the *x*'s and *y*'s in Table 22 are, another short study was conducted for this example. 30 people were surveyed, all of the patients or patients' parents when the patients were young enough to coherently respond to the questions. The respondents were allowed to skip questions that they didn't understand or found irrelevant. The following questions were asked:

- What is your preferred lower range boundary for an AP system?
- What is your preferred upper range boundary for an AP system?
- What A1C target you want the system to help you achieve?
- How often would you like the sensor to tell you your glucose?
- Thinking about basal rates, what is the lowest titration of insulin bolus increments you would like the system to have?

- What is the finest modification of basal (temporary basal) the system should provide? (Currently you can titrate your basal up and down using a percentage or unit based calculation. Given a percentage based calculation, what is the increment of adjustment you'd prefer to have – example: increase by increments of 1%, 5%, 10%, etc.)
- How many fingersticks per a day are you willing to perform to enable the Artificial Pancreas system to work.

Multiple choice answers were suggested for the questions. The results are presented in the following figures.

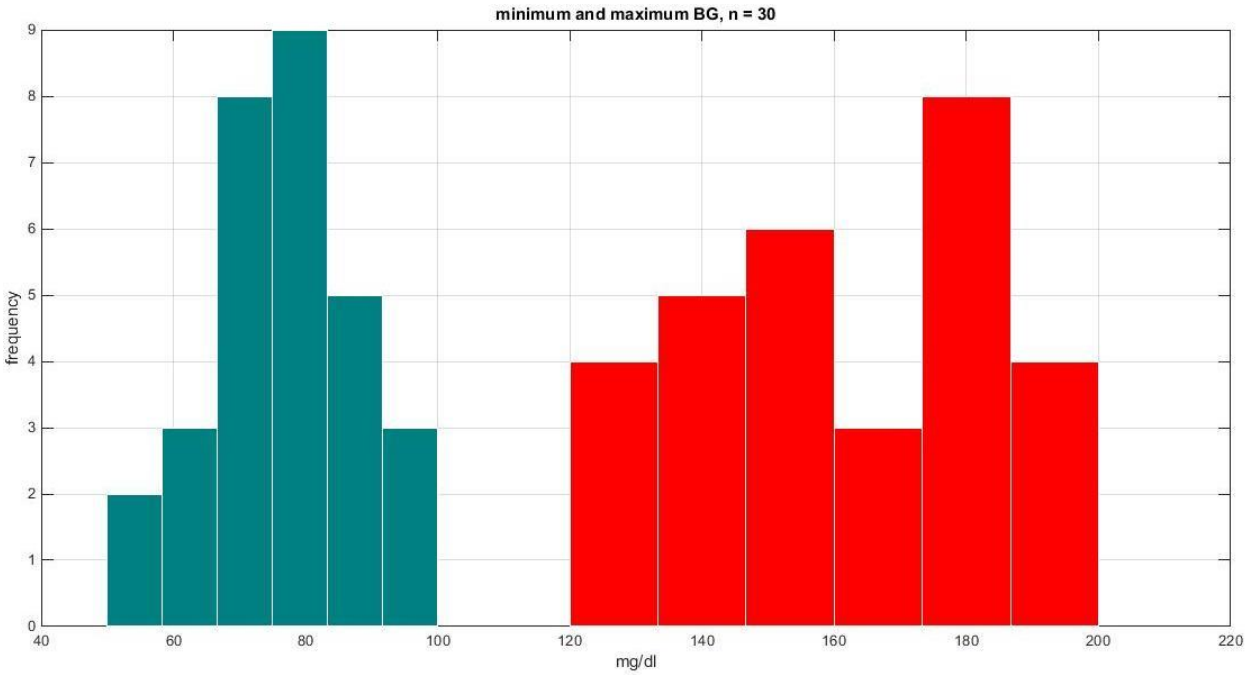

Figure 59. Minimum and maximum BG desired.

Figure 59 suggests that most of the patients would like to stay above 70 mg/dl and most (not necessarily the same) patients would like to stay below 180 mg/dl. Note that the maximum BG (red bars) has a wider distribution which reasonably suggests that minimum BG values are more important for patients than maximum BG values.

Since the minimum BG and maximum BG responses are not connected to each other, it is also worth presenting the ranges calculated from the respective minimum and maximum BG values – Figure 60.

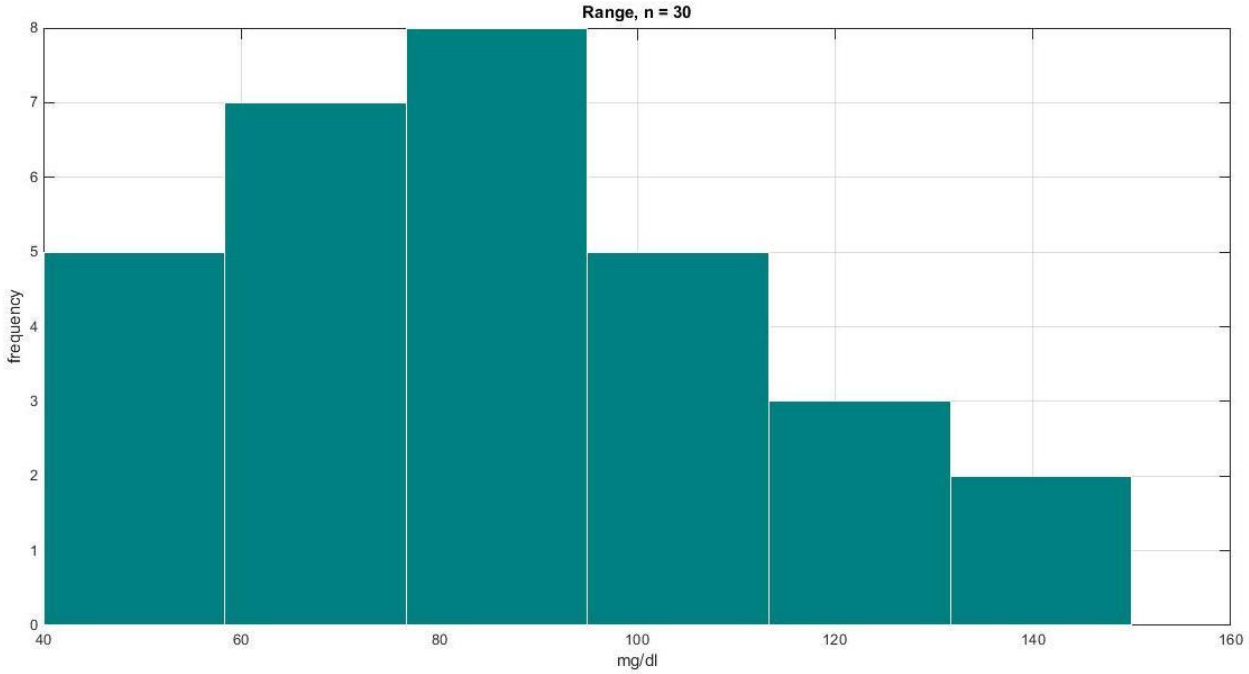

Figure 60. Range desired.

Figure 60 suggests that, on average, the acceptable width of the range is about 90 mg/dl.

Figure 61 presents the HbA1c values that the respondents named as optimal for them.

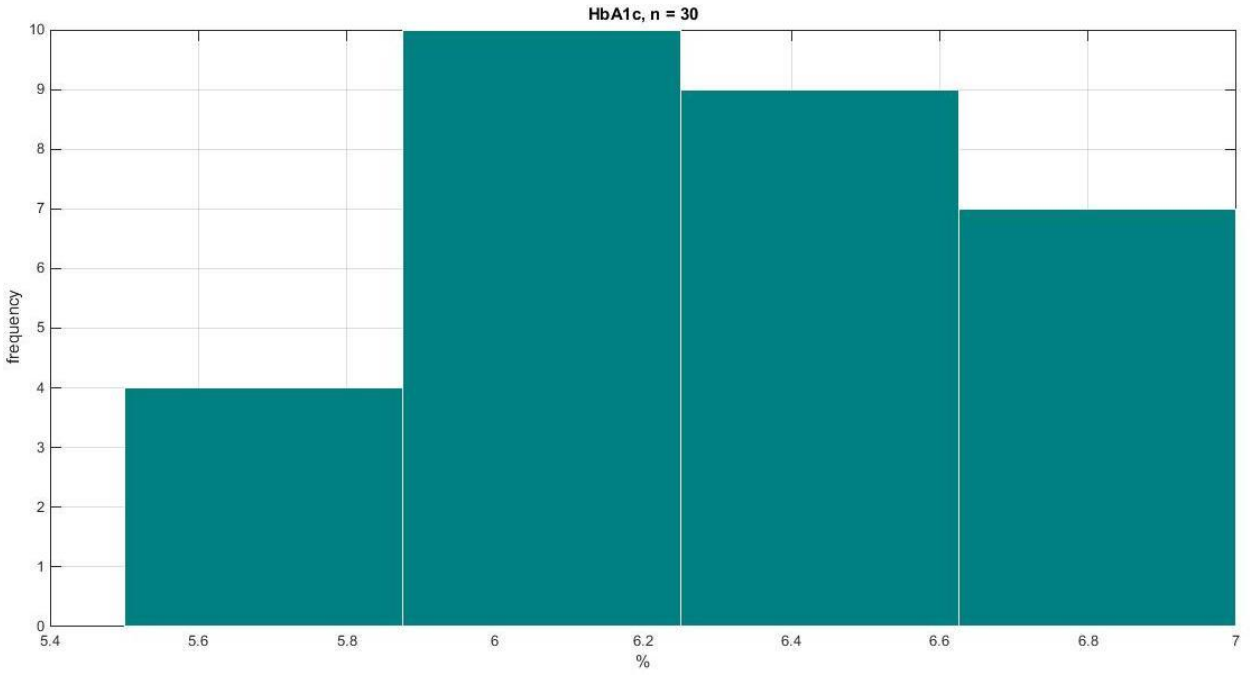

Figure 61. Desired HbA1c.

Figure 62 shows how often the respondents wanted to have access to a new CGM value.

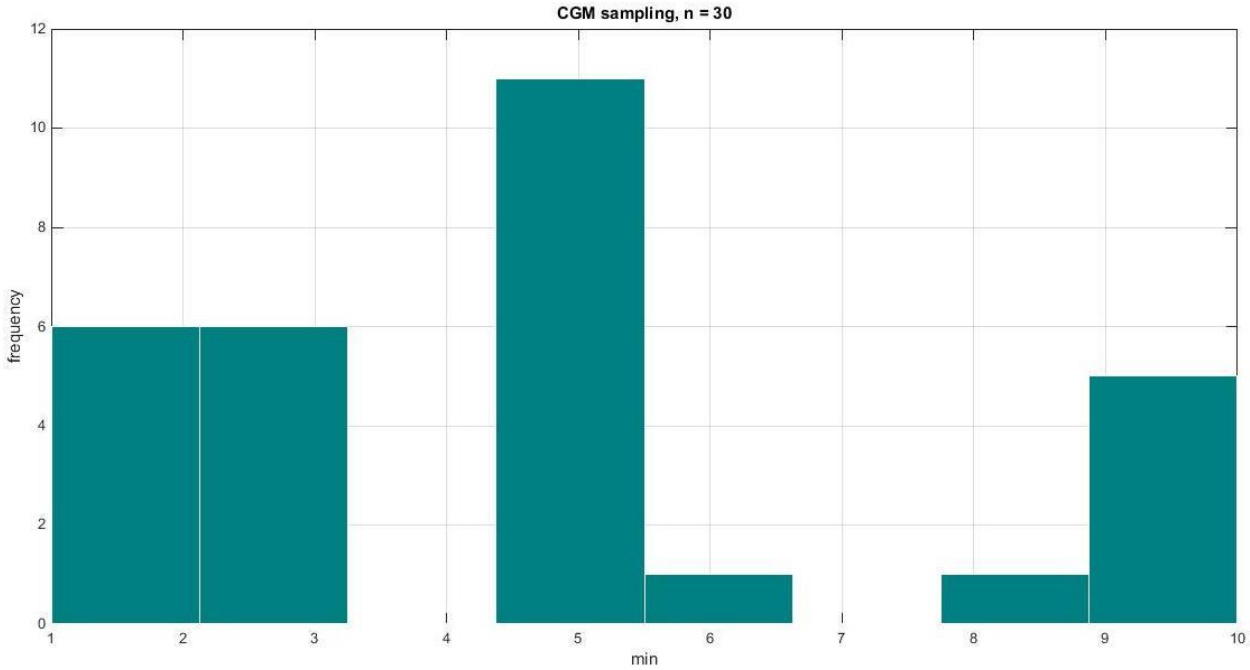

Figure 62. Desired CGM sampling frequency.

Figure 63 show how fine the respondents wanted to have their pump's increment. Majority of the patients preferred to have it as precise as 0.01 Unit.

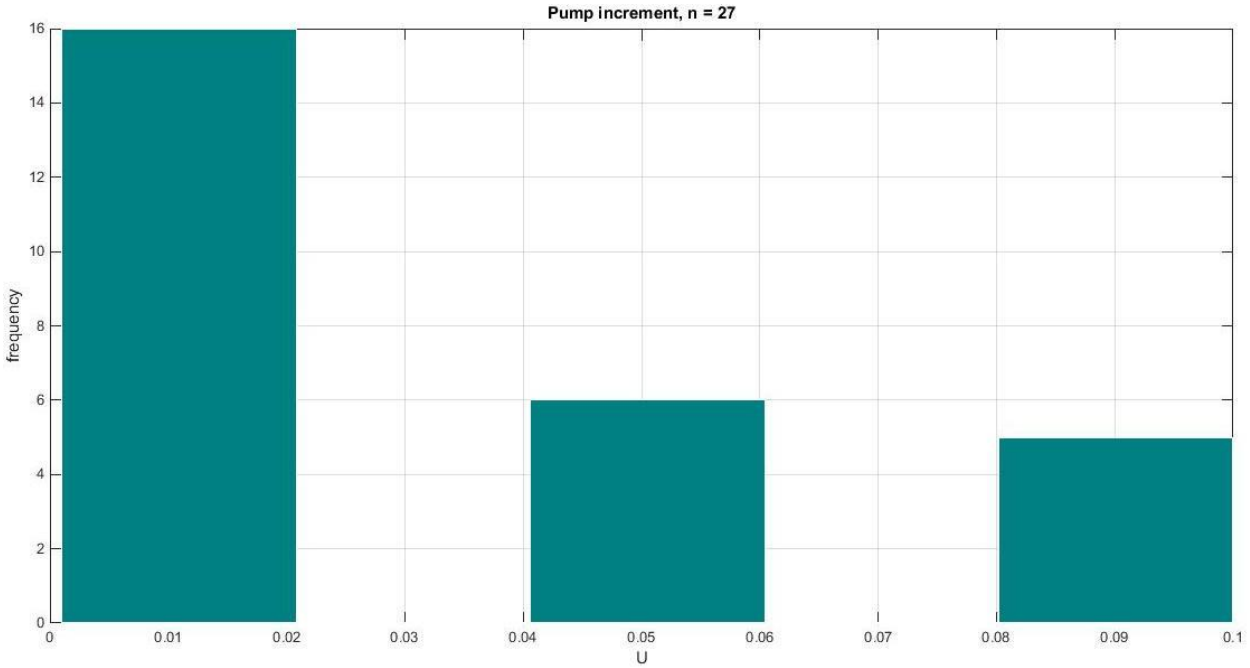

Figure 63. Desired pump increment.

Figure 64 shows how small the relative value of temporary basal must be in the view of the patients.

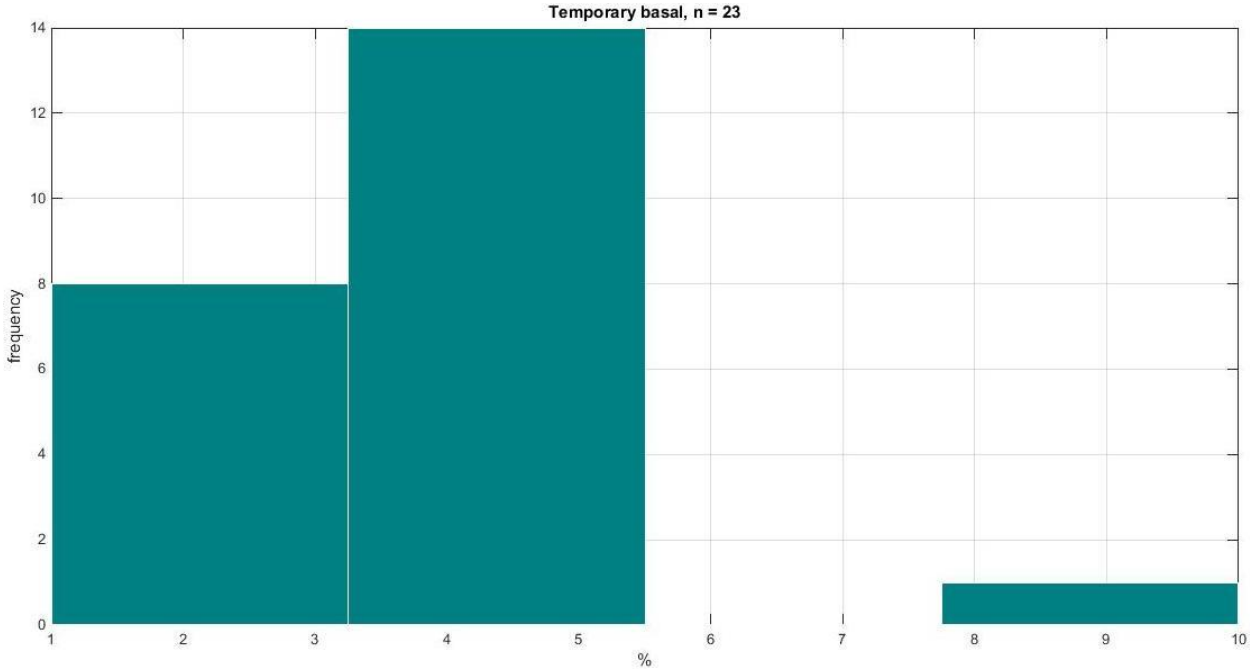

Figure 64. Desired temporary basal precision.

Finally, Figure 65 shows how the patients feel about the number of fingersticks the system would require per day for optimal performance. The distribution is bimodal with many people being comfortable with just 4 fingersticks a day and other large group being comfortable with 6-7 fingersticks.

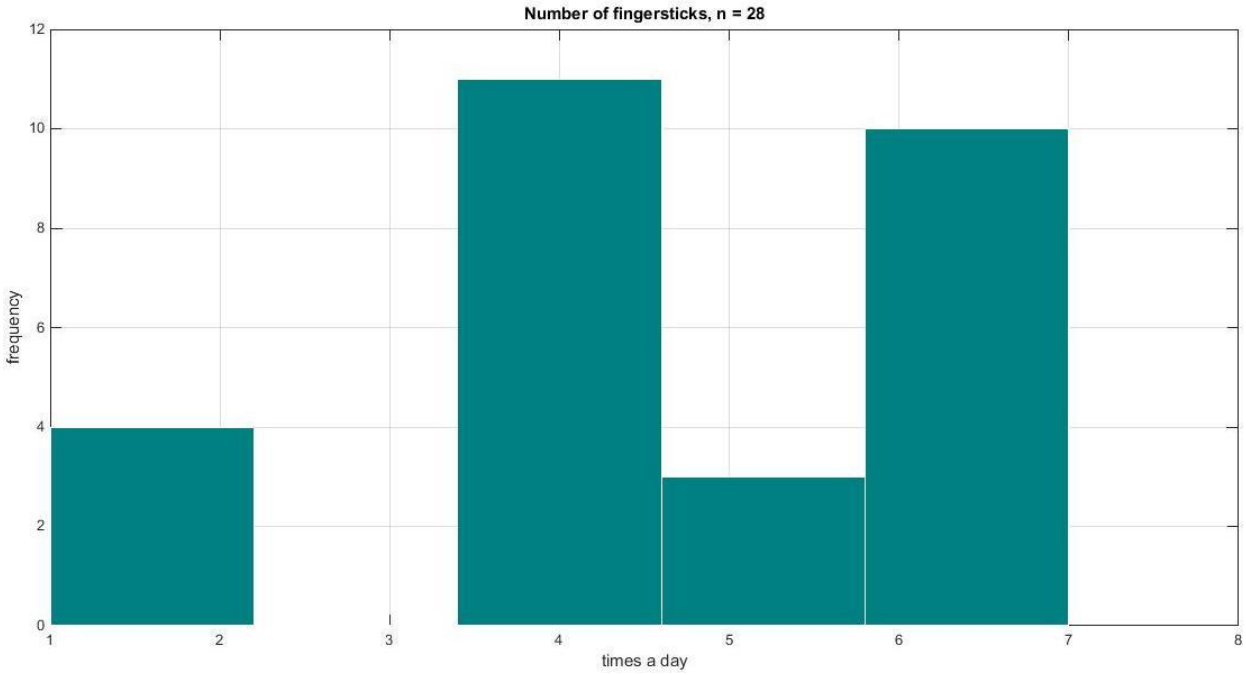

Figure 65. Acceptable number of fingersticks.

6.5.2 Subsystems

As was mentioned before, the resulted AP HRM contains 107 requirements. That is before STA. After a proper STA the number can increase several-fold. This large number is not surprising as the associated system (Artificial Pancreas) is highly complex and involves many subsystems. In fact, systems of such order always produce several HRMs where there is one overarching HRM and others are HRM of the system's subsystems. This is not surprising, as according to systems analysis [84], a system comprises subsystems, and a system is a sub-system of a bigger system.

As this work pursues not a full product development documentation, but only a formalization of the process, all sub-systems' HRM will not be presented, but a demonstrative example will be discussed. The

most common case is when a function that is complex necessitates delving into the function's sub-system thus producing another HRM. In this case:

1. The appropriate Functional Requirement of the system becomes the purpose element of the Operational Requirement of the sub-system.
2. The Non-Functional Performance Requirements of the function of the system become Non-Functional System Requirements of the sub-system.

Using familiar graphics for HRM representation, an example of this case is presented in Figure 66.

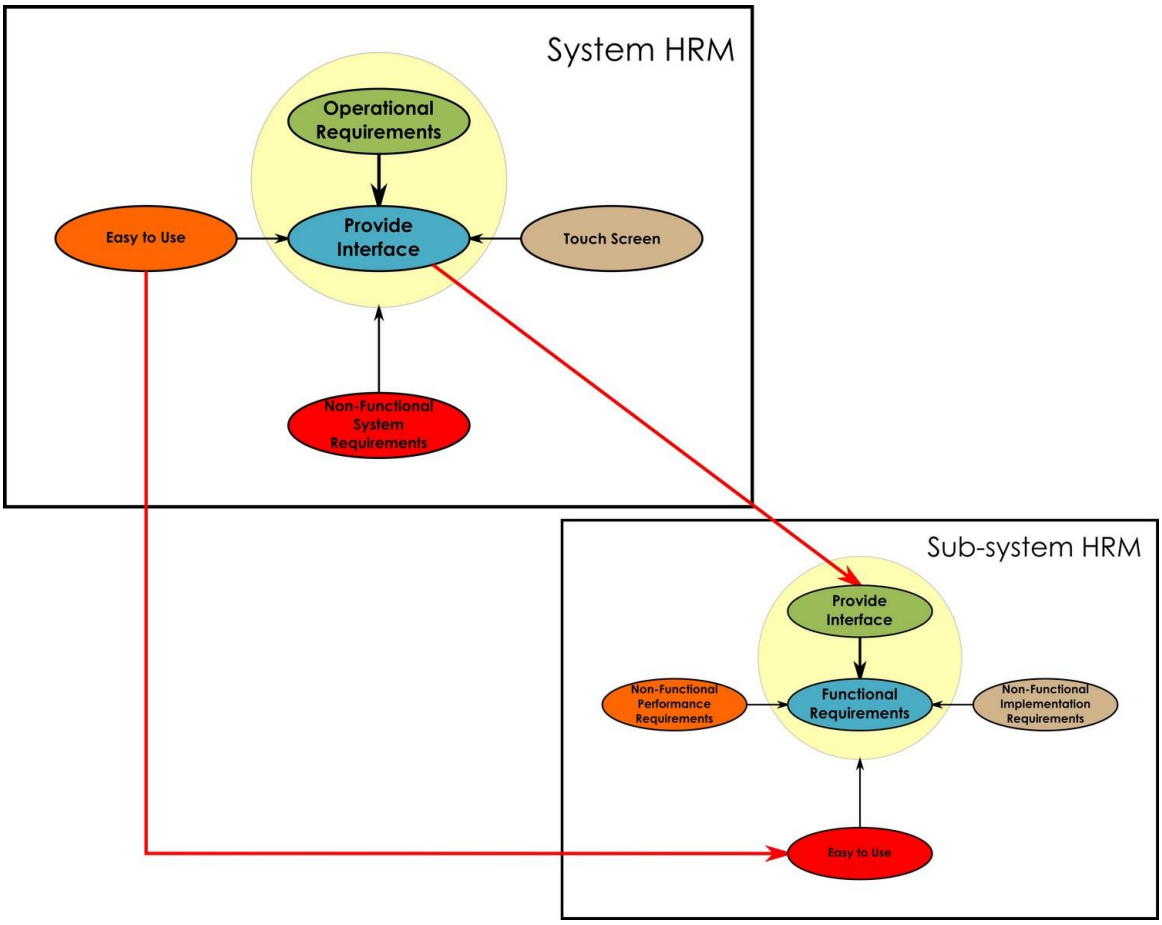

Figure 66. System and Sub-system HRMs.

There are many of the 107 HRM requirements that will require a sub-system HRM and possibly another level of HRM – sub-sub-systems. Particularly, many or all functional requirements of the Table 16 (Advanced/Other Functional Requirements) will require a sub-system HRM. For example:

- Provide remote monitoring/control
- Account for intra-patient variability
- Distinguish different highs

Sequential application of Stakeholder Mapping, surveying the stakeholders, Holistic Requirements Analysis, and Systemic Textual Analysis not only provides a framework for a system design that fits the purpose, but also guarantees that the purpose is correct.

6.6 7D Diagram

In the previous sections, a formalization of the engineering design process for Artificial Pancreas systems was presented. However, even with the more though-though design approach, complex systems like AP are exposed to a lot of risk during their operation. To address this aspect of AP systems, a risk assessment and management methodology is presented.

Ishikawa diagram is routinely used in different industries. It also comes under different names – cause-and-effect diagram and fishbone diagram and others. It shares its features with many other risk assessment and management tools in its hierarchical and modular structure in which various sources of risk and malfunction are grouped in categories. Many methodologies differ only in the structural geometry they chose to present the categories. Ishikawa diagram's general structure example is depicted in Figure 67.

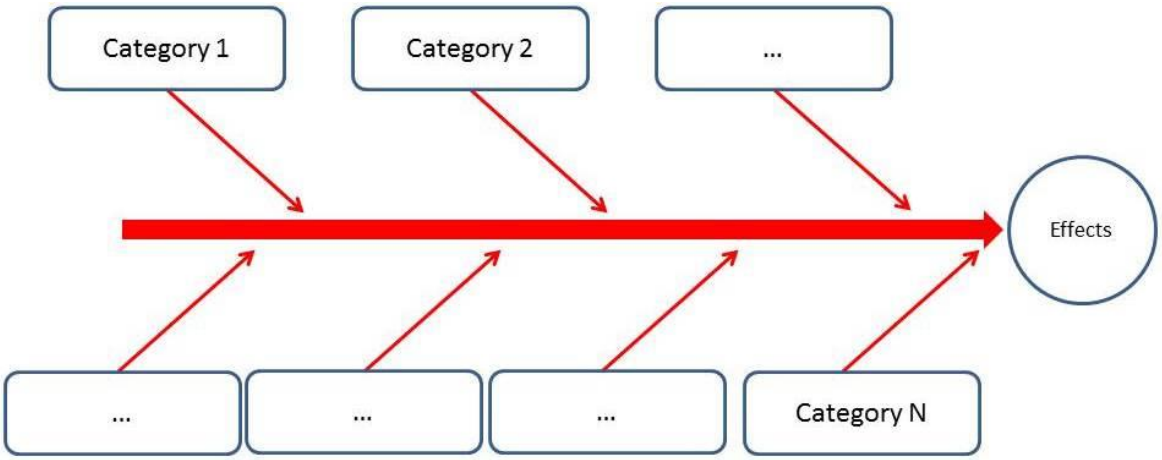

Figure 67. Ishikawa Diagram.

When using Ishikawa diagram, historically, in each industry, the model has been described by an "acronym" that would consist of the same letter repeated. For example:

- in manufacturing industry, 8 Ms:
    - Machine (technology)
    - Method (process)
    - Material (Includes Raw Material, Consumables and Information.)
    - Man Power (physical work)/Mind Power (brain work)
    - Measurement (Inspection)
    - Milieu/Mother Nature (Environment)
    - Management/Money Power
    - Maintenance
- in marketing industry, 7 Ps:
    - Product/Service
    - Price
    - Place
    - Promotion

    - People/personnel
    - Positioning
    - Packaging
- in service industry, 5 Ss:
    - Surroundings
    - Suppliers
    - Systems
    - Skills
    - Safety

For the field of AP systems, the "acronym" of 7 Ds is proposed:

- Design (underlying algorithm)
- Development (software implementation)
- Device (hardware implementation)
- Drug (medications used: insulin, glucagon, etc.)
- Deployment (environment of use)
- Diabetic (patient's behavior)
- Doctor (clinician's/physician's involvement)

Updated diagram is presented in Figure 68.

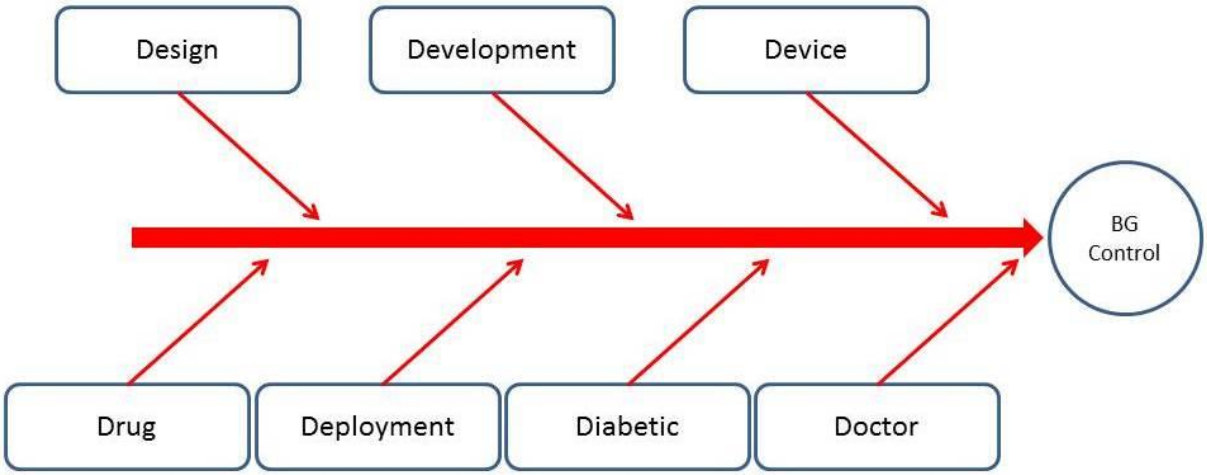

Figure 68. 7D Ishikawa Diagram.

As in any Ishikawa diagram, in our case each effect cause has several sub-causes. Some of them are shown in Figure 69.

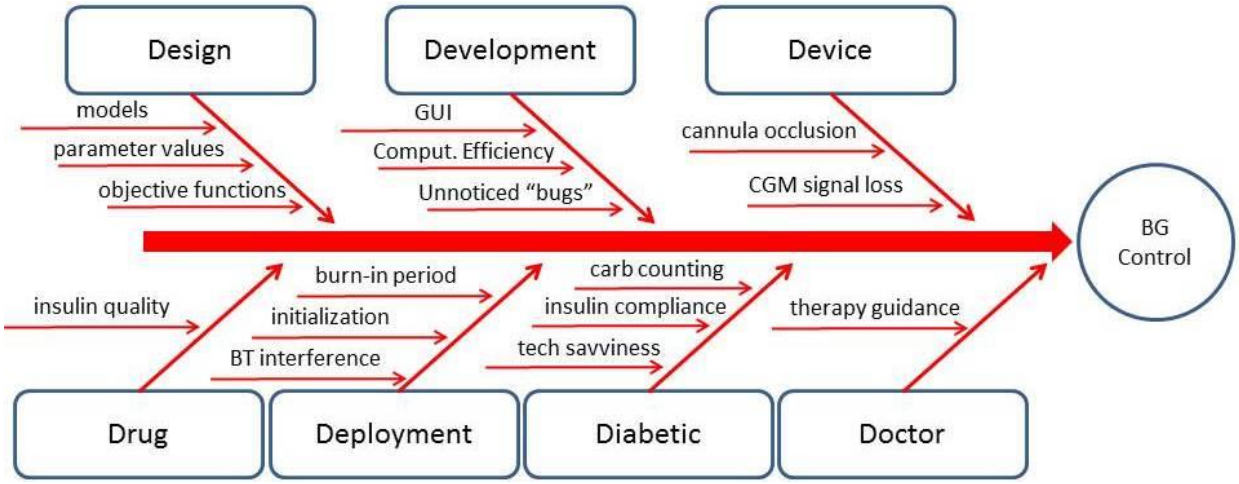

Figure 69. 7D Model with Sub-categories.

The structure nature of multilevel decomposition shows the following advantages [92]:

1. Decomposition methods can reflect the internal hierarchical nature of large-scale multiobjective systems. In AP system case, categories like Design, Development, Device, and Drug would be in

the center of the system and this center's operation is defined by the Diabetic, Doctor, and Deployment.

2. Trade-off analyses can be performed among sub-systems and the overall system. In AP system case, for example, CGM signal loss from the Device category can be addressed with proper software response (Development category) planned during the design of the algorithms (Design category).
3. Through decomposition, the complexity of a large-scale multiobjective systems can be relaxed by solving several smaller sub-problems.

Just like Hierarchical Holographic Modeling by Haimes [92], 7D model is a holistic methodology designed at capturing and representing the essence of the inherent diverse characteristics and attributes of a system – its multiple aspects, perspectives, facets, views, dimensions, and hierarchies which in AP systems are many.

Together with HRM, 7D provides a formal framework for a genuine systems approach to designing and assessing Artificial Pancreas systems.

Chapter 7

Conclusions and Contributions

In this work, we posited that in complex biomedical control systems it is beneficial to support the operator's ability to control the decision making. In particular, in the framework of diabetes technology, advice and decision support systems were considered as a reasonable precursor to fully closed-loop systems. Such advisory systems calculate numerically optimal advice when requested so by the user and then the user himself or herself decides whether to actuate the advised value.

We designed such advisors for both (i) insulin pump-equipped systems which are currently the prevalent configuration for Artificial Pancreas systems, and (ii) Multiple Daily Injections setting which has not been studied before in terms of optimal dosing. In addition, as such systems are complex, and not only include human operator but also have human as the control object, we deemed it necessary to develop a structured framework for the design of such systems. In the course of this work we came to several conclusions:

1. Model-based treatment is as robust as the models are themselves, and to the extent that the model fails to represent the reality of treatment, the configuration of the system and its control authority have to be carefully chosen. After developing a model that we deemed reliable for long-term prediction, we did observe promising results *in silico* when it was tested using the FDA accepted Simulator. However, when testing the system *in vivo*, it was found not suited for accurate long-term predictions due to inter- and intra-subject variability. The model experienced particular problems when handling dynamics of insulin transport and meal absorption, especially in the cases when meals were grossly misestimated. *In vivo* experience modified our expectations of model based advisory approach. We found that these model-based prediction challenges can be addressed by introducing certain therapy and control features. In particular, the therapy can limit

the advice requests to meal times only to avoid the complications of the post-prandial metabolical dynamics. The control strategy can also be reverted to conventional correction bolus calculation based on correction factor and IOB when the model is not tracking the real-life insulin transport dynamics.

2. In control systems where the operation is significantly influenced by human behavior, such as biomedical systems of diabetes algorithmic solutions, it is important to understand the context and requirements of the system's use before the design stage. This allows not only to avoid unnecessary implementation iterations, but also improves the design features of the system overall through abiding by all behavioral constraints that can be applied to such system.

Our contributions to algorithmic technology-based diabetes solutions are found in modeling, control, simulation, and systems design. More specifically:

1. We built a risk-space model-based advisory system with a non-patient-specific objective function. Unlike previous model-based advisory systems that generally relied upon a "population average" model and achieved individualization through careful construction of optimization objective function, the system we proposed achieved individualization of the control action through the development of a mathematical model that was adapted to patient's individual physiology. In particular, some parameters of the model for state estimation were individualized by applying optimal multiplier values. However, the objective function is adapted to timing of meals – we apply a gradient weighting on the cost matrix across the horizon putting less penalty during time right after the meal and more penalty closer to the end of the horizon. This protects the systems from overpenalizing during the most uncertainty and penalizing appropriately at the end of the horizon where it matters the most for returning the patient to the target blood glucose values. Importantly, we employed a risk space model that adequately reflects the difference in the sense of clinical importance between numerically equivalent deviations from the target.

2. We designed a long-acting insulin model to enable the design of advisory systems for MDI therapy patients and designed one such system. The new compartmental long-acting insulin model allows tracking of the dynamics of long-acting insulin glargine that is extensively used in MDI therapy for type 1 diabetes. In addition, it preserved the original compartmental structure of the traditional rapid-acting insulin transport model used in Artificial Pancreas system. Thus the new model reconciles the pharmacokinetics of insulins with different action profiles and accommodates design and simulation of real-life MDI therapies where two different insulins are used.
3. We introduced the concept of Virtual Basal Rate that allows the designer to adopt the mathematics of pump-equipped Artificial Pancreas systems for MDI therapy systems. The Virtual Basal Rate is an equivalent basal rate that would be dialed in a pump throughout a day to achieve an insulin concentration profile equivalent to the one produced by injections of long-acting insulin glargine. The deviation of this oscillating concentration profile from the average basal concentration produced by long-acting insulin only can thus be used as a "IOB" specific to MDI therapies. Importantly, we further developed the Virtual Basal Rate calculation for real patients that do not inject the long-acting insulin at exactly same time of day or skip long-acting insulin injection completely. This specific representation of the Virtual Basal Rate has the most impact in these corner cases by providing a way of tracking the "excess" or "skipped" insulin concentration for any patient only knowing their long-acting insulin injection value and the number of such injection a day (usually one or two in MDI therapy).
4. We developed a reference model for MDI therapy system testing and validation by introducing the concept of behavioral populations. In contrast to existing *in silico* population widely used in diabetes technology simulations, real-life patients on MDI therapy possess behavioral features that had not been represented in such simulators before. We translated possible behavioral profiles like "hypo-fearing" patients, "hyper-fearing" patients, or "common patients" into numerical *in silico* subjects that vary behaviorally in their therapy parameters. These behavioral

populations allow testing and validation of MDI therapy algorithms. We then used one of these populations – hypo-fearing – to validate our own MDI therapy advisory system that takes advantage of the knowledge about long-acting insulin dynamics through the Virtual Basal Rate.

5. In addition to the specific diabetes technology contributions above, we introduced a general methodology for the design of diabetes technology solutions. We identified various groups of stakeholders that affect or are influenced by Artificial Pancreas and other technological diabetes solutions. We then transformed the categories of the Holistic Requirements Model approach into a survey that could be completed by individuals from these stakeholder groups. During the poll of over 130 respondents, we gleaned invaluable information about what is required from such diabetes management systems and what the constraints are. To process the survey results, we used the thematic analysis approach. Further, we demonstrated a way to refine such results with the application of Systemic Textual Analysis and subsystem formation.
6. Finally, we employed the Ishikawa Diagram and developed our own diabetes technology specific cause-effect diagram with 7 categories corresponding to the grouped sources of risks and solutions to control and therapy problems that can arise in diabetes technology systems: Design, Development, Device, Drug, Deployment, Diabetic, and Doctor. The 7D diagram is thus equipped to encompass all aspects of creating and using a technological diabetes management solution. As a decomposition method, 7D provides a convenient way of reflecting the internal hierarchical nature of large-scale complex diabetes technology systems and facilitates trade-off analysis among the sub-systems. Importantly, it allows the designer to systematically search for a solution in various categories to address a problem that arose in any of the categories thus providing a road map to the analysis and debugging process of the design and operation of such systems.

BIBLIOGRAPHY

[1] S. Bennett and Institution of Electrical Engineers, *A history of control engineering, 1800-1930*. Stevenage; New York: Peregrinus : Institution of Electrical Engineers, 1979.

[2] H. H. Cole, "Improvement in fluting-machines," US55469 A, 12-Jun-1866.

[3] J. M. Jay, "Improvement in machines for making the spindles of wagon-axles," US47769 A, 16-May-1865.

[4] R. Brown, *Society and Economy in Modern Britain 1700-1850*, First Edition edition. London ; New York: Routledge, 1991.

[5] "Time and Timekeepers by Milham, Willis I.: New York: Macmillan Hardcover, 5th or later Edition - Yankee Peddler Bookshop, Past ABAA, ILAB." [Online]. Available: http://www.abebooks.com/Time-Timekeepers-Milham-Willis-I-New/8941048952/bd. [Accessed: 09-May-2014].

[6] W. B. Cannon, *The Wisdom Of The Body*, Rev. and Enl. Ed edition. New York: W. W. Norton and Company, Inc., 1963.

[7] T. Samad and A. Annaswamy, "The Impact of Control Technology," IEEE Control Systems Society, 2011.

[8] B. W. Bequette, "A critical assessment of algorithms and challenges in the development of a closed-loop artificial pancreas," *Diabetes Technol. Ther.*, vol. 7, no. 1, pp. 28–47, Feb. 2005.

[9] P. Stephen, C. Hughes, P. Vereshchetin, M. Breton, and B. Kovatchev, "Correction Insulin Advisory System Based on Meal Behavioral Profiles," 2011, pp. 8354–8359.

[10] A. D. A. 1701 N. B. S. Alex, ria, and V. 22311 1-800-Diabetes, "Hyperglycemia (High blood glucose) - American Diabetes Association®," *American Diabetes Association*. [Online]. Available: http://www.diabetes.org/living-with-diabetes/treatment-and-care/blood-glucose-control/hyperglycemia.html. [Accessed: 04-May-2014].

[11] A. D. A. 1701 N. B. S. Alex, ria, and V. 22311 1-800-Diabetes, "Hypoglycemia (Low blood glucose) - American Diabetes Association®," *American Diabetes Association*. [Online]. Available: http://www.diabetes.org/living-with-diabetes/treatment-and-care/blood-glucose-control/hypoglycemia-low-blood.html. [Accessed: 04-May-2014].

[12] C. Giovino, I. Ayensu, J. Tetteh, and J. S. Boateng, "Development and characterisation of chitosan films impregnated with insulin loaded PEG-b-PLA nanoparticles (NPs): A potential approach for buccal delivery of macromolecules," *Int. J. Pharm.*, vol. 428, no. 1–2, pp. 143–151, May 2012.

[13] F. Cui, C. He, M. He, C. Tang, L. Yin, F. Qian, and C. Yin, "Preparation and evaluation of chitosan-ethylenediaminetetraacetic acid hydrogel films for the mucoadhesive transbuccal delivery of insulin," *J. Biomed. Mater. Res. A*, vol. 89A, no. 4, pp. 1063–1071, Jun. 2009.

[14] A. K. Agrawal, H. Harde, K. Thanki, and S. Jain, "Improved Stability and Antidiabetic Potential of Insulin Containing Folic Acid Functionalized Polymer Stabilized Multilayered Liposomes Following Oral Administration," *Biomacromolecules*, vol. 15, no. 1, pp. 350–360, Jan. 2014.

[15] A. G. Balducci, S. Cagnani, F. Sonvico, A. Rossi, P. Barata, G. Colombo, P. Colombo, and F. Buttini, "Pure insulin highly respirable powders for inhalation," *Eur. J. Pharm. Sci.*, vol. 51, pp. 110–117, Jan. 2014.

[16] R. Salzman, J. E. Manson, G. T. Griffing, R. Kimmerle, N. Ruderman, A. McCall, E. I. Stoltz, C. Mullin, D. Small, and J. Armstrong, "Intranasal aerosolized insulin. Mixed-meal studies and long-term use in type I diabetes," *N. Engl. J. Med.*, vol. 312, no. 17, pp. 1078–1084, Apr. 1985.

[17] S. Liu, M. Jin, Y. Quan, F. Kamiyama, H. Katsumi, T. Sakane, and A. Yamamoto, "The development and characteristics of novel microneedle arrays fabricated from hyaluronic acid, and their

application in the transdermal delivery of insulin," *J. Control. Release Off. J. Control. Release Soc.*, vol. 161, no. 3, pp. 933–941, Aug. 2012.
[18] Y. Ito, T. Nakahigashi, N. Yoshimoto, Y. Ueda, N. Hamasaki, and K. Takada, "Transdermal insulin application system with dissolving microneedles," *Diabetes Technol. Ther.*, vol. 14, no. 10, pp. 891–899, Oct. 2012.
[19] G. C. Chiou, C. Y. Chuang, and M. S. Chang, "Systemic delivery of insulin through eyes to lower the glucose concentration," *J. Ocul. Pharmacol.*, vol. 5, no. 1, pp. 81–91, 1989.
[20] B. W. Bequette, *Process Control: Modeling, Design and Simulation*, 1 edition. Upper Saddle River, N.J: Prentice Hall, 2003.
[21] "The Effect of Intensive Treatment of Diabetes on the Development and Progression of Long-Term Complications in Insulin-Dependent Diabetes Mellitus," *N. Engl. J. Med.*, vol. 329, no. 14, pp. 977–986, 1993.
[22] P. King, I. Peacock, and R. Donnelly, "The UK Prospective Diabetes Study (UKPDS): clinical and therapeutic implications for type 2 diabetes," *Br. J. Clin. Pharmacol.*, vol. 48, no. 5, pp. 643–648, Nov. 1999.
[23] A. J. Kowalski, "Can we really close the loop and how soon? Accelerating the availability of an artificial pancreas: a roadmap to better diabetes outcomes," *Diabetes Technol. Ther.*, vol. 11 Suppl 1, pp. S113–119, Jun. 2009.
[24] G. Marchetti, M. Barolo, L. Jovanovic, H. Zisser, and D. E. Seborg, "An improved PID switching control strategy for type 1 diabetes," *IEEE Trans. Biomed. Eng.*, vol. 55, no. 3, pp. 857–865, Mar. 2008.
[25] C. Cobelli, E. Renard, and B. Kovatchev, "Artificial Pancreas: Past, Present, Future," *Diabetes*, vol. 60, no. 11, pp. 2672–2682, Nov. 2011.
[26] A. H. Clemens, P. H. Chang, and R. W. Myers, "The development of Biostator, a Glucose Controlled Insulin Infusion System (GCIIS)," *Horm. Metab. Res. Horm. Stoffwechselforschung Horm. Métabolisme*, vol. Suppl 7, pp. 23–33, 1977.
[27] E. B. Marliss, F. T. Murray, E. F. Stokes, B. Zinman, A. F. Nakhooda, A. Denoga, B. S. Leibel, and A. M. Albisser, "Normalization of Glycemia in Diabetics During Meals with Insulin and Glucagon Delivery by the Artificial Pancreas," *Diabetes*, vol. 26, no. 7, pp. 663–672, Jul. 1977.
[28] R. S. Parker, F. J. Doyle 3rd, and N. A. Peppas, "A model-based algorithm for blood glucose control in type I diabetic patients," *IEEE Trans. Biomed. Eng.*, vol. 46, no. 2, pp. 148–157, Feb. 1999.
[29] R. S. Parker, E. P. Gatzke, and I. Doye, F.J., "Advanced model predictive control (MPC) for type I diabetic patient blood glucose control," in *American Control Conference, 2000. Proceedings of the 2000*, 2000, vol. 5, pp. 3483–3487 vol.5.
[30] L. Magni, D. M. Raimondo, C. Dalla Man, G. De Nicolao, B. Kovatchev, and C. Cobelli, "Model predictive control of glucose concentration in type I diabetic patients: An in silico trial," *Biomed. Signal Process. Control*, vol. 4, no. 4, pp. 338–346, Oct. 2009.
[31] L. Magni, M. Forgione, C. Toffanin, C. Dalla Man, B. Kovatchev, G. De Nicolao, and C. Cobelli, "Run-to-run tuning of model predictive control for type 1 diabetes subjects: in silico trial," *J. Diabetes Sci. Technol.*, vol. 3, no. 5, pp. 1091–1098, Sep. 2009.
[32] R. Hovorka, V. Canonico, L. J. Chassin, U. Haueter, M. Massi-Benedetti, M. Orsini Federici, T. R. Pieber, H. C. Schaller, L. Schaupp, T. Vering, and M. E. Wilinska, "Nonlinear model predictive control of glucose concentration in subjects with type 1 diabetes," *Physiol. Meas.*, vol. 25, no. 4, pp. 905–920, Aug. 2004.
[33] B. Kovatchev, C. Cobelli, E. Renard, S. Anderson, M. Breton, S. Patek, W. Clarke, D. Bruttomesso, A. Maran, C. Silvana, A. Avogaro, C. D. Man, A. Facchinetti, L. Magni, G. De Nicolao, J. Place, and A. Farret, "Multinational Study of Subcutaneous Model-Predictive Closed-Loop Control in Type 1

Diabetes Mellitus: Summary of the Results," *J. Diabetes Sci. Technol.*, vol. 4, no. 6, pp. 1374–1381, Nov. 2010.
[34] R. Hovorka, J. M. Allen, D. Elleri, L. J. Chassin, J. Harris, D. Xing, C. Kollman, T. Hovorka, A. M. F. Larsen, M. Nodale, A. De Palma, M. E. Wilinska, C. L. Acerini, and D. B. Dunger, "Manual closed-loop insulin delivery in children and adolescents with type 1 diabetes: a phase 2 randomised crossover trial," *Lancet*, vol. 375, no. 9716, pp. 743–751, Feb. 2010.
[35] E. Dassau, H. Zisser, R. A. Harvey, M. W. Percival, B. Grosman, W. Bevier, E. Atlas, S. Miller, R. Nimri, L. Jovanovic, and F. J. Doyle 3rd, "Clinical evaluation of a personalized artificial pancreas," *Diabetes Care*, vol. 36, no. 4, pp. 801–809, Apr. 2013.
[36] S. D. Patek, L. Magni, E. Dassau, C. Hughes-Karvetski, C. Toffanin, G. De Nicolao, S. Del Favero, M. Breton, C. D. Man, E. Renard, H. Zisser, F. J. Doyle, C. Cobelli, and B. P. Kovatchev, "Modular Closed-Loop Control of Diabetes," *IEEE Trans. Biomed. Eng.*, vol. 59, no. 11, pp. 2986–2999, Nov. 2012.
[37] S. J. Russell, F. H. El-Khatib, D. M. Nathan, K. L. Magyar, J. Jiang, and E. R. Damiano, "Blood glucose control in type 1 diabetes with a bihormonal bionic endocrine pancreas," *Diabetes Care*, vol. 35, no. 11, pp. 2148–2155, Nov. 2012.
[38] S. D. Patek, B. W. Bequette, M. Breton, B. A. Buckingham, E. Dassau, F. J. Doyle 3rd, J. Lum, L. Magni, and H. Zisser, "In silico preclinical trials: methodology and engineering guide to closed-loop control in type 1 diabetes mellitus," *J. Diabetes Sci. Technol.*, vol. 3, no. 2, pp. 269–282, Mar. 2009.
[39] B. P. Kovatchev, M. Breton, C. D. Man, and C. Cobelli, "In silico preclinical trials: a proof of concept in closed-loop control of type 1 diabetes," *J. Diabetes Sci. Technol.*, vol. 3, no. 1, pp. 44–55, Jan. 2009.
[40] R. Gillis, C. C. Palerm, H. Zisser, L. Jovanovic, D. E. Seborg, and F. J. Doyle, "Glucose estimation and prediction through meal responses using ambulatory subject data for advisory mode model predictive control," *J. Diabetes Sci. Technol.*, vol. 1, no. 6, pp. 825–833, Nov. 2007.
[41] M. W. Percival, H. Zisser, L. Jovanovic, and F. J. Doyle 3rd, "Closed-loop control and advisory mode evaluation of an artificial pancreatic Beta cell: use of proportional-integral-derivative equivalent model-based controllers," *J. Diabetes Sci. Technol.*, vol. 2, no. 4, pp. 636–644, Jul. 2008.
[42] A. Schiffrin, M. Mihic, B. S. Leibel, and A. M. Albisser, "Computer-assisted Insulin Dosage Adjustment," *Diabetes Care*, vol. 8, no. 6, pp. 545–552, Nov. 1985.
[43] T. Deutsch, E. R. Carson, F. E. Harvey, E. D. Lehmann, P. H. Sonksen, G. Tamas, G. Whitney, and C. D. Williams, "Computer-assisted diabetic management: a complex approach," *Comput. Methods Programs Biomed.*, vol. 32, no. 3–4, pp. 195–214, Aug. 1990.
[44] O. K. Hejlesen, S. Andreassen, R. Hovorka, and D. A. Cavan, "DIAS—the diabetes advisory system: an outline of the system and the evaluation results obtained so far," *Comput. Methods Programs Biomed.*, vol. 54, no. 1–2, pp. 49–58, Sep. 1997.
[45] O. K. Hejlesen, S. Andreassen, N. E. Frandsen, T. Brandt Sørensen, S. Henrik Sandø, R. Hovorka, and D. A. Cavan, "Using a double blind controlled clinical trial to evaluate the function of a Diabetes Advisory System: a feasible approach?," *Comput. Methods Programs Biomed.*, vol. 56, no. 2, pp. 165–173, May 1998.
[46] B. P. Kovatchev, E. Renard, C. Cobelli, H. C. Zisser, P. Keith-Hynes, S. M. Anderson, S. A. Brown, D. R. Chernavvsky, M. D. Breton, A. Farret, M.-J. Pelletier, J. Place, D. Bruttomesso, S. Del Favero, R. Visentin, A. Filippi, R. Scotton, A. Avogaro, and F. J. Doyle 3rd, "Feasibility of outpatient fully integrated closed-loop control: first studies of wearable artificial pancreas," *Diabetes Care*, vol. 36, no. 7, pp. 1851–1858, Jul. 2013.
[47] K. Zarkogianni, S. G. Mougiakakou, A. Prountzou, A. Vazeou, C. S. Bartsocas, and K. S. Nikita, "An Insulin Infusion Advisory System for Type 1 Diabetes Patients based on Non-Linear Model Predictive Control Methods," in *29th Annual International Conference of the IEEE Engineering in Medicine and Biology Society, 2007. EMBS 2007*, 2007, pp. 5971–5974.

[48] K. Nemire, “Roller Coasters, Mental Models, and Product Safety,” *Ergon. Des. Q. Hum. Factors Appl.*, vol. 16, no. 4, pp. 7–10, Sep. 2008.
[49] C. Cobelli, C. D. Man, G. Sparacino, L. Magni, G. De Nicolao, and B. P. Kovatchev, “Diabetes: Models, Signals, and Control,” *IEEE Rev. Biomed. Eng.*, vol. 2, pp. 54–96, Jan. 2009.
[50] C. Dalla Man, R. A. Rizza, and C. Cobelli, “Meal simulation model of the glucose-insulin system,” *IEEE Trans. Biomed. Eng.*, vol. 54, no. 10, pp. 1740–1749, Oct. 2007.
[51] R. N. Bergman, Y. Z. Ider, C. R. Bowden, and C. Cobelli, “Quantitative estimation of insulin sensitivity.,” *Am. J. Physiol. - Endocrinol. Metab.*, vol. 236, no. 6, p. E667, Jun. 1979.
[52] C. S. Hughes, S. D. Patek, M. D. Breton, and B. P. Kovatchev, “Hypoglycemia prevention via pump attenuation and red-yellow-green ‘traffic’ lights using continuous glucose monitoring and insulin pump data,” *J. Diabetes Sci. Technol.*, vol. 4, no. 5, pp. 1146–1155, Sep. 2010.
[53] S. Patek, M. Breton, P. Vereshchetin, B. Jiang, and B. Kovatchev, “Model-Based Control of Type 1 Diabetes in Risk Space,” presented at the International Federation for Automatic Control (IFAC), Cape Town, South Africa, 2014.
[54] B. P. Kovatchev, D. J. Cox, L. A. Gonder-Frederick, and W. Clarke, “Symmetrization of the Blood Glucose Measurement Scale and Its Applications,” *Diabetes Care*, vol. 20, no. 11, pp. 1655–1658, Nov. 1997.
[55] P. S. Gillies, D. P. Figgitt, and H. M. Lamb, “Insulin glargine,” *Drugs*, vol. 59, no. 2, pp. 253–260, 2000.
[56] K. I. Birkeland, P. D. Home, U. Wendisch, R. E. Ratner, T. Johansen, L. A. Endahl, K. Lyby, J. H. Jendle, A. P. Roberts, J. H. DeVries, and L. F. Meneghini, “Insulin Degludec in Type 1 Diabetes A randomized controlled trial of a new-generation ultra-long-acting insulin compared with insulin glargine,” *Diabetes Care*, vol. 34, no. 3, pp. 661–665, Mar. 2011.
[57] F. Porcellati, P. Rossetti, N. R. Busciantella, S. Marzotti, P. Lucidi, S. Luzio, D. R. Owens, G. B. Bolli, and C. G. Fanelli, “Comparison of pharmacokinetics and dynamics of the long-acting insulin analogs glargine and detemir at steady state in type 1 diabetes: a double-blind, randomized, crossover study,” *Diabetes Care*, vol. 30, no. 10, pp. 2447–2452, Oct. 2007.
[58] L. Heinemann, R. Linkeschova, K. Rave, B. Hompesch, M. Sedlak, and T. Heise, “Time-action profile of the long-acting insulin analog insulin glargine (HOE901) in comparison with those of NPH insulin and placebo,” *Diabetes Care*, vol. 23, no. 5, pp. 644–649, May 2000.
[59] F. Porcellati, G. B. Bolli, and C. G. Fanelli, “Pharmacokinetics and pharmacodynamics of basal insulins,” *Diabetes Technol. Ther.*, vol. 13 Suppl 1, pp. S15–24, Jun. 2011.
[60] I. B. Hirsch, “Insulin Analogues,” *N. Engl. J. Med.*, vol. 352, no. 2, pp. 174–183, 2005.
[61] *Linearization Methods for Stochastic Dynamic Systems*, vol. 730. Berlin, Heidelberg: Springer Berlin Heidelberg, 2008.
[62] H. J. Stetter, *Analysis of Discretization Methods for Ordinary Differential Equations*, vol. 23. Berlin, Heidelberg: Springer Berlin Heidelberg, 1973.
[63] L. S. Farhy, E. A. Ortiz, B. P. Kovatchev, A. G. Mora, S. E. Wolf, and C. E. Wade, “Average Daily Risk Range as a Measure of Glycemic Risk Is Associated with Mortality in the Intensive Care Unit: A Retrospective Study in a Burn Intensive Care Unit,” *J. Diabetes Sci. Technol.*, vol. 5, no. 5, pp. 1087–1098, Sep. 2011.
[64] J. D. Lee and K. A. See, “Trust in Automation: Designing for Appropriate Reliance,” *Hum. Factors J. Hum. Factors Ergon. Soc.*, vol. 46, no. 1, pp. 50–80, Mar. 2004.
[65] “The Human Side of the Artificial Pancreas,” *diaTribe*. [Online]. Available: http://diatribe.org/human-side-artificial-pancreas. [Accessed: 11-Mar-2015].
[66] J. A. Shepard, L. Gonder-Frederick, K. Vajda, and B. Kovatchev, “Patient Perspectives on Personalized Glucose Advisory Systems for Type 1 Diabetes Management,” *Diabetes Technol. Ther.*, vol. 14, no. 10, pp. 858–861, Oct. 2012.
[67] “iBOLUSED Focus Group Meeting,” 2013.

[68] "Standards of Medical Care in Diabetes--2012," *Diabetes Care*, vol. 35, no. Supplement_1, pp. S11–S63, Jan. 2012.
[69] R. S. Parker, F. J. Doyle, J. H. Ward, and N. A. Peppas, "Robust H∞ glucose control in diabetes using a physiological model," *AIChE J.*, vol. 46, no. 12, pp. 2537–2549, Dec. 2000.
[70] P. Dua, F. J. Doyle 3rd, and E. N. Pistikopoulos, "Multi-objective blood glucose control for type 1 diabetes," *Med. Biol. Eng. Comput.*, vol. 47, no. 3, pp. 343–352, Mar. 2009.
[71] N. Hernjak and F. J. Doyle, "Glucose control design using nonlinearity assessment techniques," *AIChE J.*, vol. 51, no. 2, pp. 544–554, Feb. 2005.
[72] B. P. Kovatchev, M. Straume, D. J. Cox, and L. S. Farhy, "Risk Analysis of Blood Glucose Data: A Quantitative Approach to Optimizing the Control of Insulin Dependent Diabetes," *Comput. Math. Methods Med.*, vol. 3, no. 1, pp. 1–10, 2000.
[73] B. Jiang, "Dynamic Model of Glycemic Risk: Application to T1DM Bolus Advisory System in Arti_cial Pancreas Platforms.," presented at the Diabetes Technology Meeting 2013, Chicago, 2013.
[74] B. Grosman, E. Dassau, H. C. Zisser, L. Jovanovic, and F. J. Doyle 3rd, "Zone model predictive control: a strategy to minimize hyper- and hypoglycemic events," *J. Diabetes Sci. Technol.*, vol. 4, no. 4, pp. 961–975, Jul. 2010.
[75] B. P. K. Sue A Brown, "Multinight 'Bedside' Closed-Loop Control for Patients with Type 1 Diabetes," *Diabetes Technol. Amp Ther.*, 2015.
[76] B. P. Kovatchev, S. D. Patek, E. A. Ortiz, and M. D. Breton, "Assessing Sensor Accuracy for Non-Adjunct Use of Continuous Glucose Monitoring," *Diabetes Technol. Ther.*, vol. 17, no. 3, pp. 177–186, Dec. 2014.
[77] J. C. Pickup, "Point: Are Insulin Pumps Underutilized in Type 1 Diabetes? Yes," *Diabetes Care*, vol. 29, no. 6, pp. 1449–1452, Jun. 2006.
[78] "Product Monograph. Lantus. Insulin glargine (rDNA orgin). Solution for injection 100 U/mL." Sanofi-Aventis, 07-Jan-2015.
[79] M. Hompesch, S. M. Ocheltree, E. T. Wondmagegnehu, L. A. Morrow, A. P. Kollmeier, B. N. Campaigne, and S. J. Jacober, "Pharmacokinetics and pharmacodynamics of insulin lispro protamine suspension compared with insulin glargine and insulin detemir in type 2 diabetes," *Curr. Med. Res. Opin.*, vol. 25, no. 11, pp. 2679–2687, Nov. 2009.
[80] M. Lepore, S. Pampanelli, C. Fanelli, F. Porcellati, L. Bartocci, A. Di Vincenzo, C. Cordoni, E. Costa, P. Brunetti, and G. B. Bolli, "Pharmacokinetics and pharmacodynamics of subcutaneous injection of long-acting human insulin analog glargine, NPH insulin, and ultralente human insulin and continuous subcutaneous infusion of insulin lispro," *Diabetes*, vol. 49, no. 12, pp. 2142–2148, Dec. 2000.
[81] T. Heise and L. F. Meneghini, "Insulin stacking versus therapeutic accumulation: understanding the differences," *Endocr. Pract. Off. J. Am. Coll. Endocrinol. Am. Assoc. Clin. Endocrinol.*, vol. 20, no. 1, pp. 75–83, Feb. 2014.
[82] S. E. Manley, "Estimated average glucose derived from HbA1c (eAG): report from European Association for the Study of Diabetes (EASD), Amsterdam 2007," *Diabet. Med.*, vol. 25, no. 2, pp. 126–128, Feb. 2008.
[83] C. Ellingsen, E. Dassau, H. Zisser, B. Grosman, M. W. Percival, L. Jovanovic, and F. J. Doyle, "Safety constraints in an artificial pancreatic beta cell: an implementation of model predictive control with insulin on board," *J. Diabetes Sci. Technol.*, vol. 3, no. 3, pp. 536–544, May 2009.
[84] J. Gibson, W. Scherer, and W. Gibson, *How to Do Systems Analysis*, 1st ed. Wiley, 2007.
[85] S. Burge, "The Systems Engineering Tool Box: Stakeholder Influence Map." .
[86] S. Burge, "The Systems Engineering Tool Box: Holistic Requirement Model." 2006.
[87] A. G. Tuckett, "Applying thematic analysis theory to practice: A researcher's experience," *Contemp. Nurse*, vol. 19, no. 1–2, pp. 75–87, Aug. 2005.

[88] V. Braun and V. Clarke, “Using thematic analysis in psychology,” *Qual. Res. Psychol.*, vol. 3, no. 2, pp. 77–101, Jan. 2006.
[89] S. Burge, “The Systems Engineering Tool Box: Systemic Textual Analysis.” 2004.
[90] L. Ricotti, T. Assaf, A. Menciassi, and P. Dario, “A novel strategy for long-term implantable artificial pancreas,” *Conf. Proc. Annu. Int. Conf. IEEE Eng. Med. Biol. Soc. IEEE Eng. Med. Biol. Soc. Annu. Conf.*, vol. 2011, pp. 2849–2853, 2011.
[91] S. Kalra, “Smart insulins,” *JPMA J. Pak. Med. Assoc.*, vol. 64, no. 1, pp. 95–97, Jan. 2014.
[92] Y. Y. Haimes, “Frontmatter,” in *Risk Modeling, Assessment, and Management*, John Wiley & Sons, Inc., 2008, pp. i–xxiii.
[93] “Use Matlab to discretize continuous state space model,” *Matrix, Control and Vision*. .
[94] G. U. Kuerzel, U. Shukla, H. E. Scholtz, S. G. Pretorius, D. H. Wessels, C. Venter, M. A. Potgieter, A. M. Lang, T. Koose, and E. Bernhardt, “Biotransformation of insulin glargine after subcutaneous injection in healthy subjects,” *Curr. Med. Res. Opin.*, vol. 19, no. 1, pp. 34–40, Jan. 2003.

Appendix A. Matrix Representation and Discretization

All the parameters in the equations (11), (12), and (15) are either available (BW), population average (V_I, k_d, k_{cl}, a_d, a_1, a_2, and G_b) or are calculated through a regression equation (parameters p_1, p_2, p_6, p_4) when the algorithm is engaged during the system's operation. Therefore, as soon as these parameters' values are obtained, we can take the system matrices of (11), (12), and (15) and discretize these equations using MATLAB means [93]. The resulted matrices for discrete state space models are then as follows:

$$\begin{bmatrix} -\kappa_d & 0 & 0 \\ \kappa_d & -\kappa_d & 0 \\ 0 & \kappa_d & -\kappa_{cl} \end{bmatrix} \Rightarrow A_I = \begin{bmatrix} k_{11}^{dis} & k_{12}^{dis} & k_{13}^{dis} \\ k_{21}^{dis} & k_{22}^{dis} & k_{23}^{dis} \\ k_{31}^{dis} & k_{32}^{dis} & k_{33}^{dis} \end{bmatrix}, \tag{52}$$

$$\begin{bmatrix} 1 \\ 0 \\ 0 \end{bmatrix} \Rightarrow B_I = \begin{bmatrix} b_{i1}^{dis} \\ b_{i2}^{dis} \\ b_{i3}^{dis} \end{bmatrix} \tag{53}$$

$$\begin{bmatrix} -(a_d + a_1) & 0 \\ a_d & -a_2 \end{bmatrix} \Rightarrow A_Q = \begin{bmatrix} a_{11}^{dis} & a_{12}^{dis} \\ a_{21}^{dis} & a_{22}^{dis} \end{bmatrix} \tag{54}$$

$$\begin{bmatrix} 1 \\ 0 \end{bmatrix} \Rightarrow B_Q = \begin{bmatrix} b_{q1}^{dis} \\ b_{a2}^{dis} \end{bmatrix} \tag{55}$$

$$\begin{bmatrix} -p_1 & -p_2 & 0 \\ 0 & -p_4 & 0 \\ 0 & 0 & -\frac{1}{720} \end{bmatrix} \Rightarrow A_C = \begin{bmatrix} p_{11}^{dis} & p_{12}^{dis} & p_{13}^{dis} \\ p_{21}^{dis} & p_{22}^{dis} & p_{23}^{dis} \\ p_{31}^{dis} & p_{32}^{dis} & p_{33}^{dis} \end{bmatrix} \tag{56}$$

$$\begin{bmatrix} p_6 \\ 0 \\ 0 \end{bmatrix} \Rightarrow B_{CQ} = \begin{bmatrix} b_{cq1}^{dis} \\ b_{cq2}^{dis} \\ b_{cq3}^{dis} \end{bmatrix} \tag{57}$$

$$\begin{bmatrix} 0 & 0 & 0 \\ 0 & 0 & \frac{p_4}{V_I BW} \\ 0 & 0 & 0 \end{bmatrix} \Rightarrow B_{CI1} = \begin{bmatrix} b_{ci11}^{dis} \\ b_{ci12}^{dis} \\ b_{ci13}^{dis} \end{bmatrix} \tag{58}$$

$$\begin{bmatrix} 0 \\ -p_4 I_b \\ 0 \end{bmatrix} \Rightarrow B_{CI2} = \begin{bmatrix} b_{ci21}^{dis} \\ b_{ci22}^{dis} \\ b_{ci23}^{dis} \end{bmatrix} \tag{59}$$

Where the elements of the RHS matrices have values produced by MATLAB. In addition, the same approach is used to obtain the following matrix that was not included in the matrix notation of equation (12), but corresponds to equation (8) and will become useful later in the derivation:

$$[a_1 \quad a_2] \Rightarrow C_Q=[c_{q1} \quad c_{q2}] \tag{60}$$

Further, the following matrix notation for the states is adopted:

$$i(k) = \begin{bmatrix} I_{SC1}(k) \\ I_{SC2}(k) \\ I_P(k) \end{bmatrix} \tag{61}$$

$$q(k) = \begin{bmatrix} Q_1(k) \\ Q_2(k) \end{bmatrix} \tag{62}$$

$$x(k) = \begin{bmatrix} ln\left(\frac{G(k)}{G_b}\right) \\ ln\left(\frac{X(k)}{X_b}\right) \\ \dot{\Delta}(k) \end{bmatrix} \tag{63}$$

Appendix B. Optimization Model Matrix Composition and Manipulation

The evolution equation of the insulin transport state all the way to the end of the horizon can be written out using matrix notation:

$$\begin{bmatrix} i(k) \\ i(k+1) \\ i(k+2) \\ \vdots \\ i(k+N-1) \end{bmatrix} = \begin{bmatrix} I \\ A_I \\ {A_I}^2 \\ \vdots \\ {A_I}^{N-1} \end{bmatrix} i(k) + \begin{bmatrix} \mathbf{0} & \mathbf{0} & \mathbf{0} & \dots & \mathbf{0} \\ I & \mathbf{0} & \mathbf{0} & \dots & \mathbf{0} \\ A_I & I & \mathbf{0} & \cdots & \mathbf{0} \\ \vdots & \vdots & \vdots & \ddots & \vdots \\ {A_I}^{N-2} & {A_I}^{N-3} & {A_I}^{N-4} & \cdots & \mathbf{0} \end{bmatrix} \begin{bmatrix} B_I \\ B_I \\ B_I \\ \vdots \\ B_I \end{bmatrix} J_{basal} + \begin{bmatrix} \mathbf{0} \\ B_I \\ A_I B_I \\ \vdots \\ {A_I}^{N-2} B_I \end{bmatrix} u_{bolus}(k) \quad \textbf{(64)}$$

where I is an identity matrix of the size 3x3, and $\mathbf{0}$ is a null matrix of the size 3x3 or a null column of the size 3x1, depending on the context. Notice that J_{basal} does not have the step index (k) anymore – two matrices in front of it propagate J_{basal} through the horizon implicitly creating all the consecutive state values. This is possible as basal is assumed constant throughout the time horizon.

We further define matrix notation as:

$$\tilde{\imath}_{k,N} = \begin{bmatrix} i(k) \\ i(k+1) \\ i(k+2) \\ \vdots \\ i(k+N-1) \end{bmatrix}, \text{ size 3Nx1} \quad \textbf{(65)}$$

$$\mathcal{A}_I = \begin{bmatrix} I \\ A_I \\ {A_I}^2 \\ \vdots \\ {A_I}^{N-1} \end{bmatrix}, \text{ size 3Nx3} \quad \textbf{(66)}$$

$$\Gamma_{I1} = \begin{bmatrix} \mathbf{0} & \mathbf{0} & \mathbf{0} & \dots & \mathbf{0} \\ I & \mathbf{0} & \mathbf{0} & \dots & \mathbf{0} \\ A_I & I & \mathbf{0} & \cdots & \mathbf{0} \\ \vdots & \vdots & \vdots & \ddots & \vdots \\ {A_I}^{N-2} & {A_I}^{N-3} & {A_I}^{N-4} & \cdots & \mathbf{0} \end{bmatrix}, \text{ size 3Nx3N} \quad \textbf{(67)}$$

$$\mathcal{B}_I = \begin{bmatrix} B_I \\ B_I \\ B_I \\ \vdots \\ B_I \end{bmatrix}, \text{ size 3Nx1} \tag{68}$$

$$\Gamma_{I2} = \begin{bmatrix} \mathbf{0} \\ B_I \\ A_I B_I \\ \vdots \\ {A_I}^{N-2} B_I \end{bmatrix}, \text{ size 3Nx1} \tag{69}$$

The same can be done with the evolution equation of the carbohydrate transport as was done with the insulin transport equation – the state evolution all the way to the end of the horizon can be written out using matrix notation:

$$\begin{bmatrix} d(k) \\ d(k+1) \\ d(k+2) \\ \vdots \\ d(k+N-1) \end{bmatrix} = \begin{bmatrix} C_Q & \mathbf{0} & \mathbf{0} & \dots & \mathbf{0} \\ \mathbf{0} & C_Q & \mathbf{0} & \dots & \mathbf{0} \\ \mathbf{0} & \mathbf{0} & C_Q & \cdots & \mathbf{0} \\ \vdots & \vdots & \vdots & \ddots & \vdots \\ \mathbf{0} & \mathbf{0} & \mathbf{0} & \cdots & C_Q \end{bmatrix} \left(\begin{bmatrix} I \\ A_Q \\ {A_Q}^2 \\ \vdots \\ {A_Q}^{N-1} \end{bmatrix} q(k) + \begin{bmatrix} \mathbf{0} \\ B_Q \\ A_Q B_Q \\ \vdots \\ {A_Q}^{N-2} B_Q \end{bmatrix} m(\mathrm{k}) \right) \tag{70}$$

where I is an identity matrix of the size 2x2, and $\mathbf{0}$ is a null vector of size 2x1 or a null vector of size 1x2, depending on the context. Note also, that C_Q of (60).

We further define matrix notation as:

$$\tilde{d}_{k,N} = \begin{bmatrix} d(k) \\ d(k+1) \\ d(k+2) \\ \vdots \\ d(k+N-1) \end{bmatrix}, \text{ size Nx1} \tag{71}$$

$$\mathcal{C}_Q = \begin{bmatrix} C_Q & \mathbf{0} & \mathbf{0} & \dots & \mathbf{0} \\ \mathbf{0} & C_Q & \mathbf{0} & \dots & \mathbf{0} \\ \mathbf{0} & \mathbf{0} & C_Q & \cdots & \mathbf{0} \\ \vdots & \vdots & \vdots & \ddots & \vdots \\ \mathbf{0} & \mathbf{0} & \mathbf{0} & \cdots & C_Q \end{bmatrix}, \text{ size Nx2N} \tag{72}$$

$$\mathcal{A}_Q = \begin{bmatrix} I \\ A_Q \\ {A_Q}^2 \\ \vdots \\ {A_Q}^{N-1} \end{bmatrix}, \text{ size 2Nx2} \tag{73}$$

$$\mathcal{B}_Q = \begin{bmatrix} \mathbf{0} \\ B_Q \\ A_Q B_Q \\ \vdots \\ {A_Q}^{N-2} B_Q \end{bmatrix}, \text{ size 2Nx1} \tag{74}$$

Finally, the same can be done for the core model – the state all the way to the end of the horizon can be written out using matrix notation:

$$\begin{bmatrix} x(k+1) \\ x(k+2) \\ x(k+3) \\ \vdots \\ x(k+N) \end{bmatrix} = \begin{bmatrix} A_C \\ {A_C}^2 \\ {A_C}^3 \\ \vdots \\ {A_C}^N \end{bmatrix} x(k)$$

$$+ \begin{bmatrix} B_{CQ} & \mathbf{0} & \mathbf{0} & \dots & \mathbf{0} \\ A_C B_{CQ} & B_{CQ} & \mathbf{0} & \dots & \mathbf{0} \\ {A_C}^2 B_{CQ} & A_C B_{CQ} & B_{CQ} & \cdots & \mathbf{0} \\ \vdots & \vdots & \vdots & \ddots & \vdots \\ {A_C}^{N-1} B_{CQ} & {A_C}^{N-2} B_{CQ} & {A_C}^{N-3} B_{CQ} & \dots & B_{CQ} \end{bmatrix} \begin{bmatrix} d(k) \\ d(k+1) \\ d(k+2) \\ \vdots \\ d(k+N-1) \end{bmatrix}$$

$$+ \begin{bmatrix} B_{CI1} & \mathbf{0} & \mathbf{0} & \dots & \mathbf{0} \\ A_C B_{CI1} & B_{CI1} & \mathbf{0} & \dots & \mathbf{0} \\ {A_C}^2 B_{CI1} & A_C B_{CI1} & B_{CI1} & \cdots & \mathbf{0} \\ \vdots & \vdots & \vdots & \ddots & \vdots \\ {A_C}^{N-1} B_{CI1} & {A_C}^{N-2} B_{CI1} & {A_C}^{N-3} B_{CI1} & \dots & B_{CI1} \end{bmatrix} \tilde{\imath}_{k,N} \tag{75}$$

$$+ \begin{bmatrix} I & \mathbf{0} & \mathbf{0} & \dots & \mathbf{0} \\ A_c & I & \mathbf{0} & \dots & \mathbf{0} \\ {A_C}^2 & A_c & I & \cdots & \mathbf{0} \\ \vdots & \vdots & \vdots & \ddots & \vdots \\ {A_C}^{N-1} & {A_C}^{N-2} & {A_C}^{N-3} & \dots & I \end{bmatrix} \begin{bmatrix} B_{CI2} \\ B_{CI2} \\ B_{CI2} \\ \vdots \\ B_{CI2} \end{bmatrix}$$

Since our aim is to derive a closed-form solution for $u_{bolus}(k)$, we have to expand $\tilde{\imath}_{k,N}$ and write out the evolution of the insulin transport state explicitly:

$$\begin{bmatrix} x(k+1) \\ x(k+2) \\ x(k+3) \\ \vdots \\ x(k+N) \end{bmatrix} = \begin{bmatrix} A_C \\ {A_C}^2 \\ {A_C}^3 \\ \vdots \\ {A_C}^N \end{bmatrix} x(k)$$

$$+ \begin{bmatrix} B_{CQ} & \mathbf{0} & \mathbf{0} & \dots & \mathbf{0} \\ A_C B_{CQ} & B_{CQ} & \mathbf{0} & \dots & \mathbf{0} \\ {A_C}^2 B_{CQ} & A_C B_{CQ} & B_{CQ} & \cdots & \mathbf{0} \\ \vdots & \vdots & \vdots & \ddots & \vdots \\ {A_C}^{N-1} B_{CQ} & {A_C}^{N-2} B_{CQ} & {A_C}^{N-3} B_{CQ} & \dots & B_{CQ} \end{bmatrix} \begin{bmatrix} d(k) \\ d(k+1) \\ d(k+2) \\ \vdots \\ d(k+N-1) \end{bmatrix}$$

$$+ \begin{bmatrix} B_{CI1} & \mathbf{0} & \mathbf{0} & \dots & \mathbf{0} \\ A_C B_{CI1} & B_{CI1} & \mathbf{0} & \dots & \mathbf{0} \\ {A_C}^2 B_{CI1} & A_C B_{CI1} & B_{CI1} & \cdots & \mathbf{0} \\ \vdots & \vdots & \vdots & \ddots & \vdots \\ {A_C}^{N-1} B_{CI1} & {A_C}^{N-2} B_{CI1} & {A_C}^{N-3} B_{CI1} & \dots & B_{CI1} \end{bmatrix} \begin{bmatrix} I \\ A_I \\ {A_I}^2 \\ \vdots \\ {A_I}^{N-1} \end{bmatrix} i(k)$$

$$+ \begin{bmatrix} B_{CI1} & \mathbf{0} & \mathbf{0} & \dots & \mathbf{0} \\ A_C B_{CI1} & B_{CI1} & \mathbf{0} & \dots & \mathbf{0} \\ {A_C}^2 B_{CI1} & A_C B_{CI1} & B_{CI1} & \cdots & \mathbf{0} \\ \vdots & \vdots & \vdots & \ddots & \vdots \\ {A_C}^{N-1} B_{CI1} & {A_C}^{N-2} B_{CI1} & {A_C}^{N-3} B_{CI1} & \dots & B_{CI1} \end{bmatrix} \quad \textbf{(76)}$$

$$\begin{bmatrix} \mathbf{0} & \mathbf{0} & \mathbf{0} & \dots & \mathbf{0} \\ I & \mathbf{0} & \mathbf{0} & \dots & \mathbf{0} \\ A_I & I & \mathbf{0} & \cdots & \mathbf{0} \\ \vdots & \vdots & \vdots & \ddots & \vdots \\ {A_I}^{N-2} & {A_I}^{N-3} & {A_I}^{N-4} & \dots & \mathbf{0} \end{bmatrix} \begin{bmatrix} B_I \\ B_I \\ B_I \\ \vdots \\ B_I \end{bmatrix} J_{basal}$$

$$+ \begin{bmatrix} B_{CI1} & \mathbf{0} & \mathbf{0} & \dots & \mathbf{0} \\ A_C B_{CI1} & B_{CI1} & \mathbf{0} & \dots & \mathbf{0} \\ {A_C}^2 B_{CI1} & A_C B_{CI1} & B_{CI1} & \cdots & \mathbf{0} \\ \vdots & \vdots & \vdots & \ddots & \vdots \\ {A_C}^{N-1} B_{CI1} & {A_C}^{N-2} B_{CI1} & {A_C}^{N-3} B_{CI1} & \dots & B_{CI1} \end{bmatrix} \begin{bmatrix} \mathbf{0} \\ B_I \\ A_I B_I \\ \vdots \\ {A_I}^{N-2} B_I \end{bmatrix} u_{bolus}(k)$$

$$+ \begin{bmatrix} I & \mathbf{0} & \mathbf{0} & \dots & \mathbf{0} \\ A_C & I & \mathbf{0} & \dots & \mathbf{0} \\ {A_C}^2 & A_c & I & \cdots & \mathbf{0} \\ \vdots & \vdots & \vdots & \ddots & \vdots \\ {A_C}^{N-1} & {A_C}^{N-2} & {A_C}^{N-3} & \dots & I \end{bmatrix} \begin{bmatrix} B_{CI2} \\ B_{CI2} \\ B_{CI2} \\ \vdots \\ B_{CI2} \end{bmatrix}$$

We further define matrix notation as:

$$\tilde{x}_{k,N} = \begin{bmatrix} x(k+1) \\ x(k+2) \\ x(k+3) \\ \vdots \\ x(k+N) \end{bmatrix}, \text{ size 3Nx1} \tag{77}$$

$$\mathcal{A}_C = \begin{bmatrix} A_C \\ {A_C}^2 \\ {A_C}^3 \\ \vdots \\ {A_C}^N \end{bmatrix}, \text{ size 3Nx3} \tag{78}$$

$$\Gamma_{C1} = \begin{bmatrix} B_{CQ} & \mathbf{0} & \mathbf{0} & \dots & \mathbf{0} \\ A_C B_{CQ} & B_{CQ} & \mathbf{0} & \dots & \mathbf{0} \\ {A_C}^2 B_{CQ} & A_C B_{CQ} & B_{CQ} & \cdots & \mathbf{0} \\ \vdots & \vdots & \vdots & \ddots & \vdots \\ {A_C}^{N-1} B_{CQ} & {A_C}^{N-2} B_{CQ} & {A_C}^{N-3} B_{CQ} & \dots & B_{CQ} \end{bmatrix}, \text{ size 3NxN} \tag{79}$$

$$\Gamma_{C2} = \begin{bmatrix} B_{CI1} & \mathbf{0} & \mathbf{0} & \dots & \mathbf{0} \\ A_C B_{CI1} & B_{CI1} & \mathbf{0} & \dots & \mathbf{0} \\ {A_C}^2 B_{CI1} & A_C B_{CI1} & B_{CI1} & \cdots & \mathbf{0} \\ \vdots & \vdots & \vdots & \ddots & \vdots \\ {A_C}^{N-1} B_{CI1} & {A_C}^{N-2} B_{CI1} & {A_C}^{N-3} B_{CI1} & \dots & B_{CI1} \end{bmatrix}, \text{ size 3NxN} \tag{80}$$

$$\Gamma_{C3} = \begin{bmatrix} I & \mathbf{0} & \mathbf{0} & \dots & \mathbf{0} \\ A_C & I & \mathbf{0} & \dots & \mathbf{0} \\ {A_C}^2 & A_c & I & \cdots & \mathbf{0} \\ \vdots & \vdots & \vdots & \ddots & \vdots \\ {A_C}^{N-1} & {A_C}^{N-2} & {A_C}^{N-3} & \dots & I \end{bmatrix}, \text{ size 3Nx3N} \tag{81}$$

$$\mathcal{B}_{CI2} = \begin{bmatrix} B_{CI2} \\ B_{CI2} \\ B_{CI2} \\ \vdots \\ B_{CI2} \end{bmatrix}, \text{ size 3Nx1} \tag{82}$$

Appendix C. Q Matrix Composition and Use

First, several "discrete" matrices were used that had more elements to the end of the diagonal filled with one instead of zeros as more time passed after the meal. These matrices are presented in Figure 70.

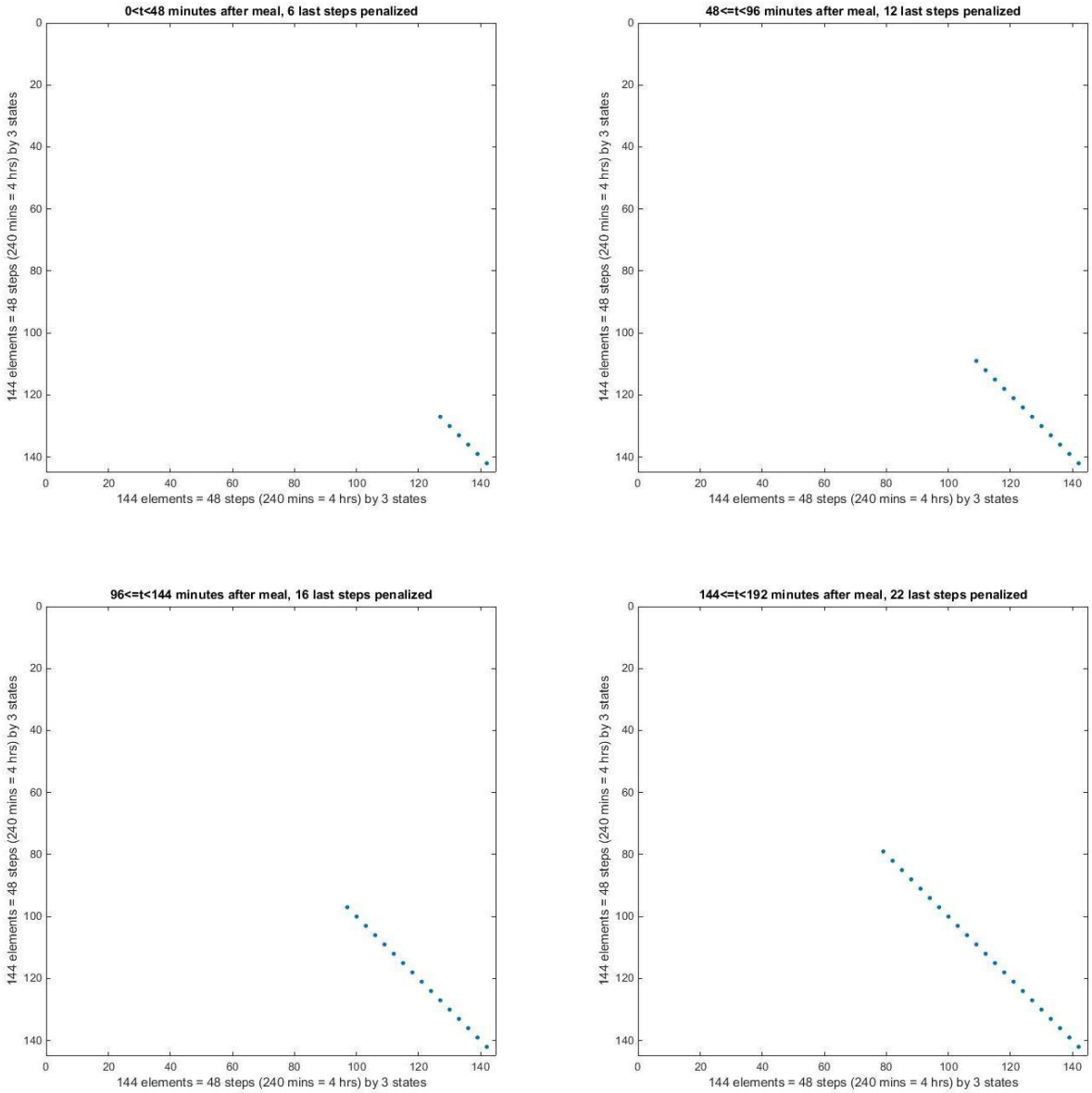

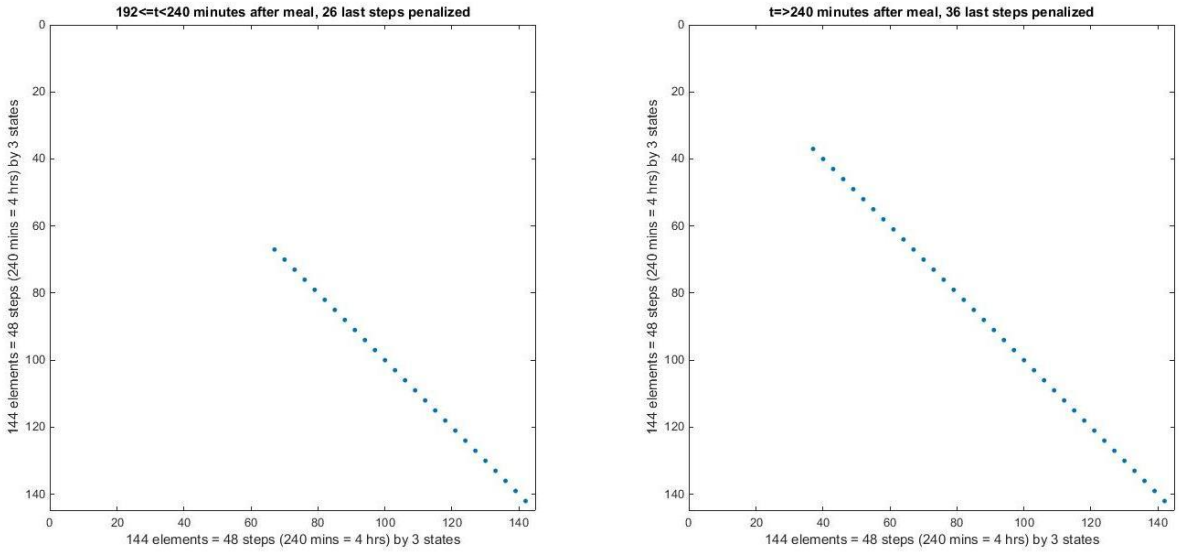

Figure 70. *Q* Matrix Variations. Blue dots show element positions with 1's.

Then, these 6 matrices were combined through interpolation of their "tails" that do not overlap between every consecutive pair of matrices to obtain the intended penalization along the horizon. Consider now a particular example. A meal was consumed at 1:00 pm and a corresponding meal bolus was taken at the time. At 1:50pm, the patient decides to administer a correction bolus as the glucose is at 170 mg/dl which for this particular patient is too high. An idealistic gradual penalization of glucose deviation that the algorithm would use in this scenario is illustrated in Figure 71.

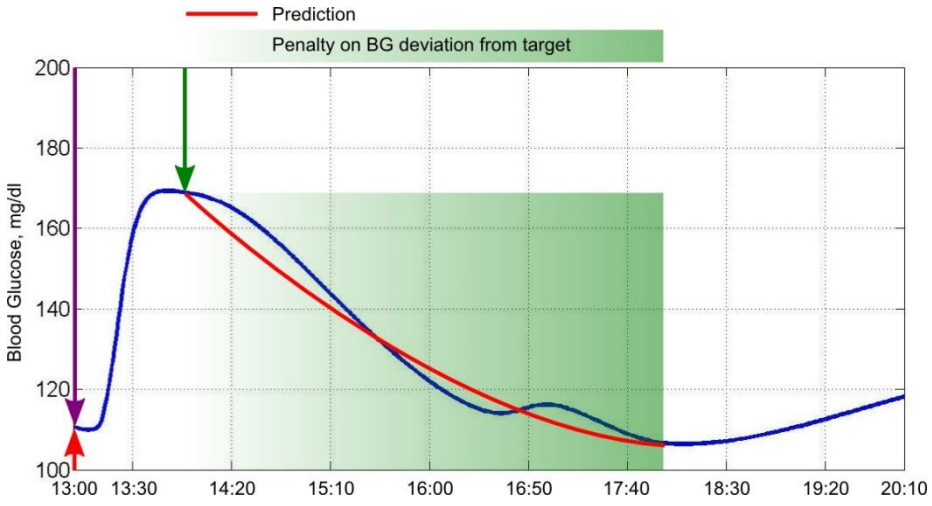

Figure 71. Penalty Increasing Later In the Horizon..

To achieve this, the diagonals of all possible Q matrices were stacked next to each other as columns of a new Q_{pool} matrix. For this particular implementation of the 4-hour prediction horizon, 5-minute discretization, and 3 core states, the Q_{pool} is a matrix of size 144x264. The matrix is presented in Figure 72.

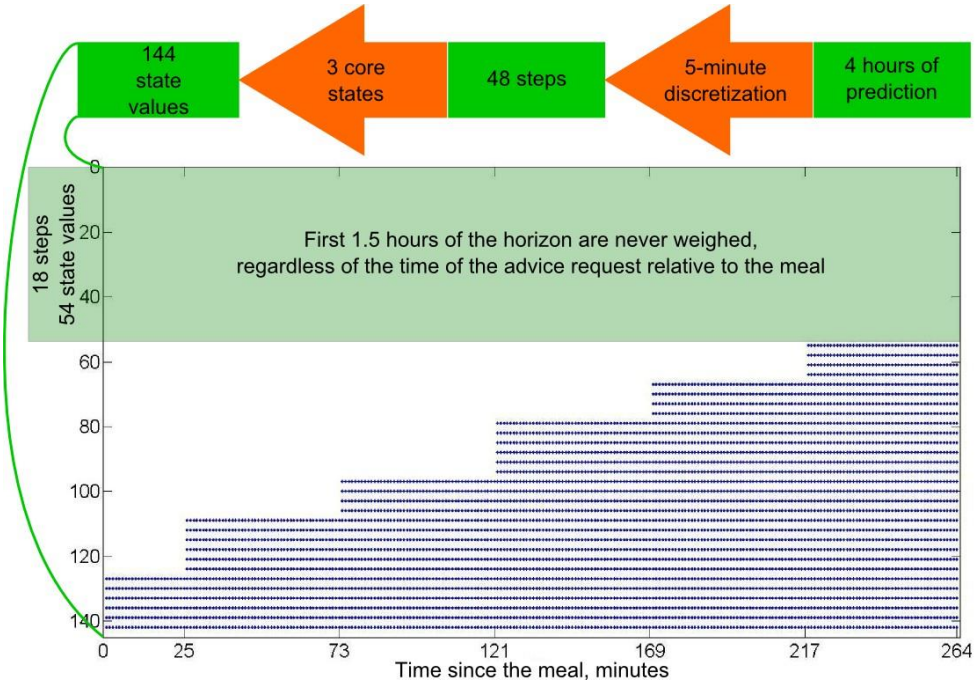

Figure 72. Q_{pool} Matrix.

As was mentioned above, the matrix is filled as a gradient, meaning that not all dots in Figure 72 represent 1's, the vertical vectors themselves consist of two subsets of different values: one set that depended on the "tails" interpolation, and the next set which is all 1's.

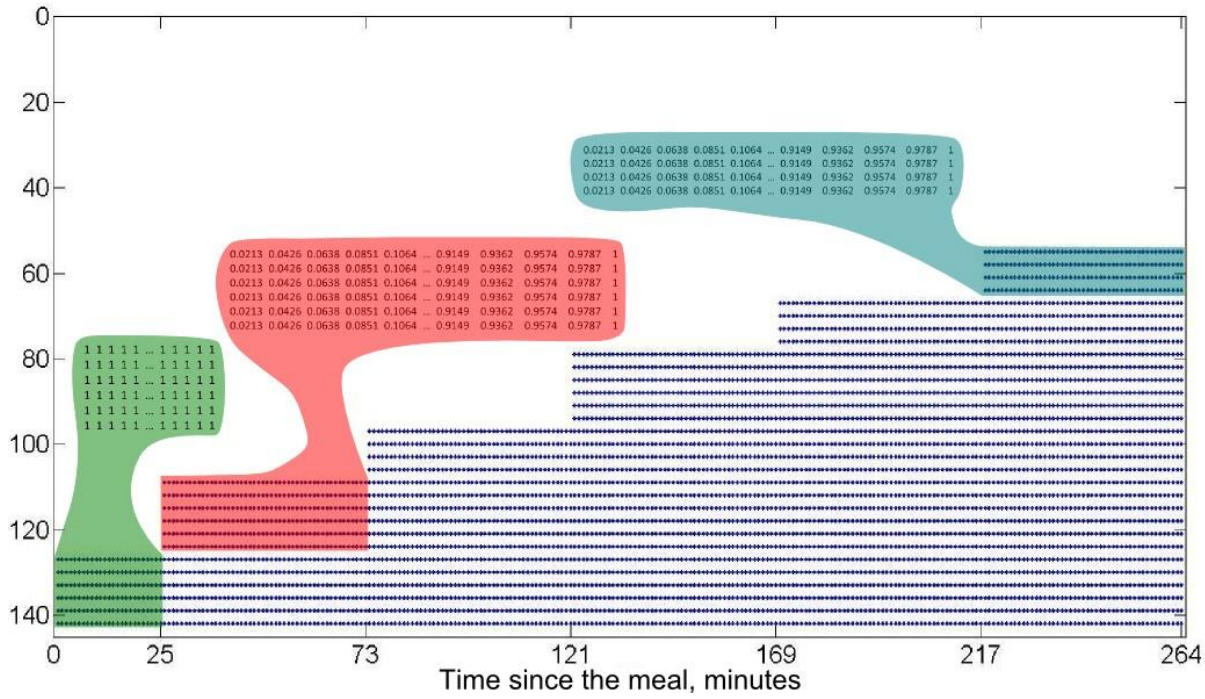

Figure 73. Q_{pool} Values Shown.

The way the algorithm "reads" and applies Q_{pool} is presented in Figure 74. In the figure, Q_{BG} is the resulting matrix that is used by the algorithm in equations (23) and (24).

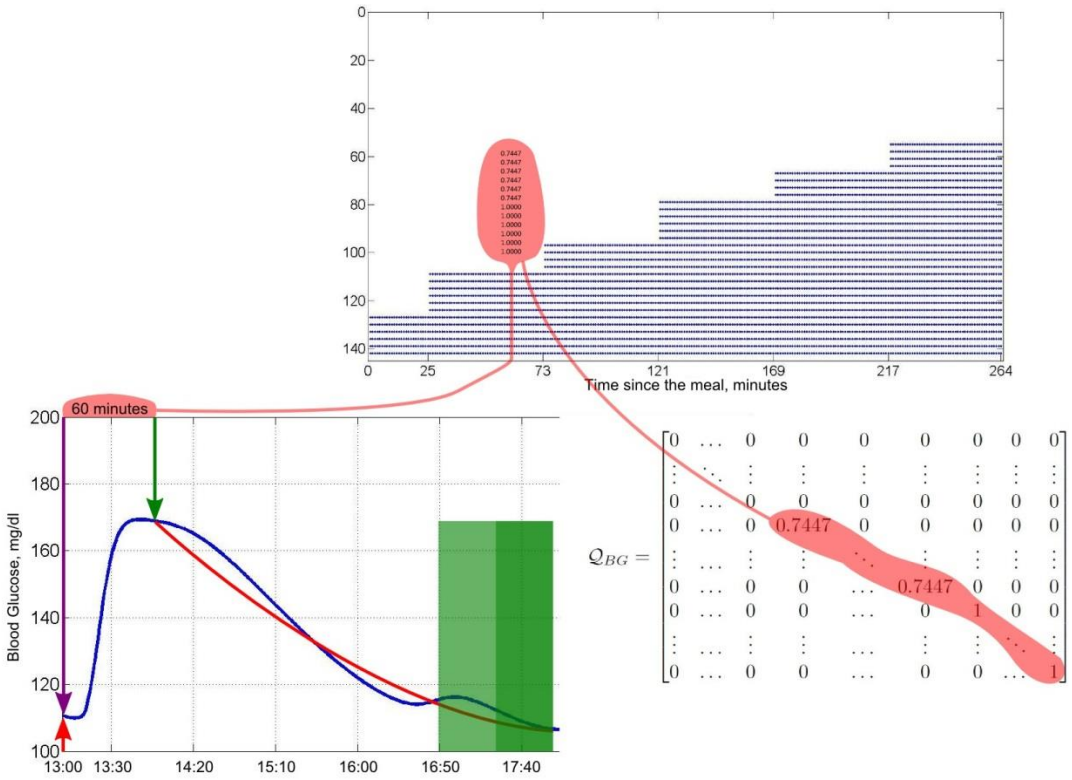

Figure 74. Example of Q_{pool} Use.

Appendix D. Notes from the Clinical Trial, Subject 1.

1	MEAL_CHO=MEDIUM + REGULAR
2	HYPO_CHO=16
3	Patient showered from 21:26 to 21:32; removed pump and did not receive any boluses during this time
4	ADVICE=subject requested advice- 0.65 units was suggested, subject accepted, actual injected insulin 0.7 units
5	CGM2=?????; Secondary CGM currently has no reading "?????"
6	ketones 0.1; repeated SMBG 275=mg/dl
7	repeated ketone=0.1
8	calibrate the secondary CGM at 296mg/dl
9	0.0 ketones
10	For lunch, correction advised was -2.87, full bolus 0.9.
11	Lunch low carb
12	13:39 calibration 189

Appendix E. Notes from the Clinical Trial, Subject 2.

1	MEAL_CHO=SLOW+LARGE; (Ruby Tuesday's- French fries, cheeseburger + bun, salad, italian salad dressing
2	System recommended 2.5, subject chose to decrease to 1.8; Initial advice requested got 1.7 advice, subject cancelled, subject requested advice again for 1.9 advice but subject lowered this to 1.7 then hit inject. The safety message chame up and the injection was cancelled. Advice then was requested again and displayed 0 to subject, subject increased to 1.8 which was then actually injected
3	KETONES = 0.2
4	KETONES=0.1
5	KETONES=0.1, at 00:02
6	CGM reading low, not correctly reading, SMBG 131mg/dl. CGM came back in 20mins.
7	patient got a headache and did a SMBG herself
8	<90 alarm
9	For lunch, correction advised was -3.58, full bolus 0.0.
10	Lunch medium regular

Appendix F. Notes from the Clinical Trial, Subject 3.

1	MEAL_CHO=41; ACTUAL VALUE= 41;MEAL GRID VALUE = 39
2	MEAL_CHO= 17; ACTUAL VALUE =17; MEAL GRID VALUE = 20
3	OTHER_PUMP_OTHER; BASAL BOLUS 0.1 NOT GIVEN AT 23:10, LOG SHOWED "INVALID REQUEST"; POSSIBLY BLOCK OF COMMUNICATION BETWEEN DIAS PHONE AND PUMP
4	SMBG=85; FOR RED LIGHT
5	SMBG=82; FOR RED LIGHT
6	SMBG=76; FOR RED LIGHT
7	SMBG=75
8	SMBG=81
9	SMBG=153
10	MEAL_CHO= 69; ACTUAL VALUE= 69; MEAL GRID VALUE= 60.
11	PUMP; BATTERY LOW AND WAS REPLACED
12	Advice suggested is 2.4, subject decided to manually decrease to 1.4
13	KETONES= 0.0
14	Subject requested advice, the value is 0 due to the blackout period, manually increased to 0.5
15	Subject started some exercise (walking around the hose) at about 11:40 and proceeded for about 10-15 minutes to see if BG reacts. Steep drop ensued as can be seen in the graph.
16	Meal of 44 actual grams estimated into the 'most carbs' group of 60 grams. At the time of the bolus request CGM was 146 mg/dl and the advice suggested -0.36 U (due to the previous long term steep downward trend). The bolus wasn't injected. Few minutes later bolus was requested again and the CGM was 129 mg/dl. At this time it was -1.07 U and the total of 2.46 was accepted and injected with actual amount injected being 2.5 due to pump rounding.
17	HYPO_CHO=16g
18	Exercise (walking) from 14:29 to 15:14.
19	Subject tried to take a bolus for snack, did not like suggestion for bolus (way too high), tried a few times and was still high, decreased to 1.22 units and tried to give it, but it never went through. Subject decided not to have a snack.
20	Advise requested: Advise given was zero. On display appeared to be 2.7 units. Patient elected to take 1.5 units.
21	Subject re-calibrated both CGMs based upon SMBG of 158.
22	OTHER_RMS_OTHER; DIAS PHONE DISPLAYED INABILITY TO CONTACT DWM SERVER, AND LAST CGM WAS 7 MIN AGO, BUT BACKUP CGM GAVE ALARM OF CGM BELOW 90
23	HYPO_CHO=16; FOR RED LIGHT
24	Open Loop at 07:27
25	test 2
26	Subject went out of range for 10 minutes- may have missed bolus and got no CGM data
27	IGNORE BG OF 200
28	Aprox. 04:50 BG<90 Traffic Light is still yellow
29	RESET_CGM_RMS; CGM was out of range and reset, think it may be due to subject sleeping across the bed and on stomach, there was no antenna on CGM receiver which would suggest out of range issue
30	CALIB_CGM=134
31	Two CGM data points Listed (think this may be due to CGM calibration)

32	CGM; Issue resolved but a data point was lost
33	CGM; Connections good, CGM missing data points on its own
34	RESTART; SUBJECT_ACCIDENT; slept on her side, stopped getting data; System taken out of Closed Loop for 10 minutes; connection issues with CGM- fixed by having subject get closer to DiAs and taking CGM in and out of dock

Appendix G. Visual Analysis of MDI Subjects.

Notice that the scale of Y axis is 0 to 400 for all subjects besides three for whom it is set individually.

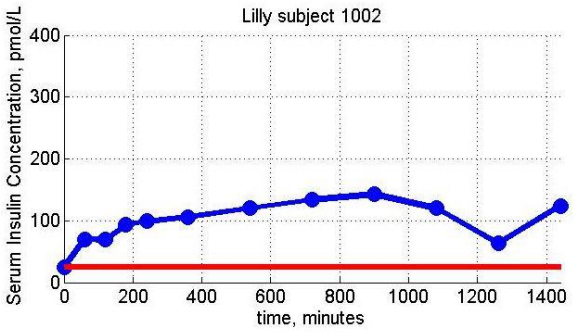

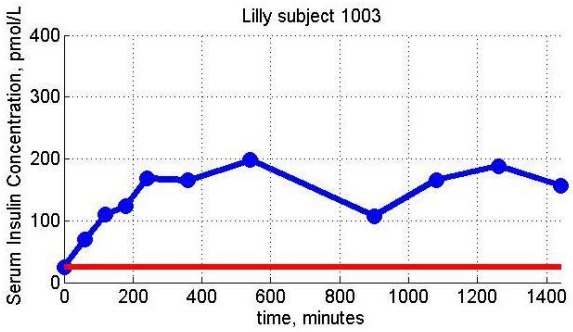

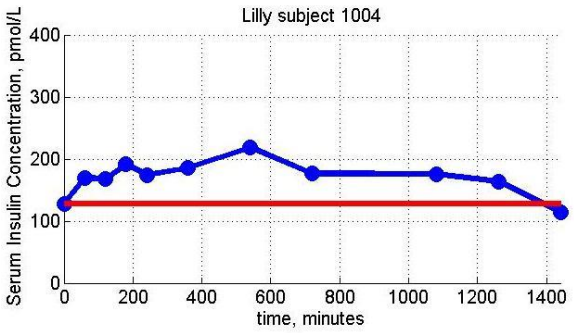

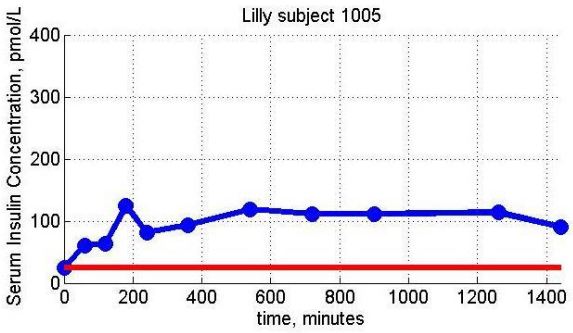

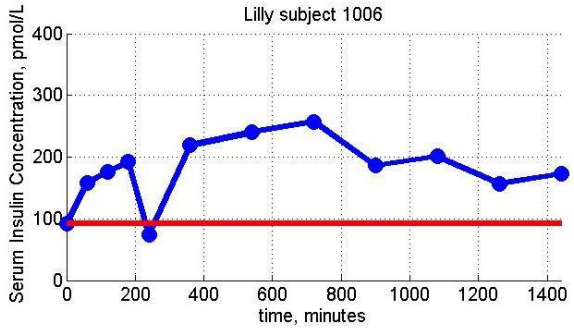

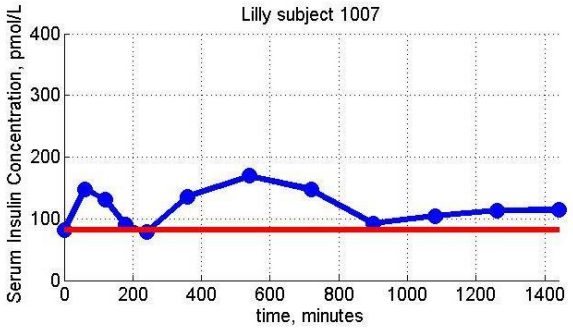

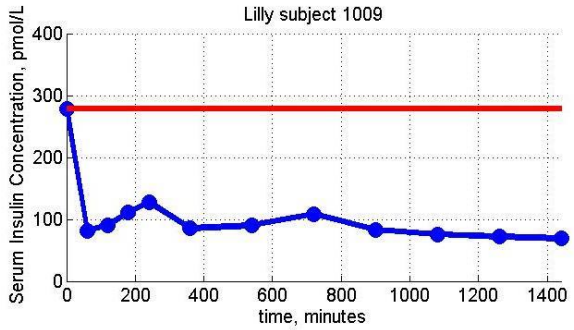

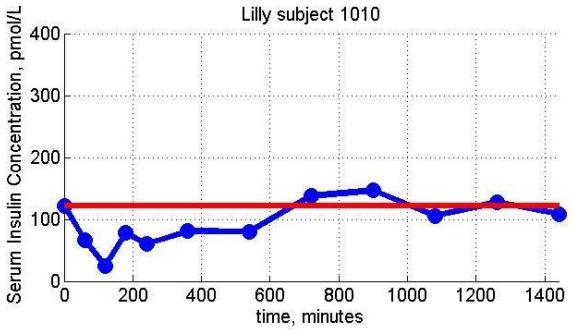

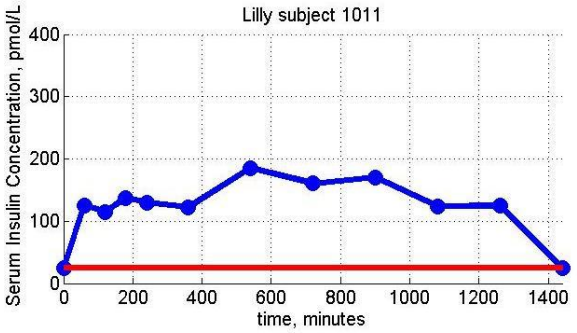
Lilly subject 1011
Serum Insulin Concentration, pmol/L
time, minutes

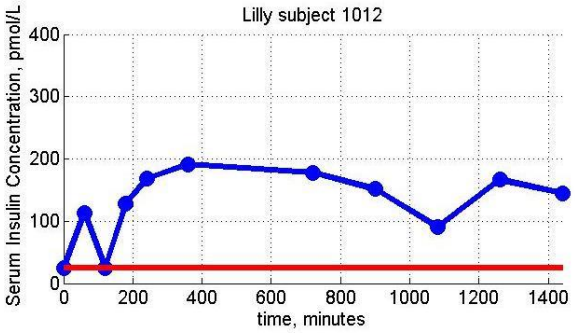
Lilly subject 1012
Serum Insulin Concentration, pmol/L
time, minutes

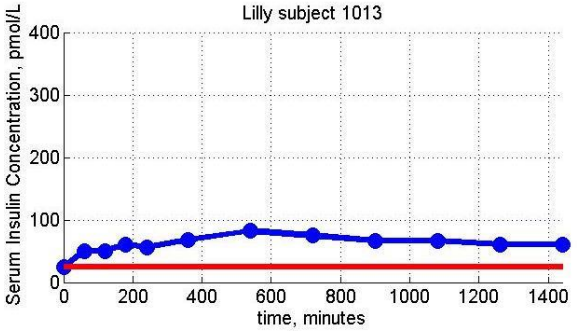
Lilly subject 1013
Serum Insulin Concentration, pmol/L
time, minutes

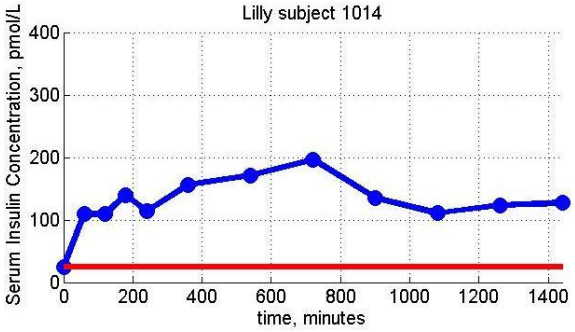
Lilly subject 1014
Serum Insulin Concentration, pmol/L
time, minutes

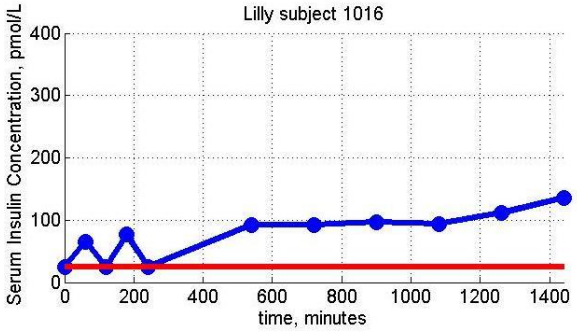
Lilly subject 1016
Serum Insulin Concentration, pmol/L
time, minutes

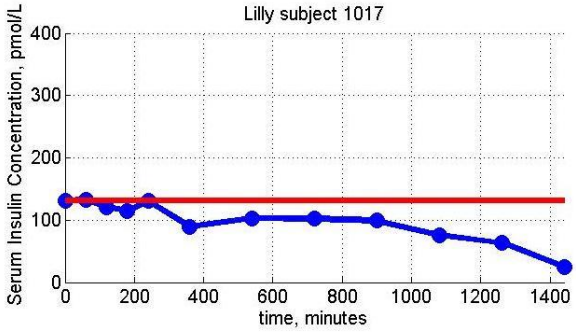
Lilly subject 1017
Serum Insulin Concentration, pmol/L
time, minutes

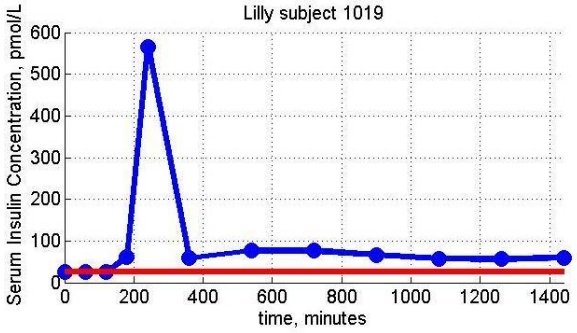
Lilly subject 1019
Serum Insulin Concentration, pmol/L
time, minutes

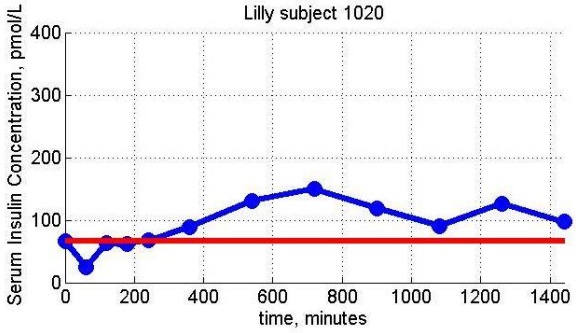
Lilly subject 1020
Serum Insulin Concentration, pmol/L
time, minutes

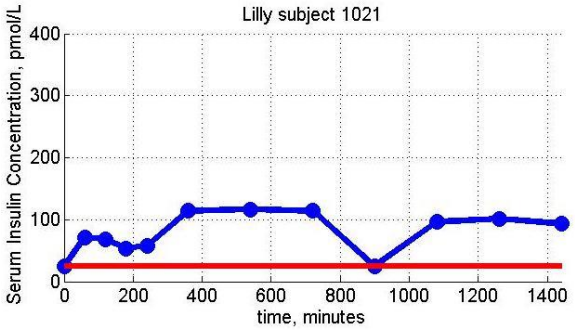
Lilly subject 1021
Serum Insulin Concentration, pmol/L
time, minutes

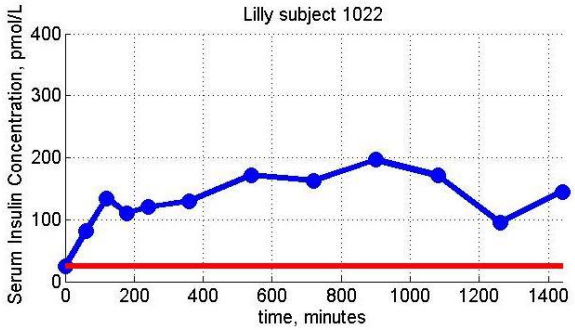
Lilly subject 1022
Serum Insulin Concentration, pmol/L
time, minutes

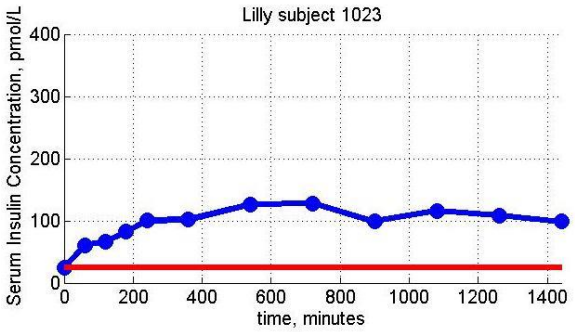
Lilly subject 1023
Serum Insulin Concentration, pmol/L
time, minutes

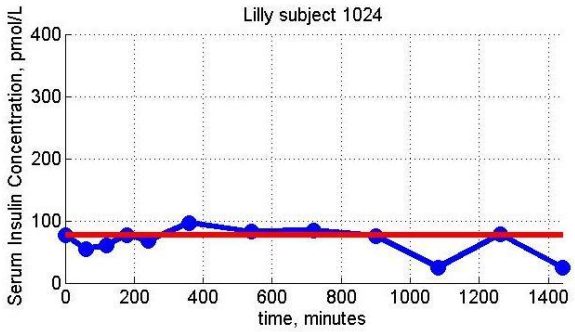
Lilly subject 1024
Serum Insulin Concentration, pmol/L
time, minutes

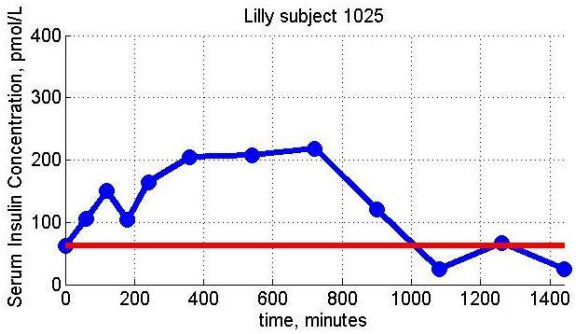
Lilly subject 1025
Serum Insulin Concentration, pmol/L
time, minutes

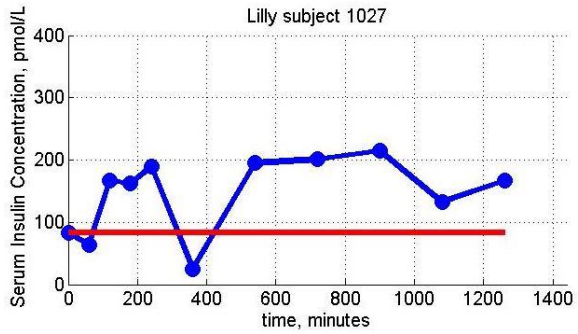
Lilly subject 1027
Serum Insulin Concentration, pmol/L
time, minutes

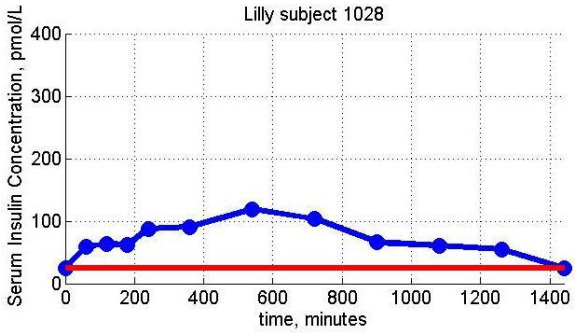
Lilly subject 1028
Serum Insulin Concentration, pmol/L
time, minutes

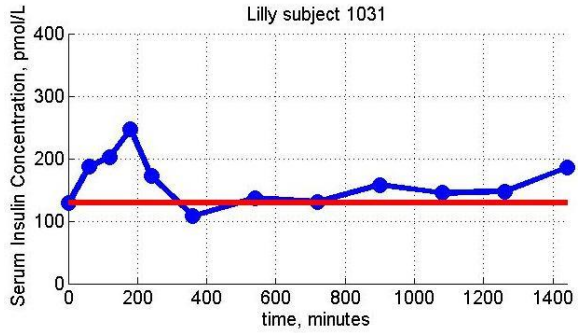
Lilly subject 1031
Serum Insulin Concentration, pmol/L
time, minutes

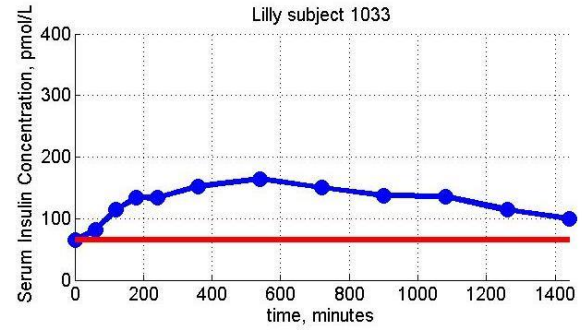
Lilly subject 1033
Serum Insulin Concentration, pmol/L
time, minutes

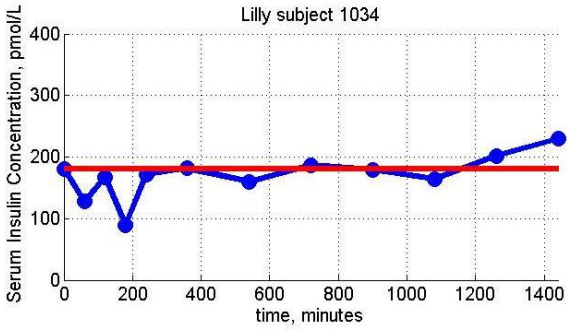
Lilly subject 1034
Serum Insulin Concentration, pmol/L
time, minutes

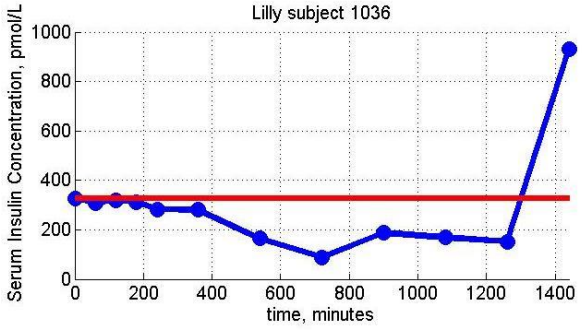
Lilly subject 1036
Serum Insulin Concentration, pmol/L
time, minutes

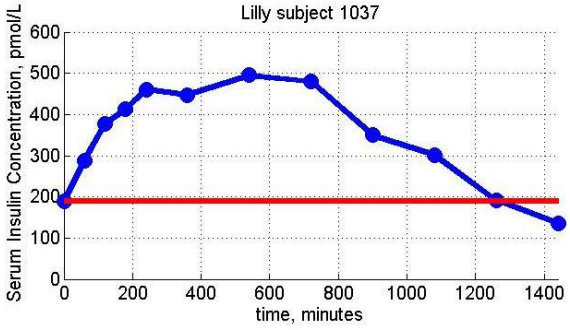
Lilly subject 1037
Serum Insulin Concentration, pmol/L
time, minutes

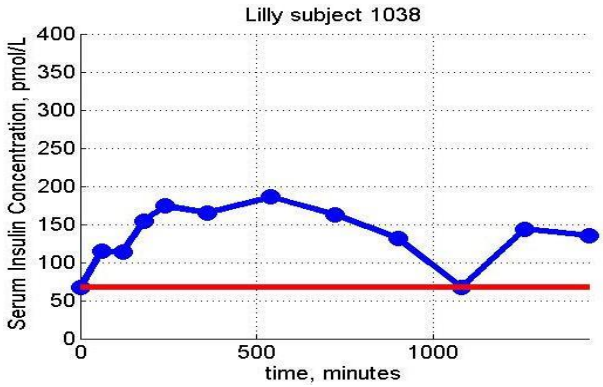
Lilly subject 1038
Serum Insulin Concentration, pmol/L
time, minutes

Appendix H. Individual Fits

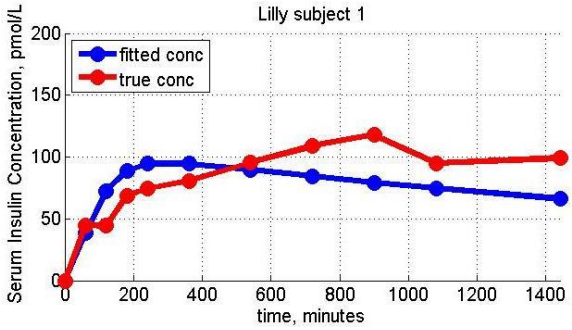

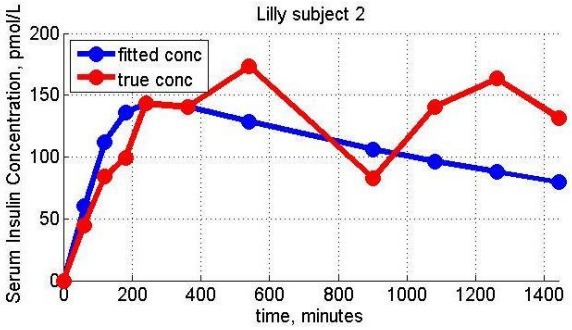

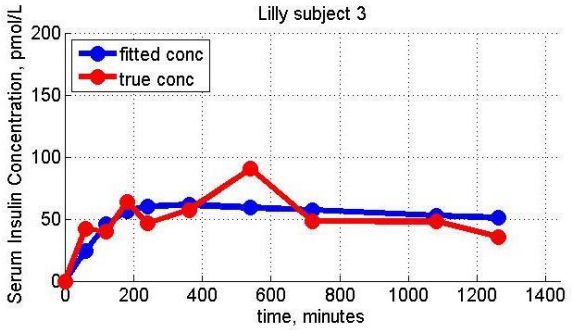

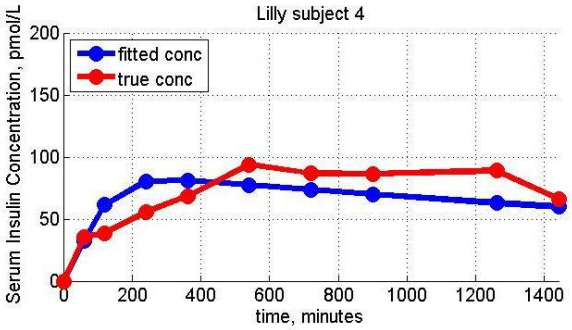

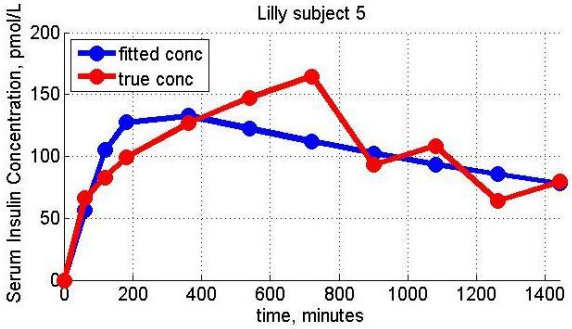

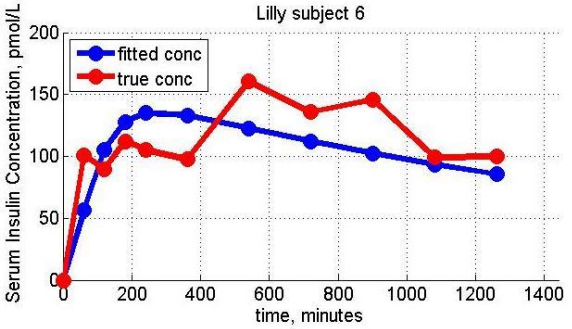

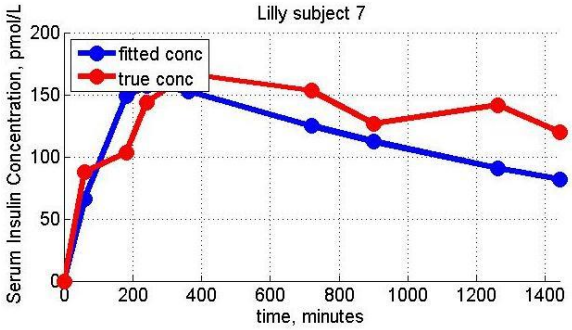

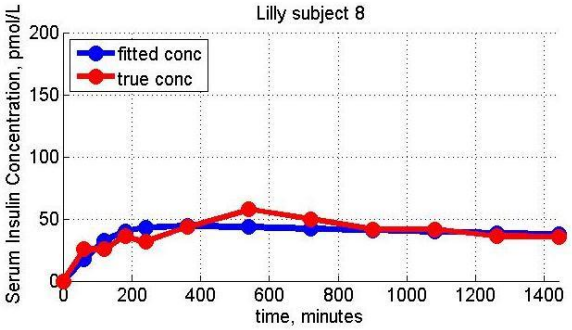

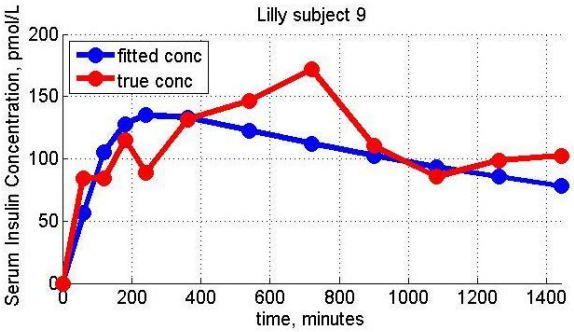
Lilly subject 9
fitted conc
true conc
Serum Insulin Concentration, pmol/L
time, minutes

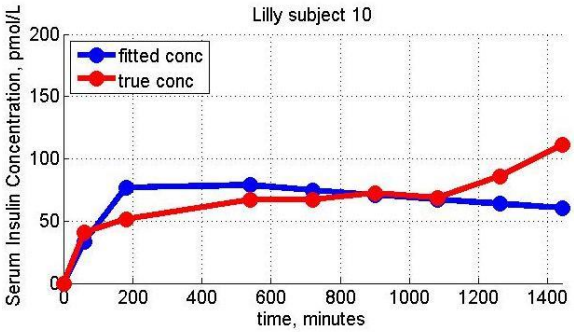
Lilly subject 10
fitted conc
true conc
Serum Insulin Concentration, pmol/L
time, minutes

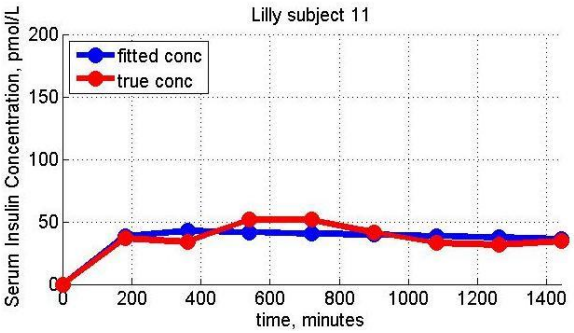
Lilly subject 11
fitted conc
true conc
Serum Insulin Concentration, pmol/L
time, minutes

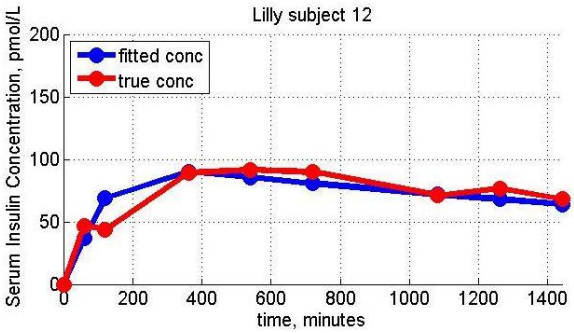
Lilly subject 12
fitted conc
true conc
Serum Insulin Concentration, pmol/L
time, minutes

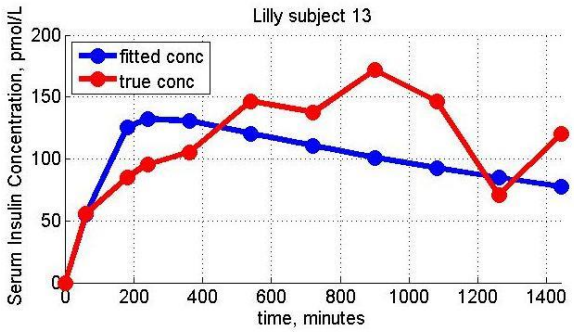
Lilly subject 13
fitted conc
true conc
Serum Insulin Concentration, pmol/L
time, minutes

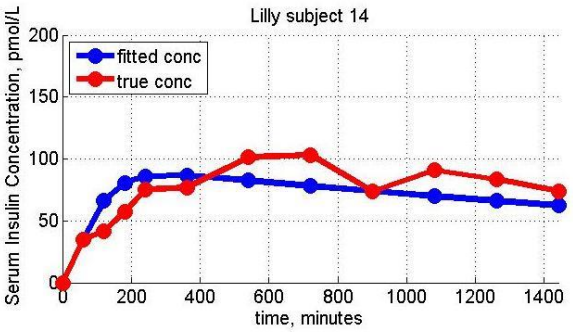
Lilly subject 14
fitted conc
true conc
Serum Insulin Concentration, pmol/L
time, minutes

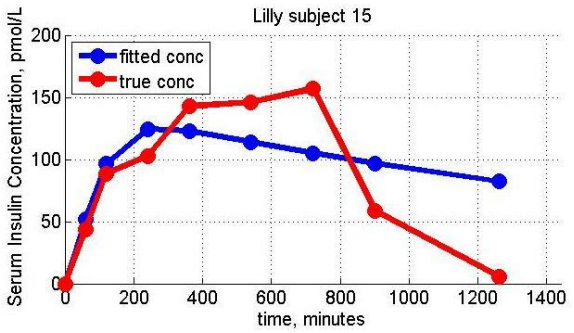
Lilly subject 15
fitted conc
true conc
Serum Insulin Concentration, pmol/L
time, minutes

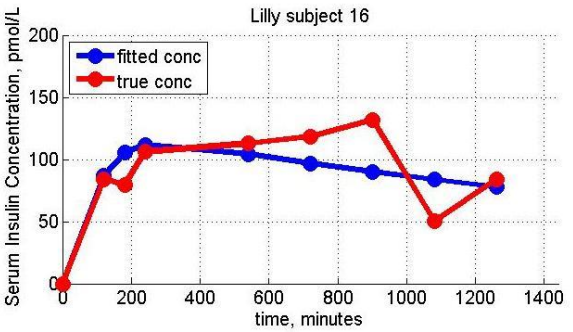
Lilly subject 16
fitted conc
true conc
Serum Insulin Concentration, pmol/L
time, minutes

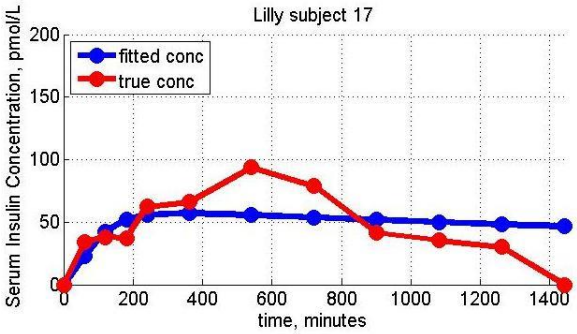
Lilly subject 17
fitted conc
true conc
Serum Insulin Concentration, pmol/L
time, minutes
0
50
100
150
200
0
200
400
600
800
1000
1200
1400

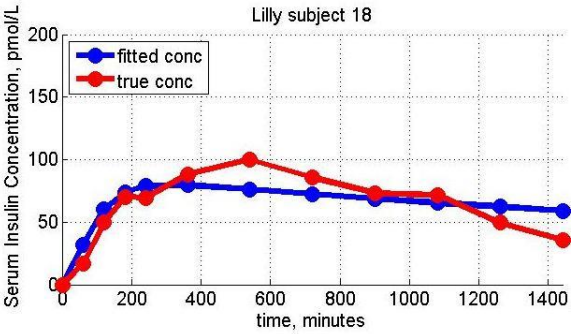
Lilly subject 18
fitted conc
true conc
Serum Insulin Concentration, pmol/L
time, minutes
0
50
100
150
200
0
200
400
600
800
1000
1200
1400

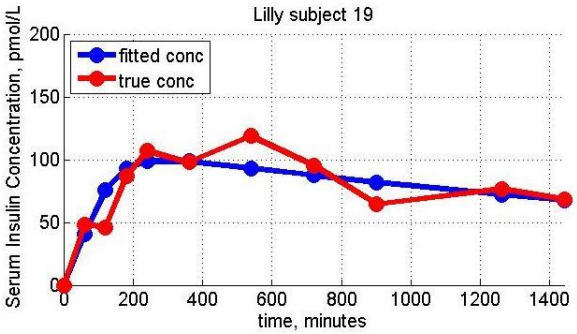
Lilly subject 19
fitted conc
true conc
Serum Insulin Concentration, pmol/L
time, minutes
0
50
100
150
200
0
200
400
600
800
1000
1200
1400

Appendix I. Simulator Modularization Details.

The pump module was removed from the Simulator and two separate pen modules were built: one pen for long-acting insulin for MDI basal injections and one pen for rapid-acting insulin for boluses (Figure 75).

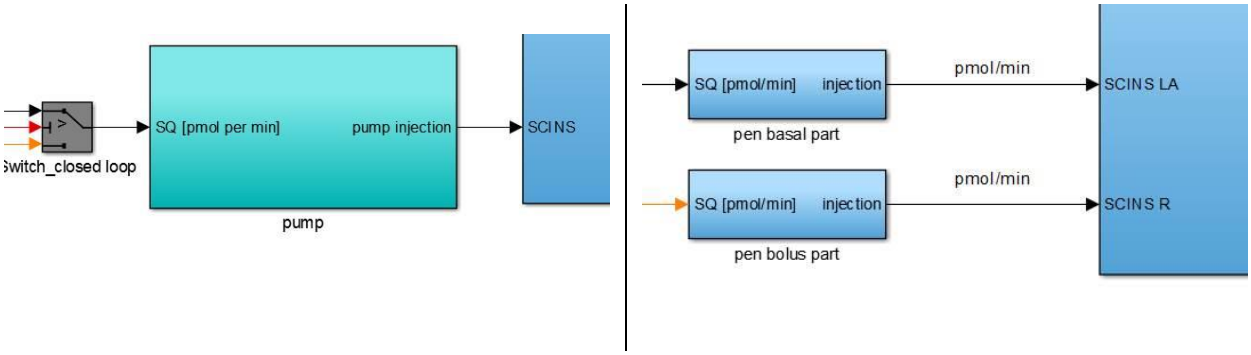

Figure 75. Pump to pens Simulator modification.

Note that in Figure 75, there is a switch before the pump module which changes the input from pre-determined scenario to the controller-initiated injections when needed (black arrow – scenario; orange arrow – controller; red arrow – switch signal). There is no such switch in the pens case because all the predetermined insulin goes through the long-acting insulin pen (top, black arrow), and the control is only applied to the rapid-acting insulin pen (bottom, orange arrow).

The second problems consisted of the fact that the Simulink implementation of the meal model [50] in the Simulator [39] included all the states in a single s-function block (Figure 76).

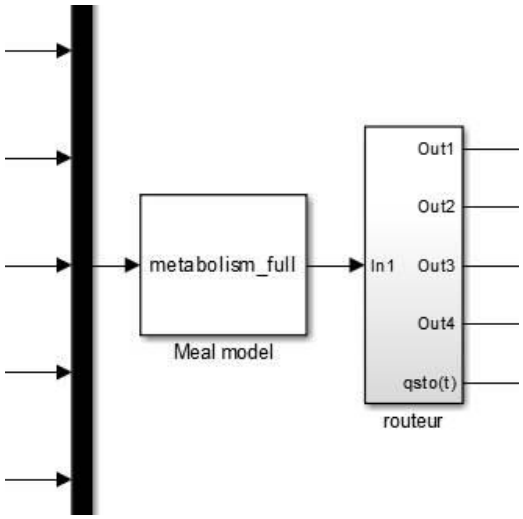

Figure 76. One-Block Meal Model.

The s-function block contained the differential equations of the meal model that took various inputs (meals, subcutaneous insulin injection, etc.) and produced the outputs (states of the model including blood glucose).

In order to add the new subcutaneous "0" compartment characterized by (34) to the Simulator, this one-block configuration was dismantled and reassembled with the insulin transport modules operating "outside" of the rest of the model (Figure 77).

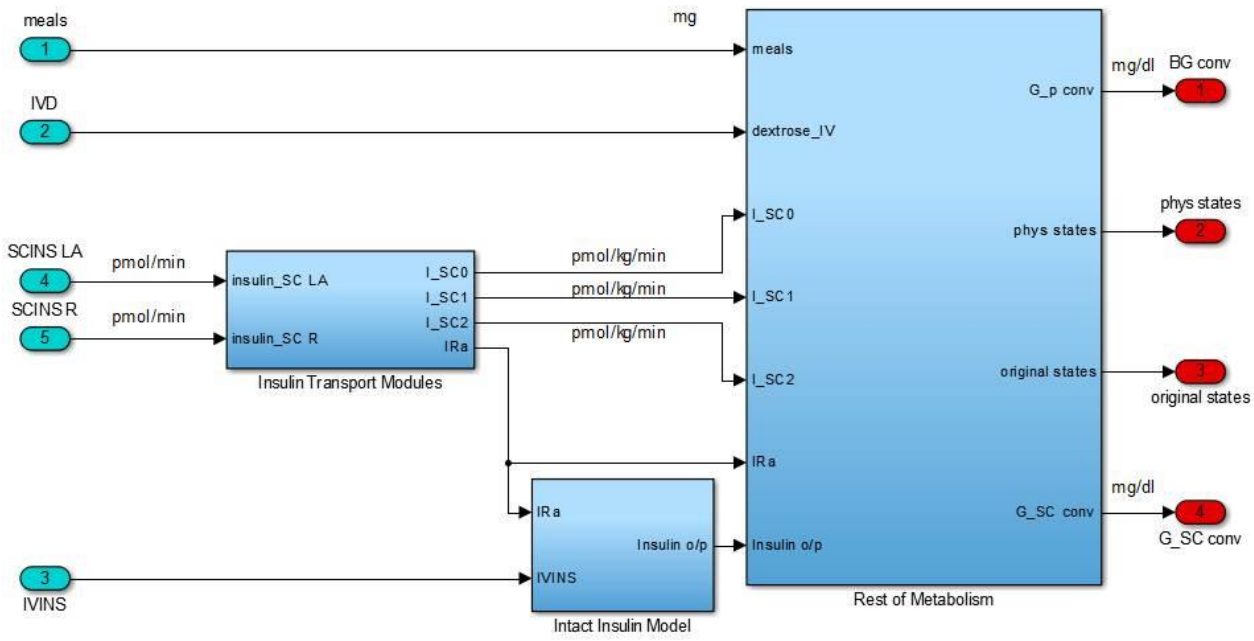

Figure 77. Insulin Transport Outside of the Meal Model.

In Figure 77, the inputs SCINS LA and SCINS R stand for long-acting subcutaneous insulin and rapid subcutaneous insulin and come from the Simulink pen implementations that inject long-acting and rapid insulins, respectively. They enter the Insulin transport modules block where the aggregate rate of appearance in plasma is determined. The assumption is made that once in plasma, the monomers of insulin show the same bioavailability, whether they came to subcutaneous tissues as hexamers of glargine or monomers of rapid-acting insulin [94]. Thus the aggregate rate of appearance corresponds to rapid acting insulin and enters the Intact insulin module where it is processed to enter the Rest of Metabolism block.

This kind of transformation is useful outside of solving this particular problem of adapting the Simulator [39] to MDI systems. Generally, such modularization of the system into the subsystems of independent dynamics of various states provides the ability to:

- easily modify a particular subsystem and quickly verify the effects of the modification to the system overall

- separate concerns specific to a particular subsystem
- minimize the dependency between the various subsystems to allow efficient maintenance of the program

Since the insulin transport model was modified, for the *In Silico* validation, insulin states initial conditions of the simulation must be revised. In the regular minimal model [51] the initial conditions are calculated through:

$$I_{SC1}{}^{0} = max\left(0, \frac{(m_2 + m_4)I_P{}^{0} - m_1 I_L{}^{0}}{(k_{a1} + k_d)}\right) \quad \textbf{(83)}$$

$$I_{SC2}{}^{0} = \frac{k_d I_{SC1}{}^{0}}{k_{a2}} \quad \textbf{(84)}$$

In the modified Simulator, the initial conditions for insulin subsystem are then calculated as

$$I_{SC0}{}^{0} = max\left(0, \frac{(m_2 + m_4)I_P{}^{0} - m_1 I_L{}^{0}}{(k_{a1} + k_d)}\right) \quad \textbf{(85)}$$

$$I_{SC1}{}^{0} = \frac{k_d I_{SC1}{}^{0}}{k_{a1} + k_d} \quad \textbf{(86)}$$

$$I_{SC2}{}^{0} = \frac{k_d I_{SC1}{}^{0}}{k_{a2}} \quad \textbf{(87)}$$

Now a simulation platform is established. Such simulation framework is essential not only for validation of an already designed system, but for the design process itself, especially when of complex systems. The new Simulator allows for two types of insulin delivery:

- daily insulin glargine injections
- injections of rapid acting insulin at meal times (or between meals) according to a prescribed "meal/correction" scenario

Thus, the simulator is uniquely equipped to support evaluation of both (i) conventional insulin pen therapy and (ii) enhanced "Smart Pen" insulin therapy.

Appendix J. Creating hypo-fearing population.

First, random values between 1.1 and 1.3 are generated. These are CR multipliers and are obtained for all *in silico* subject. Similarly, a CF multiplier for every *in silico* subject is generated. Given these modified CRs and CFs, the subjects can be titrated for their LA insulin dosage to achieve the population average HbA1c of approximately 8%.

To get a distribution around the 8% HbA1c, a random number is generated from N(8, 0.5). This results in 95% of the subjects falling within [7, 9] % HbA1c interval. Given an HbA1c value for each subject, the corresponding average BG value is calculated using the formula from [82]:

$$eAG = 18(1.583HbA_{1c} - 2.52) \quad \textbf{(88)}$$

The value of eAG is the average BG that a subject must have to achieve their given HbAc1. Examples of A1c's and average BGs produced this way are presented in Figure 78.

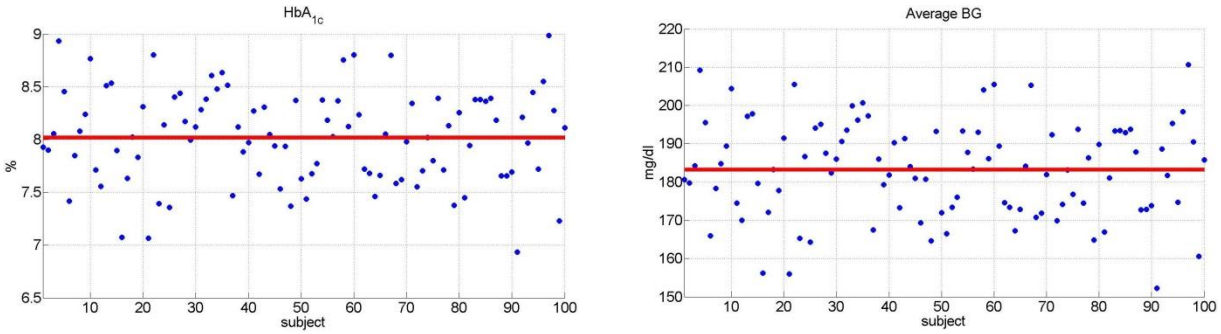

Figure 78. A1c and average BG of hypo-fearing *in silico* population.

Then the titration is conducted for each subject to bring them to the desired average BG value. The titration is done over 2-day period with meal disturbances under a realistic scenario of:

- first day
    - 0.5 g CHO/kg for breakfast at 8:00 AM
    - 0.9 g CHO/kg for lunch at 2:00 PM
    - 0.7 g CHO/kg for dinner at 8:00 PM

- second day
    - 0.5 g CHO/kg for breakfast 8:00 AM
    - 0.9 g CHO/kg for the dinner 8:00 PM

The meals are bolused according to the newly calculated carbohydrate ratios for each *in silico* subject. Moreover, if during the titration the subject went too high they were corrected according to their correction factor. The second day is designed as described to test the system's behavior in the case of a skipped meal. Thus the scenario closely emulated realistic live behavior.

Titration showed that not every subject of the Simulator can achieve the assigned average BG value. Some subjects would not go higher enough even under no basal insulin injections due to their meal boluses administered according to the modified CR. In this case, the CR was randomly modified into a larger possible CR value (under the methodology described above) which overinsulinized the subject.

Average BGs conditioned on TDDs of LA insulin from two examples of subjects who could achieve their target average BGs (195 mg/dl and 189 mg/dl respectively) are presented in Figure 79.

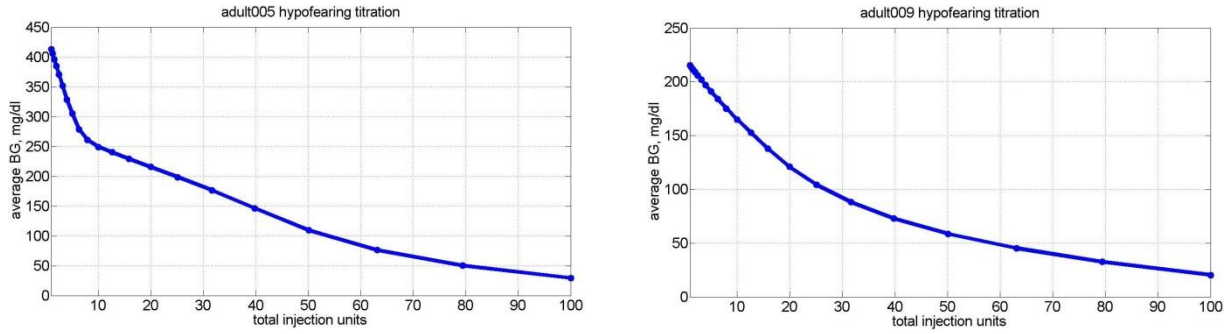

Figure 79. Average BG vs TDD of long-acting insulin; BG targets achieved.

The following two plots present examples of subjects who could not achieve their targets (192 mg/dl and 186 mg/dl respectively) – Figure 80

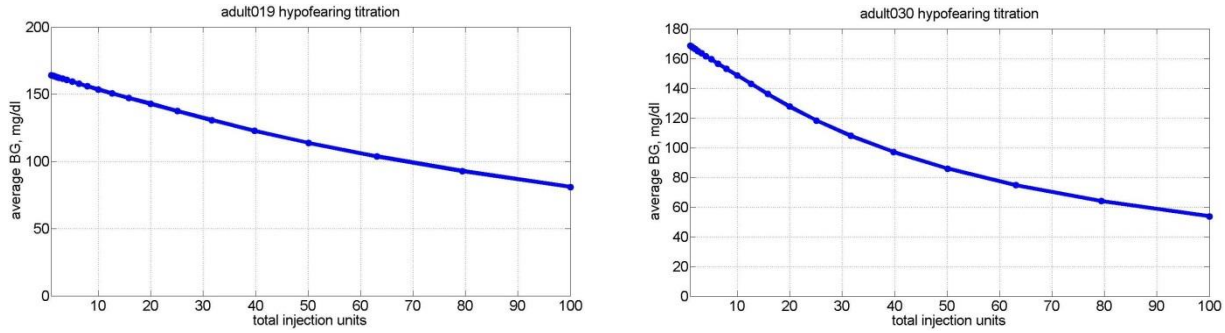

Figure 80. Average BG vs TDD of long-acting insulin; BG targets not achieved.

Third type of "behavior " during the titration is subjects who are very sensitive to basal insulin. An example of such subject is in Figure 81.

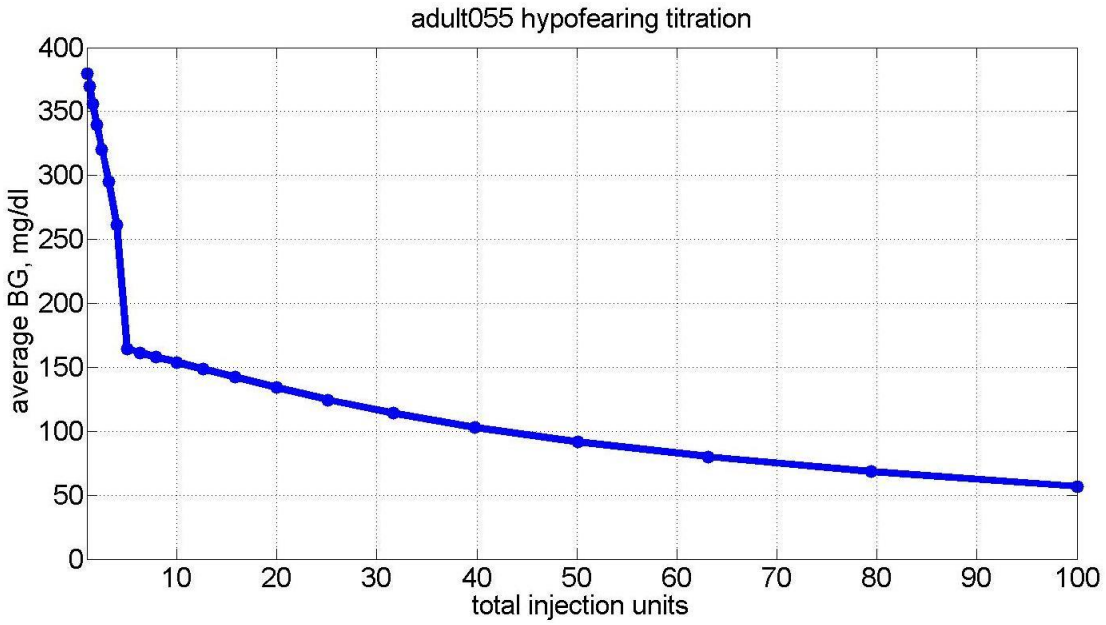

Figure 81. Subject overly sensitive to LA insulin in certain range of TDD.

Finally, fourth type of "behavior" exhibited by *in silico* subjects during the titration was "broken" curve which happens due to the corrections that result from high BG values at low LA insulin injection values. Such "breaks" could happen more than once – see examples in Figure 82

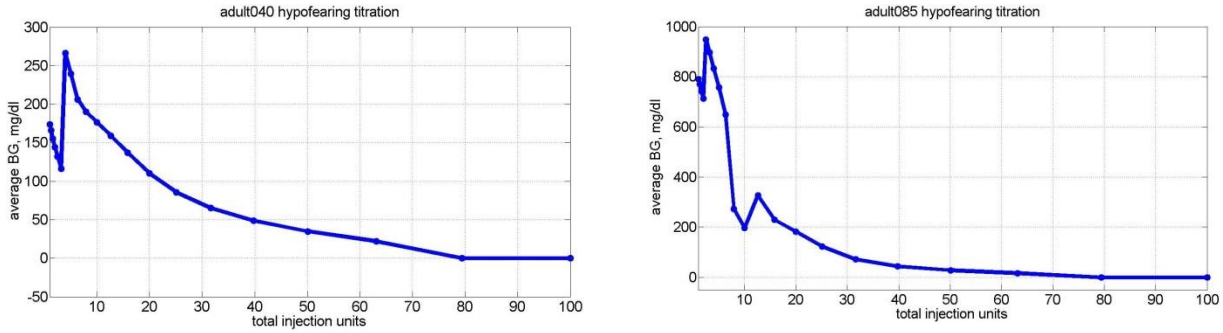

Figure 82. Influence of CF corrections in titration.

Importantly, the titration process showed that there are subjects whose daily BG fluctuation is more sensitive to LA insulin than other. This is summarized in Figure 83, where upward excursions correspond to subjects who are not too sensitive to the basal changes (the ones who could not achieve their targets by just LA insulin dose modification) and downward excursions correspond to subjects who are very sensitive to LA insulin dose modification.

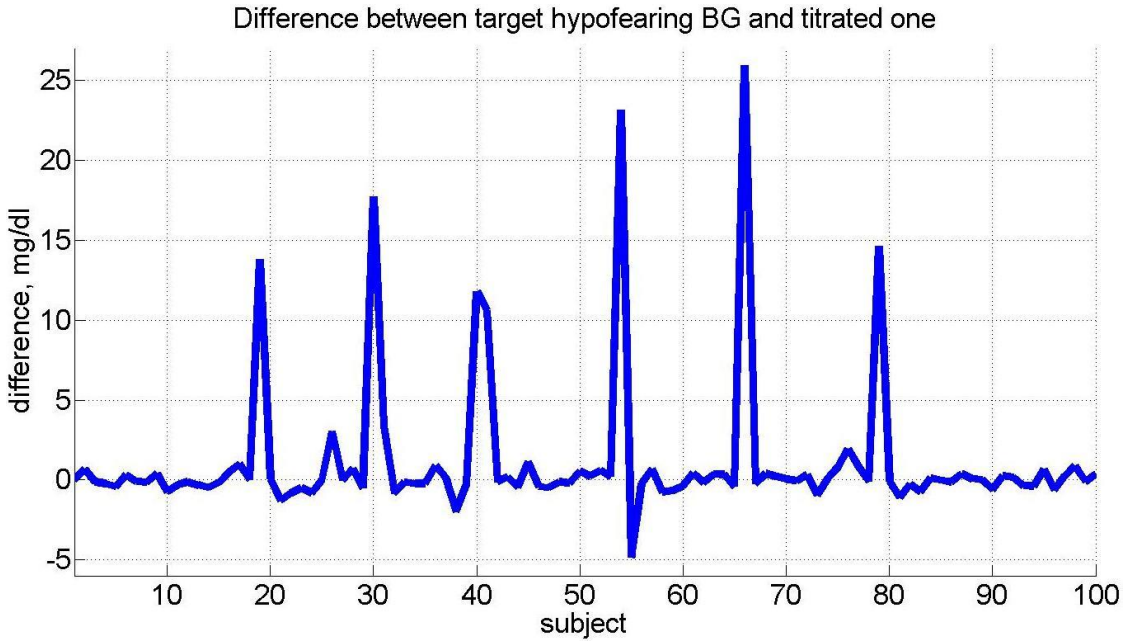

Figure 83. Difference between desired BG and the one that was achieved via titration.

Note that the word ‘sensitive’ is not used in the sense of being sensitive or not sensitive to insulin itself, but in the sense of the subjects’ therapy being overly dominated but incorrectly calibrated CR and CF that do not allow to choose an appropriate (in the context of hypo-fearing population) LA insulin dose.

Appendix K. Interface Screens.


CLOSED | 176 mg/dl | CGM PEN 8:40
For your 8:00 long-acting insulin profile injection, you already injected 6 U at 7:50
Are you sure you wa
Your last 3 injections
6 U at 7:50
10 U at 21:07
11 U at 8:03
CANCEL
APPROVE
CLOSED | 176 mg/dl | CGM PEN 11:50
Long- or Rapid-Acting?
Long
Rapid
CLOSED | 176 mg/dl | CGM PEN 11:50
Are You Going to Eat?
YES
NO
CLOSED | 176 mg/dl | CGM PEN 11:50
Blood Glucose
220
mg/dl
Meal Carbs
OR
Meal Insulin
55
g
0
U
CANCEL
Sony Ericsson
XPERIA

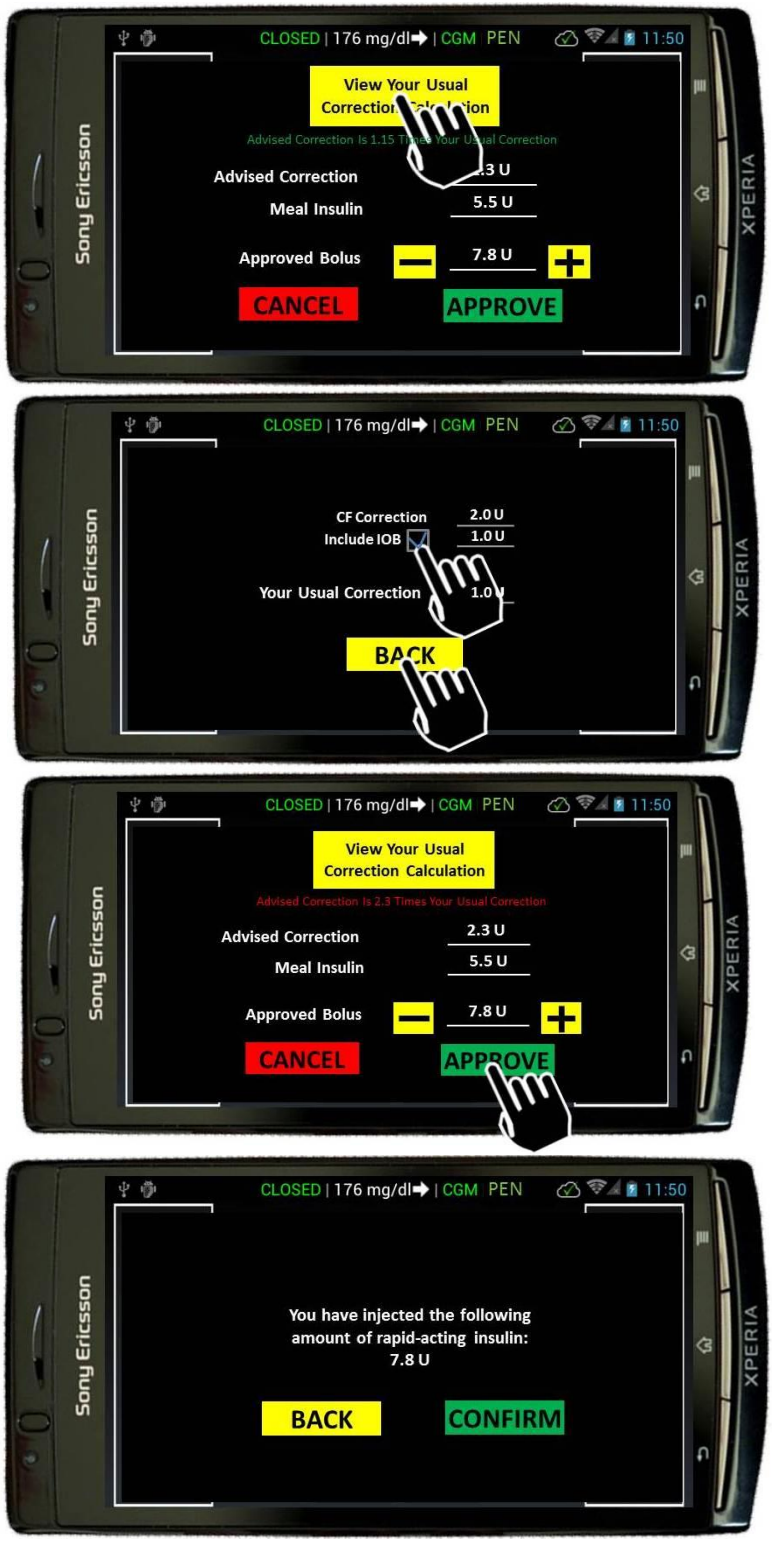
CLOSED | 176 mg/dl | CGM PEN 11:50
View Your Usual
Advised Correction
Meal Insulin
5.5 U
Approved Bolus
7.8 U
CANCEL
APPROVE
Sony Ericsson
XPERIA
CF Correction
2.0 U
Include IOB
1.0 U
Your Usual Correction
BACK
View Your Usual
Correction Calculation
Advised Correction Is 2.3 Times Your Usual Correction
Advised Correction
2.3 U
Meal Insulin
5.5 U
Approved Bolus
7.8 U
CANCEL
APPROVE
You have injected the following
amount of rapid-acting insulin:
7.8 U
BACK
CONFIRM

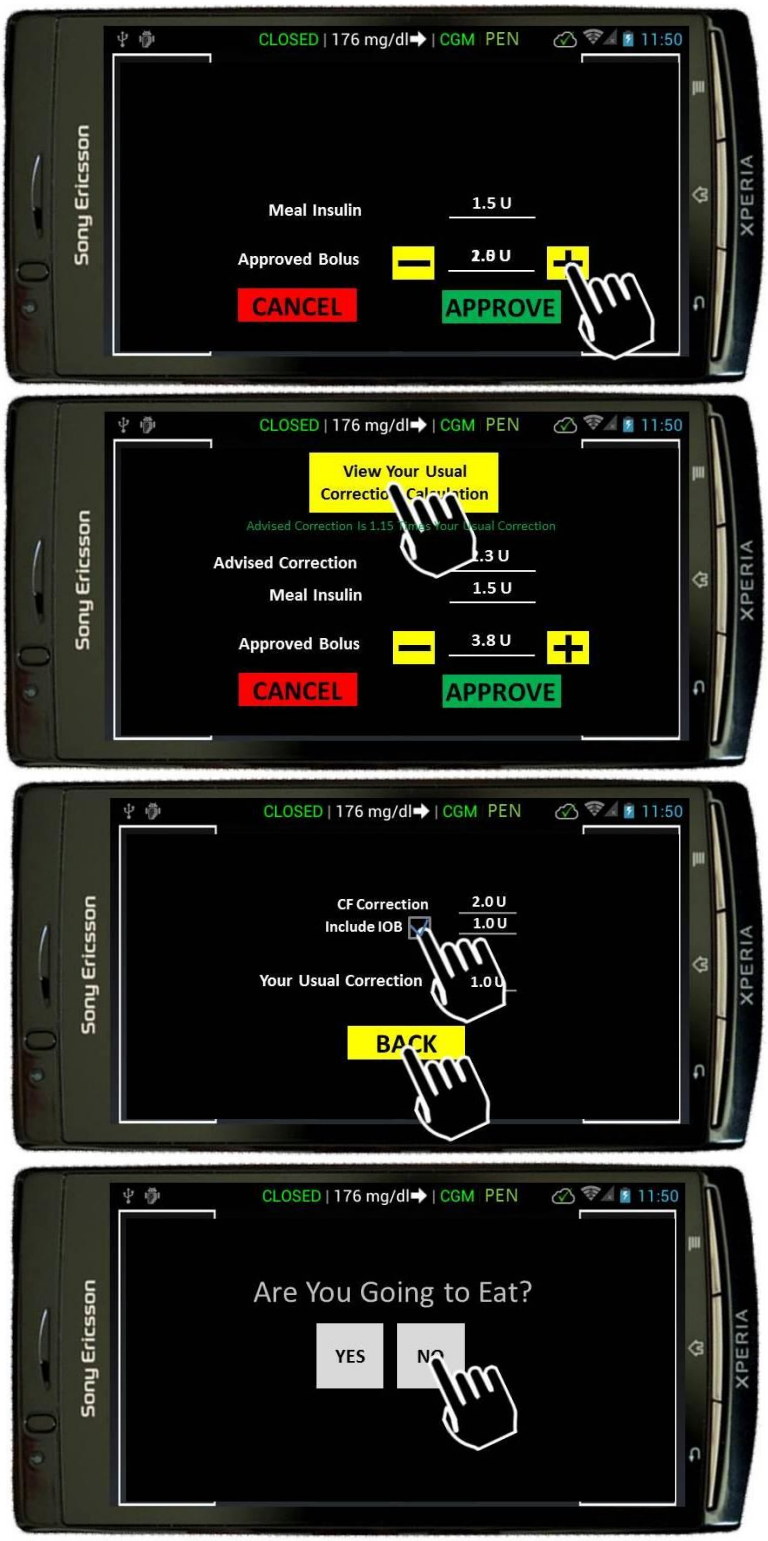
CLOSED | 176 mg/dl | CGM PEN 11:50
Meal Insulin 1.5 U
Approved Bolus 2.8 U
CANCEL
APPROVE
CLOSED | 176 mg/dl | CGM PEN 11:50
View Your Usual
Advised Correction
Meal Insulin 1.5 U
Approved Bolus 3.8 U
CANCEL
APPROVE
CLOSED | 176 mg/dl | CGM PEN 11:50
CF Correction 2.0 U
Include IOB 1.0 U
Your Usual Correction 1.0 U
BACK
CLOSED | 176 mg/dl | CGM PEN 11:50
Are You Going to Eat?
YES
NO

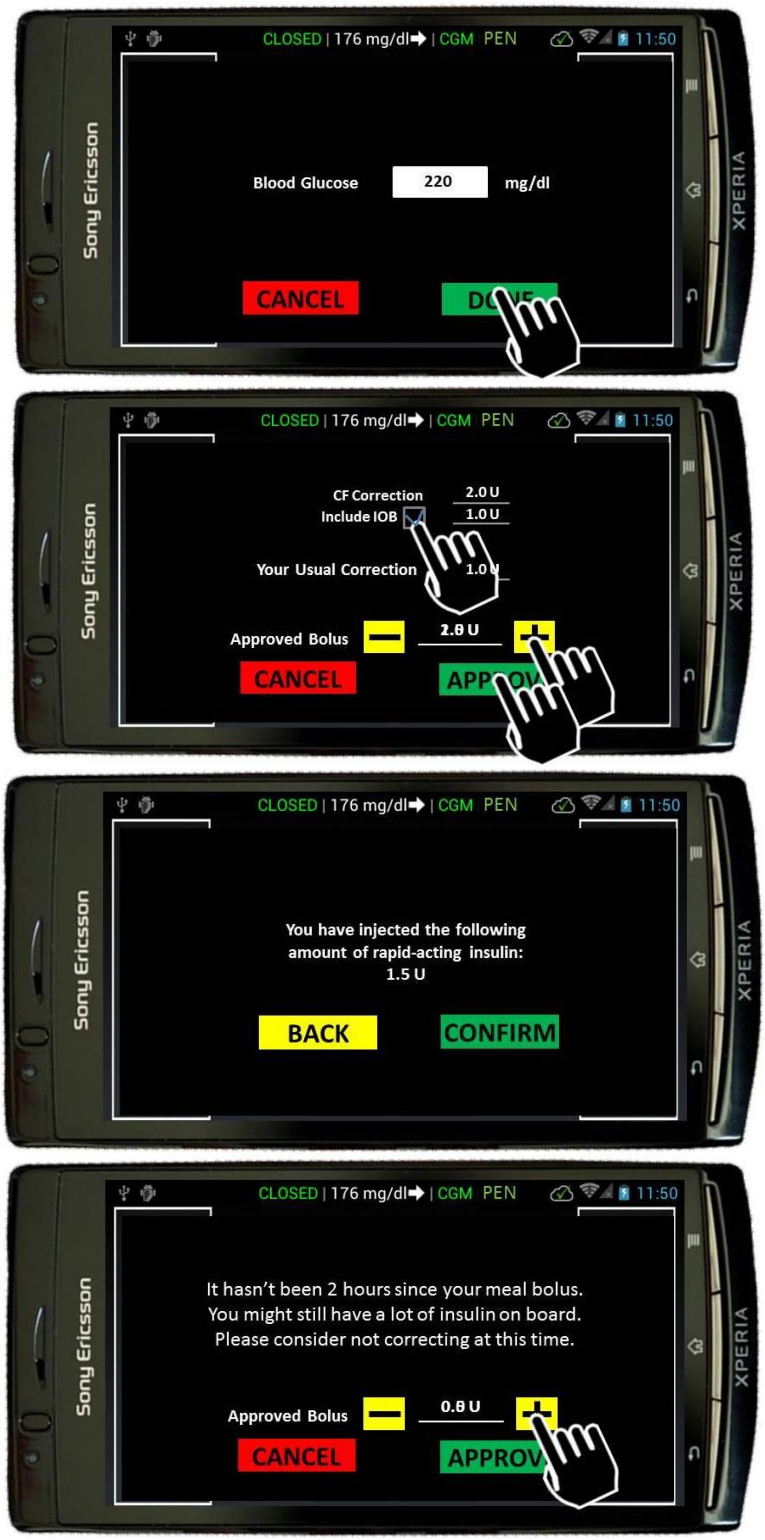
CLOSED | 176 mg/dl | CGM PEN 11:50
Blood Glucose
220
mg/dl
CANCEL
CF Correction
2.0 U
Include IOB
1.0 U
Your Usual Correction
1.0 U
Approved Bolus
2.8 U
CANCEL
You have injected the following amount of rapid-acting insulin:
1.5 U
BACK
CONFIRM
It hasn't been 2 hours since your meal bolus.
You might still have a lot of insulin on board.
Please consider not correcting at this time.
Approved Bolus
0.8 U
CANCEL
Sony Ericsson
XPERIA

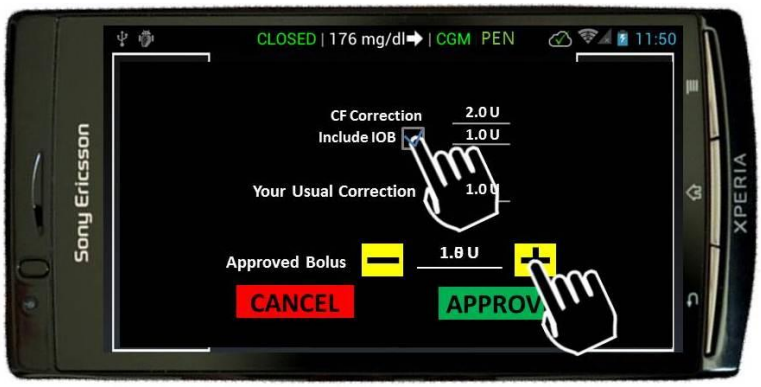
CLOSED | 176 mg/dl | CGM PEN
11:50
CF Correction
2.0 U
Include IOB
1.0 U
Your Usual Correction
1.0 U
Approved Bolus
1.8 U
CANCEL
APPROV
Sony Ericsson
XPERIA

Appendix L. Survey Thematic Analysis Examples.

One response to a question increased the score of one requirement in the corresponding category:

Response to question 1	→ Category 1, Requirement *a*	+1
	Total increment	+1

One response to a question increased the score of more than one requirement in the corresponding category:

Response to question 1	→ Category 1, Requirement *a*	+1
	Category 1, Requirement *b*	+1
	Total increment	+2

One response to a question increased the score of requirements in more than one category:

Response to question 1	→ Category 1, Requirement *a*	+1
	Category 2, Requirement *a*	+1
	Total increment	+2

One response to a question did not increase any score in its corresponding category, but increased score in other categories:

Response to question 1	→ Category 1	+0
	Category 2, Requirement *a*	+1
	Category 2, Requirement *b*	+1
	Category 3, Requirement *a*	+1

Category 4, Requirement *a*	+1
Total increment	+4

Responses to different questions increase score of the same requirement in the same category:

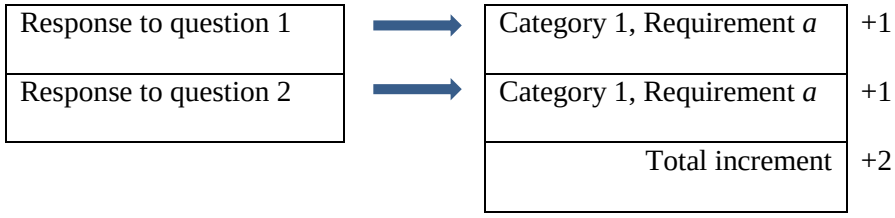

Response to question 1	→	Category 1, Requirement *a*	+1
Response to question 2	→	Category 1, Requirement *a*	+1
		Total increment	+2